THE FLOW BEHAVIOUR

of

SHALLOW FLUIDISED BEDS

by

STUART JAMES McGUIGAN

A thesis submitted to the Faculty of Engineering in fulfilment of the requirements for the Degree of Doctor of Philosophy.

Department of Mechanical Engineering
University of Aston in Birmingham
England
November 1974

SUMMARY

The flow behaviour of shallow gas-fluidised beds was studied experimentally using a rotational viscometer, and an inclined open channel.

Initially, tests were carried out with the viscometer in order to establish qualitative trends in the flow properties of a variety of materials over a wide range of fluidising conditions. Also, a technique was developed which enabled quantitative viscosity data to be extracted from the experimental results.

The flow properties were found to be sensitive to the size, size-range and density of the fluidised material, the type of distributor used, and the moisture content of the fluidising gas. Tests in beds up to 120 mm deep showed that the fluidity of the bed improves with reduction in depth; and indicated a range of flow behaviour from shear-thinning to Newtonian, depending chiefly on fluidising velocity.

Later, an apparatus was built which provided for a steady, continuous flow of fluidised material down an inclined open channel of 3m length x 0.15m square, up to a mass flowrate of 10 kg/s (35 ton/hr). This facility has enabled data to be obtained that is of practical value in industrial applications; which is otherwise difficult in view of the present limited understanding of the true mechanism of fluidised flow. A correlation has been devised, based on analogy with laminar liquid flow, which describes the channel flow behaviour with reasonable accuracy over the whole range of shear-rates used.

The channel results indicated that at low fluidising velocities the flow was adversely affected by settlement of a stagnant layer of particles on to the distributor, which gave rise to increased flow resistance. Conversely, at higher fluidising velocities the resistance at the distributor appeared to be less than at the walls. In view of

this, and also because of the disparity in shear-rates between the two types of apparatus, it is not possible as yet to predict exactly the flow behaviour in an open channel from small-scale viscometer tests.

QUOTATION

'But first I shall test by experiment before I proceed further, because my intention is to consult experience first and then with reasoning show why experience is bound to operate in such a way. And this is the true rule by which those who analyse the effects of nature must proceed.'

Leonardo da Vinci

ACKNOWLEDGEMENTS

I wish to express my thanks to the University for an appointment to the research staff which enabled me to carry out this work, and to Professor A. J. Ede for the provision of research facilities in the Department of Mechanical Engineering.

I am especially grateful to my supervisor, Professor D. E. Elliott for his continued advice and many helpful discussions throughout the course of the work. His enthusiasm was a source of considerable inspiration to me.

I would also like to express my gratitude to the following:

Messrs. E. W. Denchfield, G. O. Rickers, J. Hirons and other members of the technical staff of the Department for their considerable practical assistance.

Mr. R. R. Pugh who collaborated in the design and construction of the channel flow rig.

Drs. J. S. M. Botterill and D. J. Bossant of the Department of Chemical Engineering, University of Birmingham for our many fruitful exchanges of views.

Mrs. E. I. Lockwood of the Royal Military College of Science for typing this thesis.

C O N T E N T S

APPENDICES

CHAPTER 1

INTRODUCTION

INTRODUCTION

The concept of fluidisation of solid particles has been known for many years. The first patent of an industrial application was taken out in 1922; and since 1942 fluidised beds have been in universal use for the cracking of petroleum products.

In this, and other applications in chemical engineering, the salient advantages of the fluidised bed are the large surface area and good fluid-solid contacting which enable enhanced reaction rates; and the uniformity of temperature within the bed which assists in controlling the reactions. The latter property is consequent upon good solids mixing and good interparticle heat transfer. These features also assist in making the bed an excellent vehicle for the combustion of a wide variety of fuels at high efficiency.

As a result of the favourable combustion and the excellent heat-transfer which is obtained between the bed and immersed surfaces, there has been increasing interest in recent years in boilers and heat-exchangers employing fluidised beds. Several large-scale boiler designs employing coal combustion have been planned and a number of pilot plants constructed, but as yet only smaller scale heat-transfer applications of fluidisation have achieved commercial fruition.

Most of the large-scale boiler designs have retained the relatively deep beds employed in fluidised chemical reactors; and this creates serious design problems as it is difficult to scale-up the results from pilot tests in small beds under these circumstances. However, recent work at the University of Aston has shown that good combustion is possible in beds only a few centimetres deep. Moreover, it has been found that the heat transfer performance in such shallow beds - particularly using heat exchangers with extended surfaces - is much superior to that obtainable from deep beds. The general behaviour

of shallow beds also differs markedly from deeper ones; mainly as a result of the absence of large bubbles, which grow by coalescence as they rise through deep beds. The shallow bed is characterised by an even, rhythmic bubbling pattern giving a greater degree of homogeneity which enhances its fluid-like character. Whilst a comparative wealth of knowledge is available on deep beds, shallow beds have received little attention until the recent interest at Aston in heat-transfer systems.

One disadvantage of fluidised combustion is its relatively narrow range of stable operating temperatures, which places some limitation on the operational flexibility of plant in terms of turn-down from maximum capacity. A number of schemes have been proposed to overcome this drawback which involve circulation or transport of the fluidised material at high temperature, an artifice which is also required in other plants using fluidisation techniques. Fluidised transport is also a useful means of handling particulate materials in its own right; and offers a number of advantages, both functional and economic over alternative methods.

The wider application of fluidised flow has undoubtedly been hampered by ignorance of the character and properties of the flowing bed, which in some ways have only superficial similarity to the flow of true fluids. The fluidised state in general can be regarded as another state of matter, about which comparatively little is known compared with the other, simpler states. Consequently, research in fluidisation is rather a matter of discovery and investigation than the refinement and improvement of established techniques of which much current research work is comprised.

To the engineer, who is interested in applications rather than concepts, this must mean heavy reliance on empirical data for design purposes. This is not a satisfactory state of affairs, particularly

since in fluidisation it is often found that the range of application of empirical correlations extends very little beyond that of the conditions under which they were determined. So far, all attempts to account for fluidised bed flow behaviour from theoretical considerations have proved to be of little worth in practical situations. This is so for two reasons. Firstly, the interaction of particles on a microscopic scale is not completely understood; and secondly such knowledge as is available is not easy to apply, especially in gas-fluidised beds which are generally heterogeneous.

In this situation, the approach adopted in this work was to make a two-pronged attack. Initially, a study was made - using small scale apparatus - of a range of materials and fluidising conditions to look for trends in the flow behaviour. This apparatus enabled a cheap and rapid qualitative evaluation to be made, but it was not expected that the results would necessarily have direct quantitative application to fluidised transport. Secondly, a rig was designed which has enabled the study of channel flow at velocities and mass flowrates sufficient to provide data of direct relevance to commercial application. The rig is large by standards of university research; but its construction is considered fully justified as the best means, at the present time, of obtaining practically useful information on fluidised flow. The rig also provides a basic solids circulation facility, which will be useful for work over a much wider field than that of immediate interest.

CHAPTER 2.

LITERATURE SURVEY.

INTRODUCTION

This survey of published information on fluidisation may be conveniently divided into five sections.

The first deals briefly with the concept of a fluidised bed and the second with some aspects of the general behaviour of gas fluidised beds, particularly those which may be relevant to their flow performance. Notes are included on some of the attempts which have been made to classify the behaviour of different types of fluidised systems. The third part covers previous work on what may be broadly termed flow behaviour, and the fourth deals with electrostatic charging. The latter is known to have a profound effect upon the flow properties of some fluidised materials.

Finally a short section is included on the history and development of the industrial use of fluidisation, together with some observations regarding the potentialities of heat transfer and solids transport systems.

1. THE CONCEPT OF A FLUIDISED BED

A fluidised bed can be considered to comprise a mass of particulate material, through which passes a fluid with sufficient dissipation of energy to cause the particles to exhibit a certain degree of random mobility. This is a rather abstract and incomplete definition, and usually the bed of material is contained in a vessel with a porous base through which the fluidising medium is supplied. If the flowrate of the latter is increased from zero the fluid will initially permeate through the voids between the particles of the packed bed, without causing any particle motion. As the fluid flowrate is further increased the upward drag forces on the particles become greater and cause some expansion of the packed bed, although the particles still remain loosely arranged in a fixed structure. With a still higher flowrate the bed expands to such an extent, and the interstitial fluid velocity increases sufficiently for some of the particles to become fully supported in the fluid, thus allowing some freedom of movement. This is the beginning of the fluidised state. It is clear that the foregoing is an inherently unstable situation, for no sooner has the local movement of particles commenced than the bed structure is rearranged, causing a redistribution of fluid flow pattern throughout the bed. Thus in this condition the bed is only fluidised over part of its total volume; the fluid taking a path of least resistance as it rises through the bed. Further small increases in fluid velocity then cause further areas of the bed to become mobile, as more particles become supported by the fluid until the whole of the main body of the bed is supported.

At this point it is necessary to distinguish the behaviour of beds fluidised by liquids from those fluidised by gases. With a liquid fluidised system, further increases in fluid flowrate generally cause

a uniform progressive expansion of the bed in which the local particle voidage is substantially equal to the overall mean voidage. Gas fluidised systems, by contract, expand much less and the additional gas flow is accommodated by the formation of bubble-like cavities which form near the distributor and rise through the bed. Such bubbles are substantially if not completely free of particles thus the local voidage in a gas fluidised bed is not generally equal to the overall mean voidage. The above descriptions of gas and liquid fluidisation are not universally accurate, as it is possible for a gas fluidised bed to expand homogeneously and for a liquid fluidised bed to exhibit bubbling. However such classification is adequate as a general guide.

When a bed has been fluidised it is usual for it to be able to be able to sustain stable uniform fluidisation over a range of fluid flow velocities. The lower limit is normally fixed by the tendency for the larger particles present to segregate out towards the distributor plate. The upper limit is governed by entrainment of the smallest particles in the efflux fluid stream. This occurs at a velocity similar to the free fall velocity of the particles in the fluid. The range of stable operation depends mainly upon the size and size distribution of the particles and their density relative to that of the fluidising medium.

The fluidised systems investigated in this work are confined to gas fluidised beds which start to bubble at flow velocities close to that at which fluidisation commences. These are the types of systems which are of greatest interest in heat transfer and combustion applications. Liquid fluidised systems are at present of secondary interest in this context, and will not be discussed further. However it is pertinent to mention that their flow behaviour is likely to be

fundamentally different to that of gas fluidised beds, and more similar to that of solid/liquid suspensions and slurries.

2. GENERAL BEHAVIOUR OF GAS FLUIDISED BEDS

The behaviour of stationary (ie non-flowing) gas fluidised beds has been the subject of numerous and extensive studies, both theoretical and experimental, over a number of years and is now well reported in the literature. However, the hydrodynamics of the bed are still by no means fully understood. Furthermore, most previous authors have studied systems comprising relatively deep beds and in many cases small, low density particles such as petroleum cracking catalyst. Such systems are of most interest to chemical engineers, who up to now have been the main exponents of fluidised bed technology; but generally these systems behave in a different manner to shallow beds of denser particles. Thus although much of the work which has been done is very useful, a very critical appraisal is necessary before applying the results obtained to other systems with markedly dissimilar bed geometries and fludising conditions. Having said this, it is still often the case that results obtained from systems which appear initially to bear little similarity are quite comparable at least in qualitative terms.

The intention here is not to give an exhaustive review of all the published work on general bed behaviour. Rather it is to discuss briefly the points which are perhaps the most important and well established, and to examine where possible how far they apply to the shallow bed systems which have been studied in the present work. This is considered under a number of headings.

2.1 Minimum Fluidising Velocity

This is perhaps the most important parameter used in classifying fluid bed behaviour, and yet one of the most difficult to define

accurately and to estimate for design purposes without carrying out a practical test. It is usual to define the minimum fluidising velocity as the fluid velocity at which the pressure drop across the bed becomes equal to the weight of the bed per unit area of the distributor plate. This velocity is usually expressed as a "superficial velocity" equal to the fluid flow rate per unit area of cross section of the bed. The idealised behaviour in which a transition occurs from a fixed to a fully supported fluidised bed at a discreet "minimum fluidising velocity" rarely occurs in practice. Real systems fluidise over a range of fluid velocities, and the head loss does not become equal to the bed weight until well after U_{m_f}, if indeed it ever does. Some of the reasons for this are reported by RICHARDSON[1].

Many attempts have been made to provide expressions from which the minimum fluidising velocity may be calculated from fluid and particle properties. Most of these are based on equating the pressure drop across the bed to the weight of the particles.

$$\Delta p = h_{m_f} (1 - \epsilon_{m_f}) (\rho_s - \rho_f) g \qquad (1)$$

Expressions for the pressure drop across a fixed bed of uniform particles such as that of ERGUN[2] given below, or CARMEN[3] are then used

$$\frac{\Delta p}{h} = \frac{150 (1 - \epsilon)^2}{\epsilon^3} \frac{u_f u_o}{(\phi d_p)^2} + 1.75 \frac{1 - \epsilon}{\epsilon^3} \frac{\rho_f u_o^2}{\phi d_p} \qquad (2)$$

By equating the pressure drop given by (1) & (2) an expression for minimum fluidising velocity is obtained. Unfortunately these expressions demand knowledge of the particle sphericity and bed voidage: information which is not normally available or easy to determine with simple apparatus. Because of this WEN and YU[4] have correlated these parameters for a wide range of particle systems and proposed an expression for U_{m_f} involving only particle & gas density, gas viscosity and particle diameter:

$$\frac{d_p \, u_{m_f} \, \rho_f}{\mu_f} = \left[(33.7)^2 + \frac{.0408 \, d_p^3 \, \rho_g \, (\rho_s - \rho_f) g}{\mu_f^2} \right] - 33.7 \qquad (3)$$

The first term in (2) represents the viscous losses and the second the kinetic energy losses. According to KUNII and LEVENSPIEL[8] the former may be neglected at particle Reynolds Numbers greater than 1000 and latter at less than 20.

This leads to simpler expressions for small particles

$$u_{m_f} = \frac{d_p^2 \, (\rho_s - \rho_f) \, g}{1650 \, \mu} \qquad \text{for } Re_p < 20 \qquad (4)$$

$$\left[\text{Note } Re_p = \frac{\rho_s \, u_f \, d_p}{\mu_f} \right]$$

and for large particles

$$u_{m_f}^2 = \frac{d_p \, (\rho_s - \rho_f) \, g}{24.5 \, \rho_g} \qquad Re_p > 1000 \qquad (5)$$

Other workers have suggested equations similar to (4): Rowe[11] uses a factor of 1240 in place of 1650 and Richardson[1] suggests 1695. Other expressions have been proposed by LEVA[5], FRANTZ[6] and ZENZ OTHMER[7], the latter of which is claimed to be applicable to beds of wide size range particles.

None of these expressions is very accurate however: WEN & YU[4] report a standard deviations of ± 34% over a range of Re_p .001→ 4000. This is perhaps not surprising in view of the approximations made, and also because the packed bed equations upon which the expressions are based ignore any particle interaction forces which may be present and give rise to agglomeration, or reduced mobility on fluidisation. Fortunately it is easy to determine minimum fluidisation velocity accurately with simple apparatus provided that a small sample of the material to be fluidised is available for test. This determination is usually carried out by plotting the pressure drop across the bed against the superficial velocity, as recorded from readings taken at intervals as the fluid flow rate is reduced from a value well above

minimum fluidisation.

The resulting graph exhibits a pronounced change of slope at U_{m_f} and if tangents are drawn to the two sections of the curve, their point of intersection represents the minimum fluidising velocity. Recently an alternative method has been suggested by MOTAMEDI and JAMESON[12] involving introduction of bubbles into the bed. The method gives higher values than the pressure drop method, but there is no reason to suppose that they are more realistic, since in any case the definition of U_{m_f} is quite arbitrary.

2.2 Entrainment Velocity

This represents the upper limit of bed operation and is dependent rather on the smallest size of particles present in the bed than the mean size as is U_{m_f}. In real systems there is frequently a small percentage of very fine material in commercial materials as supplied due to degradation caused by handling. For design purposes it would be unrealistic to operate below the entrainment velocity for such particles and calculations must be based on the lowest size present in significant quantity. However precautions may be necessary in commercial plant to retain such very fine material, as it can constitute a serious health hazard even with non toxic materials.

The entrainment velocity is usually equated to the free fall velocity of a single particle in the fluid. An expression of the form

$$U_t = \sqrt{\frac{4\, g d_p (\rho_s - \rho_f)}{3 \rho_g C_d}} \qquad (6)$$

may be derived from fluid mechanics, where C_D is an empirical drag coefficient which has a value depending upon the particle Reynolds number[8]. BROWN et al[9] have suggested a graphical correlation for estimating the entrainment velocity over a wide range of C_D and Re_p.

It is useful to be able to estimate approximately the range of operation possible between the minimum fluidisation and terminal velocities. This normally lies between 10:1 and 90:1 for fairly narrow cuts of particles. However PINCHBECK and POPPER[10] have derived an expression to find the ratio of U_t/U_{m_f} at values of $C_D\ Re_p$ from 10^{-1} to 10^6, which gave reasonable agreement with experimental data.

2.3 Bubbling Behaviour of Beds

Whilst it is broadly true that liquid fluidised beds fluidise homogeneously and gas fluidised beds bubble, this is not universally accurate. WILHELM AND KWAUK[13] suggested a Froude number

$$Fr = \frac{U_m^2}{gd_p}$$

for deciding whether or not bubbling will occur: Froude numbers greater than unity corresponding to bubbling fluidisation. More recent work by ROMERO and JOHANSON[14] uses the Froude number together with a Reynolds number and fluid/solid density ratio. However work by SIMPSON and RODGER[15] on systems with Froude numbers close to unity showed that behaviour the reverse of that suggested by Wilhelm and Kwauk was possible. They considered the bed as a bundle of capillary tubes and evolved a theoretical prediction involving various dimensionless groups. Other workers[16,17,18,19] have used mathematical approaches based on the stability or growth of disturbances within the bed. HARRISON et al[20] developed a theory based on the maximum size of bubble likely to be stable in a fluidised system. An approach using the occurrence of shock waves in the bed has been used to predict the transition from homogeneous to bubbling behaviour by VANLOOP and HEERTJES[21] and works well in liquid fluidisation, but less so with gas/solid systems. Some of the foregoing are extremely complex and whilst they can distinguish successfully between gas and liquid fluidisation, none is able to predict satisfactorily whether

a given system will bubble or behave homogeneously.

It is clear that there is little real understanding of why bubbles form under certain circumstances. Perhaps the most useful work in this area is an attempt by GELDART[22] to classify powders into different behaviour groups. He has suggested four distinct types of system, as follows:

Group A Materials of small mean size and/or density less than 1.4×10^3 kg/m^3, which expand homogeneously before bubbling commences.

Group B Materials in the medium size and density ranges ($40\ \mu m < d_p < 500\ \mu m$, 4×10^3 kg/m^3 $> \rho_s >$ 1.4×10^3 kg/m^3) which bubble at or only slightly above U_{m_f}.

Group C Powders which exhibit any cohesive properties and are difficult to fluidise. Particles subject to strong electrostatic charging are said to belong to this group.

Group D Very large and/or dense particles in which bubbles rise more slowly than the interstitial gas.

It is doubtful if Group C and possibly Group D materials can be considered to behave as true fluidised beds. Certainly they are of little interest as regards flow and heat transfer performance because of their poor particle mobility.

The division between groups A and B is in terms of bubbling at or near U_{m_f} and Geldart gives an empirical criterion for minimum bubbling velocity:

$$U_{m_b} = 100\ d_{s_v}$$

The constant 100 is not dimensionless and has units of seconds^{-1}. It is claimed that the effect of changes of gas viscosity and density will be to alter the magnitude of the constant, but this has not yet been verified experimentally. This criterion clearly has no theoretical

justification, but appears to correlate the published data as well as any other, and has the advantage of simplicity.

Most published work on bubble growth within the bed has been conducted on deeper beds than have been of interest in the present work. It is evident from visual observation that bubbling patterns in very shallow beds are much different to those in deeper beds. The even and regular bubbling evident at bed depths up to about 20-30 mm gives way to a random less uniform pattern. It is probable that this coincides with the onset of bubble coalescence within the bed.

It is generally accepted that bubbles grow by coalescence and expansion as they rise up the bed. GELDART[23] has shown from measurements of bubbles bursting at the bed surface that diameter increases linearly with bed depth and also with excess gas velocity. Several authors [24,25,26] have suggested that bubble size increases with particle size, but GELDART[23] has shown by comparisons at $U_f - U_{m_f}$ rather than U_f/U_{m_f} that there is actually little change. Similarly, he has suggested that wide and narrow cuts of similar mean particle size show little difference in bubbling pattern. Other workers[22,28] may have been mislead in this respect by choosing a non-representative mean particle diameter in the case of wide size range material. GELDART[23] has also shown that bed expansion ratio h/h_{m_f} decreases with particle size and bed depth but again that particle size distribution has little effect. The foregoing observations apply to beds of Group B powders at bed depths between 50 and 300 mm.

It is well accepted that bubbles are the main vehicle for gross particle circulation in a bubbling bed, although in particulate fluidisation solids diffusion occurs also. Various authors[24,29,30] have observed that particles are carried upwards by the bubble wake and move downwards elsewhere. In small deep beds the particle motion is predominantly upwards in the centre and downwards at the walls, but

in larger beds areas remote from the walls in which substantial downflow occurs are apparent. It has been suggested by TOOMEY AND JOHNSTONE[31], and later DAVIDSON and HARRISON[32] that, in a bubbling bed, the particulate phase is at the minimum fluidising condition and that all the excess gas flow passes through the bed as bubbles. This is referred to as the 'two phase theory' of fluidisation and it is supported by experimental findings[33]. Studies of single bubbles passing through incipiently fluidised beds have confirmed this and it is probable that the theory is a reasonable overall model of the behaviour of freely bubbling beds also. However it is likely that in a violently bubbling bed, the particulate phase comprises local areas of greater or lesser aeration due to bubbling passage; though the overall dense phase voidage still remains at U_{m_f}. Such behaviour would have a profound effect upon the flow properties, but its existence could not easily be confirmed experimentally in a two dimensional bed.

A phenomenon which occurs in tall narrow beds is "slugging". This is also familiar in gas/liquid columns, and occurs when bubbles grow to a size equal to the column diameter. The slugs of gas so formed rise up the bed at regular intervals and particles rain down around their periphery. Slugs are of little importance in shallow bed work, but are likely to be seriously detrimental in vertical fluidised transport. According to ZENZ and OTHMER[7] and KADLEC[39] slug flow is common in tubes up to 50 mm diameter, but the author has frequently observed slugging in columns of three times that size.

Theoretical treatment of fluidised bed slugging is possible using equations developed for liquid slug flow. However STEWART[40] has developed a correlation to predict whether slugging is likely in columns of greater than unit aspect ratio. Further information, and a review of published data on slugging is presented by HOVMAND and DAVIDSON[40A].

Many workers have studied the rise of single bubbles, and of these, the theoretical analysis due to DAVIDSON[34] gives perhaps the best understanding and agreement with experience[35]; though JACKSON[36] and MURRAY[37] have presented other treatments. Davidson found that, for bubbles which rose more slowly than the interstitial gas (as usually found in large particles), the gas passed up through the bubble but became circulatory around its horizontal diameter. Thus an annulus of gas rises with the bubble. In fine particle systems the bubbles rise faster than the interstitial gas, and gas flows upward through the bubble, but downwards around the outside and in again at the base. Thus solids are carried upward in the bubble wake. It is well established in the literature that the rise velocity of a single bubble is given by an expression due to DAVIES and TAYLOR[38] for bubble rise in an inviscid liquid. This is of the form:

$$U_b = k(g\, d_b)^{\frac{1}{2}}$$

where $0.57 < k < 0.85$ in fluidised beds. Clearly this can only be expected to yield approximate results, especially in freely bubbling beds.

Though studies of single bubbles are useful, their existence is rather artificial. The bubbling characteristics of a real system are complicated by bubble interaction and local departures[77] from idealised behaviour.

2.4 Segregation

According to RICHARDSON[1], segregation - that is settling out of the larger particles present in a bed, is more likely in liquid fluidised systems than in bubbling gas fluidised beds. Nonetheless, segregation can be a serious problem in gas fluidised systems comprising a wide size-range of particles. When segregation does occur in gas fluidisation it is usual for the segregated particles to

settle out completely and form a stagnant layer on top of the distributor. In liquid systems it is often possible for the separated layers both to remain fluidised, but with the lower, larger size layer at reduced voidage - a less deleterious condition.

In studying the effects of segregation, WEN and YU[4] reported that segregation is likely in a two component mixture when the ratio of the minimum fluidising velocity of the components is greater than two. RICHARDSON[1] and JOTTRAND suggest that segregation is less likely at low voidage. These and other fairly self evident conclusions have been drawn by other workers and there is little more published data for gas fluidised beds except that of BOLAND[42].

His conclusions are useful and may be summarised thus:

1. Bubbling beds give good mixing as long as all constituent particles will fluidise together.

2. The maximum possible segregation depends upon the standard deviation of the initial mixture. Segregation is negligible for a standard deviation below 50 μm.

3. The presence of segregation can be detected from the curve of pressure drop against fluidising velocity. For increasing superficial velocity the usually flat portion of the curve beyond U_{m_f} exhibits a series of waves. The 'valleys' correspond to dumping of particles of a certain size.

4. Segregation is promoted by vibration of the bed.

5. Segregation behaviour on defluidisation depends upon the rate of reduction of gas flowrate.

It is of note that the phenomenon of (3) above has been observed by the author even in very shallow beds. Boland presented a correlation for the range of gas velocities over which segregation is likely to occur.

Range of velocity over which segregation occurs. $= U_q - U_p = .0078$ (Std Deviation in μ m)$^{1.42}$

$U_p \simeq U_{m_f}$

2.5 Effects of Distributor, Immersed Surfaces and Vertical Walls

The effect of the distributor plate through which the fluidising gas is supplied is usually neglected in correlations for predicting bulk bed behaviour. However it is true to say that identical beds may, in practice, behave as completely different systems when fluidised by different types of distributor. The latter is particularly true of shallow beds, when the distributor clearly has a proportionately greater effect upon bed performance.

In shallow bed heat-transfer systems distributors are normally restricted to either porous media or pierced plates with closely pitched holes. Other distributor types, like bubble caps, slots, tuyeres or simple orifices, such as are used in deep bed reactors, cannot be used because sufficient lateral gas diffusion to give uniform fluidisation cannot occur until some distance above the plate. The latter condition would merely lead to spouting or channelling in a shallow bed. Besides giving local evenness of fluidisation, two other attributes are desirable of the distributor: it should provide substantially equal gas velocity to all areas of the bed, with the minimum pressure drop necessary to achieve that aim.

In deep beds a general criterion for even distribution over the bed area is that the plate pressure drop should be at least 0.4 of the bed pressure drop[43]. However HIBY[43A] has suggested the lower value of 0.15 for $U/U_{m_f} < 2$. Shallow beds however may be operated at much lower values: successful industrial installations in which the ratio is as low as 0.05 are reported[43]. However the value chosen depends upon many other factors, some of which are summarised by

WHITEHEAD[43], GREGORY[44] and ZUIDERWEG[45]. Clearly large beds will tend to greater unevenness than smaller ones, as will the existence of a solid feed at one point and a drain at another. Once solids build up or local defluidisation has occurred, the effect may 'snowball' quite rapidly due to preferential airflow in the areas not so affected. Generally systems which must operate near U_{m_f} are more susceptible to maldistribution effects. The magnitude of pressure drop and flow rate across pierced plates may be estimated roughly from orifice theory, but for porous materials either the manufacturer's data or a practical test are the normal means. Different samples of commercially available porous materials which are supposedly the same often exhibit considerable differences in permeability due to poor quality control: a further source of difficulty when designing large systems.

Evidence of the distance from the distributor over which its effects are felt is somewhat conflicting. MORSE and BALLOU[46] made tests on 'uniformity of fluidisation' with capacitance probes, and reported distributor effects up to 16 inches above the plate in deep beds, above which level no differences were apparent. Conversely GROHSE[47] noted different behaviour throughout deep beds. It is likely that the effect will depend upon the departure of the plate from homogeneous porosity and the effect this has upon bubble formation and initial growth near the plate.

The influence of obstructions in the bed depends upon their shape and orientation. Generally their presence is deleterious to uniformity and particle mobility. The effect is bubble coalescence around downward facing surfaces causing loss of contact with the dense phase; whereas upward facing surfaces become heaped with defluidised particles unless irrigated with additional gas. The published literature is

diverse in the reported effects of different types of obstructions, due to the pronounced influence of differing shapes and spacing. The latter is too involved to report in detail here, but is well covered by HARRISON and GRACE[48] who also cite the work of many other authors.

It is generally reported that particle packing density is reduced in proximity to the walls of a bed. BENENATI and BROSILOW[49] measured wall effects up to a distance of about 10 particle diameters in packed beds and YAGI and KUNII[50] reported disturbances of similar magnitude using a technique of "freezing" the bed with molten wax. However it is conjectural whether or not these findings are relevant to a bubbling bed. It can be visually observed that particle down-flow occurs at the wall, indicating that the wall layers are not so well fluidised as the body of the bed. This would suggest reduced particle separation, and therefore closer packing, in all layers except that immediately adjacent to the wall where the packing is reduced for geometrical reasons.

The only real conclusions which can be drawn concerning the effects of the containment and any internals in the bed is that any generalisations regarding their effect must be regarded with extreme caution. This is particularly so where the geometrical configuration or operating conditions of the equipment differ from those under which the observations were made.

2.6 Liquid Analogy for Fluidisation

The very name of fluidised beds suggests similarity with liquid behaviour and various attempts have been made to draw analogies between the two states. The chief exponents of this approach are Gelperin and Einstein of the USSR. Some of the analogies used are quite reasonable but are probably of more value in relation to liquid systems than bubbling gas fluidised beds.

As an introduction to the concept, EINSTEIN[51] and GELPERIN cite the applicability of Archimedes Law to fluidisation. Clearly this is only valid if the floating bodies are large enough to be unable to integrate with the particle arrangement in the bed.

Perhaps the commonest analogy is between fluidising velocity and temperature. The temperature in a liquid is a measure of the kinetic energy of the molecules (Brownian movement) but there is no evidence that the particle kinetic energy in a fluid bed increases in the same manner with fluidising velocity. Clearly some particles in a bubbling bed have high kinetic energy, but this is bubble oriented not random as for liquid molecules. The concept of an overall increase in kinetic energy with fluidising velocity is contrary to the two phase theory of fluidisation. Similarly, analogy is drawn between melting and boiling, and minimum fluidising and elutriation respectively. Again it is evident that there is little more than superficial similarity, particularly in real systems in which there is a particle size distribution.

The same argument may be applied to most comparisons between the two states: there is a superficial similarity in their behaviour but this is not substantiated by closer scrutiny. Certainly such analogy is of value in describing fluidisation to the layman, but perhaps has little quantitative usefulness.

2.7 Heat Transfer in Fluidised Beds

Immersed and wall heat transfer surfaces have been widely used for a number of years in fluidised reactors as a means of controlling reaction rates. However, it is only recently that the full potential of the excellent heat transfer performance attainable has been appreciated.

Two realistic models of bed to surface heat transfer have been proposed. The first, due to MICKLEY[52,53,54] and co-workers, considers pockets of gas and solids to approach the surface, reside for a certain small time and then recede again into the isothermal bed. BASKAKOV[55] has modified this theory by considering the geometry of a sphere contacting a surface.

The second model, proposed by BOTTERILL[56,57] and co-workers considered a single sphere surrounded by gas at the bulk bed temperature coming into contact with a surface. Botterill plotted isotherms for various particle residence times, and showed why good heat transfer performance is possible at low residence times. The model has since been improved to take account of particle properties, packing, and gas conductivity[58,59,60]. The Mickley and Fairbanks approach is adequate for small particles and long residence times; but in the more interesting and useful regime of short residence times the Botterill model is superior. An approach similar to Mickley and Fairbanks, but accounting for particle/surface contact by considering the probability that the particle will have a certain packing density near a surface has recently been proposed by KUBIE[60A]. This has been shown to give good predictions for heat transfer to a flat plate at both long and short residence times. The realisation of low particle residence times and heat transfer performance of the same order as those achieved by Botterill with small immersed probes is not easy in a practical situation.

Any immersed surfaces tend to reduce particle mobility, cause local defluidisation, or promote shielding by a gas boundary layer; all of which are prejudicial to good particle/surface contact at low residence times. Large round horizontal tubes - the easiest commercially usable arrangement - are particularly bad in this respect, especially when spaced closely together in the bed. (A correlation for heat transfer to an immersed tube due to VREEDENBURG[61] is available, but is of limited accuracy). Contrary to liquid systems, the situation is not improved by flowing the solids past transverse tube arrays[62]. Thin vertical surfaces presenting minimum projected area normal to the gas flow are better; and excellent results are possible using heavily finned small diameter tubes. With such arrangements the solids motion and bubble growth patterns depart radically from those in the unconstrained bed. Very effective particle/surface contact is possible, particularly when the surfaces are placed close to the distributor[64,66].

The first published finned tube results (PETRIE et al[63]) were not particularly encouraging. However, recent work by ATKINSON[64], and SINGH and WOOTEN[65], following some preliminary tests by the author[66], have enabled operating conditions nearer the optimum to be established. With such configurations, new concepts of compact, high efficiency, low pressure drop heat exchange systems are possible. This area is currently the subject of intense interest and industrial development potential (see below).

3. FLOW BEHAVIOUR OF FLUIDISED BEDS

3.1 Introduction

Fluidisation has been widely used in chemical engineering for over 30 years and the first substantial work[67] on flow behaviour was published in 1949. Yet it is true to say that there is still no thorough understanding of the mechanism by which fluid beds flow. Simplified models

have been developed, but in spite of considerable mathematical complexity in some cases, none is really adequate. Other workers have produced correlations for behaviour derived from small scale experiments, but again none of these is really useful in giving quantitative predictions in real flowing bed situations.

The foregoing is not intended to imply criticism; for the difficulties, both theoretical and practical, are considerable. In particular it is extremely difficult to make quantitative measurements of flow behaviour, particularly with small scale apparatus. A further point is that it is fruitless to attempt to classify the flow behaviour of the full spectrum of fluidisation by one set of criteria. Even within the bounds of gas fluidisation, work has been executed in such widely varying conditions that direct comparisons are often impossible. In fact in many cases it is surprising that the results from such clearly differing systems and experimental techniques are so qualitatively similar.

The literature on flow behaviour is examined here in two sections: the first dealing with small scale viscometric studies, and the second with the more limited information on transport.

3.2 Small Scale Viscometer Studies

The first reported work on fluid bed viscosity, together with other properties, is due to MATHESON et al[67]. They used a Stormer (falling weight) rotational viscometer with a paddle shaped rotor of 1.5 in. length x .75 inch width. This was mounted symmetrically in beds of only 1 inch diameter x c. 2.5 in. deep, and rotated at 200 r.p.m. The foregoing clearly bears little resemblance to a large freely fluidised bed; but nevertheless some of their findings established a basic trend which has been confirmed in principle by most subsequent experiments, including the present work.

The results obtained are qualitative; that is, no calibration of their instrument was possible. (Other authors have since tried to ascribe quantitative values to their data: which attempts have no justification). Also, the "viscosities" given are point values, rather than apparent viscosities taken from the slopes of stress/shear rate curves: hence they take no account of any Non-Newtonian behaviour. The work showed that the "viscosity" of the bed reduces markedly with gas velocity just above U_{m_f}, and then tends to stabilise to a fairly constant value at higher air flow rates. The break-point of the curve was found to be sharply defined with small particle sizes but more gradual with large ones. However if their results are replotted as μ/μ_{min} against U_f/U_{m_f}, it can be shown that the curves are very similar for all particle sizes.

They also reported that the "viscosity" increased with both particle size and particle density for narrow size ranges. The "viscosity" was found to be greater for spherical material than for particles of angular shape. This was attributed to dense-packing in the case of the spheres, but the differences were quite small and may have been due to differences in effective diameter of the two particle types. In this context it is always difficult to be sure that one is comparing like with like. It is usually suggested that the surface mean diameter should be used in comparing fluidising properties of irregular particles; but this may not always give adequate comparison, and is sometimes difficult to determine accurately.

Matheson et. al. also presented graphs showing that the "viscosity" of wide size range cracking catalyst was lower than that for narrow cuts, and that the addition of a small proportion of fines produced considerable reduction in viscosity. However GELDART[68] has recently shown that the above results are explained by changes in the surface mean size of the

material. He replotted their data on this basis and found that the wide and narrow cut results fell on the same curve. It is interesting to note that shortly after the publication of Mathesons' results a theory was developed by TRAWINSKI[69], based on their findings, to explain the lower viscosity of wide size mixtures. This considered the fines to form a mono-layer around the large particles and thus act as a lubricant. Trawinski suggested that the ideal two component mixture would be such that all large particles were completely covered by a single layer of small ones. However, such predictions are not borne out in practice, probably because such a two component mixture would not fluidise in the manner envisaged.

It was further suggested by Matheson that fluid bed viscosity should be a function of the volume in which individual particles are able to move; which parameter depends upon the bed expansion without bubbling. They plotted "viscosity" versus bed expansion at U_{m_f} over particle specific gravity, and found that data for several materials correlated fairly well. Some of the scatter in the results could be explained by difficulty in determining bed expansion at U_{m_f} accurately, but subject to this latter limitation the correlation may be quite useful.

Photographs were also shown illustrating the rise of bubbles in tall narrow columns of fluidised solids and liquids. Comparison was drawn between the even, small bubbles evident in columns of 45 μm catalyst and alcohol, and slugging behaviour in the case of 150 μm catalyst and a viscous mineral oil. The analogy was not pursued very far, but could be useful in studying fluidised upflow and downflow in pipes.

Similar apparatus to that of Matheson et al was used by KRAMERS[70], but differed in using a 'dumb-bell' type of rotor in lieu of a paddle,

and was somewhat larger. The bed was 86 mm diameter x c. 180mm deep and the vertical position of the rotor was adjustable. A number of materials were used, but the results presented deal only with two cuts of river sand of 105-150 μm and 150-210 μm. A maximum rotor speed of 30 rpm was used for all tests, and as with the previous work, this means that the true shear rate would not be constant under Non-Newtonian conditions.

For this reason the results presented of shear force versus fluidising velocity could be misleading. However the latter show that the flow resistance increases with distance from the distributor; a feature which has been confirmed in the present work. The curves at all bed depths are of similar shape to those of Matheson, and become asymptotic to one another as the fluidising velocity is reduced. The curves differ from Matheson's in that the resistance rises with fluidising velocity instead of reaching a terminal value at high fluidising velocities. The coarser material exhibited about 25% greater flow resistance than the fine.

Curves of shear stress versus rotor speed are also presented and show shear-thinning behaviour, especially at low fluidising velocity. Here again though, difficulty in interpretation arises because rotor speed cannot be taken as directly proportional to shear rate.

DIEKMAN and FORSYTHE[71] also carried out viscometer tests using a Brookfield instrument, with the object of correlating viscometric data with deaeration in aerated vertical transport lines. The material used was 30-150 μm cracking catalyst and this was saturated with gaseous ammonia before use; a treatment said to reduce electrostatic charging.

The rotor was a hollow mesh cylinder of 2.3 in diameter and was placed at an unspecified height in a bed of 4 in diameter x 8 in deep. Again no calibration of the instrument was possible.

The method used was to plot viscosity against settling time and obtain a "fluidity index". This was shown to bear some relation to flow behaviour in commercial transport units, although this was not expressed quantitatively. It was further inferred that flow quality improved with a reduction in particle size. A curve was also presented of viscosity against fluidising velocity and changes in surface appearance of the bed ascribed to different parts of the curve. The behaviour exhibited was similar to that observed by previous workers. The de-aeration work is not of direct interest in the present study, in which the materials used settle almost instantaneously. Also, the use of an unmodified Brookfield viscometer in even gently bubbling beds gives rise to undesirable disturbances of the rotor by bubble action.

A different experimental approach was employed by PETERS and SCHMIDT.[72] They used a falling ball method in a column of sand 40 mm diameter x 600 mm long, fluidised with air. They first calibrated their apparatus with suitable liquids and then measured the Archimedes buoyancy forces in fluidised beds. This was claimed to make possible quantitative assessment of fluid bed viscosity. There seems to be little justification for this, since the tube wall effects would probably be quite different in the two cases, and Non-Newtonian materials are not amenable to the simple Stokes' Law treatment used for Newtonian liquids[73]. The change of bed viscosity with vertical location would cause further difficulty in interpreting the results. It would also appear that the bubbling of the bed may prevent the ball falling concentrically.

In spite of these difficulties, the results presented of viscosity against fluidising velocity for coarse and fine material show qualitative similarity to those of Matheson et al[67]. However it must be concluded that the falling sphere viscometer is of limited value in bubbling fluidised bed work.

FUKUKAWA and OHMAE[74] studied a number of bed properties including viscosity. The apparatus used was similar to that of Matheson et al[67] but somewhat larger. A rotor speed of 113 rpm was used and the instrument calibrated in liquids. Such a calibration has no theoretical justification and again the results must be considered qualitative. The material used was poly vinyl acetate spheres of diameters between 277 and 755 μm.

The shear curves obtained were not presented graphically, but were stated to be shear thickening - in contrast to the observations of previous workers. However, the true shear rate at the rotor surface cannot be estimated accurately for the type of rotor used. Results were also obtained of the variation of viscosity with fluidising velocity. These were said to be similar to those of Matheson[67] and Diekman[71] but were presented graphically in a manner which precludes direct comparison.

It was suggested that bed viscosity is proportional to the free volume within the bed, and that for particulate fluidisation this is equal to the volume expansion over that at U_{m_f}.

$$\text{ie} \quad \mu = K V_{m_f}/(V-V_{m_f})$$

This follows similar reasoning to that of Matheson[67] and gives good agreement with experimental data. The value of K appears to increase slightly with particle size. However, it is difficult to judge if this approach would be of value in the presence of Non-Newtonian behaviour.

Further work using a Stormer viscometer was carried out by SHUSTER and HAAS[75]. They postulated that three regions of flow behaviour should be evident as the fluidising velocity is increased from zero. Firstly the viscosity will fall rapidly near U_{m_f} as particles are freed from the packed state. Secondly it will increase again as particle circulation commences, and thirdly another reduction of viscosity will be apparent as the bed density is reduced at higher air rates. This is a reasonable

explanation and accords generally with observed tests, but does not take account of change in local behaviour which can markedly modify the relative importance of the phenomena described.

The apparatus used was a Stormer viscometer with a paddle rotor, whose position was adjustable both radially and vertically within a 5-3/4 in diameter x 5.6 in deep bed. Beds of glass beads sieved into narrow cuts between 76 and 1020 μm were fluidised over mesh screen and porous metal distributors. Measurements indicated substantially Newtonian behaviour under all conditions and results were said to be highly reproducible. The latter is difficult to believe in the light of the current work, especially as no precautions were taken against electrostatics or moisture variations.

Tests were carried out at rotor positions of 1, 2 and 3 inches from the distributor, and results presented as viscosity versus u_f. With the porous plate the viscosity was found to increase with rotor height. This was less marked with the mesh screen, in that the bed was more viscous near the plate. The viscosity was everywhere greater with the screen distributor. These findings were explained in terms of a low, even bubbling behaviour with the porous distributor. This seems reasonable, but it is surprising that such a fine screen should cause so marked a change in behaviour. Other effects were also reported due to enveloping of the rotor completely by bubbles, but these are discounted as being "apparatus effects" rather than changes in behaviour.

Changes of radial position of the rotor produced no effect in the case of the porous plate distributor, but with the screen the central area of the bed was noted to be less viscous due to preferential airflow.

Tests on mixtures of different size particles led to the overall conclusion that the viscosities of the mixtures were higher than those of the fine cuts. However the curves presented are rather ill defined and comparisons were made at equal fluidising velocities for mixtures of

different mean size. In the highly fluidised regions, mixtures were found to obey Kendahl's rule, viz:

$$\log \mu_{mix} = x_a \log \mu_a + x_b \log \mu_b$$

where a and b are the constituents and x is the volume fraction present.

This work was the first to indicate the importance of the distributor in its effect upon bed flow behaviour.

FA-KEH LIU and ORR[76] used a Brookfield viscometer for investigating changes of viscosity with vertical position in a 1.75 inch diameter bed of up to 18.5 inches depth. They used a hollow cylindrical rotor element, thus measuring pure shear as opposed to form drag, but again made unjustified claims regarding calibration with liquids and quantitative shear rate measurements. Also, it appears from the diagram and description of their apparatus that gross disturbances of the rotor would be inevitable in a bubbling bed, although no mention is made of this.

They reported three regions of behaviour, corresponding to the lower, middle and upper thirds of the bed height. The behaviour in the lower third was found to accord generally with that reported by previous workers. This similarity encompassed the effect of increasing airflow, increasing particle size and increasing bed height. In the middle third of the bed, the viscosity was found to be relatively insensitive to airflow rate, with a gradual increase with increasing fluidising velocity. In the upper third, the viscosity increased markedly with fluidising velocity to a maximum value, after which it fell away again.

At first sight the last mentioned condition suggests that near the top of the bed the viscosity of the semi and incipiently fluidised bed is less than the fully fluidised bed. This would also apply, to a lesser degree, to the middle section of the bed. However, whilst no details are given of the size range of the particles used, it is thought that these phenomena were due to segregation. Segregation is known to have a marked

influence on flow behaviour and some would be almost inevitable in such a deep bed near U_{mf} even with quite a closely sized material. Also, in a bed of these proportions U_f would certainly increase slightly towards the top, for a given gas flow, due to gas expansion. With this in mind, the following explanation is suggested. At the lowest gas flow the smallest particles migrate towards the top so that, at equilibrium, the lower part of the bed is defluidised, whereas the upper sections are quite mobile, giving low viscosity. As the air rate is increased, segregation progressively diminishes so that the lower part of the bed fluidises and so the viscosity then reduces. Conversely in the upper part of the bed, which has already fluidised, the mean particle size has increased and bubbling becomes more violent, so increasing the viscosity in that region. Further support is given to the foregoing hypothesis by the shear diagrams obtained, although as pointed out, there may be misleading due to invalid assumptions regarding true shear rate.

Perhaps the most comprehensive viscometric study to date is that of SCHÜGERL, who has reported work in this field since 1959. An extensive account of his work, and a review of other findings is given in reference 77.

The apparatus used comprises a rotational viscometer with hollow cylindrical rotors of varying diameter and 100 to 300 mm in length. These were mounted concentrically within another cylinder suspended in the bed. Full details of the apparatus and calibration techniques used are reported by SCHÜGERL, MERZ and FETTING[78]. Unlike any previous work, the calibration used can be said to give quantitative values of the true viscosity at the surface of the rotor, provided certain assumptions are satisfied. The only drawbacks are that the relatively small internal rotor diameter and shearing field between rotor and cup would be likely to cause changes in local fluidisation pattern and inhibit bubble growth.

Also the length of the rotor would preclude both local measurements near the distributor, and a detailed investigation of the vertical viscosity profile within the bed.

Schügerl suggests that fluid bed viscosity is due to internal friction between the particles. The particle forces said to be responsible for this are the static inter-particle forces (electrostatic, van der Waals, and capillary forces due to moisture) together with dynamic forces due to particle agitation.

It would appear that, in addition to the latter, viscous forces within the fluidising medium are also important when the local particle velocity due to shear approaches or exceeds the fluidising intersticial velocity. It is claimed by Schügerl and others, that shear rates which cause the latter condition should not be used, because it does not represent the true bed viscosity. This is perhaps true as far as dense phase viscosity is concerned, but the author feels that the behaviour at such high shear rates still represent a definite bed property in the context of flow through fluidised conduit. Clearly, high shear rates will be used in commercial transport systems, and are therefore of greater interest than dense phase behaviour as the shear rate tends to zero.

According to Schügerl, the flow equation of a fluidised system may be represented by an expression of the form:-

$$\text{Shear rate } \frac{du}{dy} = f(\tau) = A \sinh (B\tau)$$

where A and B are constants such that:

$$A = \alpha_1 \exp (- B e_1)$$

and α_1, e_1 and B depend upon size and type of material being fluidised and the fluidising velocity. With further simplifying assumptions it was suggested that :

$$\mu_o \simeq 4.7 \quad \frac{\text{dyne. sec}}{\text{cm}^2} \quad \text{for} \quad U_f \gg U_{m_f}$$

$$d_p > 100\ \mu m$$

$$\mu_o \simeq 117\, d^{1.5} \quad \frac{\text{dyne sec.}}{\text{cm}^2} \quad \text{for } U_f \gg U_{m_f}$$

$$dp < 100\ \mu m$$

Schügerl suggests that the "intrinsic viscosity" of a fluidised bed can be explained by the theory of rate processes due to EYRING[79]. This yields an expression similar to that given above in which the constants A and B are again related to particle properties and packing density. The treatment lends further support to the hypothesis that the bed viscosity is proportional to the free volume of the particle and also its kinetic energy, but does not fit experimental data particularly well.

Whilst it is true that the shear diagrams of fluid beds in some cases may be approximated by sinh functions of the type indicated, other algebraic functions could also be fitted with equal accuracy. There are many situations, cited by Schügerl, in which marked deviations from smooth functions are evident. Thus although the rate theory concept may be of some value in understanding the mechanism of fluidised flow, such an approach is as yet not capable of predicting flow behaviour accurately in a design situation.

The general conclusions from the experimental work of Schügerl follow those of previous workers regarding the effects of particle size, density and fluidising velocity. No quantitative measurements were made of the influence of bed height, rotor position or air distribution.

From studies of the flow equations of various materials, Schügerl suggests that only at shear rates approaching zero can a shear independent viscosity be defined. Above a limiting shear rate, the bed structure is changed causing a change in flow behaviour. Such changes of structure were found to be very small, and could not be detected by X-ray photography.

Study was made of incipiently fluidised beds, and these showed marked departure from the proposed Sinh function approximation. Behaviour similar

to Bingham plastics was observed in that the materials exhibited a yield stress. After this point was reached however the stress was shown to decrease rapidly at very low shear rates, followed by a fairly linear increase as shear rate was increased further. This yielding behaviour was found to disappear at a fludising velocity near U_{m_f}, as might be expected. The behaviour in this region during repeated tests was found to be dependent upon recovery time from the previous run. The latter was in some instances several hours, and could have been due to segregation effects.

Two other flow irregularities are cited by Schügerl. The first is a reduction of shear stress at a certain shear rate, due to separation of the dense phase from contact with the rotor caused by centrifugal force. The second is a sudden increase of shear stress with shear rate, said to be brought about by an increase in packing density due to shear. However this increase could alternatively have been due to a sudden change in true shear rate at the rotor surface. The value of the critical shear stress at which the above mentioned breakaways occur is given as depending upon the energy of the particles present relative to their mobility.

Viscometric data contrary to that of any previous or subsequent work was presented by LEEDEN and BOUWHUIS[80]. They suggested that the concept of viscosity was inapplicable to particulate fluidised beds, and that the flow behaviour is described by a maximum shearing stress or angle of friction. Their experiments were carried out in a particulate bed of 300 mm depth and variable radius. A Brookfield viscometer with hollow cylindrical rotors of varying lengths was used. The fluidising velocity used is not stated but the bed expansion was 1.07. The material was aluminium silicate of approximately 60 μm mean size.

The following conclusions were drawn:

1. Shearing stress at rotor independent of shearing rate.

2. Shearing stress at rotor independent of vertical position

3. " " " " " " rotor surface roughness

4. " " " " " " bed diameter

5. " " " " is the same for fluidisation with air and water

The above findings are inexplicable in the light of other work. The only conclusion that can be drawn is that severe agglomeration was occurring and that rotor movement resulted from sliding friction at its surface, with the bulk of the bed remaining stationary. In view of the small particle size this is possible for the air fluidised case, but seems unlikely in the water fluidised tests. A theoretical treatment of this form based on a combination of Bingham's equation and soil mechanics theory has been proposed by MARTYUSHIN and KHARAKOZ[81] for the flow of an incipiently fluidised bed. They did not verify this model experimentally however, and it is not borne out by Schügerl's work with such systems.

Experiments with liquid fluidised beds, using a high viscosity oil as the fluidising medium and a falling sphere method were reported by PRUDHOE and WHITMORE[82]. The found the behaviour to be described by the equation

$$\text{fluid bed viscosity, } \mu = \frac{\mu_f}{1 - 2.5c}$$

where c = vol. concentration of solids.

The work will not be discussed further since the system clearly has little resemblance to a bubbling bed, but it is interesting to note that the behaviour of such a bed is that of a fully Newtonian liquid.

HAGYARD and SACERDOTE[83] examined the behaviour of air fluidised shellac spheres between 305 and 125 μm diameter using a torsional pendulum viscometer. This instrument is not capable of measuring non-Newtonian behaviour and used a solid cylindrical bob which would undoubtedly cause preferential airflow past its surface. The results presented all show a very large degree of scatter, and although smooth

curves have been drawn, in many cases these appear to bear little relation to the observed behaviour. The well established curve of viscosity versus fluidising velocity is evident, but the data is too scattered to fully substantiate the claim that the minimum viscosity is independent of particle size. Data was also presented for binary particle mixtures, but here again the results presented are of insufficient accuracy for firm conclusions to be drawn.

It must be concluded from the results presented that the type of viscometer used is unsuitable for accurate measurements in fluidised systems.

Following Furukawa and Ohmae's work on gas fluidised viscosity, HETZLER and WILLIAMS[84] extended their free volume concept in an analogy of liquid fluidisation with glass-forming liquids. They obtained a correlation for μ_o for liquid systems and showed that this also gave good agreement with Furkawa and Ohmae's results for air fluidised plastic particles.

The correlation takes the form:

$$\mu_o = 0.667\,\mu_f\, v_f^{4/3} \left\{ \sqrt{\rho_s}\; U_{m_f}/d_p \epsilon \right\} \exp\,(3.75/\epsilon)$$

The viscosity at zero shear rate is perhaps of limited usefulness in a non-Newtonian bubbling bed, and the correlation has been verified only for non-bubbling systems. Nevertheless it lends further support to the hypothesis that the viscosity of the dense phase may be a function of the particle free volume.

A different approach to viscosity measurement was used by GRACE[85]. Arguing that the presence of any shearing surface in the bed will disturb its natural behaviour, he studied the wake angles of bubbles observed by various workers and calculated values of viscosity based on comparison with bubble wakes in liquids. Comparisons were made at equal values of a bubble Reynolds number, defined as:

$$R_e = \underbrace{\frac{d_e u_b \rho}{\mu}}_{\text{liquid}} = \underbrace{\frac{d_e u_b \rho_s (1 - \epsilon_{m_f})}{\mu}}_{\text{fluid bed}}$$

$$\text{where } d_e = \left[\frac{6(\text{Vol. of bubble})}{\pi}\right]^{1/3}$$

Though this is a justifiable comparison, the only available liquid data in the appropriate Reynolds number region is subject to considerable scatter. Also the method involves the measurement of quantities which are difficult to determine accurately. The results compare quite well with similar calculations made by STEWART[35] and viscometer determinations of SCHÜGERL[77], but it is not clear whether the comparisons were made in strictly similar fluidising conditions. A drawback of the method is that no estimation of non-Newtonian behaviour is possible.

3.3 General Conclusions from Viscometric Studies

Most of the work reported has established similar qualitative trends regarding the effects of fluidising velocity, particle size, particle density and bed depth. It is surprising that results obtained from viscometers measuring form drag or displacement are so similar in a fluidised system to those measuring pure shear. Some of the anomalies reported can now be explained in the light of improved knowledge of general bed behaviour. There appears to be no clear indication of the way in which bubbles affect the viscosity. The influence of bubbles seems to depend strongly on the size and number of bubbles and the extent to which bubble gas is exchanged with the surrounding dense phase.

In view of the reported non-Newtonian behaviour, any viscometer which cannot measure non-Newtonian flows is of little value in a fluidised system. Similarly, a viscometer which measures properties over a considerable bed height is of limited usefulness because of the dependence of viscosity with vertical position. Criticism has been made that immersed shearing surfaces disturb the fluidisation pattern.

However such disturbances also occur at the walls of a flowing bed, so the results from immersed shear surfaces should be more relevant to real transport situations than those obtained by other methods. The same is true of disturbances to the normal bed structure brought about by rapid shearing.

A particularly important discovery is that of Schügerl regarding the yield stress/relaxation behaviour of an incipiently fluidised bed. This clearly shows the lack of hydrodynamic similarity between dense phase behaviour in vigorously bubbling beds, and incipient beds with artificially introduced single bubbles. This disparity casts serious doubt on the relevance of single bubble studies to real bubbling beds.

None of the theoretical treatments proposed can adequately represent real bed behaviour in all circumstances. The best agreement is confined to non-bubbling, low shear situations. It is regretable that no work has been carried out towards relating viscometric (or theoretical) results to any fluidised transport data.

3.4 Studies of Flowing Bed Systems

The study of flowing fluidised beds has received little attention compared with that of stationary bed shear behaviour. This is probably due to the relative complexity of the apparatus necessary.

Considerable work has however been carried out on fluidised bed efflux via nozzles, orifices[87-91] and pipes[92]. A review of much of this work is given by MASSIMILLA[93]. Dilute phase transport finds quite wide industrial application and has also been studied by a number of workers. A review of work on this mode of transport is given by WEN[94,95] et al and KUNII and LEVENSPIEL[8]. Hydraulic transport of particulate material in water has also been investigated by ELLIOTT and GLIDDON[96]. It is likely that some of the findings from such work will be helpful in explaining the behaviour of fluidised systems, but none is directly concerned with flow of material over a fluidising distributor.

Vertical fluidised transport has been studied little, although it is used in some industrial applications. No substantial published work is known to the author, although some equations governing aerated vertical flow are proposed by KUNII[8]. Segregation and slugging are likely to be problems in conventionally designed tall beds. Preferential aeration could probably be used to advantage, but the effect of such measures could only be determined by experiment. Vertical flow systems are to be the subject of future study, and would find wide application of uniform non-slugging flow could be achieved.

The first published work on horizontal fluidised channel flow was presented by SIEMES and HELLMER[97]. Their apparatus comprised a rectangular channel 2m long x 150 mm wide, whose inclination could be varied between 1 and 6°. Fluidising air was supplied to the porous distributor by a blower, and maintained at the surprisingly high relative humidity of 80-90%. Solids were fed from a hopper at rates of .08 to 4.0 kg/sec and the solids flow rate measured by timed weighing of the

of the efflux stream. The material used was sand of mean particle size 210 μm and minimum fluidising velocity .02 m/sec.

It was assumed that the flow of material was laminar and Newtonian under all conditions. The former condition was said to be satisfied at Reynolds numbers below 1300, although the reason for the choice of this value is not clear. Photographs taken at different flow rates exhibited surface velocity profiles close to parabolic, as would be expected for laminar flow. However, it seems unlikely in the light of previous work[77] that the flow would be fully Newtonian.

Two approaches were used in examining the results. These were firstly that the channel behaved as it would for liquid flow, with equal shear stress on all wetted surfaces; and secondly that there was no shear stress at the distributor. It was assumed that the flow obeyed the Navier-Stokes equation, and by comparing values of viscosity calculated using the two approaches it was inferred that slip was occurring at the distributor. However the calculations assume that bed viscosity is independent of depth. The latter is now thought to be unlikely, so that whilst slip may certainly occur in some conditions, the values of slip coefficient presented cannot be considered accurate. The results given suggest that the slip coefficient increases with flow velocity and channel inclination, but decreases with fluidising velocity. Results are also presented indicating the reduction of viscosity with increasing fluidising velocity, thus confirming the findings of viscometric studies. A quantitative comparison with viscometric data is also given but, as mentioned above, this is not really justified because of inaccurate viscometer calibrations.

An analogy between increasing fluidising velocity and increasing temperature in liquids in their effect upon viscosity was proposed by NĚUŽIL and TURCAJOVÁ.[98] They used an inclined channel of fluidised

corundum, but no further details of fluidising conditions or methods of measurement are given. The method used was to compare the parameters with their value at reference conditions as a means of non-dimensionalising the result. A correlation is presented which gives reasonable agreement with the experimental results and also with other published data. However no account is taken of the increase in viscosity which can occur at higher fluidising velocities.

Further work using an inclined channel has been carried out by QUASSIM[99]. He has derived equations for the flow of a non-Newtonian fluid in a duct, but some of the assumptions used introduce lack of generality. Even so, the mathematics is relatively complicated. A model is also proposed for the viscosity of a bubbling bed in terms of dense phase viscosity and bubble voidage. In spite of several simplifying assumptions, the use of the model involves solving eight equations in eight unknowns, not all of which are readily measurable.

Some of the experimental findings are somewhat puzzling. Flow curves are presented at increments of fluidising velocity and appear to range randomly between shear thinning and shear thickening behaviour. Also, it is difficult to appreciate how shear rates of the order of 10^4 sec^{-1} were possible. Several other anomalies of behaviour are reported and it is suspected that practical problems with the apparatus may have caused some difficulty. Neither of the models presented can be said to accurately represent the behaviour of the bed.

Work on channel flow has recently been carried out by BOTTERILL and co-workers, following on from earlier studies of flow past heat transfer surfaces in fluidised beds mentioned above (section 2.7). The earliest work[100] concerned flow past arrays of tubes and helped to explain certain peculiarities previously measured in heat transfer experiments. The pressure loss across a bank of tubes was found to

vary with spacing and geometrical configuration. These and later experiments (BOTTERILL and VAN DER KOLK[101]) were carried out in a horizontal continuous loop duct in which solids circulation was achieved by a variable speed paddle arrangement. Tests were carried out using various sizes of sand and alumina in channels up to .7 ft^2 cross section at flow velocities up to 1.3 ft/sec. The latter were measured by timing a float over a given distance; a method which could give misleading results. A further limitation is that the measurements are taken under accelerating flow; probably not significant in itself, but the head loss so caused could give rise to uneven fluidisation along the length of the test section.

Initial experiments with sand suggested Bingham plastic behaviour, especially at low fluidising velocities, although no measurements were taken at very low shear rates. A minimum was observed in a plot of plastic viscosity versus fluidising velocity at about 3 U_{m_f}.

Later tests with alumina (Bauxilite) showed a range of behaviour from Bingham plastic through shear thinning to shear thickening. The two latter modes were attributed respectively to increased dense phase voidage and slip at the distributor plate. The latter phenomena also explain increases in viscosity with bed height and channel width, although there were some inconsistencies in the results. It is possible that some anomalies could have resulted from the use of the equivalent diameter concept for non-Newtonian channel flow.

The above results were compared with early results from this work (ref 102; appendix III) and showed some similar qualitative trends. No quantitative likeness was apparent however: this was probably due to inaccurate calibration of the viscometer.

Further tests in the same apparatus were made using a device for measuring local flow velocity, to enable velocity profiles to be constructed. These, and measurements of shear stress on the vertical

walls of the channel are reported by BOTTERILL and BESSANT[103]. The velocity profiles plotted suggest a change from liquid-like flow to semi-plug flow with slip at the distributor, with increasing fluidising velocity. However, no measurements were possible closer than 28 mm to the distributor.

The flow equation for the test conditions could be described adequately by a power law expression of the form,

$$\tau = k^1 \left(\frac{du}{dy}\right)^{n^1}$$

where τ = mean shear stress

$\frac{du}{dy}$ = mean shear rate

k^1, n^1 = constants

Values of k^1 and n^1 of 1.3 N/m^2 s^{-n} and 0.55 were appropriate to a channel of 140 mm wide x 118 mm deep. Using these values, velocity profiles calculated by the method of WHEELER and WISSLER[104] gave good agreement with measured profiles under some conditions.

In a later paper, BOTTERILL and BESSANT[105] have compared wall shear stress measurements with those derived from flow head loss. It was found that, at high fluidising velocities, the flow approached a condition corresponding to zero shear stress at the distributor. Recent confirmation of this effect has been provided by tests using a very shallow inclined channel of variable width. With the assumption of no horizontal velocity profile it has been possible, using a modification of a technique due to SUZUKI and TANAKA[106], to estimate slip velocities at the distributor surface.

3.5 Conclusions from Flowing Bed Studies

The results obtained from flowing bed experiments are clearly more directly relevant to fluidised transport than are viscometric studies. The main drawback is the complexity and lack of flexibility of the apparatus required.

Further development in measurement techniques for some of the parameters involved is undoubtedly required. The work of Botterill and Bessant has been hampered by experimental difficulties, although some of these are consequent upon their apparatus not being originally designed for flow measurements.

With the present level of knowledge on fluidisation it appears that the non-Newtonian liquid analogy treatment of Botterill et al[102,105], based on macroscopic flow measurements is of more value than microscopic modelling techniques such as that of Quassim[99]. However, even the former approach is likely to involve considerable further study before it can be used to describe the whole range of conditions likely to be encountered in practical systems. It may therefore be preferable, in the short term, to devise correlations of flow behaviour similar to those available for liquid channel flow. Such methods give no real insight into the mechanisms of flow, but are useful for design purposes as long as their limitations regarding accuracy and generality of application are recognised. A difficulty with whatever technique is used is that experimental study is often of necessity carried out at much lower rates of shear than would be economical to use industrially. This is a serious limitation for highly non-Newtonian systems such as fluid beds.

4. ELECTROSTATIC CHARGING IN FLUIDISED BEDS

The presence of electrostatic charges in fluidised beds is known to alter the character of fluidisation. Generally the presence of electrostatic potential causes agglomeration, or at least restriction of movement, of particles within the bed. The effect, at a given superficial fluidising velocity, is therefore to cause loss of fluidisation, channelling of the fluidising gas and adherence of particles to the bed walls and immersed surfaces. Its effect is more serious in, but not confined to, systems of small, light particles. Several fluidised flow

studies[67,74,77,83,97] have taken arbitrarily chosen precautions against charging, but none has really examined their effectiveness or consistency.

Electrostatic charging is caused principally by friction as two surfaces are brought into contact, (HARPER[107]). In general, electric potentials are high and currents minute, so that leakage and dissipation of charges can occur easily even on relatively poor conductors. The highest potentials are usually generated by contact between different materials, but dissimilar faces of crystals of the same material can give rise rise to high charges also[107]. Electrostatic charging is prevalent in pneumatic conveying systems because of the high particle velocities, and is often a serious handicap to their performance.

Relatively little quantitative data is available on electrostatics even for a non-fluidised particle system, and it is difficult to predict what charges are likely to occur in a particular system, or what their effect will be. Generally, systems in a dry environment are most subject to charging as even minute amounts of surface moisture sometimes allow charges to leak away at least partially, if not completely. Consequently, very small changes in moisture level often exert a dramatic influence on behaviour.

A substantial experimental investigation of electrostatic charging in fluidised beds has been made by CIBOROWSKI and WLODARSKI[108], who detected potentials as high as 15 kV on an electrode immersed in beds of sand and other high dielectric materials. They reported that up to 30 minutes was necessary for the establishment of equilibrium charge levels; the latter depending upon the relative rate of generation and leakage of charge. Potential was found to vary directly with fluidising velocity and, surprisingly, to be little affected by change in particle size over a range from 300-750 μm. It was found that the potential in the bed reached a maximum, with reduction in air humidity, at a fluidising air moisture level between 0.2 and 1.0% w/w; after which further

reductions in moisture caused a reduction in potential. The humidity of the air surrounding the apparatus also had a marked effect upon the potential. Particle agglomeration and adherence to the bed walls was easily visible at the point of maximum potential. It was found that the measured minimum fluidising velocity increased in this region, but not in a manner that could be related to potential. Also, the latter effect was found to completely disappear, in the case of sand, above 80°C although changes in potential were still apparent. This would suggest that the presence of the moisture has other effects than merely acting as a vehicle for charge leakage. The change in fluidising velocity with moisture highlights the limitations of the various correlations for U_{m_f} - none of which take account of interparticle forces.

KISEL'NIKOV et al[109] found that the greatest potentials, with beds of about 140 mm depth, occurred at between .6 and .75 of the total height. They also showed that charge accumulated exponentially with time, although no values of the time constant are quoted.

KATZ[110] investigated means of reducing electrostatic charging in fluidised beds of glass beads and found that humidified fluidising gas was effective, but surface moisture then caused agglomeration of the particles. Treatment of the particle surface with conducting material was also found to cause agglomeration.

A detailed investigation of the influence of rising bubbles on charge generation was reported by GELDART[111] et al. It was found that the highest charges occurred around the bubble boundary, as might be expected in view of the increased particle agitation in that region. This study was carried out in a two dimensional bed at incipient fluidisation and it might be expected that different conditions would be extant in freely bubbling beds, particularly shallow beds.

By working at a range of fluidising air humidities, Geldart showed that charges are still generated at high humidity levels, but in the

latter condition are able to leak away by virtue of the reduced resistivity of the bed. The latter was found to fall from 1.8×10^{13} ohm cm. at zero relative humidity to less than 10^{12} ohm cm. at 90% R.H. Tests using conducting and insulating bed containment walls showed that though the former allowed leakage of charges local to the wall, there was little apparent effect upon the bulk of the bed. Increased charging was evident with larger particles and this was attributed to the larger frictional forces involved in their contacting.

Several methods of reducing electrostatic charging, or its effects, have been proposed. It has been shown by FORREST[112] that surface water films only have significant effect in decreasing the electrical resistance of hydrophilic materials such as glass, sand etc. and have little effect on materials such as polythene. However, according to Geldart a relative air humidity of 60-70% is sufficient to allow complete charge dissipation in some fluidised systems, although the generality of this is not known. Other conductive surface coatings are only effective if they do not restrict particle mobility for other reasons. Ionisation of the fluidising air by electrical discharge, and radioactive techniques, have been tried by LOEB[113] and others but seem to be of limited effectiveness and restricted in application.

Though it is desirable to earth any conducting parts of a fluidised bed environment for safety reasons, this will not necessarily influence the charges in the bulk of the bed. There are two reasons for this. Firstly, high potentials induced in non-conducting particles cannot dissipate because no leakage path is available. Secondly, it is quite possible for similar, but opposite, charges to be generated on different particles within the bed, so that they tend to agglomerate, yet do not give rise to any appreciable net potential (KUNKEL[140]).

An encouraging feature of electrostatic charging phenomena, from the point of view of combustion and heat transfer systems, is that the effects appear to be less serious at high temperatures. Ciborowski[108] et. al. reported reductions in potential over a temperature range of 20 — 108°C. Also, no evidence is to hand regarding difficulties due to charging in high temperature systems, whereas numerous troubles are reported with industrial and laboratory systems at ambient temperatures.

5. SOME NOTES ON INDUSTRIAL APPLICATIONS

The first commercially operational fluidised bed was a plant for gasification of powdered coal opened in Germany in 1926 following a patent granted to WINKLER[114] 1922. The next significant development was precipitated by the wartime requirement to convert light oils and kerosene to nigh octane aviation fuel for piston engined aircraft. The process involves splitting up of the higher hydrocarbons ("cracking") and the Thermofor Catalytic Cracking process utilising a fluidised alumina catalyst was developed in the USA. The significance of fluidisation of the catalyst was in the large exposed surface area allowing higher reaction rates, and the fact that continuous replacement of spent catalyst using a flowing system was possible. The latter feature was by no means without problems and spawned considerable research efforts on pneumatic and other modes of solids transport.

The catalytic cracking process lead to further widespread realisation of the potential of fluidisation in chemical engineering. The principal advantages, in addition to the aforementioned, are the excellent fluid-solid contact and heat transfer, and also the thermal uniformity and inertia which allows simplified control of reactions whose rate is temperature sensitive. The number and type of processes using fluidised reactors is now legion: the fluidised medium forming either the catalyst or one of the reactants. A concise, but comprehensive review of chemical

processes employing fluid beds is given by KUNII[8]. The special properties of the fluidised state have also been used to advantage in other fields such as drying of granular materials and plastic coating of small components. Substantial problems were encountered due to differences in behaviour between small pilot plants and the full size units; even today little is known about some phenomena in large scale devices. Some of the problems encountered, such as elutriation and segregation have since been turned to good effect in separation of materials of different size and density by fluidisation.

It was necessary in some reaction processes to provide immersed surfaces in the bed as a means of adding or extracting heat to regulate the reaction. It soon became apparent that extremely high heat transfer coefficients were possible between the bed particles and such surfaces, which discovery has lead to the conception of using fluidised beds as heat exchangers of high specific performance.

There has been interest in the UK for a number of years in large fluid bed boilers for steam raising for electrical power generation.[115] Pilot scale studies on coal combustion have been carried out by the National Coal Board culminating in a combustor of 23 kg/h capacity. Work has also been carried out by the Central Electricity Generating Board and the British Coal Utilisation Research Association. The Esso Company have investigated large scale oil burning units. The results of these investigations have been used in design studies of boilers of up to 660 MW capacity for power generation and other steam raising applications. No plants on this scale have been actually constructed at the time of writing however. In recent years this work has been somewhat overshadowed by concentration on nuclear steam raising systems, and also on so far abortive work on magneto hydrodynamics. However it is possible that with the current emphasis on energy conservation and the relatively slow progress of nuclear development that

fluidised coal combustion will again receive more attention.

The use of pressurised combustors enables the already compact fluidised boiler to be further reduced in size, and such systems are receiving attention in America. The degree of compactness attainable with pressurised boilers makes it possible to envisage the use of factory prefabricated boilers with sufficient output for power generation applications. The relatively low temperature operation of fluidised combustion is very favourable to life of the plant and in reducing internal fouling by combustion products. A further important feature is the low environmental pollution, particularly regarding nitrogen oxides.[144] It is possible to burn low grade and other unusual fuels whose use would not normally be possible or economic, and the removal of toxic sulphur oxides is possible. Some aspects of the technology of large scale combustion and boiler plant were presented in Ref. 115. Though the design studies presented illustrate the feasibility of fluidised boilers, advances in fluid bed technology mean that the designs are now outdated and further improvements are possible.

Some of these have been outlined by ELLIOTT[116], as have some of the problems - particularly that of control and turn-down. Because of the relatively narrow operating range of fluidised boilers, governed at the lower limit by inefficient combustion and at the upper by ash sintering, only small load changes can be catered for by changes in bed temperature. An attractive way[117] of overcoming this involves transporting, and possibly storing, large quantities of solids. The need for this facility was a major reason for undertaking the present programme of flow studies. A further problem with large scale combustion is fuel distribution - particularly in coal and oil burning systems. This is receiving attention but has yet to be solved in an entirely satisfactory manner.

The advantages of fluidised combustion mean that previously unattractive thermodynamic cycles may warrant reappraisal. Also because of the relatively soft powdery nature of fluid bed coal ash, directly

fired coal burning gas turbines are feasible[115,117].

Whilst it is not to be expected that large scale fluidised combustion and heat transfer systems can be developed overnight for industrial use, their intrinsic attractiveness relative to conventional systems is clear.

Perhaps of more immediate industrial interest are smaller scale applications of fluidised bed combustion and heat transfer. It has been satisfactorily demonstrated that gas, coal[118] and light oil[119] can be burnt in very shallow beds with excellent results and that heat can be efficiently extracted therefrom with extended surface heat exchangers[64-66]. ELLIOTT[120] and MOSS[121] have described applications, both tried and projected, involving small and medium scale combustion of gas and oil respectively. A particular advantage of shallow beds with finned heat exchangers is the combination of low pressure drop and high heat transfer coefficients attainable. The former is particularly important in small scale devices where the blower size must be minimised; and also in waste heat recovery applications, in which a high pressure drop can rarely be tolerated.

Small LP gas fired fluidised beds for heat treatment of metal components are now in commercial production[122]. These achieve significant improvement in performance and start-up time over conventional lead bath andother equipment, at comparable or reduced capital cost. With electrical heating and controlled fluidising atmospheres, closely controlled carburising and other surface treatment is possible without the health hazards associated with conventional cyanide plants.

Larger units utilising the same principles are now being produced for the continuous heat treatment of wire. A small, high efficiency domestic gas-fired central heating boiler has undergone extensive trials and a small industrial package boiler for water heating or low pressure steam raising is now the subject of a development study[123].

Fluidised transport has, by comparison with other applications, received little attention. In chemical plant employing fluidised reactors

it is more usual to transport the material to and from the reactor by either pneumatic or mechanical means. This is surprising, for fluidised transport has several advantages over either system, particularly over the relatively short distance involved in this type of application. Pneumatic transport requires very high air velocity, and therefore the specific power consumption is high. Also degradation, blockage and abrasion of carrying lines, electrostatic charging, and material recovery often present serious problems. It is difficult to make direct comparisons, but the air power required for fluidised transport is probably an order of magnitude lower than for pneumatic conveying. Mechanical systems involving belts and bucket conveyors have a very low power requirement, but capital cost is much higher than fluidised systems because of the large amount of hardware involved. Fluidised conveying is perhaps the only method suitable for high temperature solids transport. Mechanical systems using conventional materials would be unsuitable at high temperatures. Pneumatic systems would be subject to tremendous heat losses via the conveying air, unless this could be recycled or the heat otherwise utilised.

The only commercial fluidised conveyors in quantity production in the UK are made by Polysuis Ltd (see App. II). They manufacture a range of units up to 1 m wide, capable of handling up to 2000 m^3/h of a wide range of granular and powdered materials. However the design of these units is based solely upon past experience and pilot tests on the material to be handled[124], and use of the large sizes has so far been restricted to low density materials. A scheme for a fluidised conveyor has been patented by Squires[125] in which the motive force is provided by the fluidising air instead of by gravity as in an inclined channel. The free board above the bed is enclosed, with outlets at the solids efflux end of the channel. Thus the free-board gas is caused to flow over the surface of the bed at high velocity which is said to cause flow of the solids in the bed. It is not known whether this system has been successfully run, but the solid

flow so induced would certainly be very dependent on the depth of material in the channel. However, this could be an attractive scheme for operation at or near one particular design flow rate.

Fluidised transport has clearly been used industrially with some success: but for its further exploitation there is evidently a need for quantitative data on flow, preferably in the form of readily usable design equations.

The development potential for fluid bed technology at all industrial size levels is enormous, particularly in the heat transfer and solids transport fields which to date have received little attention. Significant advances at this stage can be achieved in spite of an often scanty appreciation of the physical principles involved. This is perhaps the most interesting period for the practical engineer, but it is to be hoped that increased experience with industrial systems will lead to a fuller understanding of the basic mechanics of fluidisation.

CHAPTER 3.

SMALL SCALE VISCOMETER WORK.

1. INTRODUCTION

The object in undertaking a small scale viscometer study was to carry out a broad investigation of the parameters likely to influence the flow behaviour of shallow fluidised beds, and the heat transfer performance of surfaces immersed in shallow beds. The apparatus enabled the effect of such variables as particle properties and bed geometry to be assessed much more easily than would have been possible with a large flowing bed.

It was not anticipated that viscometric measurements would give exact predictions of channel flow behaviour. The main aim of the work was to provide a qualitative knowledge of shallow bed flow characteristics; although a method has been developed which yields quantitative viscosity data.

Although previous workers have measured fluid bed viscosity, few results are available for freely bubbling shallow beds. Only the method of SCHUGERL[78] has enabled evaluation of any non-Newtonian properties, and his apparatus is unsuitable for localised measurements in shallow beds. Nevertheless, previous studies have been very useful as a background to the present work, and in many cases the results obtained have been surprisingly similar, in view of the differences in measurement technique.

2. DEVELOPMENT OF THE APPARATUS

2.1 Definition of the Problem

A method was required of obtaining shear diagrams for fluid beds over as wide a range of shear rates as possible, in order to assess any non-Newtonian behaviour. It was desired to examine properties at different levels in shallow beds, so that the device chosen had to measure as near "point" properties as possible. It was also desired to measure pure shear, as would occur in a real flow situation; so that any device involving displacement of particles other than in the direction of shear could not be used. Lastly, a method was required which could be used

in vigorously bubbling beds with minimal interference with the normal bubbling and gas flow patterns therein. Clearly any shear forces imposed on the bed will disturb the fluidisation compared with its usual state. Therefore an immersed probe was required which would have little effect when no shearing was taking place.

2.2 Selection of Type of Viscometer

The need to measure non-Newtonian behaviour precluded all the common types of viscometer other than capillary or rotational instruments. Other types are either incapable of measuring non-Newtonian behaviour, or their flow fields are too complex to be readily handled mathematically. The capillary viscometer is obviously unsuitable for use in fluidised systems, so that the choice was restricted to some type of rotational viscometer.

Most of such instruments available commercially are either of the concentric cylinder or cone and plate variety. These enable the rate of shear at the shearing surface to be estimated quite easily[73], but involve the use of thin films of fluid and so are again unsuitable for use in fluid beds. A cylindrical rotor immersed in an infinite fluid field can be used to measure non-Newtonian flows. The main disadvantage is that the maximum shear rate is limited by the tendency for secondary flows to develop in the sheared fluid. Apart from this limitation, the method is suitable for use in fluid beds, provided a rotor can be devised which causes minimum disturbance of the fluidisation and yet is still amenable to calculation of the shear rate. Previous fluidised bed viscometer studies have not fulfilled both of the latter conditions completely.

A hollow cylindrical rotor with thin walls, as used by Schügerl[78], enables determination of the shear rate at its outer (convex) surface. However, Schügerl used rotors up to 300mm long, and of small diameter, which would certainly have caused some constraint on normal bed behaviour at their internal surfaces.

It was therefore decided to use a hollow cylindrical rotor of much lower aspect ratio, the final dimensions chosen being shown in Figure 2.1. These dimensions were based on those of a rotor used successfully by GIDDON[126] in determining the viscosities of non-Newtonian coal ash/water slurries. Several rotors were turned from brass tube and given different surface finishes, whose significance is discussed below. The walls were made as thin as possible to give minimum projected area in the vertical direction and thus cause minimum disturbance to the path of the fluidising gas. Support was provided by steel wires of 1.5mm diameter, which when tested separately were shown to cause a resistance less than 1% of that of the rotor. The effect of the resistance of the wires was in any case, later eliminated by the method of calibration.

2.3 Brookfield Viscometer Rig

The initial viscometer work, using the rotor described above, was carried out using a modified Brookfield Syncro-Lectric viscometer, model RVT. (A description of this instrument is given in ref 73, p 139 and the manufacturers address in Appendix II). The instrument has a range of eight rotational speeds between 0.5 and 100 rev/min and a full scale torque of 7.19×10^{-4} Nm.

For normal use in liquids the Brookfield is provided with a universal joint in the shaft supporting the rotor. This enables the rotor to rotate about its own centre, obviating errors due to eccentricity or lack of straightness of the shaft. Because of this joint the rotor was subject to serious disturbances in bubbling beds caused by the passage of bubbles. To eliminate this a P.T.F.E bearing, lubricated by a bleed from the fluidising air supply was provided to support the rotor shaft. This proved to be an effective cure for the trouble and the bearing did not cause any significant frictional drag when the assembly was tested in air. These initial tests were carried out in a bed of 140 mm diameter, having a

FIG 2·1

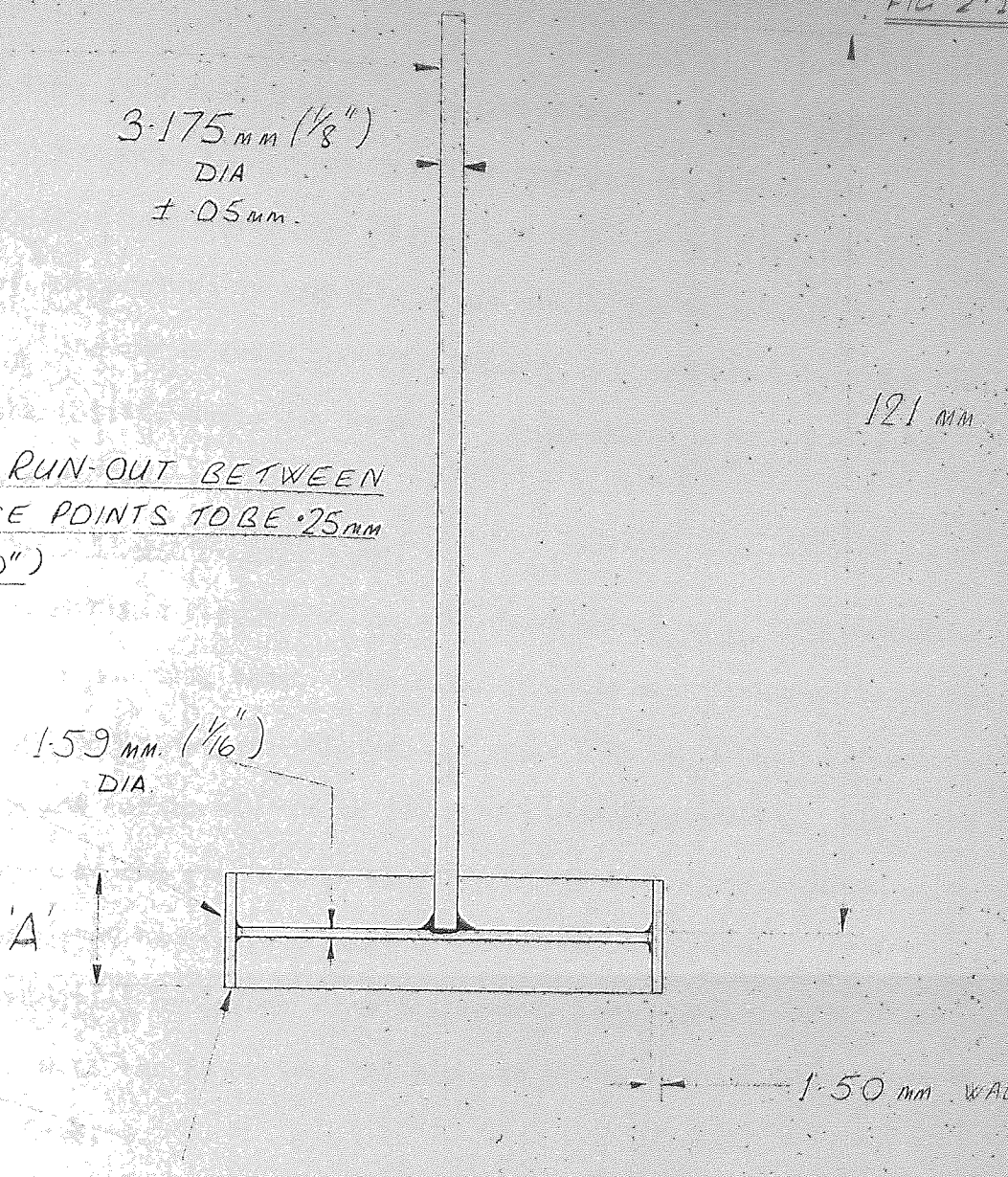

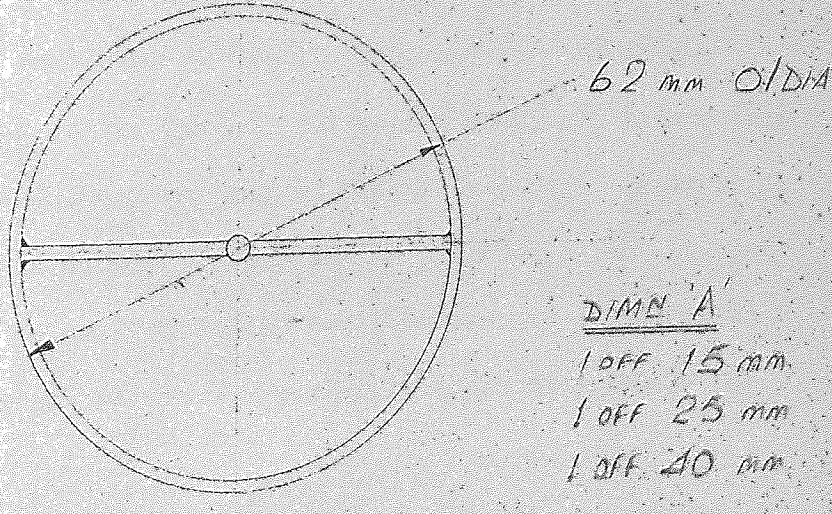

DIMN 'A'
1 OFF 15 mm
1 OFF 25 mm
1 OFF 40 mm

ASSEMBLE WITH SOFT SOLDER

DRAWN: S McGUIGAN

MATERIAL - MILD STEEL EN 8

porous ceramic tile distributor. The fluidising air was provided by a small B.V.C. electric blower and the flow rate measured with a 2½A rotameter, (for calibration see Fig 2.2). No provision was made for control of temperature or humidity of the air supply at this stage. The position of the rotor could be varied axially and radially within the bed, but for the initial tests was centrally positioned at a height of 2.5mm above the distributor.

2.4 Stormer Viscometer Apparatus

The Brookfield viscometer had some shortcomings as regards operation in vigorously bubbling beds. The chief of these were disturbances of the rotor caused by inadequate support, and gross rotational speed variations due to the low torsional rate of the torque measuring device. Also, the torque capacity and speed range were insufficient to allow complete investigation of the desired range of fluidising conditions. It was therefore decided to design a new viscometer, incorporating ideas which experience with the Brookfield had shown to be desirable for operation in fluidised beds.

The Stormer viscometer is one of the simplest and most robust types available commercially. The torque on the rotor spindle is provided by a falling weight which is attached to a bobbin on the rotor spindle and works in the manner of a ship's capstan. The angular velocity of the rotor is recorded on a revolution counter. Thus in the case of the Stormer, it is the shear stress which is maintained constant, rather than the angular velocity (and therefore rate of shear) as for the Brookfield. Because a much more rigid support bearing can be provided in the Stormer and there is no spring to cause torsional oscillations, it was expected that a viscometer operating on the same principle would be suitable for the present work.

The same design of rotor as used with the Brookfield is employed,

CALIBRATION OF 24A ROTAMETER FOR AIR AT 20°C IN BROOKFIELD BED

FIG 2.2

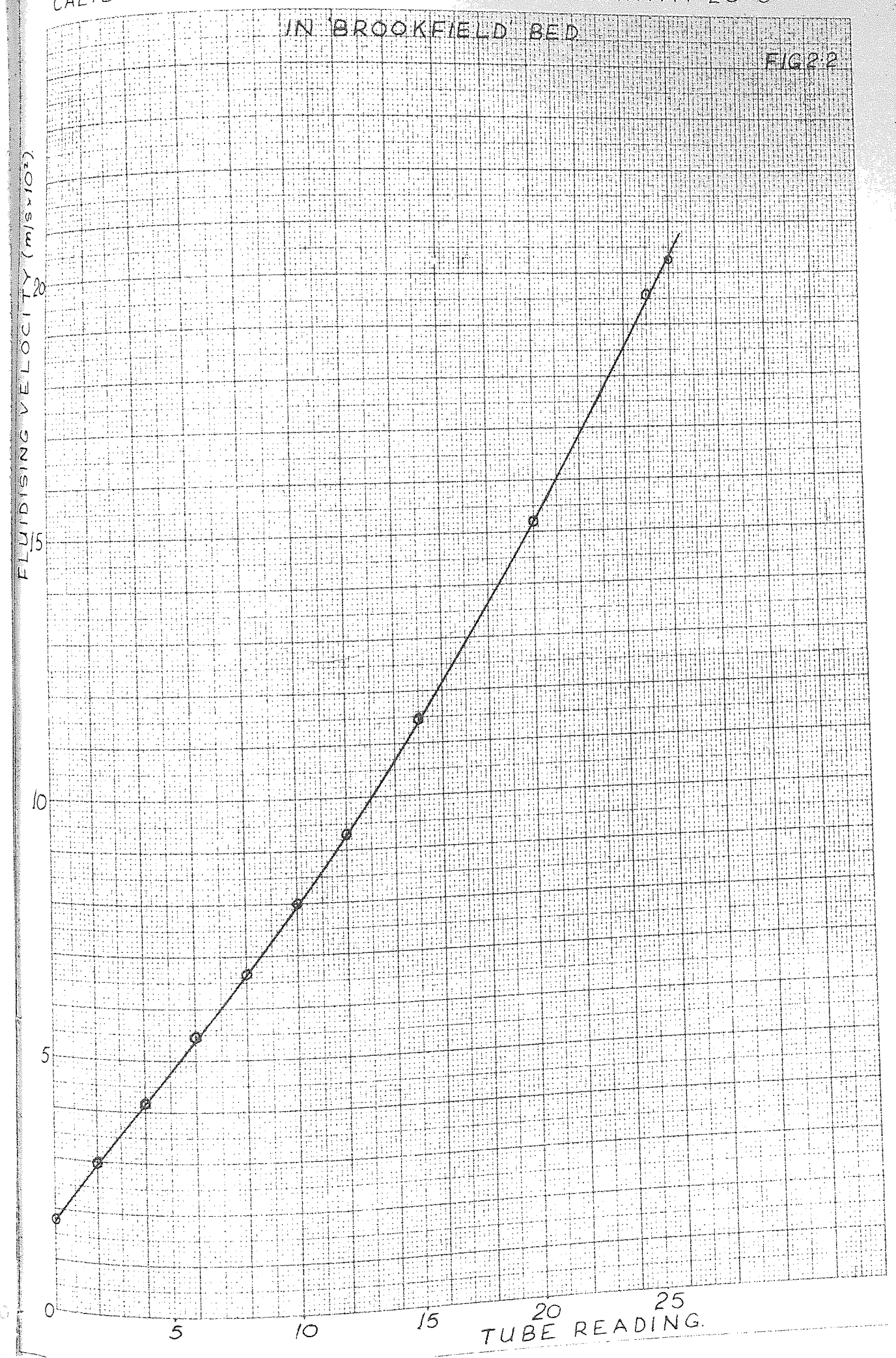

except that the support shaft was increased in diameter to completely eliminate any buffeting of the rotor by large bubbles. The rotor shaft is collet located in a short arbor mounted in two ball-races in a head stock positioned above the bed container. To ensure minimum friction in the bearings, they were initially assembled with greater than usual interference in the headstock and then 'run-in' when the headstock was fully assembled. The running-in was accomplished by feeding a mixture of paraffin and powdered "tripoli" through the bearings for several hours whilst rotating the arbor in a drilling machine. During operation the bearings are run completely dry (ie without lubricant) to reduce friction; in which condition a torque of only 7×10^{-5} Nm is required to drive the rotor assembly at 12 sec^{-1} in air. The normal minimum operating torque is more than an order of magnitude greater than this at the same speed. The headstock is sealed against dust and purged with a small filtered air bleed to prevent ingress of electriated particles from the bed. In spite of these precautions some trouble was experienced with entry of dirt, which could be removed by washing liberally with acetone or a similar solvent without dismantling the head.

The rotor is driven by a falling weight turning a bobbin attached to the arbor, in the manner described above. The headstock incorporates a brake for the spindle, and a spring-loaded locking device. The inertia of the rotating parts is kept to a minimum so that the spindle is able to accelerate up to its maximum operating speed from rest in one or two revolutions, with the rotor in air.

The speed of rotation of the spindle is measured by means of a photo-electric device triggered by a perforated plate mounted on top of the driving bobbin. The detection circuit is shown in Figure 2.3. The signal was normally fed to a Venner TSA 6634/2 digital counter which indicated the average rotor speed over a period of ten seconds. However

FIGURE 2-3

ROTOR TACHOMETER CIRCUIT

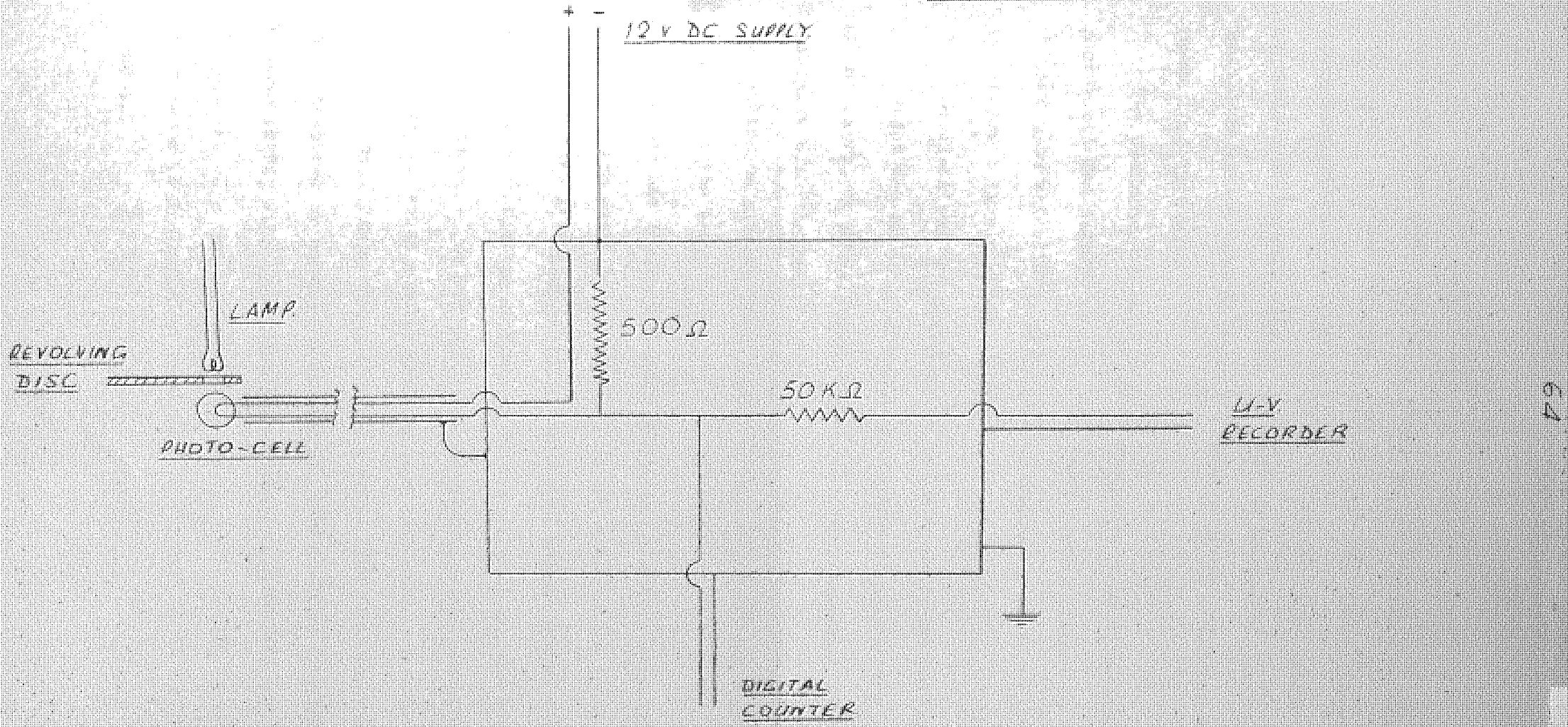

FIGURE 2·4

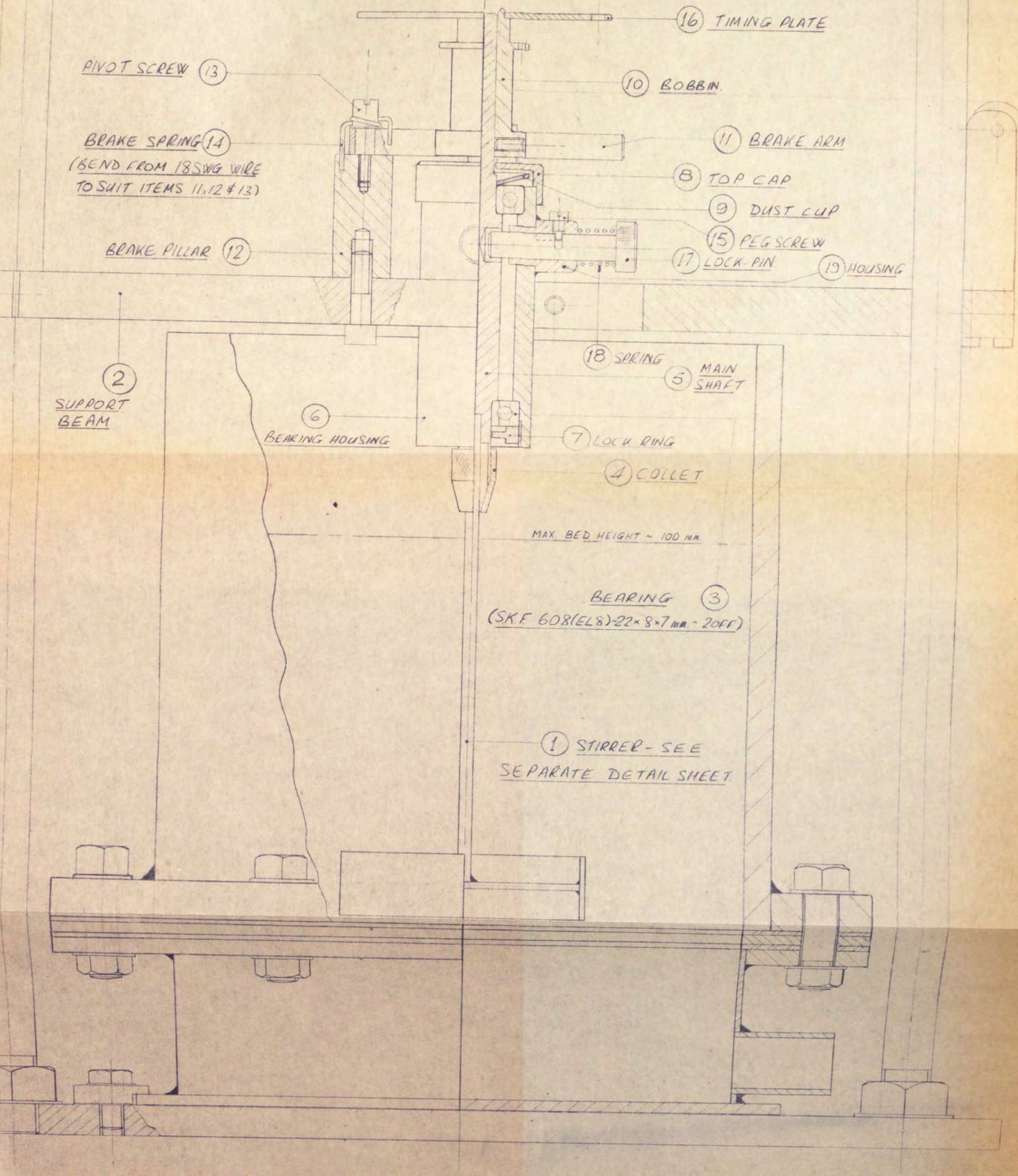
16 TIMING PLATE
PIVOT SCREW 13
10 BOBBIN
BRAKE SPRING 14
(BEND FROM 18SWG WIRE
TO SUIT ITEMS 11,12 & 13)
11 BRAKE ARM
8 TOP CAP
9 DUST CUP
15 PEG SCREW
BRAKE PILLAR 12
17 LOCK-PIN
19 HOUSING
18 SPRING
5 MAIN SHAFT
2
SUPPORT
BEAM
6
BEARING HOUSING
7 LOCK RING
4 COLLET
MAX. BED HEIGHT ~ 100 MM.
BEARING 3
(SKF 608(EL8)-22×8×7 MM. - 20FF)
1 STIRRER - SEE
SEPARATE DETAIL SHEET

FIG. 25 PRESSURE PROBE

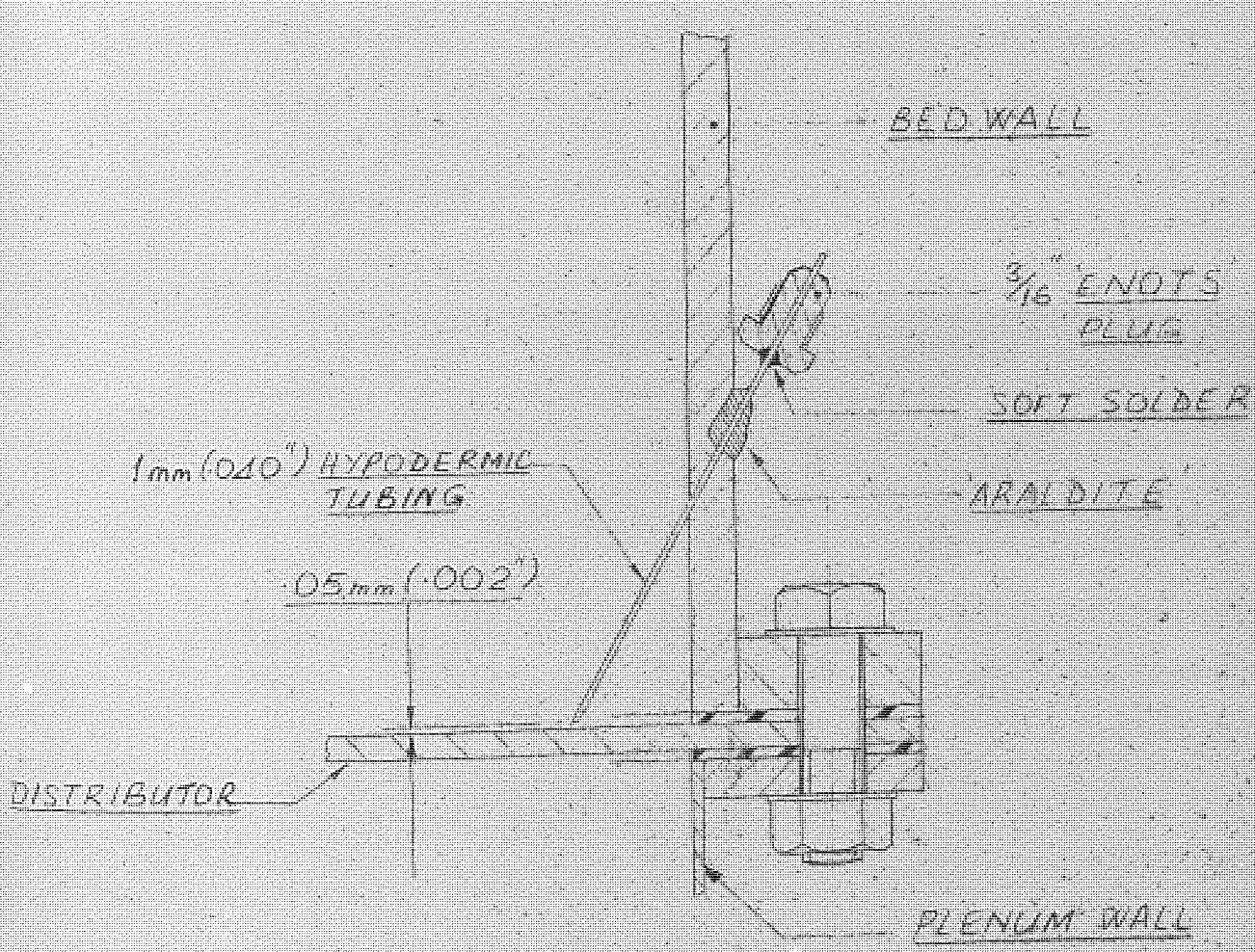

The air supply to the bed is provided either by a self contained B.V.C blower, or from a suitably regulated high pressure compressed air line. Carbon dioxide from a cylinder was also used on occasion. The supply is first taken through a heat exchanger, whose main function is to maintain the air temperature at between 20 and 25°C. It can also be used to study the effect of varying the air temperature over a limited range.

The air is then passed through either a drying tower or a humidifier, according to the conditions required. The humidifier was not fitted initially but was incorporated after the effect of air humidity had been found sufficiently important to warrant closer investigation. The humidifier comprises a chamber with a porous base containing water, through which the air is bubbled. The issuing air is almost saturated at the temperature of the water, so that ambient relative humidity is readily varied by changing the water temperature. This is achieved either with an immersed heating element or by feeding warm water to the chamber at a suitable rate. The drying tower comprises a perspex tube approximately 1.5 m long x 120 mm bore containing granular silica gel. Copper gauze provided at the top and base of the column prevents egress of silica gel.

The air flow is then metered by a bank of three Rotameters (sizes 14A, 24A, and 35A) to cater for the range of fluidising velocities required. Calibration curves for the Rotameters are given in Figures 2.6 - 2.8. The static pressure upstream of the Rotameters is maintained at approx 500 mm water to ensure consistent readings. The air temperature is measured with mercury in glass thermometers.

Initially the humidity of the fluidising air was not recorded. Later it was measured with a capacitive probe (Manufacturers AM Lock and Co.) placed in the efflux air stream from the bed. The Lock humidity meter was not really suitable for the work as it was insensitive in the low humidity region, but was to hand when the investigation of humidity

CALIBRATION FOR 14A ROTAMETER USING AIR AT 20°C

500 mm H_2O IN 140 mm DIA. BED.

FIG. 2·6

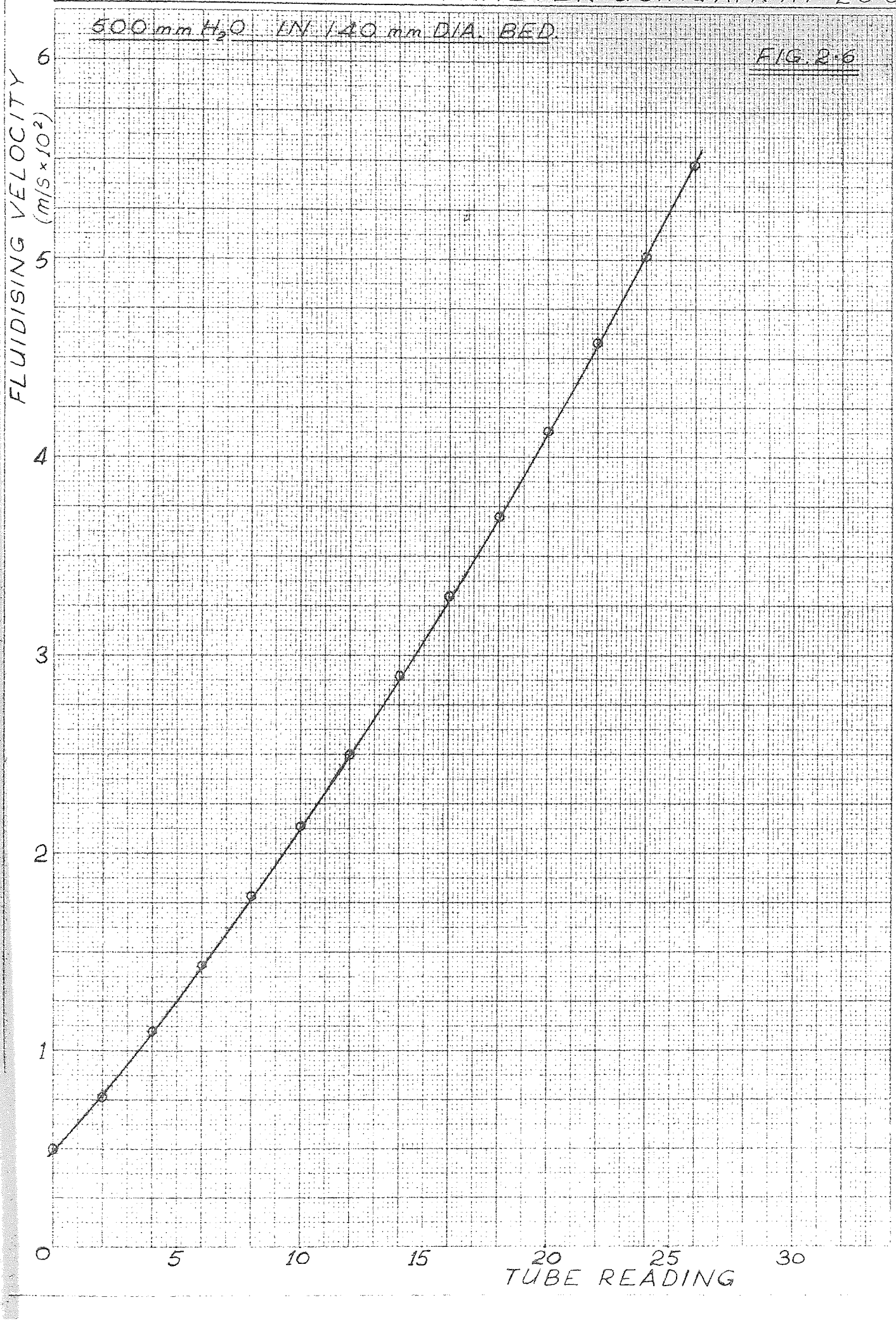

CALIBRATION OF 24A ROTAMETER FOR AIR AT 20°C 500 mm H_2O IN 140 mm DIA BED

FIG 2.7

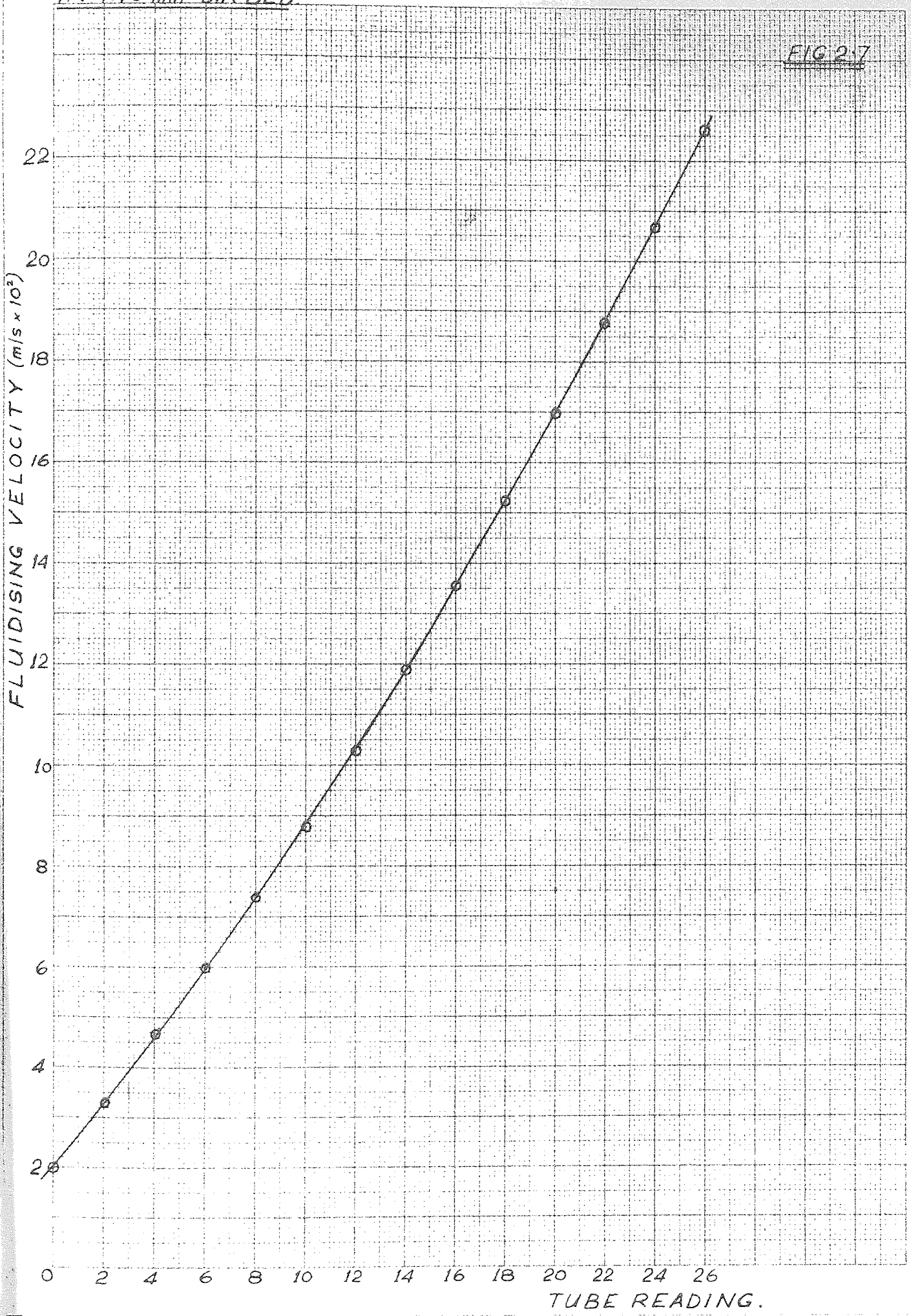

CALIBRATION OF 35A ROTAMETER FOR AIR AT 20°C
500 mm H_2O IN 140 mm DIA BED.

FIG 2·8

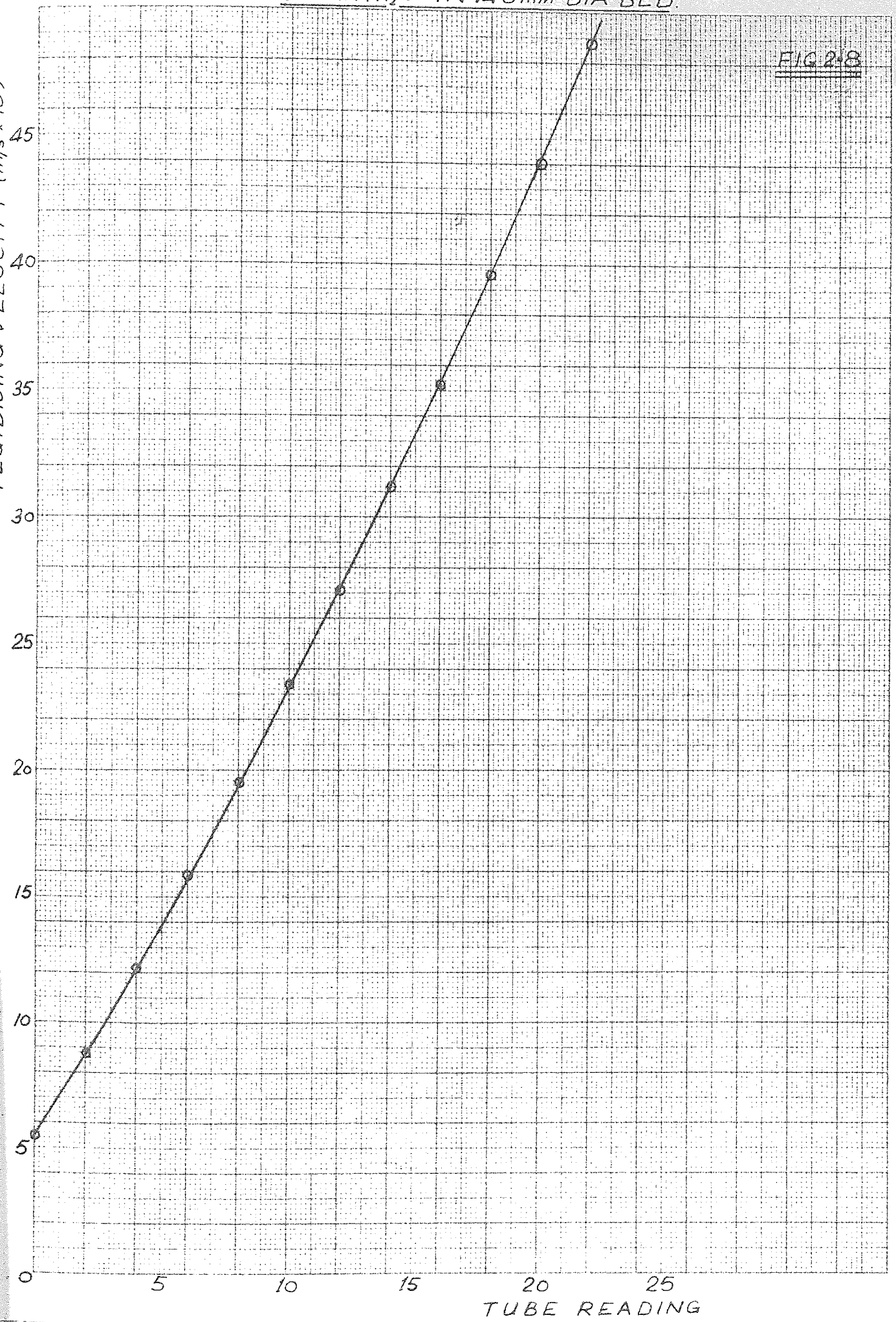

effects started. Later it was replaced by a Shaw Moisture Meter with a probe in the supply air stream just prior to the bed plenum chamber, which position facilitates control of air humidity as the element responds more quickly to small changes. The Shaw meter has not proved entirely satisfactory in use, as the calibration of the element tends to vary over a period of months. However it provides good sensitivity at low humidity.

The apparatus has proved to be reasonably easy and convenient to use for the work undertaken. A difficulty is that the viscometer must be capable of measuring a wide range of viscosities (at least 2 orders of magnitude) to cover all the fluidising conditions encountered. It must be extremely sensitive for use in very shallow beds of light particles and yet robust enough to withstand buffeting by large bubbles in deeper beds of dense material. Though the sensitivity is adequate, with careful operation, for the largely qualitative studies undertaken here, greater sensitivity would be required for accurate quantitative determinations under some conditions. This could be easily achieved by using a larger rotor, but would necessitate a larger fluid bed, and therefore more material for a given test. A diagram of the apparatus is shown in Ref. 102 (Appendix III), and a general view of the equipment in Fig. 2.9.

3. CALIBRATION OF THE VISCOMETER ROTOR

3.1 Theory of Viscous Flows

When two layers of a viscous fluid are subjected to a shearing stress, shear occurs such that the velocity gradient between the two layers is a function of the applied stress:

$$\tau = f\left(\frac{du}{dy}\right) \qquad 3.1$$

For many fluids, termed the Newtonian fluids, the velocity gradient or rate of shear is proportional to the applied stress:

$$\tau = \mu\left(\frac{du}{dy}\right) \qquad 3.2$$

MAKER'S CALIBRATION CURVE FOR SHAW HYGROMETER: NORMAL ELEMENT.

FIG 2·11

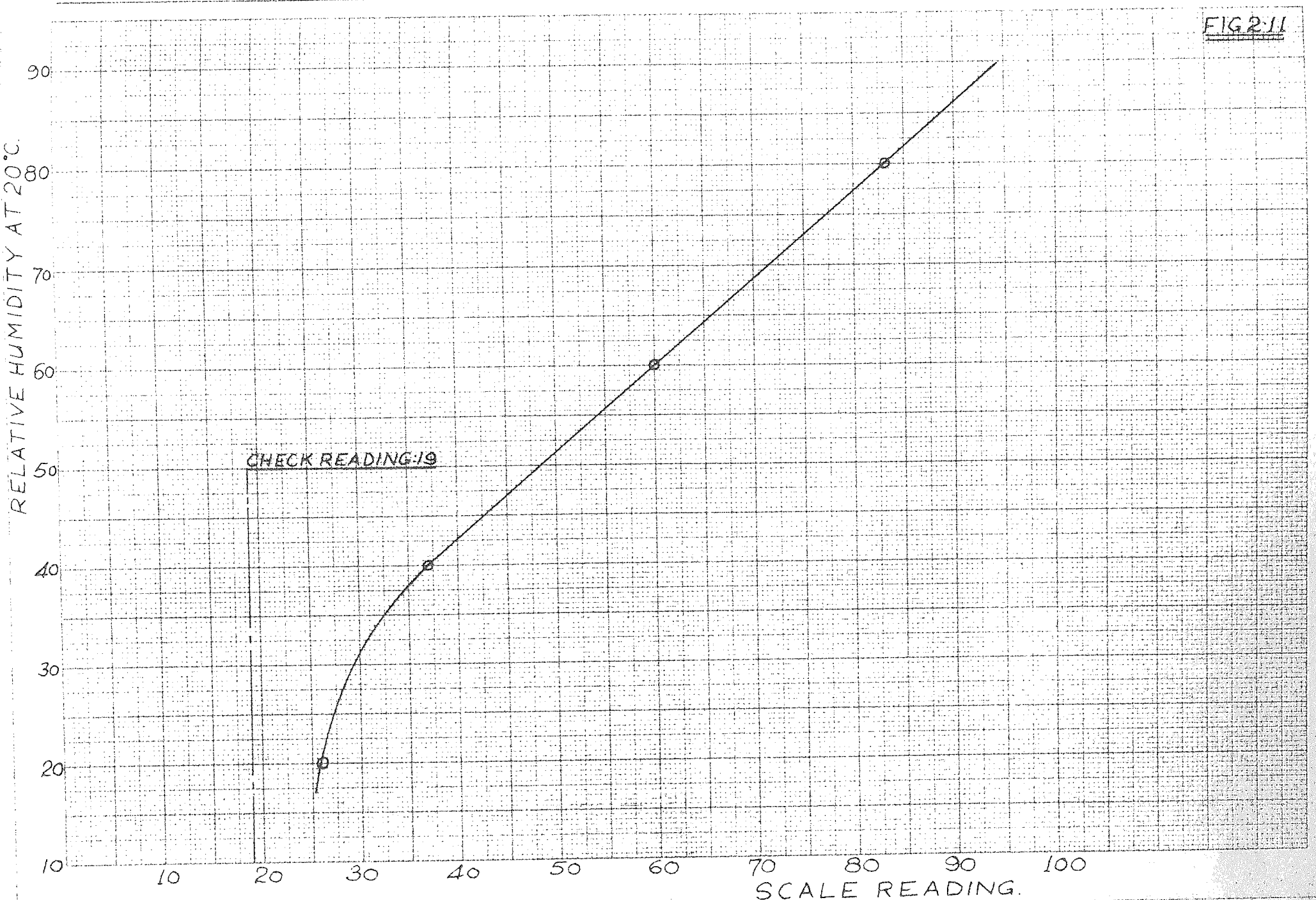

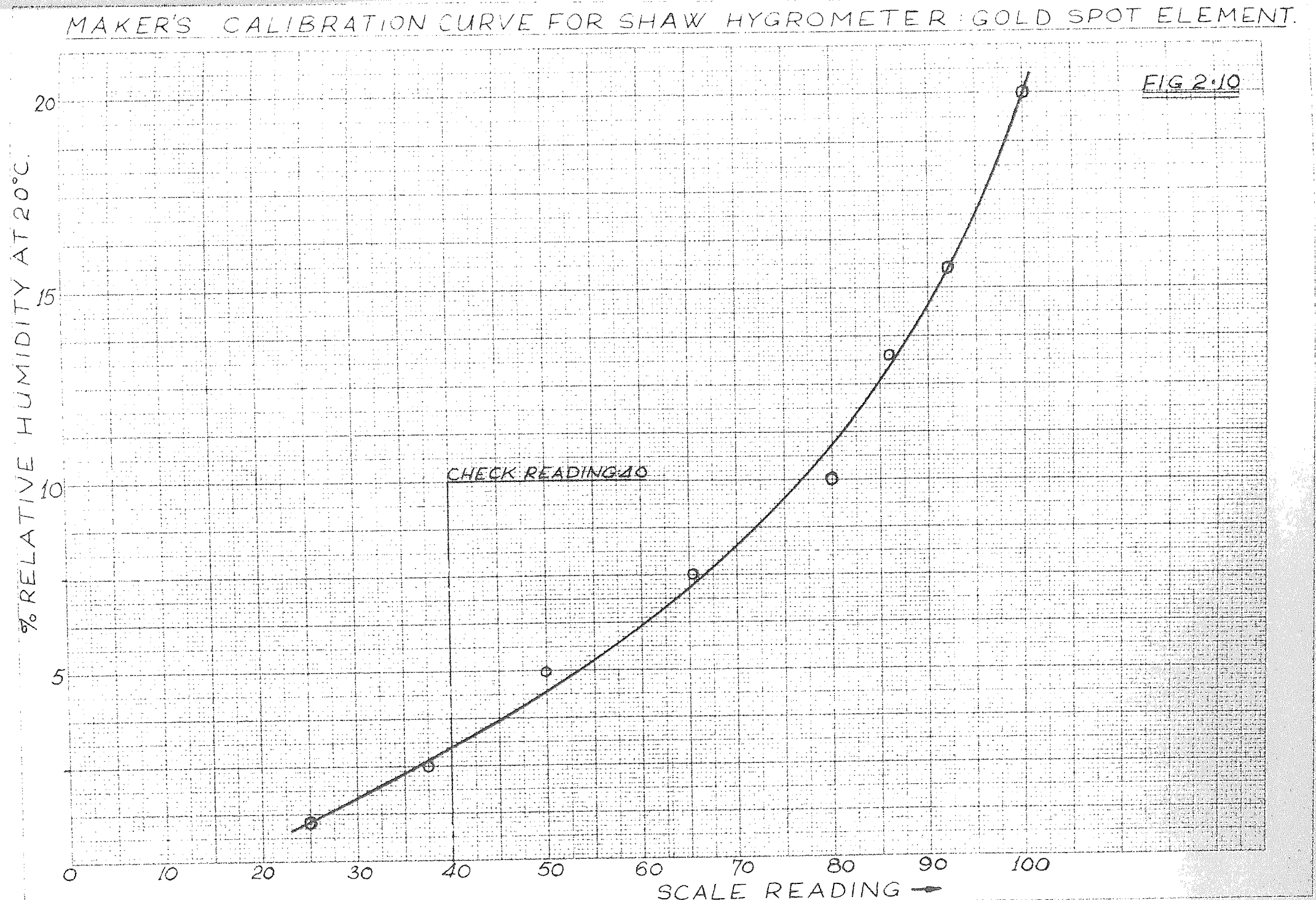
MAKER'S CALIBRATION CURVE FOR SHAW HYGROMETER : GOLD SPOT ELEMENT.
FIG 2·10
% RELATIVE HUMIDITY AT 20°C.
20
15
10
5
CHECK READING 40
0
10
20
30
40
50
60
70
80
90
100
SCALE READING

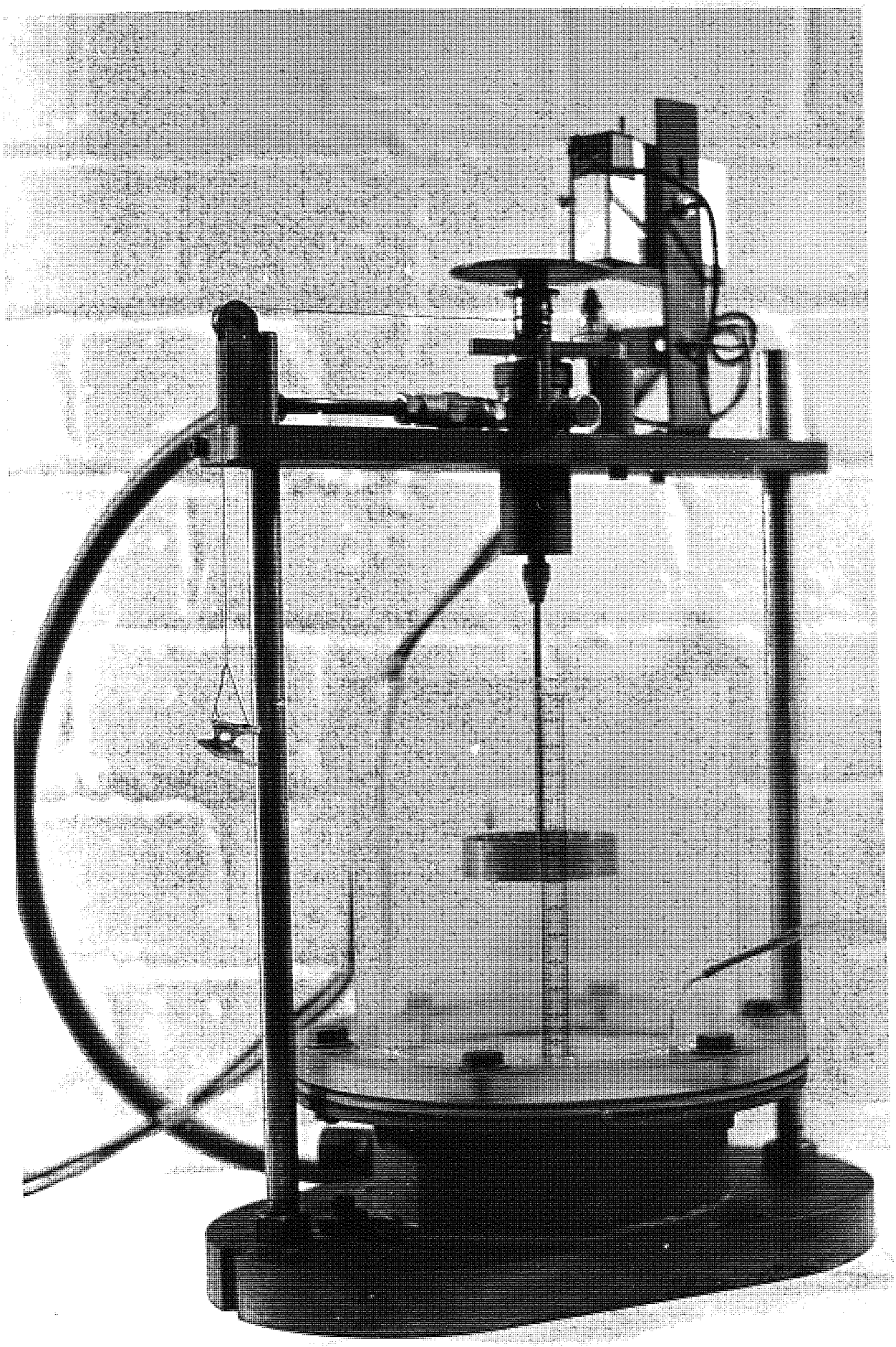

FIG. 2·9 (a).
STORMER PATTERN VISCOMETER.

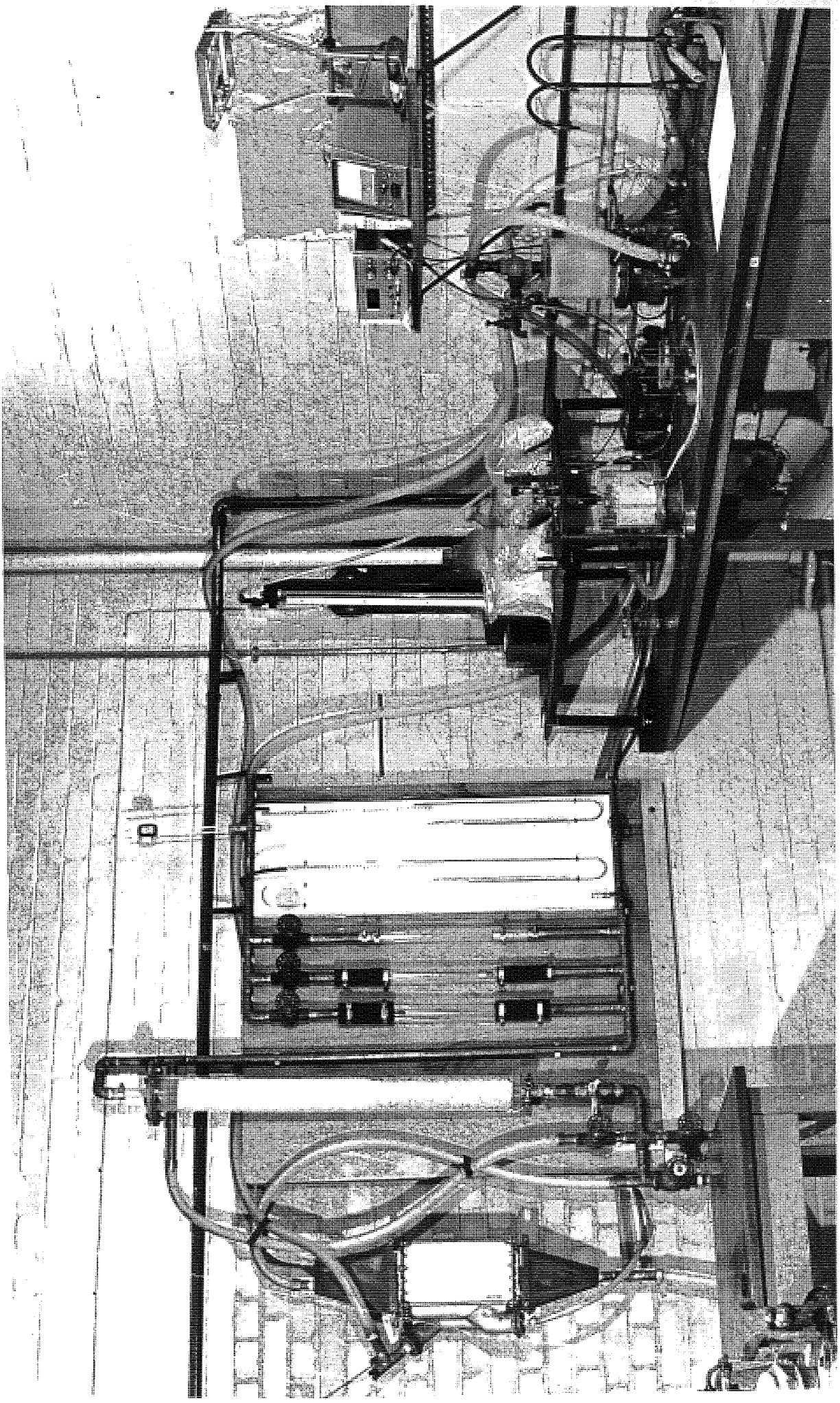

FIG. 2·9(b) VISCOMETER RIG ~ OVERALL VIEW.

The constant of proportionality μ, is the coefficient of viscosity of the material.

Some fluids, particularly those containing large molecules, and slurries of particulate matter, depart from Newtonian behaviour as a result of rearrangement of the particles brought about by the shearing action. For these materials the viscosity is not a constant, but varies with shear rate. Both shear-thinning (pseudoptastic) and shear-thickening (dilatant) behaviour has been observed, although the former is more common. The behaviour of these materials can usually be described, at least approximately, by a power law:

$$\tau = K^1 \left(\frac{du}{dy}\right)^n \qquad 3.3$$

This is sometimes referred to as Ostwald's Equation, K^1 and n being termed the indices of consistency and flow respectively. It can be seen that Newtonian fluids are a special case of this equation in which n = 1, and K^1 then becomes the viscosity, μ. Some shear-thinning materials tend towards Newtonian behaviour at high shear rates, so that it is possible to estimate a viscosity at infinite shear, μ_∞. Other expressions have been proposed for describing various non-Newtonian fluids[127].

Some fluids exhibit a yield stress, below which no shear takes place:

$$\tau = \tau_y + K^1 \left(\frac{du}{dy}\right)^n \qquad 3.4$$

Many of these display proportionality of stress and shear rate after yield has occurred. These are the Bingham plastic fluids, for which an apparent viscosity can be defined as:

$$\mu_a = (\tau - \tau_y) \Big/ \left(\frac{du}{dy}\right) \qquad 3.5$$

The flow behaviour of some fluids depends upon their previous shear history. Both time-thinning (thixotropic) and time-thickening (rheopectic) fluids are known and the process is normally reversible, so that the shear diagrams take the form of an hysterisis loop whose enclosed area depends upon the rate of change of shear stress. Such behaviour is again the

result of structural changes in fluids containing large molecules or particles.

Materials such as bitumen, flour dough and some jellies are found to deform and recover elastically at shear stresses below that necessary to sustain flow. These are termed visco-elastic materials. Little theoretical treatment of their properties has been presented, although an empirical method due to OLDROYD[128] is available.

Fortunately, neither visco elasticity nor time dependence have been observed with fluidised beds in the present work.

The above descriptions apply to viscous or laminar flow only. A laminar flow may be defined as one in which no stable eddy currents exist, even at microscopic level. At high shear-rates, fluid layers cease to slide over each other and the flow breaks up into small eddies or turbulent regions. Such turbulence develops first in the centre of the duct in channel or tube flow and gradually spreads outwards towards the walls until finally only a small "laminar boundary layer" remains. The latter condition is referred to as turbulent flow; the mathematical representation of which is not easy, although an approximate expression has been derived by VON KARMANN[129]

$$\tau = \frac{\rho K^2 (du/dy)^4}{(d^2u/dy^2)^2} \qquad 3.6$$

where K is a constant

The usual criterion for distinguishing laminar and turbulent flow of Newtonian fluids is the Reynolds number.

$$R_e = \frac{\rho u d}{\mu} \qquad 3.7$$

The transition Reynolds number is usually around 2000 for flow in circular pipes, although in practice transition begins at this value and continues for some time before flow is fully turbulent. The concept may be extended to other channel geometries by applying the concept of a hydraulic diameter, equal to the flow area divided by the wetted perimeter.

Transition normally occurs later in shear thinning fluids and earlier in shear thickening ones so that the Reynolds number criterion cannot be used for non-Newtonian flows. METZNER and REED[130] have developed a generalised Reynolds number for power-law fluids in tube flow:

$$N_{R_e} = \frac{\rho U^{2-n} d^n}{\gamma} \quad \text{where } \gamma = 8^{n-1}K^1 \qquad 3.8$$

Alternatively the Fanning or D'arcy Friction Factors may be used as a criterion for transition in tube flow for all time independent fluids with no yield value, the value of f_f at transition being 0.008 .

$$f_f = \frac{D\Delta P}{4L} \Big/ \frac{\rho U^2}{2g} \qquad 3.9$$

The latter has more theoretical justification than the Reynolds number since it represents the ratio of the viscous shear stress to the specific inertia force; which parameters largely determine the stability or otherwise of eddy currents.

3.2 Theory of the Rotational Viscometer

The main difficulty in interpreting data from a rotational viscometer lies in estimating the true shear rate at the surface of the rotor. This does not generally bear a simple relationship to the angular velocity. Commercial viscometers usually have a cylindrical rotor running with a very small radial clearance in a cylindrical cup. Among other advantages this allows, for most purposes, the assumption of a linear shear gradient across the gap; so that the rate of shear is easily calculated.

Where it is necessary to have a large clearance around the rotor, as in a fluidised bed, the shear rate can only be readily estimated if the flow equation of the fluid is known. A general method of shear rate determination, for any fluid, which utilises an infinite series solution has been presented by KREIGER and MARON[131]. The series may normally be truncated to three terms without loss of accuracy. However, as the gap width between rotor and cup is increased, more terms are necessary

and the method becomes cumbersome to handle.

Fortunately, Kreiger and Maron have also shown[132] that a closed solution is possible for the shear rate at a rotor in an infinite flow field, and this can be applied to cases where the flow equation is not known or required. The postulation of an infinite flow field requires in practice that the fluid velocity is reduced substantially to zero at the walls of the vessel containing the fluid under test. This condition is closely approached for a system with the geometry and flow regimes of interest here, which was confirmed during the calibration of the viscometer.

The only other disadvantage in using an 'infinite' flow field is that the Reynolds number, for a given rate of shear, is higher than when a narrow field is used. This means that the maximum shear rate attainable is limited by the onset of turbulence or secondary flows. A criterion for predicting the latter is presented in section 3.6 below.

3.3 Theory of Cylindrical Rotor in an Infinite Flow Field

The theory of a cylindrical rotor shearing an infinite fluid flow field will now be presented.

The following assumptions are made:-

1. There are no velocity gradients other than in the plane normal to the rotor surface
2. The flow is laminar
3. The fluid velocity at the rotor surface, relative to the rotor, is zero.

Consider a rotor of length ℓ and radius R, rotating with angular velocity Ω under the influence of a torque M. The velocity gradient at a distance r from the rotor axis, where the fluid rotates with angular velocity ω is then:

$$\frac{du}{dy} = -r\frac{d\omega}{dr} \qquad 3.10$$

and the shear stress, τ is:

$$= \frac{M}{\pi \ell} \frac{1}{2\pi r} = \frac{M}{2\pi r^2 \ell} \qquad 3.11$$

Substituting into Eq. 2.1

$$-r \frac{d\omega}{dr} = f\left(\frac{M}{2\pi r^2 \ell}\right) \qquad 3.12$$

From 2.11 $\frac{d\tau}{dr} = \frac{-2M}{2\pi r^3 \ell} = \frac{-2\tau}{r}$

Rearranging: $\frac{dr}{r} = -\frac{d\tau}{2\tau}$

Substituting in Eq 2.1

$$d\omega = \frac{1}{2} \frac{f(\tau)}{\tau} d\tau$$

Integrating between the rotor ($\omega = \Omega, \tau_R = \frac{M}{2\pi R \ell}$)

and infinity ($\omega = 0, \tau = 0$)

$$\int_{\Omega}^{0} d\omega = \frac{1}{2} \int_{\tau_R}^{0} \frac{f(\tau)}{\tau} d\tau$$

$$\text{ie } \Omega = \frac{1}{2} \int_{0}^{\tau_R} \frac{f(\tau)}{\tau} d\tau \qquad 3.13$$

Differenting & rearranging :

$$\text{Shear rate at rotor surfaces } f(\tau_R) = 2\tau_R \frac{d\Omega}{d\tau_R} \qquad 3.14$$

$$\text{Now } 2\tau_R \left(\frac{d\Omega}{d\tau_R}\right) = 2 \frac{d\Omega}{d\, \ell_n \tau_R}$$

Thus for a power law fluid the shear rate may be found from the straight line gradient of Ω vs $\ell n\, \tau_R$. Otherwise it can be obtained by measuring the local gradient of Ω vs τ_R at the desired value of τ_R.

Clearly in the real flow field there will be vertical velocity gradients due to the presence of the ends of the rotor distorting the shear field. To eliminate the errors thus caused it is usual[127] to calibrate the rotor in a fluid of known viscosity; although an approximate analytical correction is also available[73].

The calibration involves measuring rotor torque versus speed in the reference fluid and back calculating to obtain an equivalent length of rotor, ℓ_e. However the method is only generally applicable to Newtonian

fluids: for non-Newtonians, the calibration fluid must have a similar flow equation to the unknown fluid and an equivalent length is determined at each rate of shear used. The latter is clearly a cumbersome technique and for approximate work, particularly with rotors of large aspect ratio, Newtonian calibration is adequate. This method was used for rotor calibration during the early part of the present study[102], but it was soon realised that it is unsuitable for a hollow rotor of low aspect ratio. Also, it is now realised that fluid beds are hydrodynamically anisotropic, so that this method is inapplicable even if the flow is Newtonian in the plane of measurement. A more refined calibration technique has now been developed: this is described in section 3.5 below.

3.4 Initial Calibration with Brookfield Viscometer

The first method of rotor calibration involved estimating an equivalent length of rotor to correct for shear taking place on the inner and edge surfaces of the rotor. The method of KREIGER and ELROD[133] was used to calculate the results. Various tests were performed using aqueous sugar solutions with concentrations between 60 and 70% over a temperature range of 20 to 30°C. Using tabulated viscosity data[134], and with the assumption of shear on the outer surface of the rotor only in the calculation, an equivalent rotor length of 122% was obtained. This was confirmed ± 1% for all tests, and the value was used to calculate the results presented in Ref 102.

However, it is now realised that, in a fluid bed, the vertical and horizontal velocity profiles around the rotor may be different due to anisotropy of flow behaviour. This means that the foregoing method of calibration could give rise to serious errors, particularly with a low aspect ratio rotor as used in the present work.

3.5 Two Rotor Method

To overcome the above shortcoming, a method of measurement using two rotors of the same diameter but different axial length was developed. The technique was to obtain torque/angular velocity diagrams with both rotors under the same conditions. By subtracting the torque ordinates at equal values of shear rate, the inner surface and end effects are eliminated, so that an outer surface shear stress based on the difference in load and shear area between the two rotors may be calculated.

The validity of the method was checked by calibration using aqueous glycerol solution of various concentrations from 80 to 100%, covering a range of viscosity of $0.1 - 2.0 \frac{Ns}{m^2}$. Comparison with established viscosity data[135] gave a maximum discrepancy of 9%; the mean error for 20 separate tests being under 4%. A specimen calibration is set out below (Section 5.1) The validity of the assumption of an infinite flow field was checked by placing anular rings between the stirrer and the wall of the containing vessel. When the gap between stirrer and ring exceeded about 20 mm, the presence of the ring had negligible effect on the stress/angular velocity curve. This indicates that the velocity gradient was reduced effectively to zero at the outer wall, thus allowing the assumption of an infinite flow field. The foregoing was confirmed both with glycerol and fluid beds of various materials. The gap width used throughout the viscometer work was 40 mm.

It is of interest that the correct shear area to use with this method is that representing the difference in <u>outer</u> surface area only of the two rotors. The only physical interpretation which can be put on this is that the fluid inside the rotor behaves as a solid plug. That this is not so, both for liquids and fluidised beds, is clear from visual observations. All that can be said is that the method works well in practice.

It is unlikely that the above order of accuracy will always be achieved when using the method for fluidised beds. Error will be incurred due to the vertical viscosity profile in the bed causing differences in "end effect" between the large and small rotors, particularly in very shallow beds where the upper edge of the large rotor is near to the bed surface. Such error cannot be estimated or eliminated. However since no more rigorous method is available, the procedure is considered acceptable for the present study.

3.6 Criterion for Onset of Secondary Flows

It was noted above that departure from laminar flow is usual at Reynolds numbers greater than 2000; at which point the logarithmic plot of R_e against Friction Factor ceases to be linear. METZLER and WILLIAMS[84] applied this concept to rotational viscometers by defining a Reynolds number as:

$$R_e = \frac{4 \pi R^2 \rho \Omega}{\mu}$$

The use of this Reynolds number reliably predicted the onset of secondary flows when their viscometer was tested in liquids, and also gave indications of secondary flows in fluid beds.

This criterion was therefore adopted in the present work, to determine whether or not secondary flows would be likely. It was found that only for very light particles at high rates of shear and fluidising velocity were Reynolds numbers approaching 2000 encountered.

It now appears unlikely that the concepts of laminar and turculent flow can be rigorously applied to fluidised beds. However it is probable that particle separation or slip occurs between the bed and the shearing surface at high rates of shear. It would thus seem desirable to use some criterion for an upper limit of the applicability of the viscometer work.

4. EXPERIMENTAL PROCEDURE

4.1 Start-up and Preliminary Precautions

The following procedure was used:

1. Switch on air supply from blower or main, with bed inlet pipe disconnected.

2. Adjust air supply to give a suitable fluidising velocity for the test in hand.

3. Switch on humidity meter, allow the warm up, and set check-reading.

4. Adjust by-pass and control valves on heat exchanger, humidifer or drying tower to give required air conditions.

5. Switch on, and adjust sensitivity of, photo electric counter circuit.

6. Plot rotor speed vs load on pan with rotor in air to allow for frictional losses.

7. Adjust rotor position and fill bed with material to desired depth.

8. Connect air inlet pipe to bed and check circuit for any leaks.

9. Readjust humidifier, drying tower or heat exchanger as necessary and verify air supply to bearing purge line.

4.2 Test Procedure

The basic test procedure was straightforward: it involved merely adding appropriate weights to the pan, releasing the rotor and noting the resultant speed of rotation. The output from the digital counter displayed the number of revolutions of the rotor over a time interval of ten seconds. Several such intervals were normally observed and the mean rate of rotation noted. Consistency of readings was good under well fluidised conditions, but often was poor near incipient fluidisation, where small changes in bed density caused large changes in effective viscosity. It was often

extremely difficult to obtain repeatable results at low fluidising velocities, particularly at low rates of shear.

It was necessary to keep a close watch on the fluidising air humidity, and to make trimming adjustments to the humidifier power or water supply, in order to maintain a constant relative humidity. When altering the air humidity, particularly near saturation conditions, a long settling time was necessary before taking further readings, to allow for absorption or desorption of water on to the air supply lines.

Other difficulties or precautions necessary for particular tests are noted in discussing the results of the test concerned.

4.3 Shut-down Procedure

Only two special precautions were necessary upon shutting down the apparatus. Firstly, the entire air circuit was purged with dry air to prevent condensation of water vapour in the air lines or corrosion of the various metal fittings. Secondly, a further plot of load against speed was made with the rotor in air to ensure that no substantial changes in bearing friction had occurred (due to ingress of foreign matter for example) which would upset the readings taken.

4.4 Size Analysis of Particles

The particles to be fluidised were graded by sieving with British Standard sieves (BS410.1962). Because of the relatively small weight of solids required for the viscometer, it was feasible to sieve each whole batch of particles used. This eliminates any errors in obtaining a representative sample of large batches.

For single cuts of particles between two adjacent sieve meshes, the geometric mean of the two sieve apertures was taken as the mean particle size,

ie Mean diameter, $d_m = \sqrt{d_1 \, d_2}$

It is well established[3,23] that when specifying a mean particle size

for wide size range material in a fluidised bed, the best dimension to use is the surface mean diameter. Where hydrodynamic drag forces are involved, this diameter reflects the greater contribution of the smaller particles present, due to their greater surface area per unit mass. However, as shown below, fluid bed flow properties depend upon the size range as well as the mean size of the particles; also mixtures of particles of different density cannot be characterised in terms of a mean particle size.

The surface mean diameter, d_{sv} is given by:

$$d_{sv} = \Sigma w / \Sigma \left(\frac{w}{d_m} \right)$$

where d_m = geometric mean of sieve apertures.

w = weight of material of diameter d_m.

The procedure followed for sieving was that set out in ref. 136.

5. RESULTS

5.1 Specimen Calibration of Viscometer Rotor with Glycerol

To check the validity of the two rotor method of viscosity estimation, three stirrers of length 15, 25 and 40 mm were tested in glycerol solutions of varying concentration. The test presented here is for 100% glycerol at 19.5°C

Radius of Stirrers = 30.25 mm

Height of Stirrer 1 = 15.0 mm

" " " 2 = 25.0 mm

" " " 3 = 40.0 mm

Effective radius of driving bobbin = 7.25 mm

Gradient of load vs angular velocity plot (Fig.5.1):

Stirrer 1 = $\frac{2.6}{5.0}$ $\frac{\text{gmf sec}}{\text{pulse}}$

Stirrer 2 = $\frac{11.3}{5.0}$ "

Stirrer 3 = $\frac{15.1}{5.0}$ "

From Eqn. 2.14

CALIBRATION OF ROTOR WITH GLYCEROL - LOAD ON SCALE PAN vs ROTATIONAL SPEED OF ROTOR.

FIG 5.1

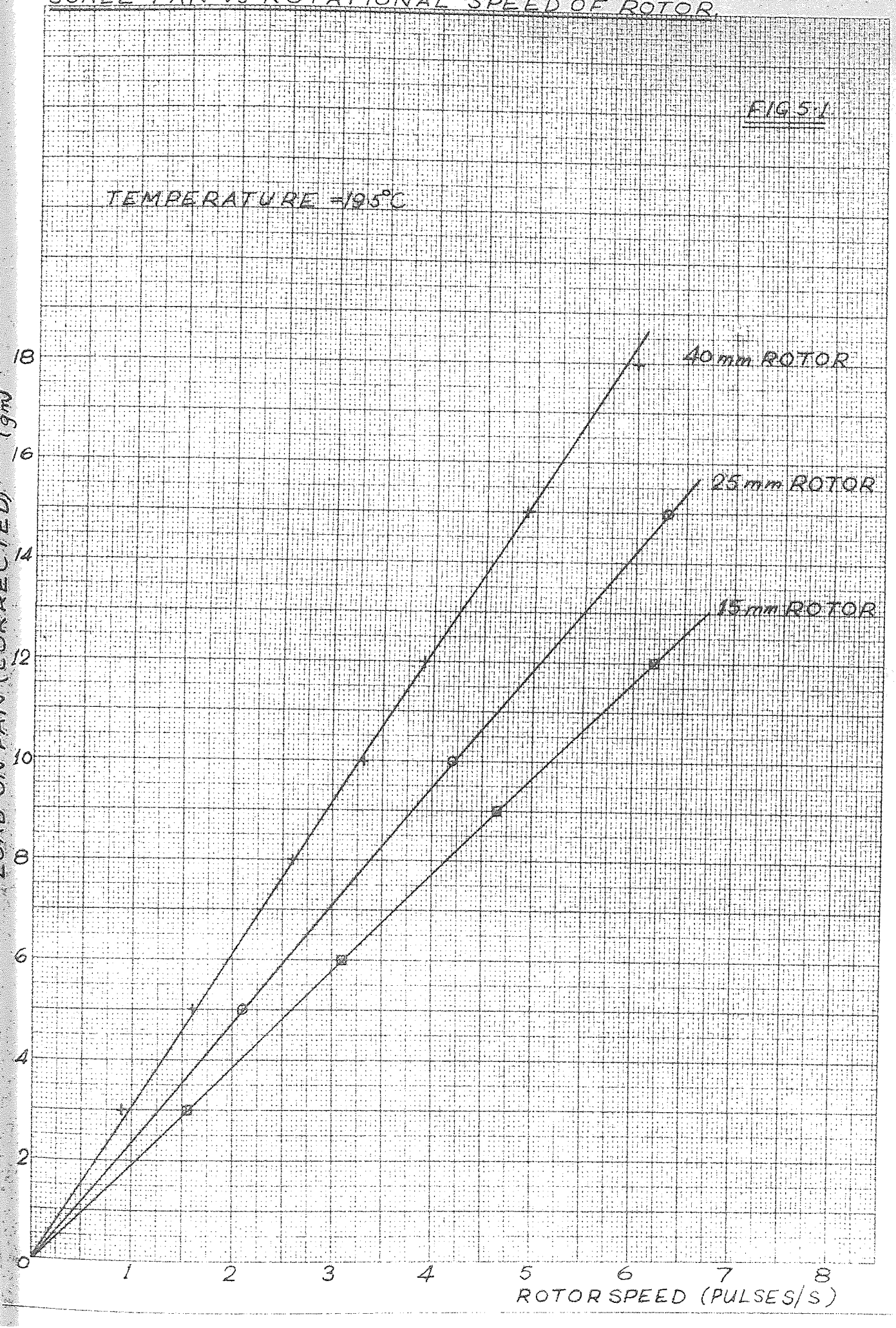

Shear rate at rotor surface $= 2\tau_R \left(\frac{d\Omega}{d\tau_R}\right)$

$\therefore$ For a Newtonian fluid, where $\frac{d\Omega}{d\tau_R}$ is constant,

$$\text{Viscosity } \mu = \frac{d\tau_R}{2d\Omega} = \frac{\text{Gradient of Shear Stress/angular velocity plot}}{}$$

$$\therefore \text{Viscosity } \mu = \frac{G}{2} \frac{\text{gm sec}}{\text{pulse}} \times \frac{7.25\text{mm}}{30.25\text{mm}} \times \frac{9.81\text{m}}{\text{sec}^2} \times \frac{36 \text{ pulse}}{2\pi \text{ radian}} \times \frac{1}{a_s \text{ m}^2} \times \frac{1 \text{ kg}}{10^3 \text{ gm}}$$

$$= \frac{6.736\ G}{a_s} \times 10^{-3} \frac{\text{kg}}{\text{m sec}}$$

where G = difference in gradients of load/angular velocity plots for stirrers concerned $\left(\frac{\text{gm sec}}{\text{pulse}}\right)$

a_s = difference in outside area of stirrers (m^2)

$\therefore$ Taking: Stirrers 1 and 2

$$\mu = 6.736 \times 10^{-3} \times \frac{(11.8 - 9.6)}{5.0} \times \frac{1}{1.9 \times 10^{-3} \text{m}^2}$$

$$= \underline{\underline{1.550 \frac{\text{kg}}{\text{m sec}}}}$$

Stirrers 2 and 3

$$\mu = 6.736 \times 10^{-3} \times \frac{(15.1 - 11.8)}{5.0} \times \frac{1}{2.85 \times 10^{-3}}$$

$$= \underline{\underline{1.560 \frac{\text{kg}}{\text{m sec}}}}$$

Stirrers 1 and 3

$$\mu = 6.736 \times 10^{-3} \times \frac{(15.1 - 9.6)}{5.0} \times \frac{1}{4.75 \times 10^{-3}}$$

$$= \underline{\underline{1.559 \frac{\text{kg}}{\text{m sec}}}}$$

The published value of the viscosity of glycerol at $19.5^{\circ}C$ (interpolated from ref 135) is $1.49 \frac{\text{kg}}{\text{m sec}}$ $\therefore$ mean error $\simeq 4.3\%$

An accuracy of this order was considered quite adequate, especially as most of the error could probably be attributed to local temperature variations in the liquid during the determination. The latter are impossible to avoid when using a wide flow field with a viscous liquid.

5.2 Main Viscometer Tests

i. Introduction

The aim of the initial work with the viscometer was to investigate the effect upon viscosity of as many as possible of the variables likely to influence the appearance and behaviour of the bed.

It is evident in retrospect that the test programme was perhaps rather haphazard, but this was governed by the desire to investigate new facets of flow behaviour, as they came to light.

It became clear as the initial testing proceeded, that the quantitative repeatability of the results was not good; although generally repeatability of form or qualitative trends was excellent. Much of this anomalous behaviour was eventually traced to variations in fluidising air humidity, even though precautions had been taken to maintain a constant humidity. The foregoing means that most of the early data obtained is not of quantitative usefulness because the testing conditions cannot be fully specified. However, this is not seen as a serious drawback. It is now realised that so many and complex are the factors affecting fluid bed flow, that extrapolation of data to conditions only differing slightly from those under which it was obtained cannot be expected to be precise.

Notwithstanding this, it is considered that the viscometer work has been useful in establishing trends of shallow bed flow behaviour which would have been difficult to observe with larger scale apparatus.

ii) Variation of Apparent Viscosity with Fluidising Velocity

The variation of bed viscosity with fluidising velocity was examined in detail for many different fluidising conditions. However the general shape of the curves obtained was always similar and it is pertinent to discuss this first before considering the effect of individual variables.

The tests were in all cases performed by increasing the fluidising air flow to a point just below the onset of elutriation of particles and noting the torque required to turn the rotor at the desired angular velocity. The fluidising velocity was then progressively reduced until the bed became defluidised and the rotor torque at the appropriate speed noted for each fluidising velocity. The latter procedure was used rather than increasing the fluidising velocity from zero in order to eliminate differences in behaviour due to the initial packing conditions. The latter can influence bed behaviour well above Umf, especially for wide size-range material. A further difficulty with wide size material is that segregation can occur even at quite high fluidising velocities, under which conditions a long time is required before a steady state is reached.

The data obtained from the above test does not, strictly speaking, yield a true viscosity versus fluidising velocity curve unless the flow is assumed Newtonian. If the flow is not Newtonian, firstly the true rate of shear is not constant, and secondly the viscosities obtained are point values rather than tangents to a true stress versus shear rate curve. The alternative, to obtain true viscosity versus fluidising velocity, is to obtain a family of stress/shear rate curve at different fluidising velocities; and extract the data so obtained to plot a single curve of viscosity versus fluidising velocity at a particular shear rate. This would be an extremely laborious process, and several trials runs indicated that the resultant curves only differed significantly from the approximate ones in the region around U_{mf}, where the flow is very non-Newtonian. The flow is generally very unpredictable near U_{mf}, and also highly viscous, so that this region is of little interest in an engineering context. For this reason it was decided that the approximate method would be adequate, at any rate for the initial qualitative work.

FIG 5.2

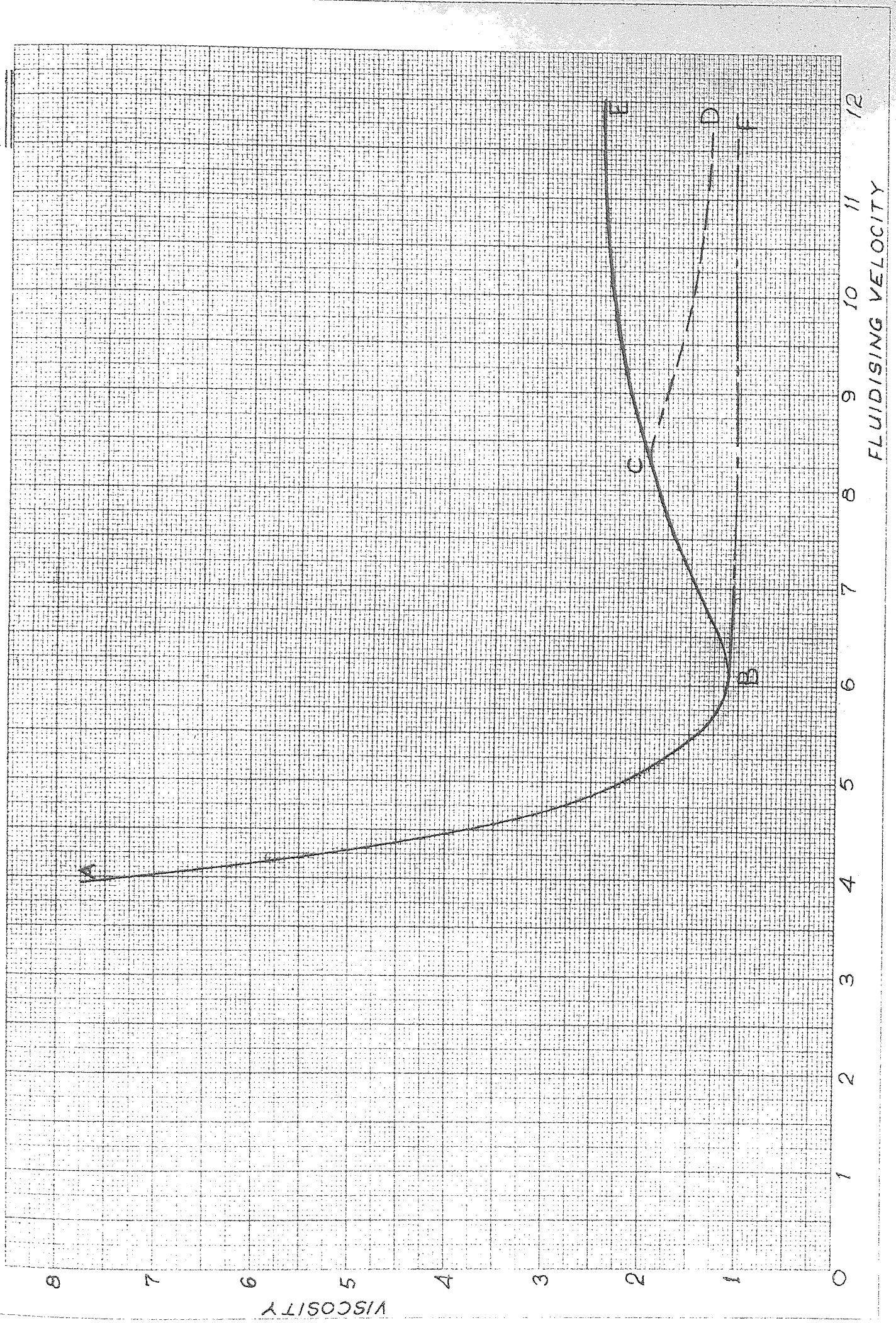
VISCOSITY vs. FLUIDISING VELOCITY - TYPICAL CURVES.
VISCOSITY
FLUIDISING VELOCITY
0
1
2
3
4
5
6
7
8
9
10
11
12
A
B
C
D
E
F

VISCOSITY AND PRESSURE DROP ACROSS BED vs. FLUIDISING VELOCITY
FOR DUNE SAND SAMPLES

FIG 5·3

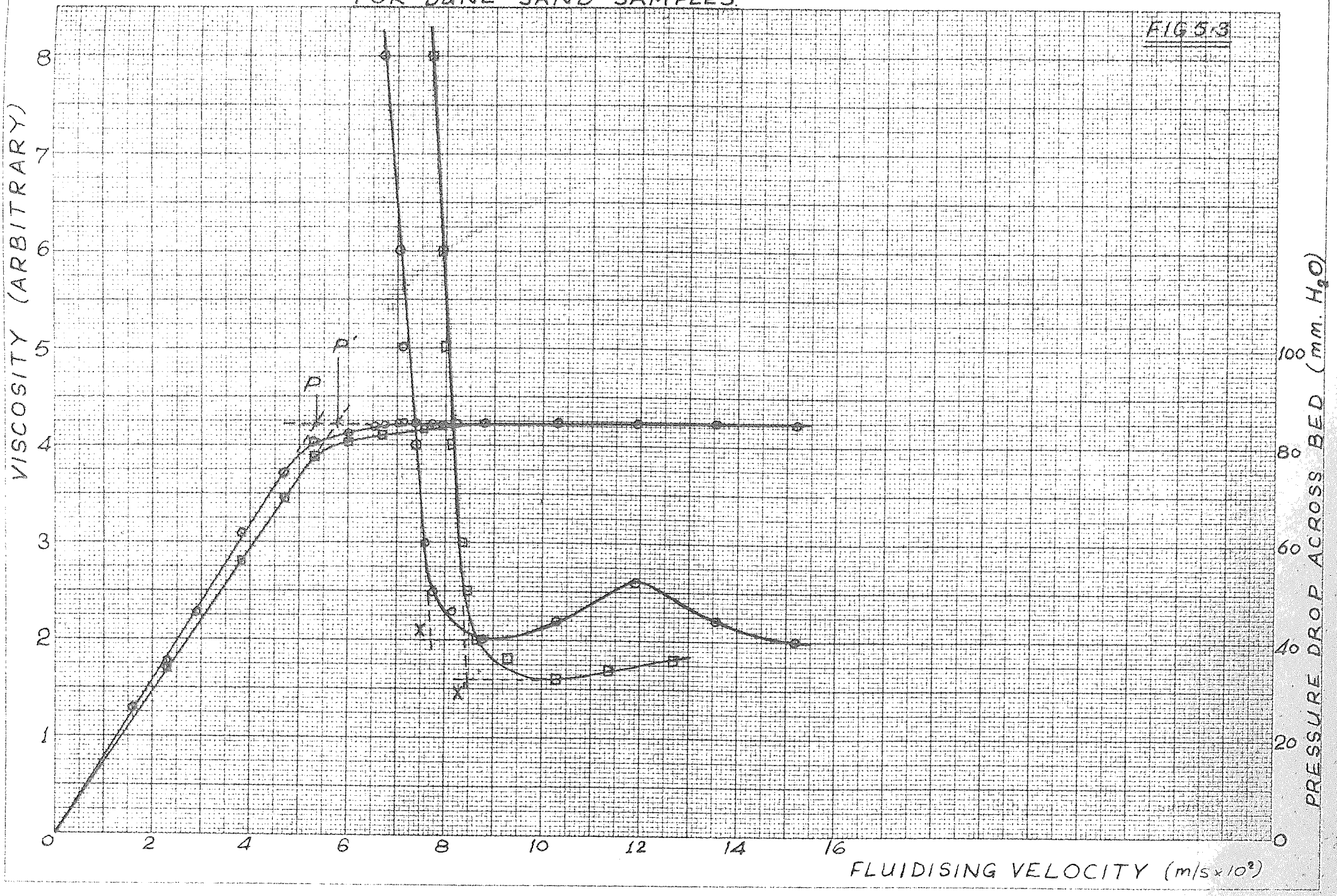

The manner in which "viscosity" varies with fluidising velocity has been observed by many previous workers under various conditions (see section 2, part 3.1).

The curves obtained for shallow beds in the present work are similar in general form to those reported by most previous investigators. Results typical of those obtained are presented in Figure 5.2, in which three types of behaviour are evident. In all cases, as the fluidising velocity is increased, the viscosity first falls sharply to a minimum at the point 'B' on Figure 5.2, which is at a velocity of about 60 mm/sec in this case. It is useful here to give a name to the point 'B', and it will be termed the "minimum apparent viscosity" of the bed. By plotting the pressure drop across the bed as well as viscosity against fluidising velocity as in Figure 5.3, it is evident that the bed does not achieve any substantial fluidity until well beyond the point normally defined as "minimum fluidisation". (The latter is the point P on Fig 5.3 at the intersection of the tangents to the two sections of the pressure drop curve). The exact fluidising velocity at which the minimum viscosity occurs is difficult to decide. However, by drawing a horizontal tangent through the minimum viscosity, and another to the steep part of the curve a more definite point X is obtained which may be used to compare the behaviour of the different materials. This point could perhaps be described as the "Flow Deterioration Velocity" since below this velocity the viscosity increases so rapidly that the flow properties would cease to be useful in an engineering situation. The flow deterioration velocity does not appear to bear any simple relationship to the minimum fluidisation velocity.

After the viscosity has fallen to its minimum value, at B on Fig 5.2, it normally increases again slowly with rising fluidising velocity, and may continue to rise until elutriation commences as in BE on Fig 5.2.

Alternatively, it may rise at first after reaching the minimum and then stabilise or even fall slightly with rising velocity as indicated by curve CD. In some circumstances the viscosity appears to remain constant, after falling to the minimum, as shown in BF on Fig 5.2. The latter behaviour has been associated by previous workers with particulate fluidisation, but was frequently observed in the present work which has been concerned only with materials which bubble at or almost immediately after fluidisation.

The above behaviour patterns were explained earlier[102] by considering the way in which gas passes up through the dense phase of the bed. Over the section AB of figure 5.2 the dense phase is thought to be expanding fairly homogeneously with increasing airflow (though clearly some bubbling is also occurring) thus allowing good particle mobility and therefore low viscosity. If the viscosity then follows curve BF, it is thought that the dense phase remains homogeneous whilst the extra gas flow is accommodated by increased size or number of bubbles. This type of behaviour was most often, though not always, found in very shallow beds of smaller material possessing the familiar even, rhythmic bubbling pattern with perhaps less gross particle circulation than in deeper beds.

The cases in which the viscosity increases with rising air flow are attributed to two main phenomena. The first is that the bubbles, as they rise through the bed and coalesce, drain some gas from the dense phase and give rise to areas of much reduced particle mobility and possibly even local defluidisation. Clearly even quite small areas such as this will result in a large increase in wall drag on an immersed surface and a corresponding increase in viscosity. Secondly, any gross circulation of particles upward and downward through the rotor, caused by ascending bubbles, will require an extra torque on the rotor in order to impart angular acceleration to the particles as they pass through it. Clearly

both the latter phenomena violate the concepts of laminar liquid flow, but are nonetheless considered to be definite bed properties, which will be equally as important in other fluidised flow situations as in the viscometer. Also, both phenomena are more likely to occur at the top of deeper beds, and in cases where local particle mobility is reduced by inter-particle forces. The viscosity data obtained in such circumstances confirm this as is discussed in later sections.

The foregoing explanations cannot really be supported by direct experimental evidence, without undertaking studies of local voidage and particle mobility: but may provide at least some insight into what is going on within the bed.

There does not appear to be any very definite criteria by which the likelihood of any one of the above three trends occurring can be predicted. Indeed, in some cases different samples of the same material behaved differently at fluidising velocities both above and below the point of minimum viscosity. The latter point was, however, normally repeatable to within three or four per cent.

iii) Effect of Fluidising Velocity on Non-Newtonian Behaviour

Shear diagrams for a number of different fluidising conditions and materials are presented in figures 5.4 to 5.10. It is clear from the latter that flow behaviour generally becomes more Newtonian in character as the fluidising velocity is increased. Most of the tests are for a bed depth of 20 mm, for which condition the flow normally approximates to Newtonian behaviour above a superficial velocity of about 2 U_{mf}. At lower fluidising velocities the shear diagrams in all cases display shear-thinning (pseudo plastic) behaviour. This can be clearly attributed to the improvement in quality of fluidisation local to the rotor brought about by the shearing action.

SHEAR STRESS vs SHEAR RATE FOR 200 μm SILICA SAND.

FIG 5.4

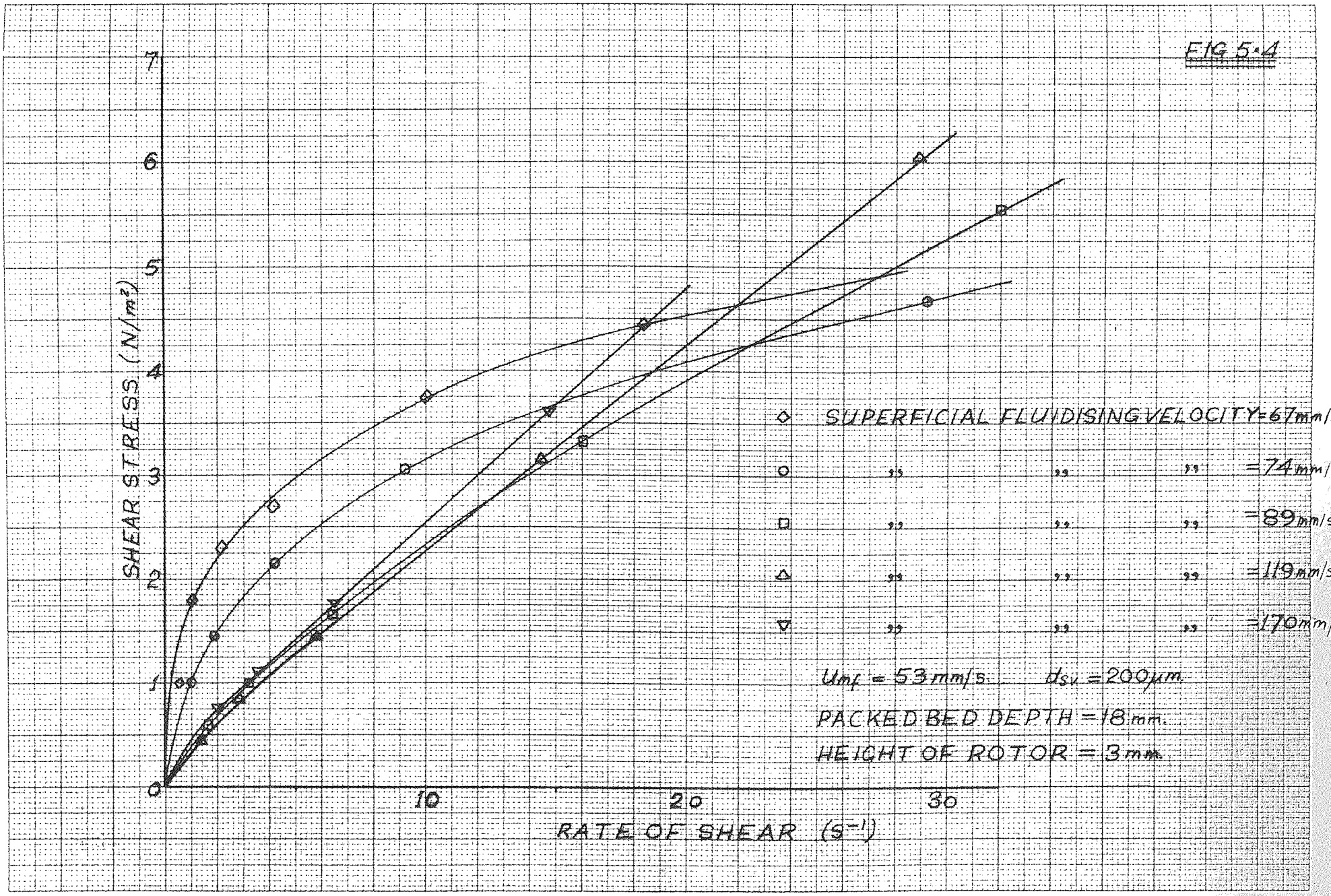

SHEAR STRESS vs SHEAR RATE FOR DUNE SAND.

FIG 5·5

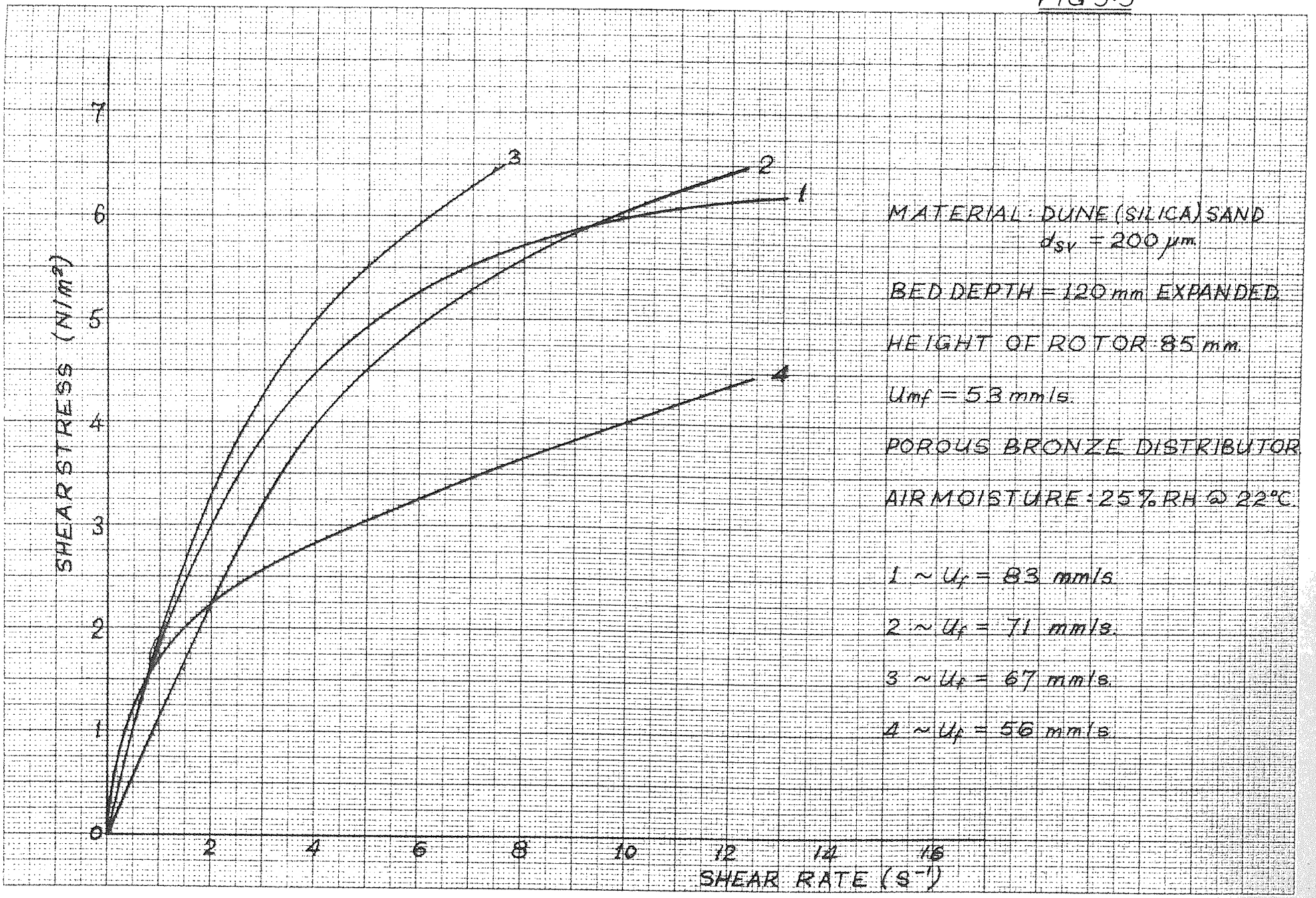

SHEAR STRESS VS. SHEAR RATE FOR 140μm DIA. ZIRCONIA

FIG 5·6

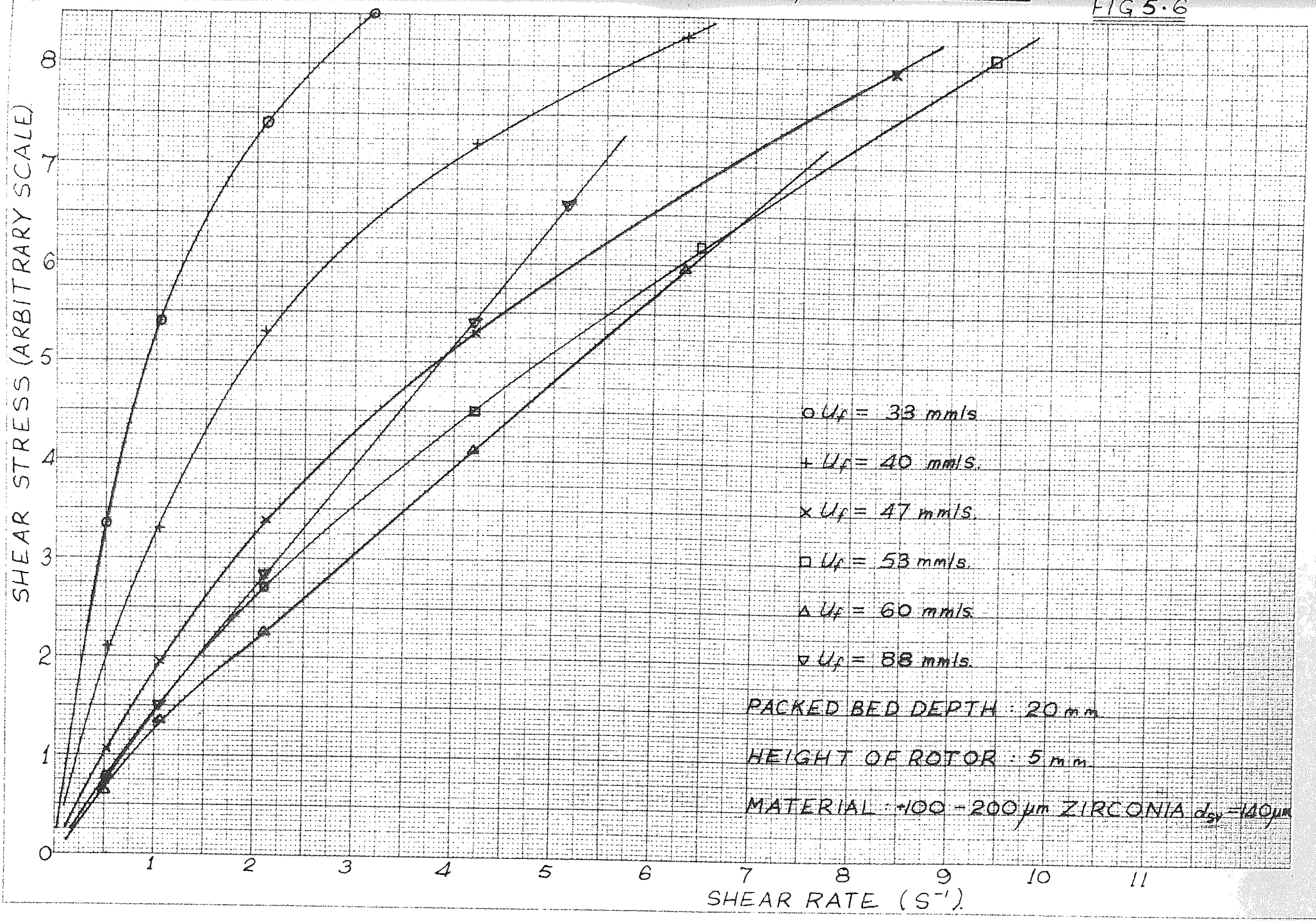

FIG 5.7

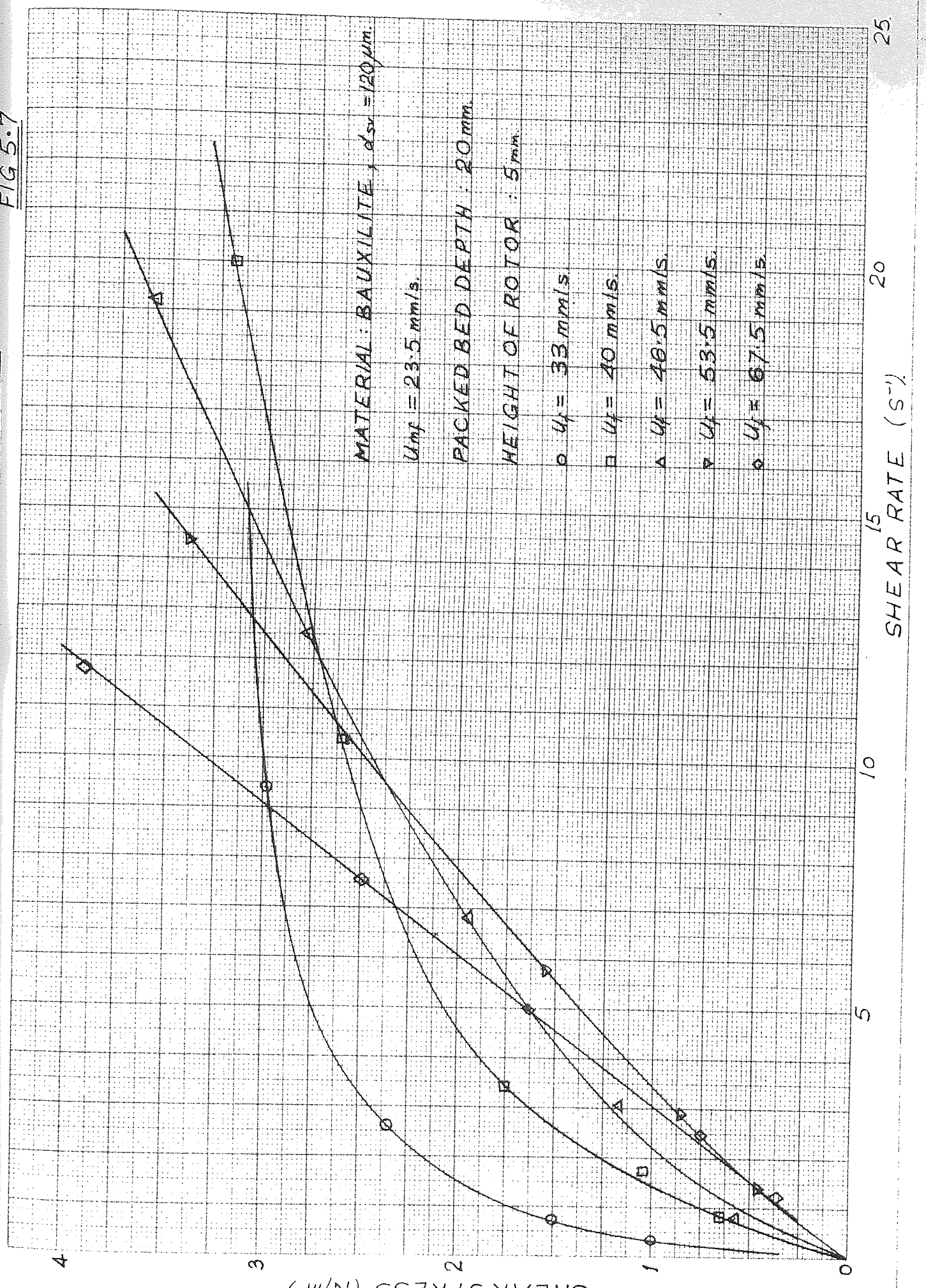

VARIATION OF SHEAR STRESS VS. SHEAR RATE FOR BAUXILITE.

SHEAR STRESS VS SHEAR RATE FOR 233μm DIA. COPPER SHOT.

FIG 5·8.

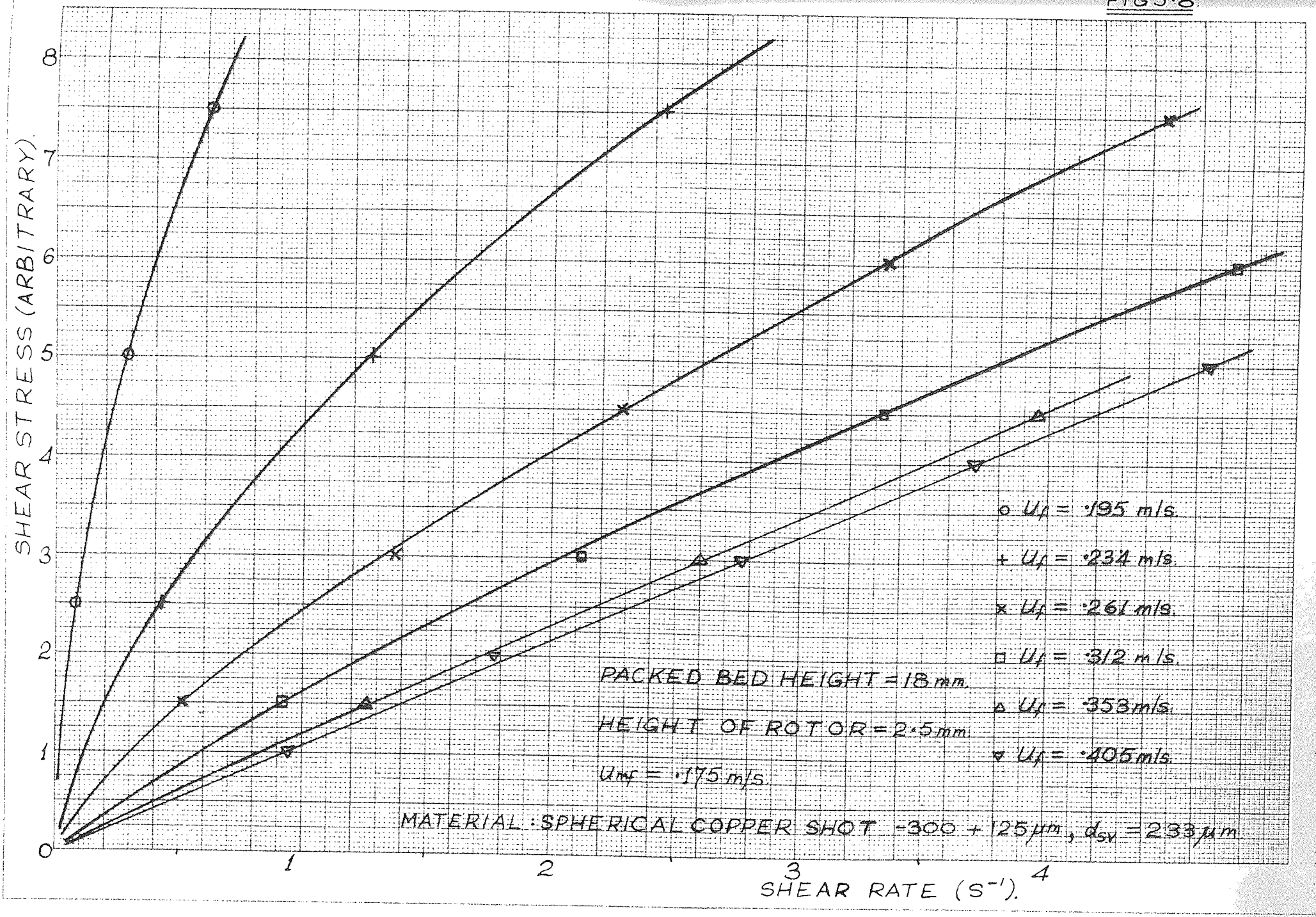

FIG 5.9

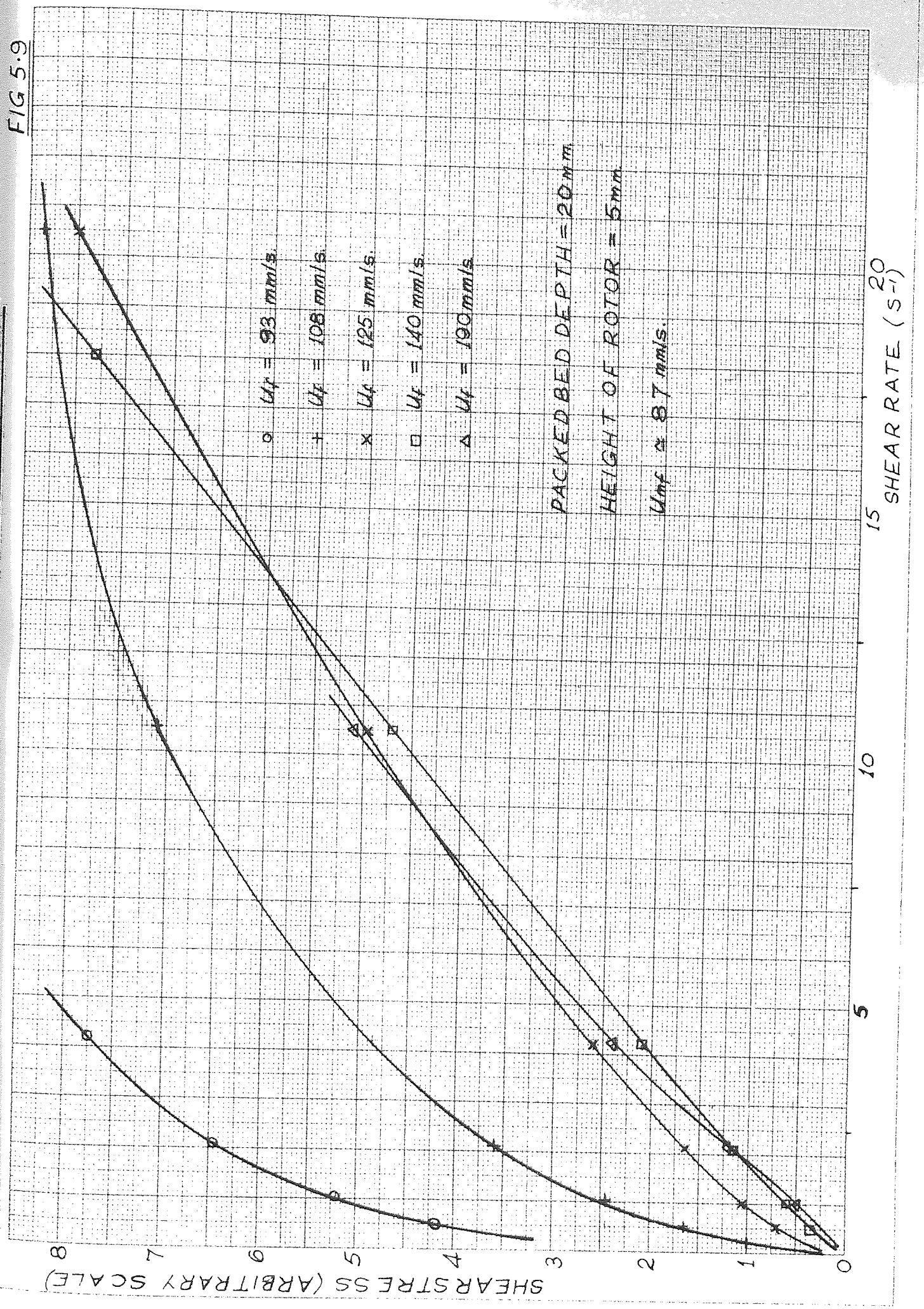

ROTATIONAL VISCOMETRY FOR FLUID BED COAL ASH.

SHEAR STRESS vs SHEAR RATE FOR SAND/ZIRCONIA/MOLOCHITE MIXTURE

FIG 5-10

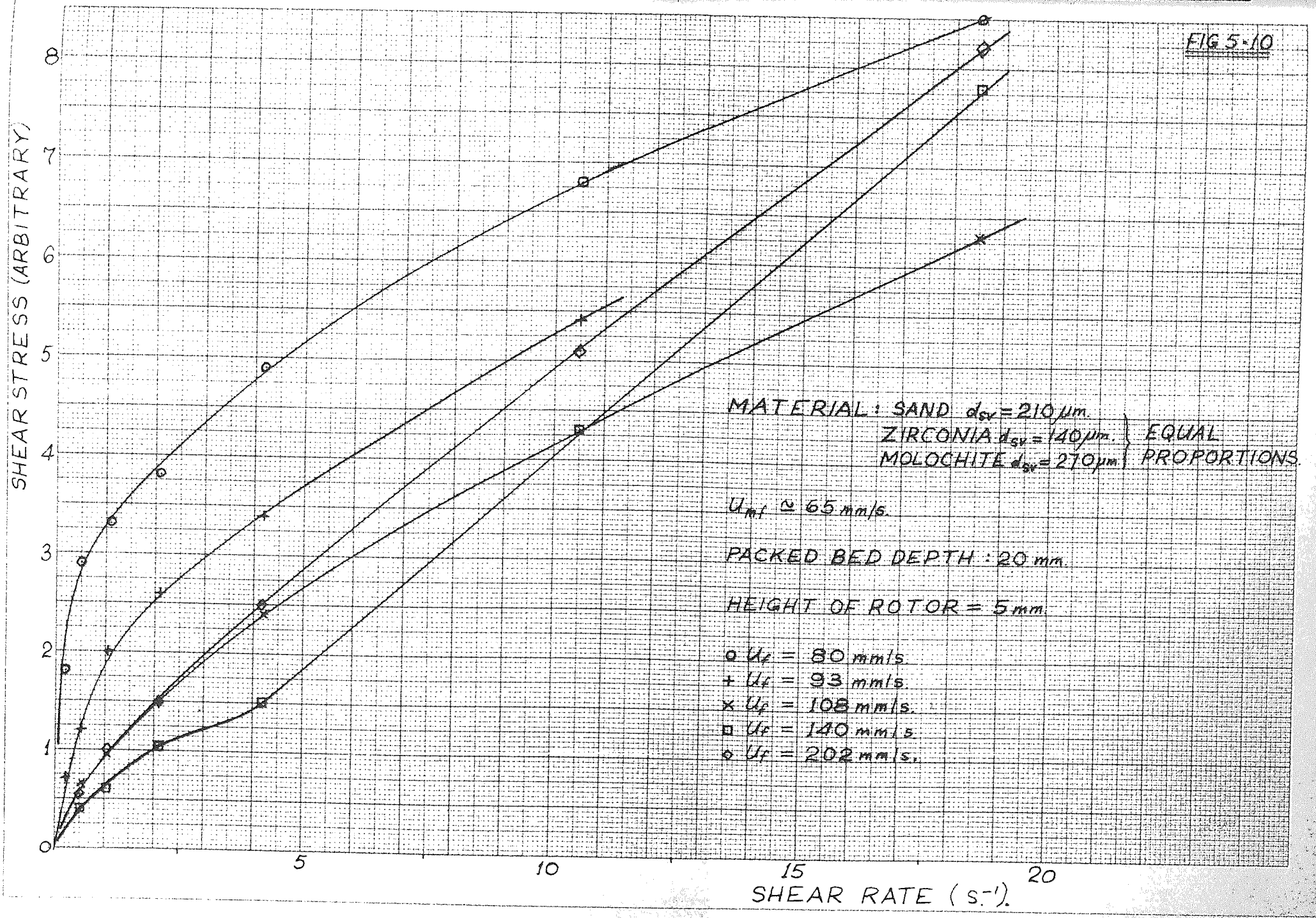

Visual observation of the bed surface under these conditions showed a well defined area of preferential bubbling around the rotor, often leaving the remainder of the bed surface almost innocent of bubbles. This preferential bubbling naturally increases particle mobility close to the rotor, thus allowing shear to occur much more easily than in the bulk of the bed. Such gross disturbance of the bed has previously been cited as limiting the relevance of small scale viscometer tests. However, under similar fluidising conditions, identical behaviour has been observed in fluidised channel flow (see below, section 4). In the channel, preferential bubbling occurred at the walls - again the region of maximum velocity gradient - and was accompanied by an improvement in flow, although the situation was somewhat complicated by segregation of the wide size-range material used. It is therefore considered that such phenomena again represent a definite property of the bed rather than merely an apparatus effect. However, such a flow situation certainly violates the condition of an infinite flow field and therefore limits the applicability of the concept of viscometric flows to incipiently fluidised beds.

The situation has some similarity to a Bingham fluid, for in both cases the shearing action causes a rearrangement of particle structure; though in the fluid bed case this is on a macroscopic rather than molecular scale.

Further similarity to Bingham behaviour was found for some materials at low fluidising velocities, in that a yield stress below which shear would not commence was evident. This effect was restricted to a few of the wide size-range materials tested, which start to fluidise over a range of gas velocities, so that the term minimum fluidising velocity has little meaning. A typical curve, for a wide size-range silica sand, is shown in figure 5.11: in which it can be seen that the behaviour is not

SHEAR STRESS vs RATE OF SHEAR FOR WIDE SIZE RANGE SILICA SAND.

FIG 5·11

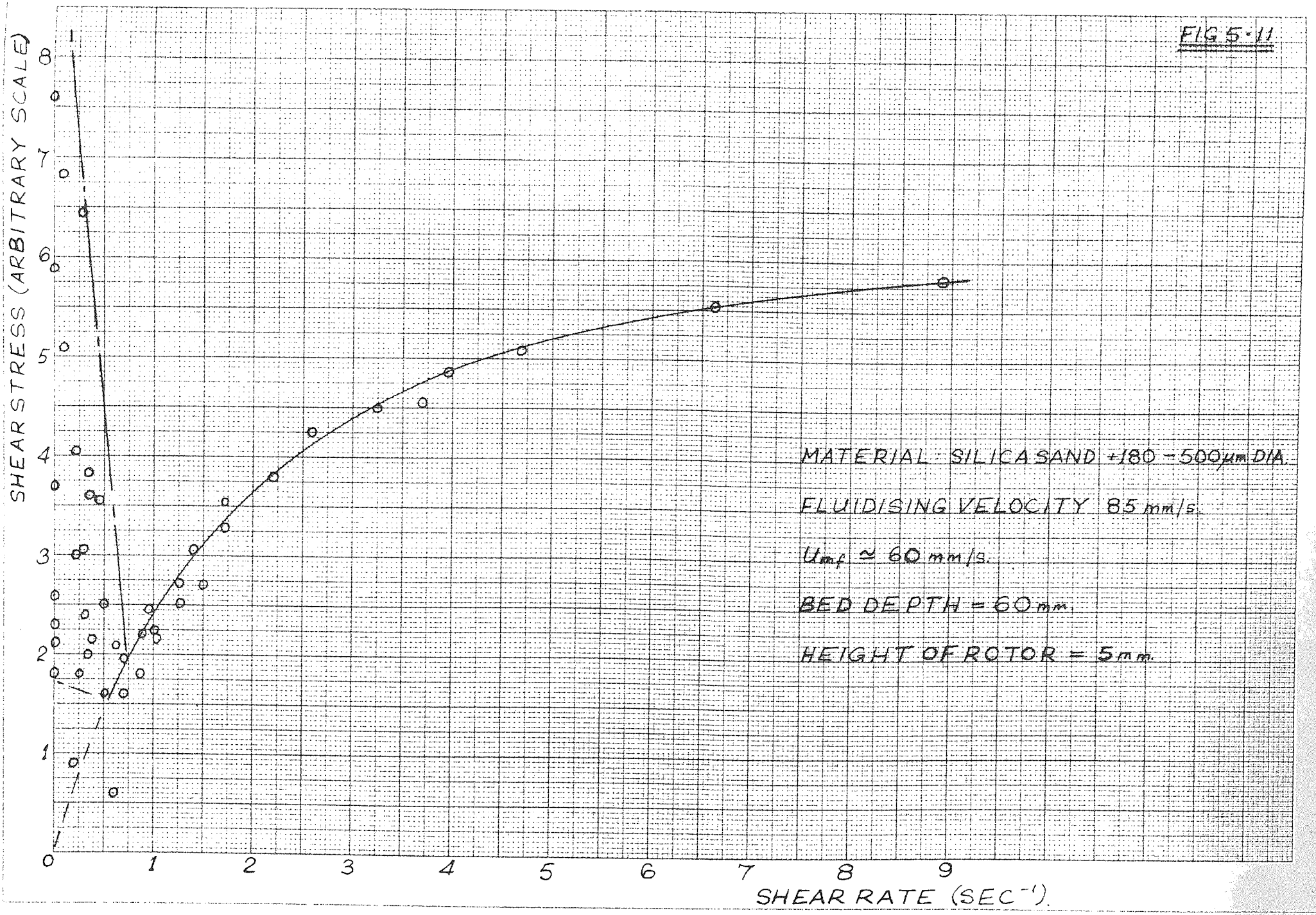

truly Bingham, since the yield value does not represent an extrapolation of the shear diagram through the shear rate axis. Indeed, it is apparent that the yield stress does not have any fixed value, but that once shear has started, flow will continue at stresses much lower than the yield stress. It is also clear from the scatter of points on Figure 5.11 that the bed is extremely unstable in this region, so that accurate measurements are impossible. The instability is caused by slight, and uncontrollable, redistributions of air flow over the bed area which could be the result of differential settlement of large and small material. Because of this instability no detailed study was made of behaviour at low shear rates and fluidising velocities. However it is now known that similar phenomena occur in a fluidised channel, (see Section 4) and can lead to total collapse of the flow at velocities well above minimum fluidising. This could be of considerable importance in industrial applications, particularly with respect to start-up and shut down of the plant. Similar behaviour has been observed by Schügerl[77,78] in what were termed "partially fluidised beds", though no mention is made of the unpredictability of behaviour at near zero shear rates that was observed in the present work.

It is noticeable from Figures 5.4 - 5.11 that the departure from Newtonian behaviour appears to be least for the denser materials, zircon sand and copper shot. These materials were characterised by a very even, regular, rhythmic bubbling pattern, which further confirms that non-Newtonian behaviour is due to local lack of homogeneity of the bed.

It is of interest that for the sands (Figs 5.4, 5.5) and also for Bauxilite (Fig 5.7) and coal ash (Fig 5.9) the shear diagrams for the lower fluidising velocities cross those for the higher ones as the shear rate is increased. This may also have occurred for the zirconia and copper (Fig 5.6), if higher shear rates had been used. These results are

probably again explainable in terms of preferential bubbling near the rotor by virtue of the shearing action; or possibly that particle separation from the rotor surface was occuring.

It would be expected from the foregoing that in the channel flow situation, where shear-rates of several hundred sec^{-1} are attainable, the flow properties at these low fluidising velocities (i.e. around 1·5-2·0 U_{mf}) would be markedly superior to the properties at higher velocities. This was not borne out in the present channel flow studies however, nor has it been reported by previous workers. It is thought that this may be due in part to segregation of large particles in the channel flow situation, which does not occur in the same manner in the viscometer. It is possible that, if such segregation could be reduced, the improved flow obtainable in the viscometer would be realised in the channel. This will be discussed in more detail later.

iv) Effect of Density of Fluidised Solids.

It was tentatively suggested earlier in this work[148] that the minimum apparent viscosity of the bed varies directly with the density of the fluidised particles. This seems a reasonable proposition, for clearly both the gravitational and buoyancy forces will be proportional to density for a given particle geometry, but it is difficult to verify with any accuracy. Other variables such as particle shape, effect of moisture, and bubbling behaviour cannot be eliminated when making comparisons between different materials. The only fact which can be stated with certainty is that dense particles tend to have higher viscosity than light ones, but it is doubtful if any precise law connecting the two properties could be propounded as yet.

The above observations apply to beds in which all the particles have the same density. Mixtures of different density particles may exhibit lower

viscosities than would be expected from the densities and proportions of the constituents (see 5.2 (v)).

(v) Effect of Particle Size and Size Distribution

The influence of particle size on bed viscosity is well illustrated in Figure 5.12. This is a plot of shear stress against fluidising velocity, at a constant shear rate, for a silica sand of wide size range sieved into three narrower cuts. It is evident from the curves that particle diameter has a relatively minor influence: a three-fold increase in mean particle size gives only a 50% increase in the minimum apparent viscosity. Clearly though, the fluidising velocity at which the minimum occurs increases with the size of particles because of corresponding increase in minimum fluidising velocity.

The fourth curve on Fig 5.12 is that for the unsieved sand from which the three narrow cuts were obtained. The minimum apparent viscosity of the raw sand occurs at a fluidising velocity appropriate to its mean particle size, but its magnitude is less than that given by a line passing through the minima for the sieved fractions. Also, it is noticeable that the viscosity remains near its minimum value over a greater range of fluidising velocities in the case of the raw sand. These two features suggest that wide size-range materials have superior flow properties to narrow cuts. Similar behaviour was reported by Matheson et al[67] for binary mixtures of narrow cut material, but their results are difficult to interpret since no details are given of the fluidising velocities. Their experiments are also open to doubt for other reasons which were discussed in Section 3. Geldart has suggested that Matheson's conclusions stemmed from an incorrect choice of mean particle diameter and has replotted the results[68] in a manner which shows that single and binary component mixtures of the same mean size have the same viscosity. The picture is

SHEAR STRESS VS. FLUIDISING VELOCITY FOR SIEVED FRACTIONS OF SILICA SAND.

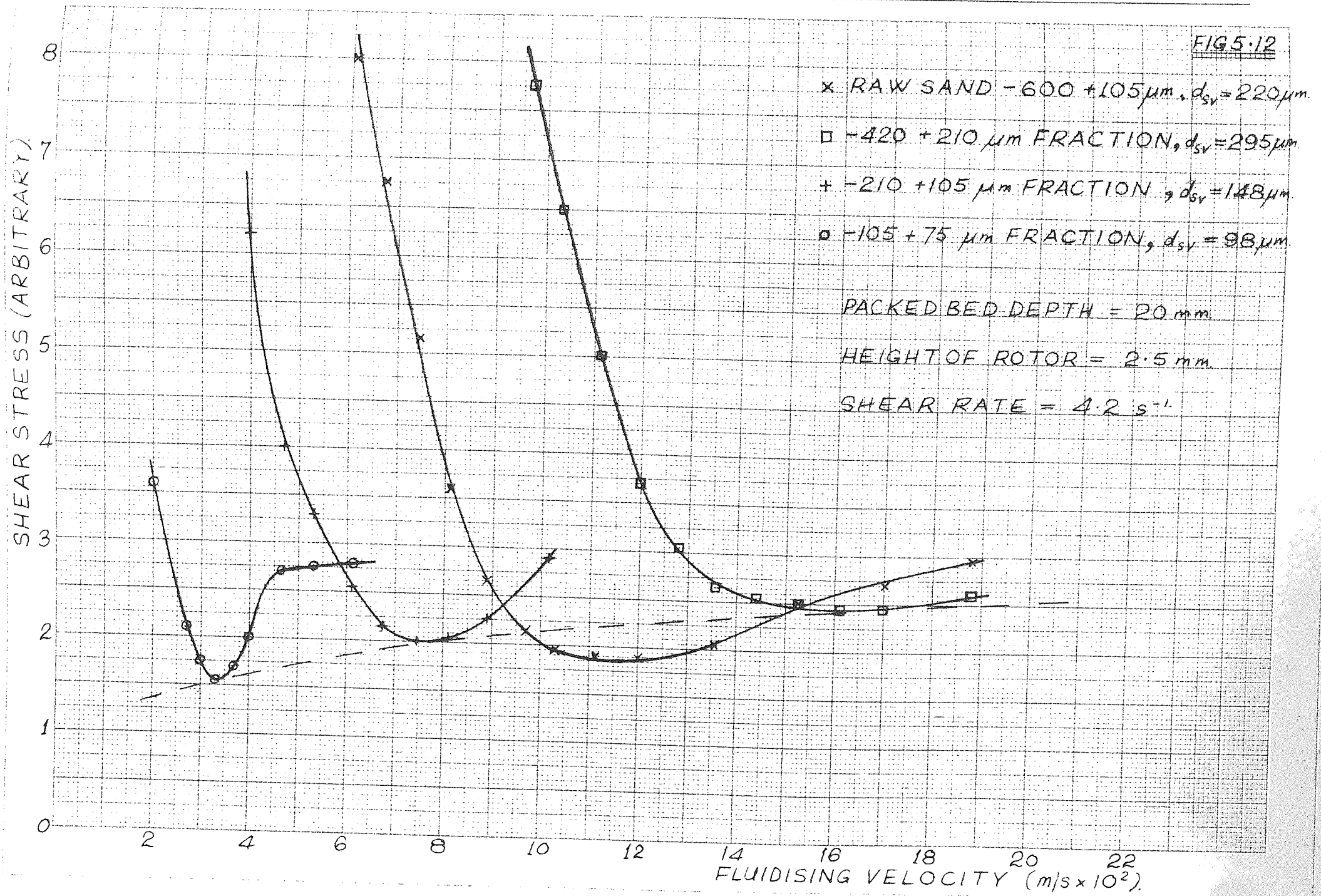

therefore somewhat confused, but what is of interest is that Matheson's results show more than an order of magnitude increase in viscosity for a particle size increase from 50 to 150 microns. Such a trend was certainly not evident in the present work.

There is little other information on the effect of size distribution on the viscosity of fluidised systems, although Elliott and Gliddon[96,126] have reported that a wide size distribution is beneficial to the flow of ash/water slurries in hydraulic transport. The best results were obtained with mixtures of maximum packing density. No measurements were made of bed density or expansion in the tests of Fig 5.12, but it seems likely that dense packing mixtures could be beneficial in fluidised systems also. This would be worth further investigation.

The main difficulty in using wide size-range material is segregation and settling of the large particles on the distributor. This is most likely at low fluidising velocities and with porous as opposed to pierced distributors. Work with channel transport has shown that the effects there are much worse than in a sheared stationary bed. Serious segregation has been observed even at fluidising velocities more than twice the minimum, although this may take several hours to develop (see below).

A possible method of overcoming such segregation is to mix small diameter dense material and larger lighter particles, so that the minimum fluidising velocities of the individual materials are closer together. This was tried for a number of silica sand/zirconia mixtures and the results are shown in Figures 5.13 - 5.15. It is clear that, in all three cases, the addition of a small proportion of coarse material to the fine zirconia gives a significant reduction in minimum apparent viscosity with no increase in fludising velocity. In Fig 5.13 where

FIG 5·13

305 μm SILICA SAND.

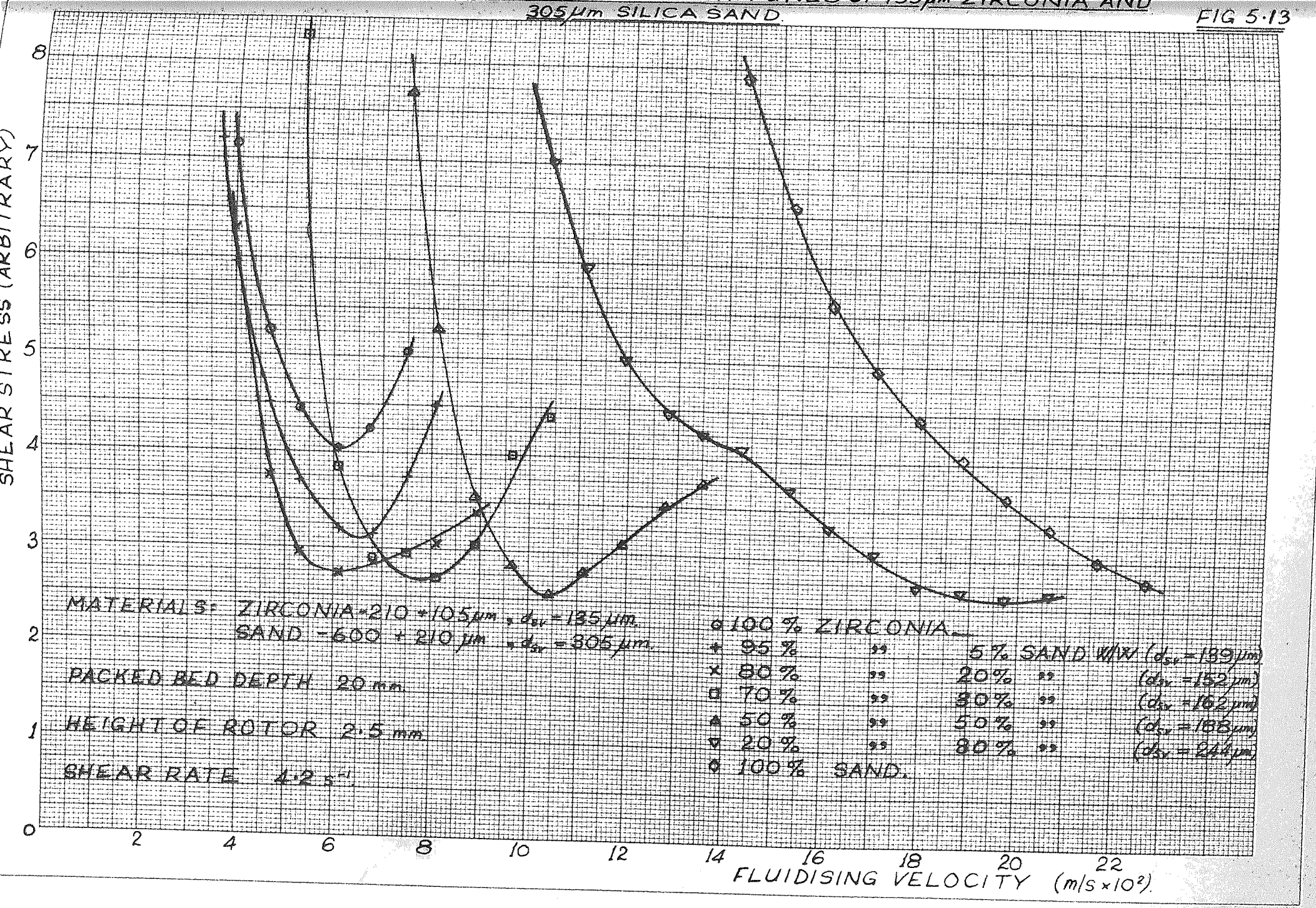

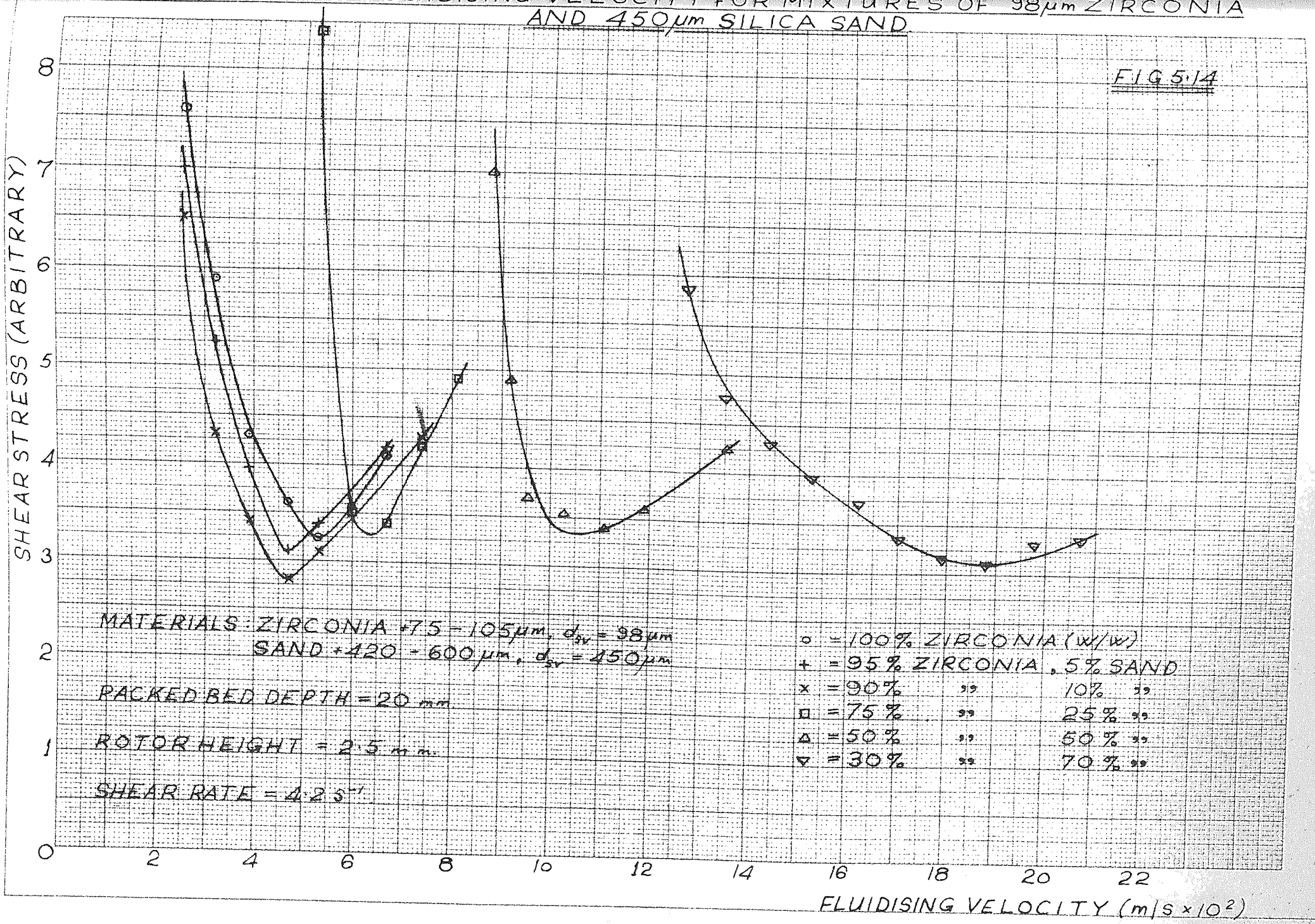
SHEAR STRESS vs. FLUIDISING VELOCITY FOR MIXTURES OF 98μm ZIRCONIA AND 450μm SILICA SAND
FIG 5.14
SHEAR STRESS (ARBITRARY)
FLUIDISING VELOCITY (m/s × 10²)
0
1
2
3
4
5
6
7
8
2
4
6
8
10
12
14
16
18
20
22
MATERIALS: ZIRCONIA +75 - 105μm, d_{sv} = 98μm
SAND +420 - 600μm, d_{sv} = 450μm
PACKED BED DEPTH = 20 mm
ROTOR HEIGHT = 2.5 mm.
SHEAR RATE = 4.2 s⁻¹
o = 100% ZIRCONIA (w/w)
+ = 95% ZIRCONIA, 5% SAND
x = 90% " 10% "
□ = 75% " 25% "
△ = 50% " 50% "
▽ = 30% " 70% "

SHEAR STRESS VS FLUIDISING VELOCITY FOR MIXTURES OF 98μm ZIRCONIA AND 295μm SILICA SAND.

FIG 5.15

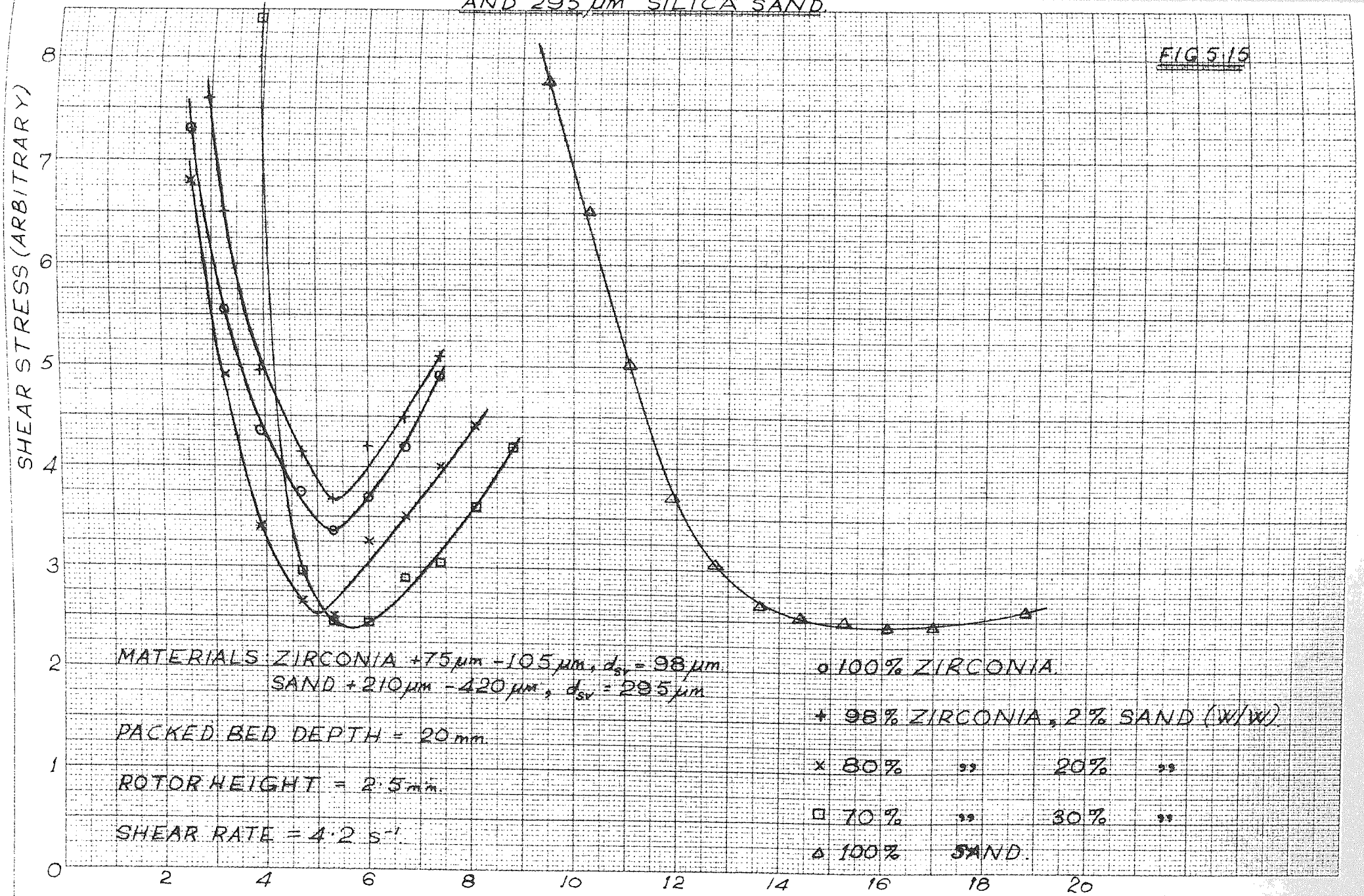

the viscosity of the pure zirconia is higher than that of the pure sand, the addition of only 20% of sand is sufficient to reduce the viscosity substantially to that of the pure sand. In Fig 5.14, where the size difference between the two fractions is greater, the viscosities of the pure materials are approximately equal. Here the addition of 10% of sand produces a mixture whose minimum apparent viscosity is below that of either of the component materials. Fig 5.15 shows curves for the Fine (d_{sv} = 98 μ) zirconia mixed with a medium-range cut of the silica sand. Here the addition of 2% of sand causes an increase in viscosity compared with the pure zirconia and not until the addition of 20% of sand is the viscosity markedly reduced.

Clearly such mixtures do not follow the previously noted trends regarding particle size and density effects. In Fig 5.13 for example, the 95/5 curve represents a 30% reduction in viscosity over the pure zirconia, and yet the particle size and density change only from 135 to 139 μm and 4.5 to 4.38 respectively. Thus Geldart's conclusions[68] regarding mean particle size are definitely inapplicable to mixed density distributions. The changes in behaviour probably arise from changes in particle packing arrangement or bubbling pattern. No measurements were made of bed expansion and bulk density: but these would in any case be difficult to interpret unless the volume of the bed occupied by bubbles could be simultaneously measured. There did not appear to be a great visual difference in bubbling behaviour of the pure and mixed materials, although the bubbling was perhaps slightly more even for the latter.

In most cases there was surprisingly little segregation once the point of minimum apparent viscosity had been reached. This was evident by visual observation of the bed surface, and by rapidly cutting off the

air supply and taking samples from the packed bed with a small spoon. Some separation could be detected in mixtures containing a high proportion of large material but this may have been due to fines filtering down through the coarse matrix after the air supply was cut off. However in those mixtures with up to about 25% of coarse sand the latter appeared to be almost completely suspended in the fine zirconia. This was true even of the materials used in Fig 5.14, whose individual minimum fluidising velocities differed by almost an order of magnitude. A possible explanation is that the fine material tends to fill the interstices in the matrix of large particles. This would give rise to much higher air velocities around the particles for a given superficial fluidising velocity and thus give improved particle mobility for a particular air flow rate.

The foregoing tests clearly show that it is possible to create free-flowing mixtures by blending materials of different densities. It remains to be confirmed that similar behaviour will occur in channel flow, but if so the method could profitably be applied to industrial processes in which such a choice of particle properties could be employed. It would also be of interest to examine mixtures of particles with a greater density difference than those so far tested, so that for a given size difference the fluidising velocities would be even closer together.

(vi) Effect of Depth of Bed and Location of Viscometer Rotor

It has been found that the minimum apparent viscosity of the bed increases with the bed depth, and also that the measured viscosity of a given bed varies with the axial location of the rotor relative to the distributor plate. Figure 5.16 shows the "viscosity profile" in the vertical direction through a bed of zirconia of 75 mm packed depth fluidised over two different distributors. It can be seen that with

the rotor placed 50 mm from the distributor, the type of plate has little influence on the viscosity once the bed is well fluidised. (This was also true at 60 mm, although the curves are not shown as they are virtually coincident with the 50 mm ones). However as the rotor is moved nearer to the distributor the viscosity increases markedly in the case of the pierced plate, whereas the converse is true for the porous plastic plate. In the latter case the viscosity measured with the rotor at 6mm from the plate is approximately 40% of its value with the rotor at a height of 50 mm.

The reason for this inviscid layer is thought to be that the fluidisation in this region tends to be particulate rather than aggregative. Since the bed possesses no surface tension like a liquid, there should be no tendency for bubbles to form on the plate at particular localities. Therefore until bubbles have grown by coalescence as they rise through the bed the fluidisation is likely to remain particulate, with reasonably uniform voidage and therefore good particle mobility. Quantitative results of a test on a silica sand fluidised at approximately 1.4 U_{mf} are shown in Fig 5.16A: these exhibit a similar improvement in viscosity near the distributor.

Confirmation of the existance of an inviscid layer near porous distributors is furnished by the surprisingly high heat transfer performance obtainable[66] with extended surface heat exchangers in shallow beds. More recent work by Atkinson[137] has shown that the heat transfer coefficient attainable is increased as the heat exchanger is moved nearer the distributor. Since heat transfer performance depends strongly on particle mobility it is to be expected that heat transfer and viscosity data will exhibit similar trends of behaviour. The results of a test by Atkinson using a bed of similar material and depth to Fig 5.16 are plotted in Fig 5.19, in which it can be seen that the

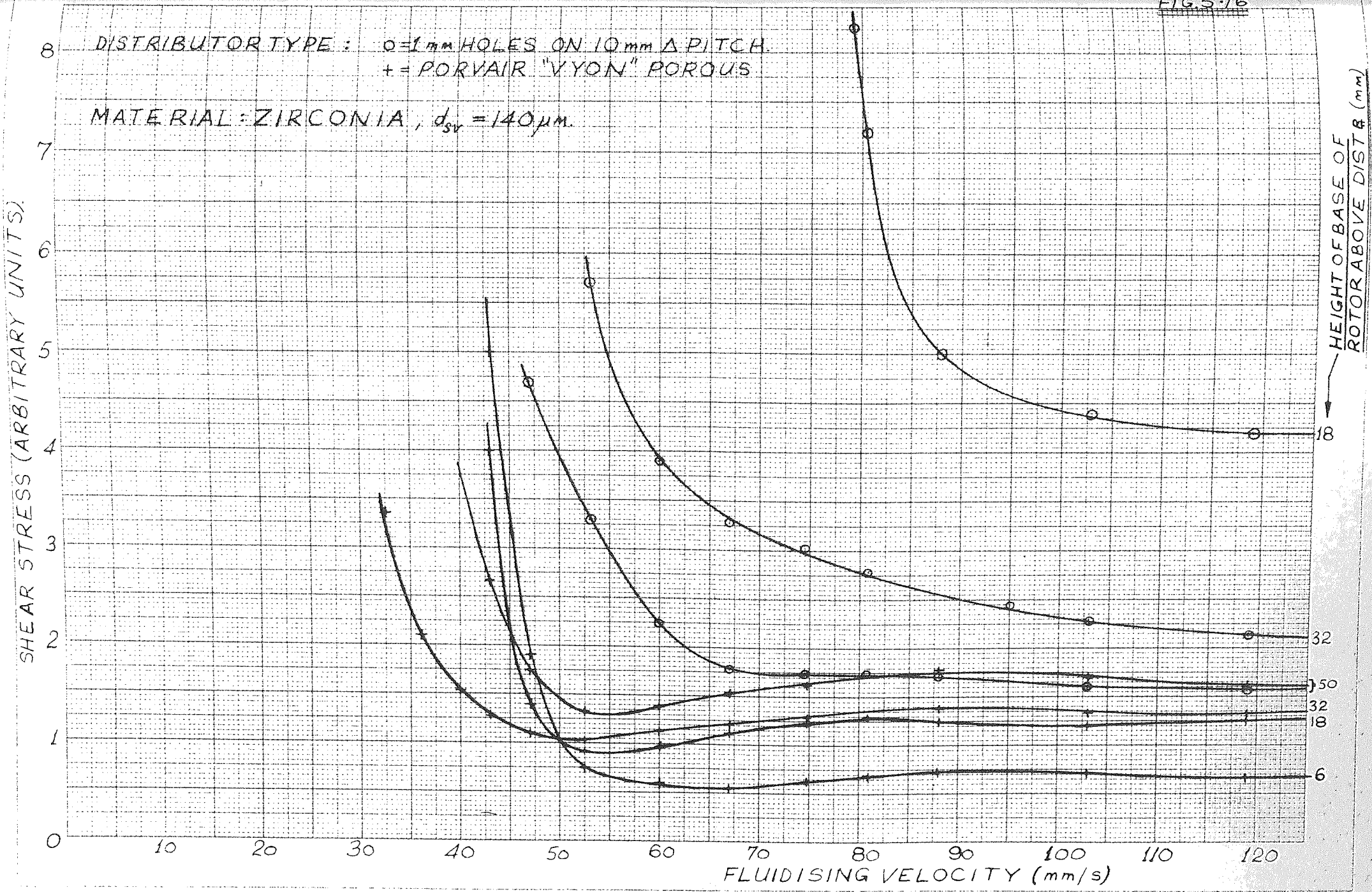
DISTRIBUTOR TYPE : o = 1 mm HOLES ON 10 mm △ PITCH.
+ = PORVAIR "VYON" POROUS
MATERIAL : ZIRCONIA, d_{sv} = 140 μm.
SHEAR STRESS (ARBITRARY UNITS).
FLUIDISING VELOCITY (mm/s)
HEIGHT OF BASE OF ROTOR ABOVE DIST.A (mm)
0
1
2
3
4
5
6
7
8
10
20
30
40
50
60
70
80
90
100
110
120
18
32
50
32
18
6

FIG 5.16A

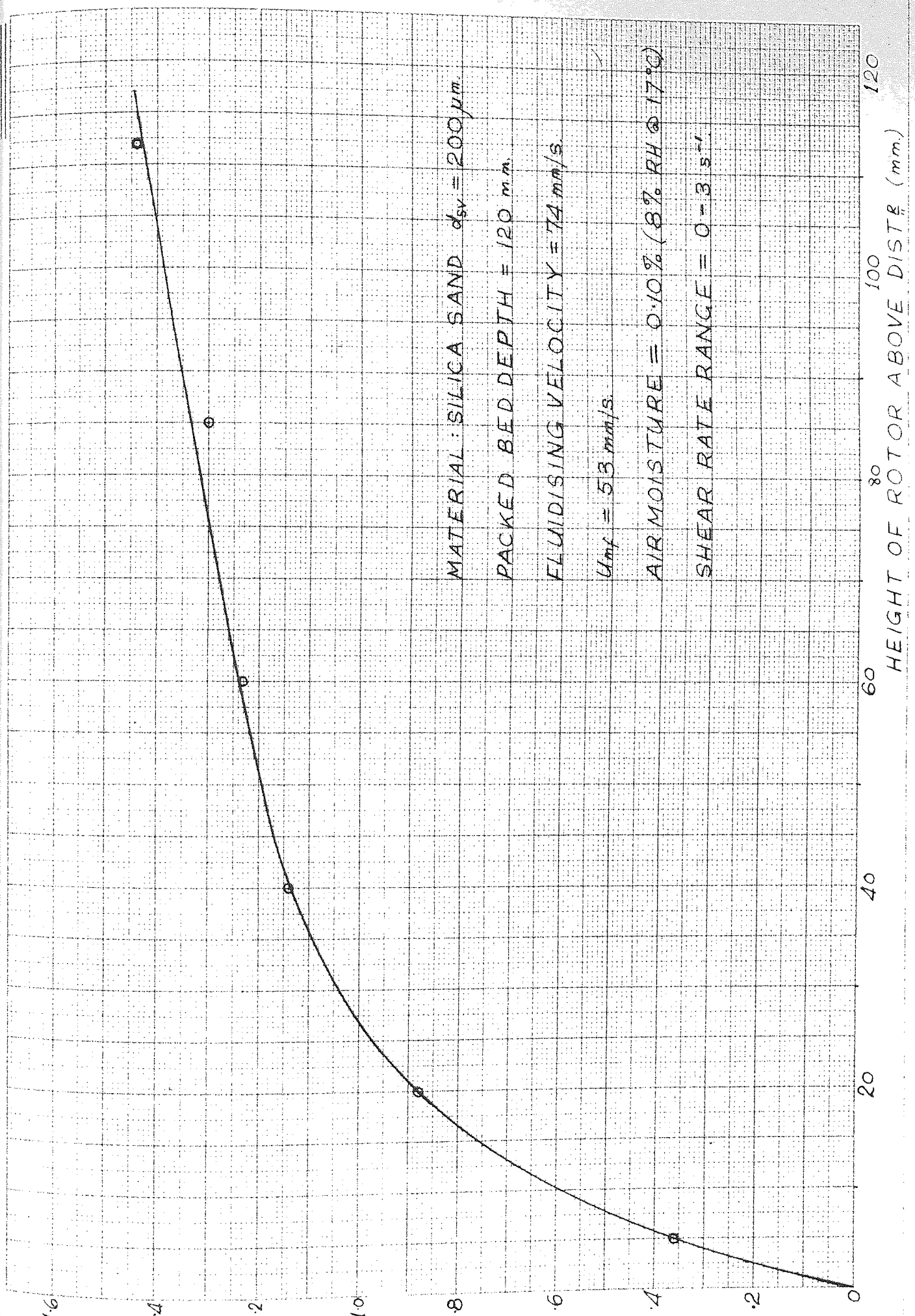
MATERIAL : SILICA SAND $d_{sv} = 200 \mu m$
PACKED BED DEPTH = 120 m.m.
FLUIDISING VELOCITY = 74 mm/s.
U_{mf} = 53 mm/s.
AIR MOISTURE = 0·10% (8% RH @ 17°C)
SHEAR RATE RANGE = 0 - 3 s^{-1}
VISCOSITY (Kg/m.s)
1·6
1·4
1·2
1·0
·8
·6
·4
·2
0
20
40
60
80
100
120
HEIGHT OF ROTOR ABOVE DISTR (mm.)

conditions for best heat transfer are also those in which the viscosity is lowest.

In the case of a pierced distributor, the area near the plate comprises alternate regions of particles with a high vertical velocity entrained in the gas issuing from the holes, and virtually stagnant areas in between[138]. Neither of these is conducive to good particle separation and the resulting local viscosity is more than three times the value at a rotor height of 50 mm. It can also be seen that flow deterioration near the pierced plate occurs at a superficial velocity nearly twice as high as for the porous plate. This is again probably due to stagnant regions near the plate as a result of gas by-passing. Examination of the pressure drop versus fluidising velocity curves for these tests, Fig 5.20, supports this; for the pressure drop for the pierced plate is everywhere lower than that for the porous plastic one. It is interesting to note from Fig 5.20 that the pressure drops for both distributors are asymptotic to values which are less than that corresponding to the total weight of material in the bed. This suggests that either there are always some particles stagnant on the distributor surface, or that particles are in a dynamic equilibrium with the distributor surface in a similar manner to the molecules of a liquid and its containing vessel. This is at variance with the accepted postulation that a fluid bed is completely supported by the fluidising gas, but it appears to the author to be a more reasonable description of the real bed behaviour.

Results similar to those above were obtained for other materials under similar conditions and it is evident that the type of distributor plate used has considerable influence on bed viscosity, up to a distance of about 50 mm from the plate.

Tests with different distributors have not yet been carried out for fluidised channel flow, either in the present or previous published work.

The viscometer results clearly suggest that porous distributors would be preferable, especially for channels of low aspect ratio, but caution is necessary as the behaviour may be modified by the increased tendency to segregation at low fluidising velocities. It is possible that less segregation would occur with pierced than with porous plates. However, in view of the superior performance of the porous plate in the above tests, drilled plates were not used for any further experiments in the present work.

Figure 5.17 shows the effect of increasing the depth of the bed whilst the rotor is maintained at a fixed height of 5 mm above the distributor. It can be seen that the magnitude of the minimum apparent viscosity increases about fourfold as the bed depth is increased from 17.5 to 40 mm. The minimum occurs at a slightly lower fluidising velocity as the depth is increased; although it was found that the minimum fluidising velocity, as measured by the pressure-drop across the bed, did not change with the depth. A further point to note is that the viscosity remains near its minimum value for a much more restricted range of fluidising velocity as the depth is increased. The latter point was not evident with some other materials tested, though most deep beds showed a greater tendency for the viscosity to increase after reaching its minimum value than did shallow ones. This is attributed to lack of homogeneity.

Figure 5.21 shows the results of a similar test on a silica sand over a greater range of bed heights, at a constant fluidising velocity of about 1.4 U_{mf}. Here, as the bed depth approaches 120 mm (the maximum depth that could be used) the viscosity is increasing much more slowly. Thus it is possible that the viscosity at the base of the bed tends to a constant value as the depth is further increased.

The viscosity at the surface of the bed changes with depth in a similar manner to that at the base. Fig 5.22 shows how the viscosity

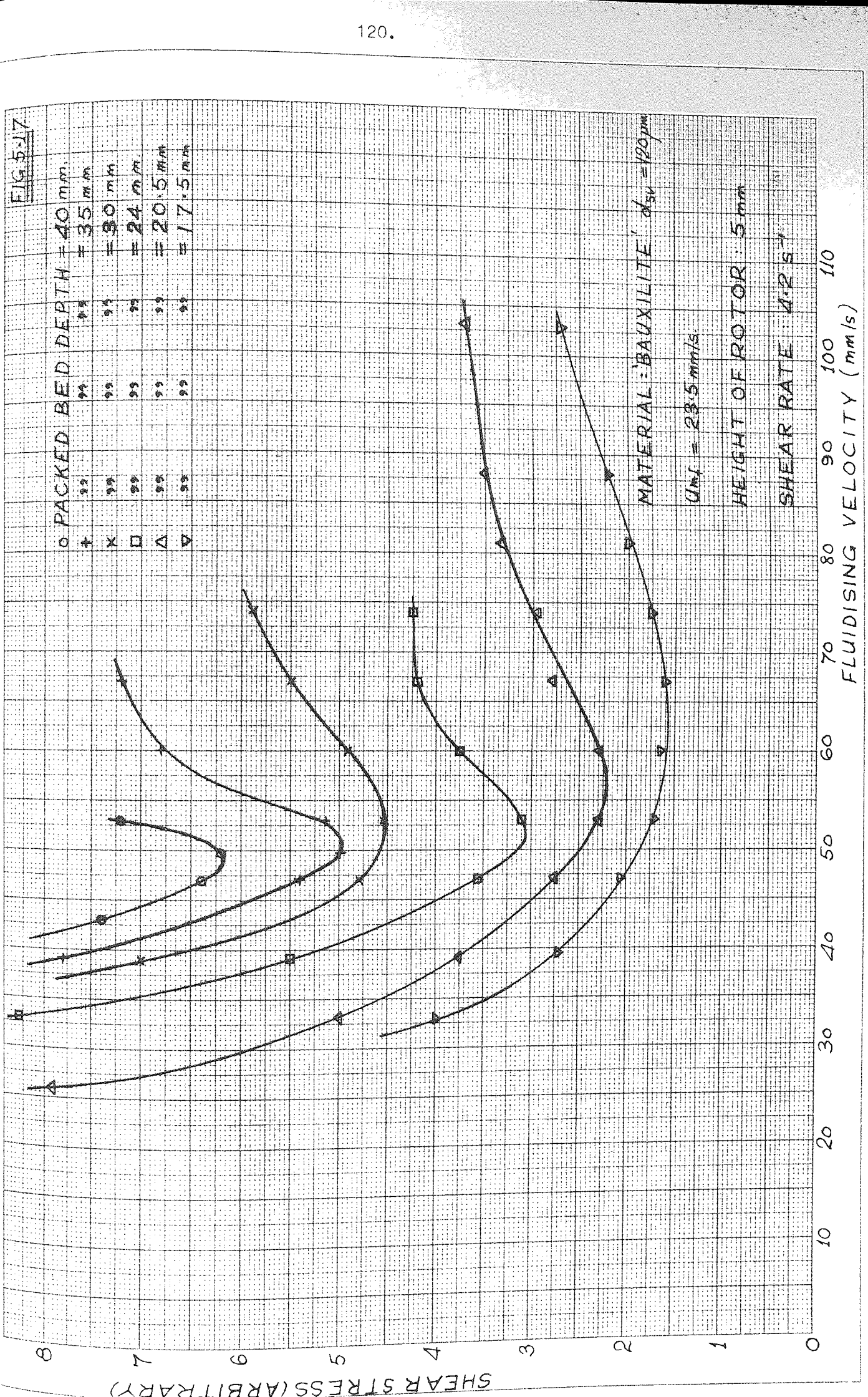
FIG 5.17
○ PACKED BED DEPTH = 40 m.m.
+ " = 35 m.m.
× " = 30 m.m.
□ " = 24 m.m.
△ " = 20.5 m.m.
▽ " = 17.5 m.m.
MATERIAL = 'BAUXILITE' d_{SV} = 120 μm
U_{mf} = 23.5 mm/s.
HEIGHT OF ROTOR : 5 mm
SHEAR RATE : 4·2 s⁻¹
FLUIDISING VELOCITY (mm/s)
SHEAR STRESS (ARBITRARY)
0
1
2
3
4
5
6
7
8
10
20
30
40
50
60
70
80
90
100
110

FIG 5·18

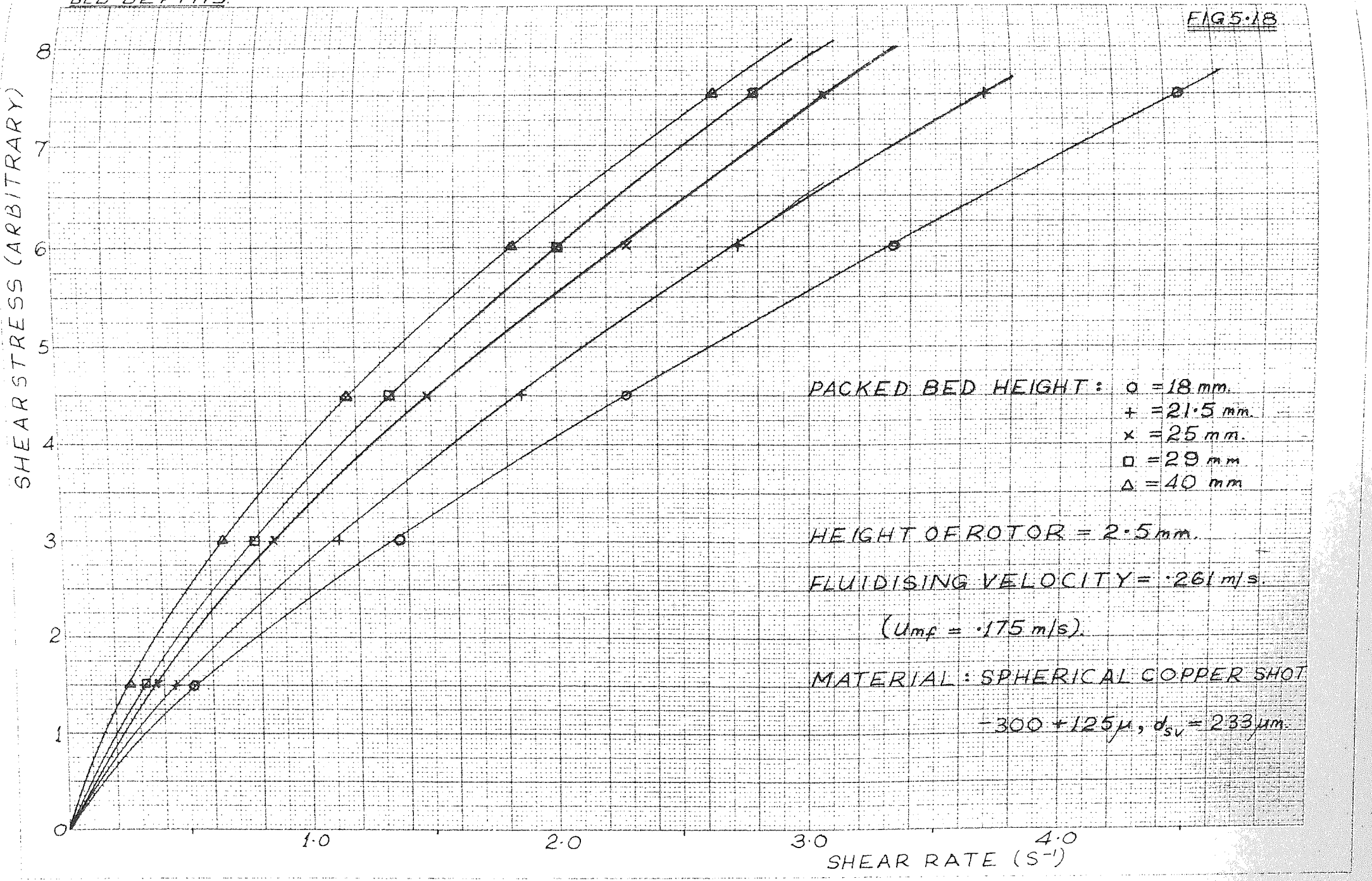
SHEAR STRESS (ARBITRARY)
0
1
2
3
4
5
6
7
8
1·0
2·0
3·0
4·0
SHEAR RATE (S⁻¹)
PACKED BED HEIGHT: o = 18 mm.
+ = 21·5 mm.
× = 25 mm.
□ = 29 mm
△ = 40 mm
HEIGHT OF ROTOR = 2·5 mm.
FLUIDISING VELOCITY = ·261 m/s.
(Umf = ·175 m/s).
MATERIAL: SPHERICAL COPPER SHOT
−300 +125 μ, dsv = 233 μm.

FOR DIFFERENT HEAT EXCHANGER POSITIONS. (ATKINSON. 157)

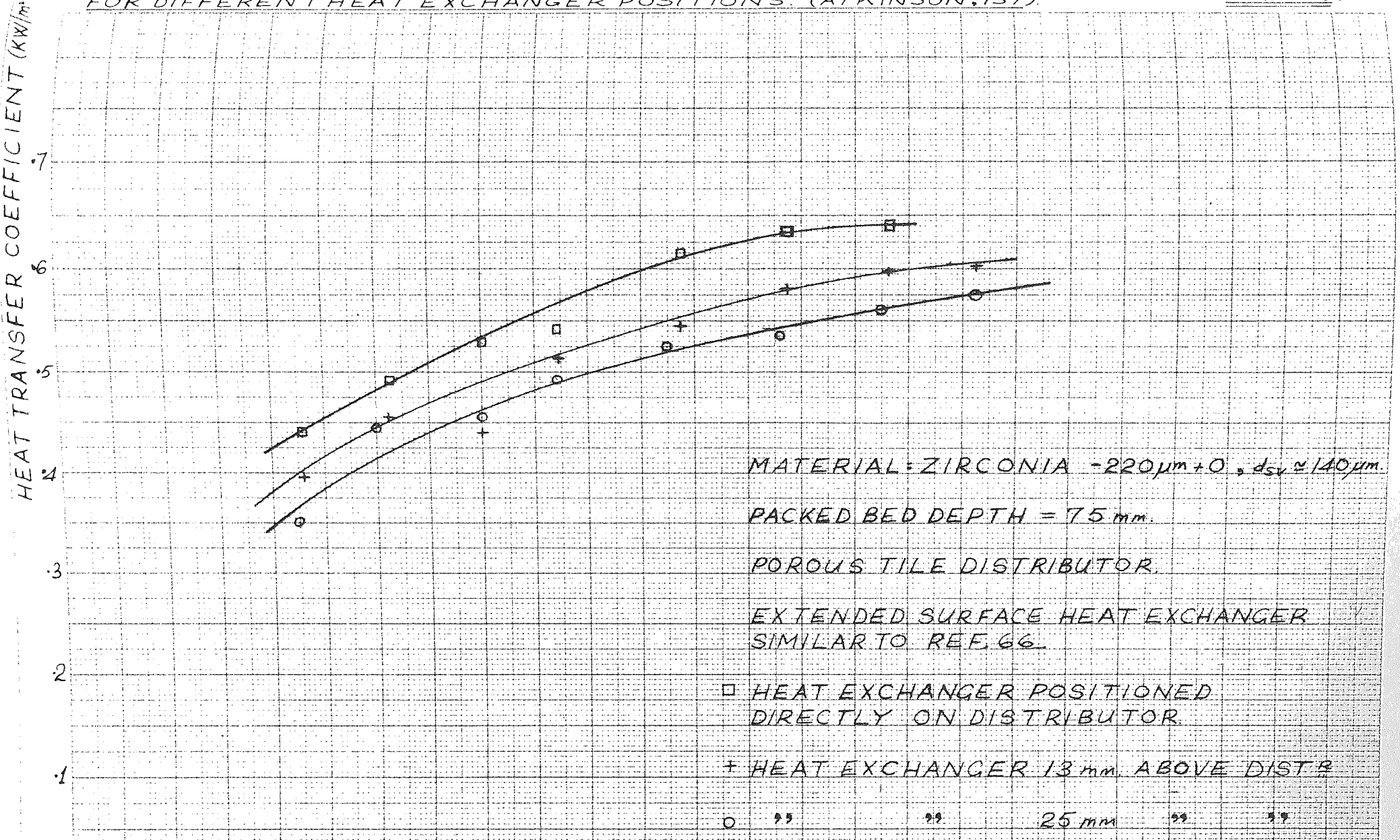

FIG 5·20

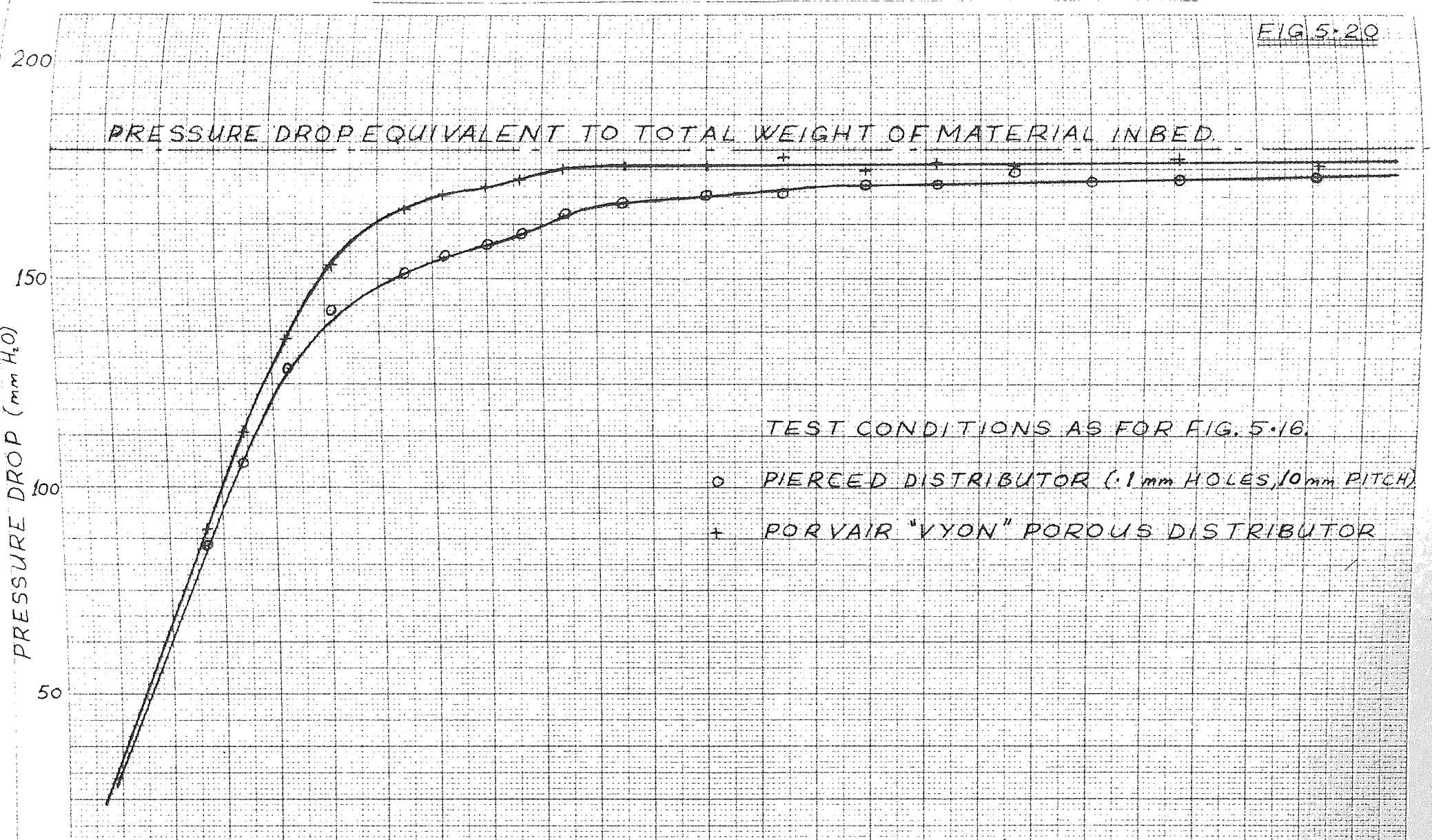
PRESSURE DROP EQUIVALENT TO TOTAL WEIGHT OF MATERIAL INBED.
TEST CONDITIONS AS FOR FIG. 5·16.
o PIERCED DISTRIBUTOR (·1mm HOLES, 10mm PITCH)
+ PORVAIR "VYON" POROUS DISTRIBUTOR
PRESSURE DROP (mm H2O)
0
50
100
150
200
10
20
30
40
50
60
70
80
90
100
110
120
FLUIDISING VELOCITY (mm/s)

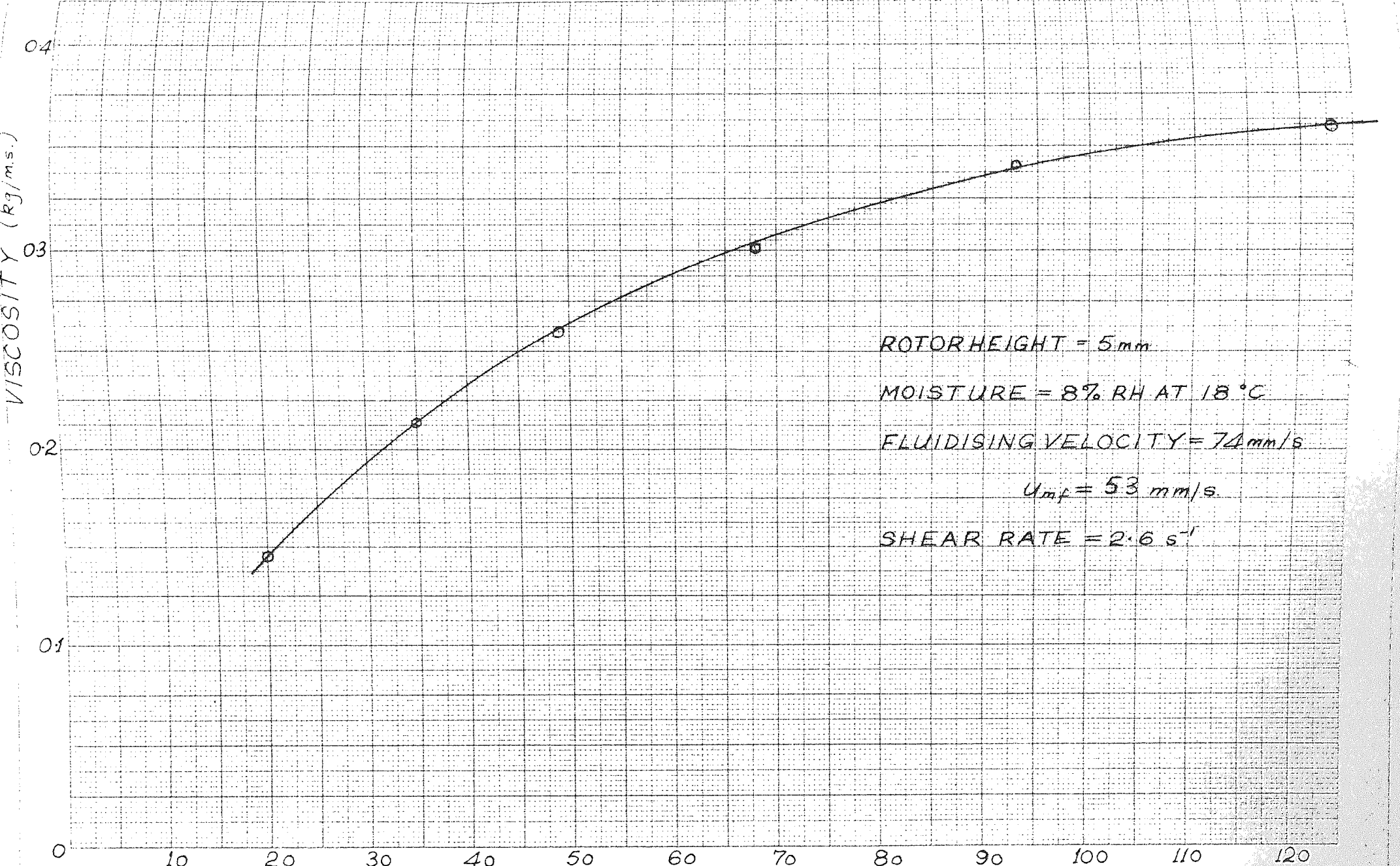
VISCOSITY (kg/m.s.)
0·4
0·3
0·2
0·1
0
10
20
30
40
50
60
70
80
90
100
110
120
EXPANDED BED DEPTH (mm) →
ROTOR HEIGHT = 5mm
MOISTURE = 8% RH AT 18 °C
FLUIDISING VELOCITY = 74mm/s
U_{mf} = 53 mm/s.
SHEAR RATE = 2·6 s^{-1}

VISCOSITY AT SURFACE OF ROTOR VS FLUIDISING VELOCITY FOR SAND AT DIFFERENT BED DEPTHS

FIG 5.22

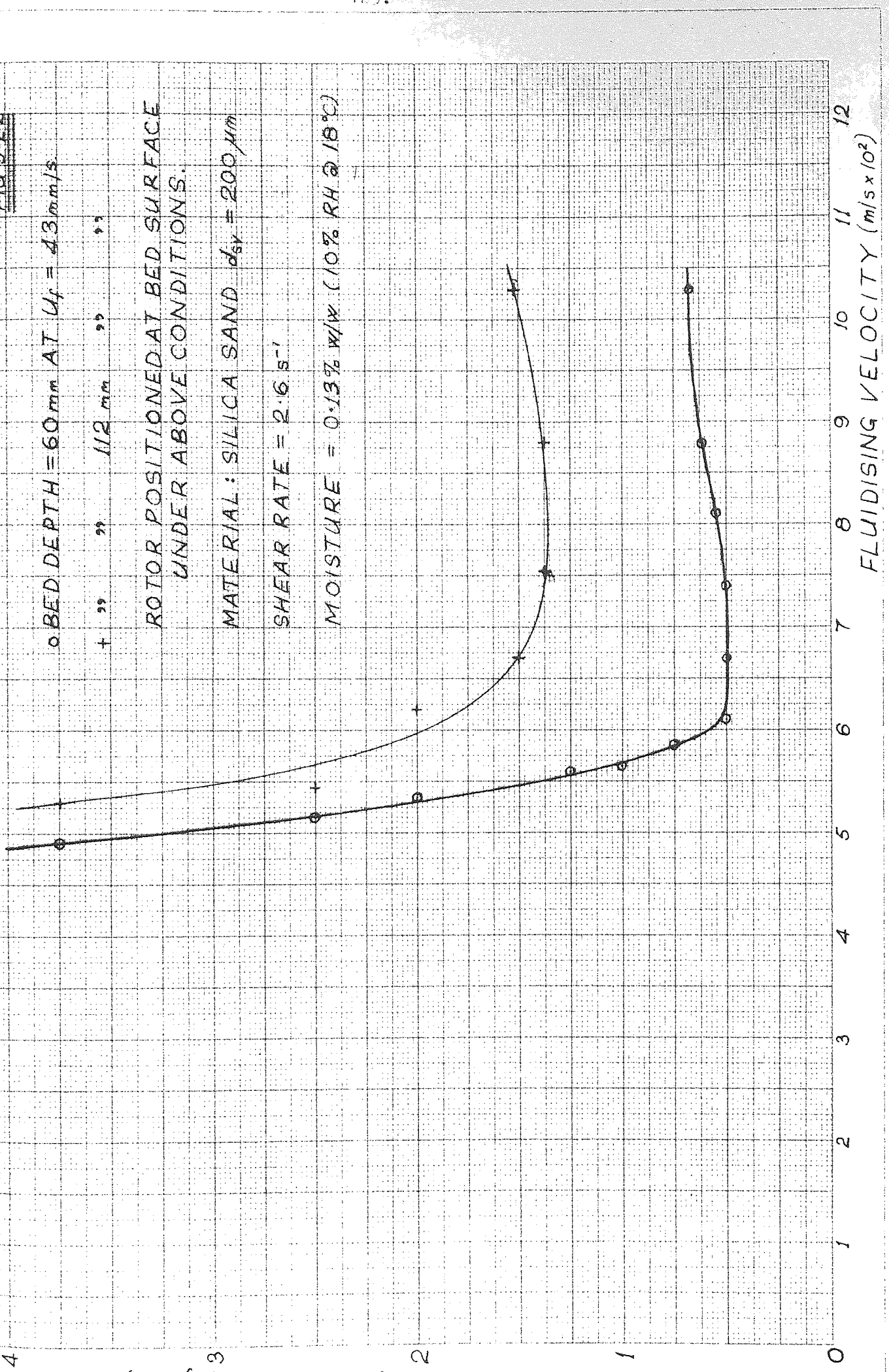

near the surface varies when the bed depth is increased from 60 to 112 mm. The material is the same is in Fig 5.21 and the surface viscosity is greater than the base viscosity under corresponding conditions since a porous distribution was used.

The influence of bed depth upon viscosity appears to be smaller in the case of denser material than for the lighter sands used for the majority of the tests. Figure 5.18 shows the shear diagrams for copper shot ($\rho \simeq 8.7$) at a number of bed depths. The viscosity is increased by about 60% as the depth increases from 18 to 40 mm. It is also apparent that there is little change in the non-Newtonian behaviour of the bed with depth. However it is likely that there would be a greater change in behaviour at lower fluidising velocities when the shear diagram becomes more pseudoplastic.

It is thought that the dependence of viscosity on bed depth is again a function of the homogeneity of fluidisation. The region in which the viscosity changes most rapidly - that is from about 20-50 mm bed depth - corresponds to that in which the bubbling changes from the even, rhythmic pattern typical of very shallow beds, to the more random bubbling associated with deeper beds. The latter are characterised by large bubbles 'exploding' at the surface causing solids efflux into the free-board, rather than the 'boiling' action of shallow beds. It is considered that the lack of homogeneity and possibly local defluidisation caused by such gross disturbances in deep beds are responsible for the poorer flow properties therein. Since the flow deteriorates so rapidly near the point of minimum fluidisation, very small regions of partial defluidisation would be sufficient to exert a large influence on the measured viscosity. A further factor is the increased particle circulation induced by the rising bubbles in deeper beds, which is likely to increase the measured viscosity as noted in part 5.2 (ii) above.

vii). Effect of Moisture Content of Fluidising Gas

The humidity of the gas used to fluidise the bed has been found to exert a marked influence on the flow properties of certain bed materials.

The effect was first detected as a lack of repeatability of results obtained from tests on a bed of silica sand under supposedly identical conditions, which was eventually traced to increases in fluidising air humidity during the course of a test. The latter was due to a reduction in efficiency of the silica-gel drying tower with time, which at that time could not be detected as the humidity of the fluidising air was not monitored. Since the moisture content of the air was initially assumed constant, a number of other explanations were investigated. These included segregation of the particles, blocking of the distributor plate and changes in air temperature due to the work done in compression by the blower. No changes in any of the latter were detected which had any influence upon the flow behaviour.

Several attempts were also made at this stage to detect electrostatic charging of the particles, which according to a number of previous workers[67,71,76,83] has a deleterious effect on the flow properties. The existence of charging was examined by withdrawing samples of particles from the fluidised bed on an insulated spoon, and testing for charge with a simple gold-leaf electroscope. No evidence of charging was found in these tests, almost certainly because the fluidising air humidity was too high to allow charge build-up. This was confirmed indirectly in that a heap of material on an earthed spoon would, if brought into contact with the previously charged electroscope, discharge it within a second or so. The latter indicated that the conductivity of the material in this condition would be more than adequate to disperse to earth any charges generated by particle motion in the bed. This was further confirmed by adding powdered graphite to the bed material which

did not change either the magnitude or repeatability of the viscosity results significantly, although as suggested by previous workers[76,83] it increased the conductivity of the particles somewhat.

In view of the surprisingly high conductivity of the sand, it was decided to measure its moisture content. A weighed sample was heated in an oven for several hours and placed in a desiccator for a week before reweighing. The loss in weight was less than 0.1% but the conductivity was reduced by more than an order of magnitude. When the dried material was tested in the viscometer its viscosity was initially more than double its normal value. However it fell to lie within the scatter band of previous results after fluidising for approximately two minutes with supposedly dry air from the drying tower. It was thus suspected that the scatter was caused by changes in the fluidising air humidity, although this could not be confirmed at this stage as no humidity measuring equipment was available. A test was performed using dry fluidising air from a high pressure cylinder, in which conditions the bed viscosity stabilised to a value close to that at the commencement of the dried sand test.

The foregoing description is included to illustrate the difficulty encountered in establishing that air humidity has a significant effect on fluidised bed flow behaviour. Once this had been established, the moisture content of the air entering the bed plenum chamber was monitored and means devised to enable the effect of varying its relative humidity to be studied. These tests will now be described.

Initially, tests were carried out by fluidising the bed at a constant superficial velocity and then varying the moisture content of the fluidising air whilst other conditions were maintained constant.

Results obtained for silica and zircon sands are presented in Figures 5.26, 5.27. It is evident that the viscosity in each case

falls to a minimum value at an air moisture content of about 0.2% (15% RH). As the air humidity is reduced from the latter value the bed viscosity increases rapidly and the bed takes on a structured, agglomerated appearance with particles adhering to the bed walls and rotor spindle. Similar behaviour has been observed by Ciborowski et al[108].

This condition is attributed to the build up of electrostatic charges on the particles, which at such low moisture levels are insufficiently conductive to allow the charge to leak away. The latter was confirmed by attempting to discharge the electroscope in the manner described above, which indicated qualitatively that the particle resistivity rises sharply when the air moisture falls below about 20% RH at 25°C.

Previous investigators[10b,109] have measured electrostatic potentials of 2 kV in beds of fluidised sand and higher potentials in beds of other non-conducting materials. No quantitative measurements of potential have been attempted in the present study as no suitable electrometer was to hand. However, qualitative tests with the electroscope upon samples of particles withdrawn from the bed indicated that there was usually little net charge present. An explanation for this has been put forward by HARPER[107], who suggests that crystalline solids having two or more dissimilar faces (of which quartz and sands are examples) are capable of charging with opposite polarity on the different faces. If these charges are unable to leak away because of low surface conductivity, crystal faces holding charges of opposite sign will be attracted to one another, and thus cause agglomeration of the particles. Clearly with a large number of particles half of which are positively charged and the other half negatively, there need not necessarily be any resultant potential. This is further confirmed by the fact that in the present work, there appeared to be no difference in flow behaviour under

ary conditions whether or not the viscometer rotor or metal distributor plate were earthed. Also the substitution of a metal bed-wall for the usual perspex one had no effect other than to eliminate the adherence of a mono-layer of particles to the walls. The foregoing confirms the findings of LOEB[113], who points out that earthing the containment vessel of a non-conducting fluidised material is ineffective in reducing the charge on material remote from the vessel walls.

The build-up of charges was so serious in the case of the silica sand that the bed defluidised completely at about 5% RH (.05% air moisture) so that much of the fluidising air passed through the bed via channels or blow-holes. This suggests that the particle cohesive forces are here of similar magnitude to the gravitational/buoyancy forces. According to HARRIS[139], interparticle attraction due to a combination of electrostatic and van der Waals forces may reach 10^{-7} N, which is roughly equal to the weight of a sand particle of diameter 100 μm.

An attempt was made to reduce charge build-up at low air moisture levels by mixing about 30% of electrically conducting magnetite (Fe_3O_4) particles with the zircon sand of Figure 5.27. The results are shown in Figure 5.29, and indicate that although the minimum viscosity is increased slightly, there is no longer a sharp deterioration in flow at low air humidity. No definite explanation of this can be put forward, but it seems likely that the conducting particles act as a vehicle for the dissipation of charges built up on the zircon particles.

The increase in viscosity at the wetter end of the air humidity spectrum is thought to be due to absorption of moisture on to the surface of the particles, rather than static electricity. In the wet region the surface conductivity of the particles was sufficiently high to discharge the gold-leaf electroscope instantaneously and should therefore allow immediate dissipation of any electrostatic potentials between

FIG. 5.23

SHEAR STRESS vs FLUIDISING VELOCITY FOR SILICA SAND AT DIFFERENT AIR MOISTURE LEVELS

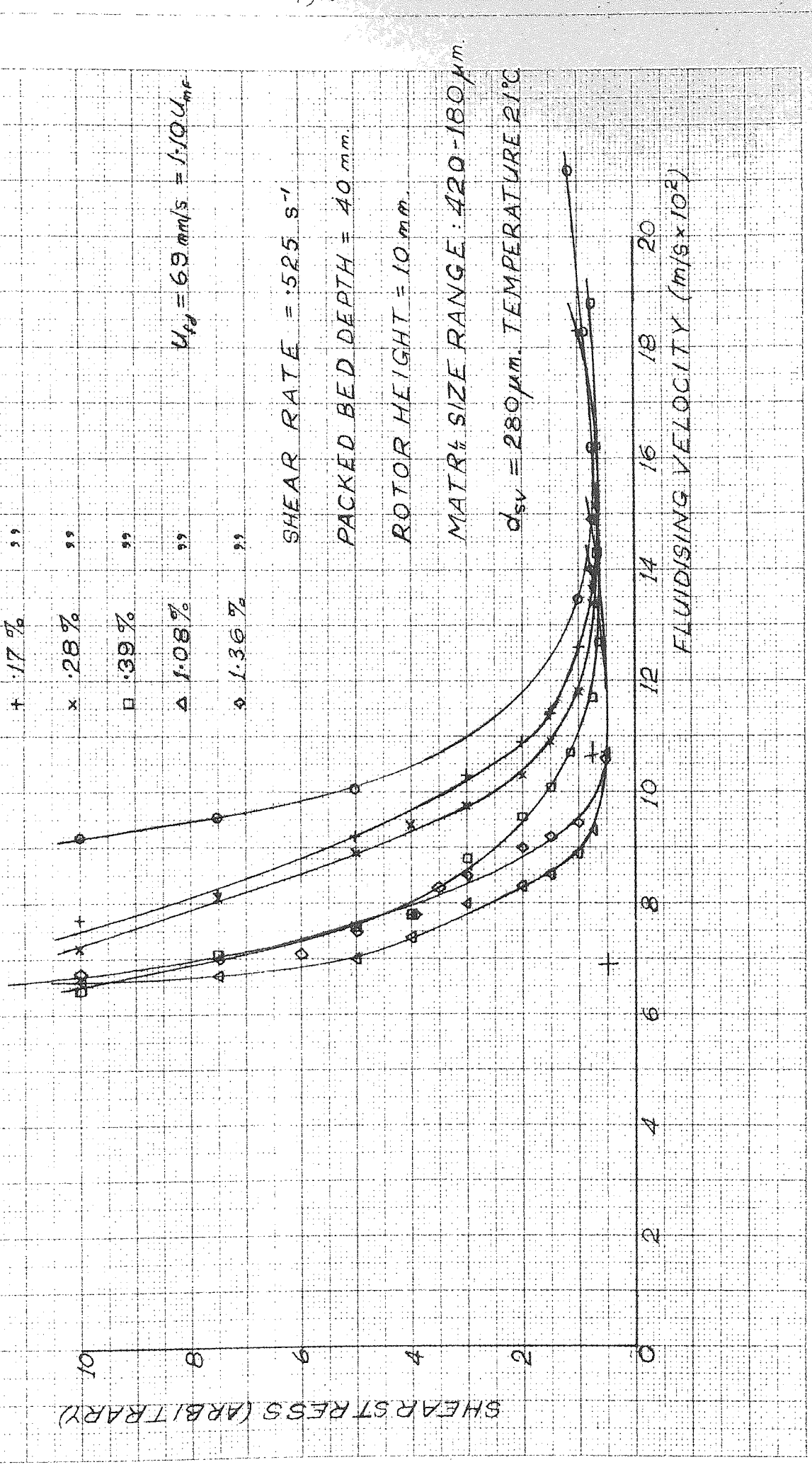

PRESSURE DROP ACROSS BED vs. FLUIDISING VELOCITY FOR SILICA SAND AT DIFFERENT AIR MOISTURE LEVELS.

FIG. 5·24

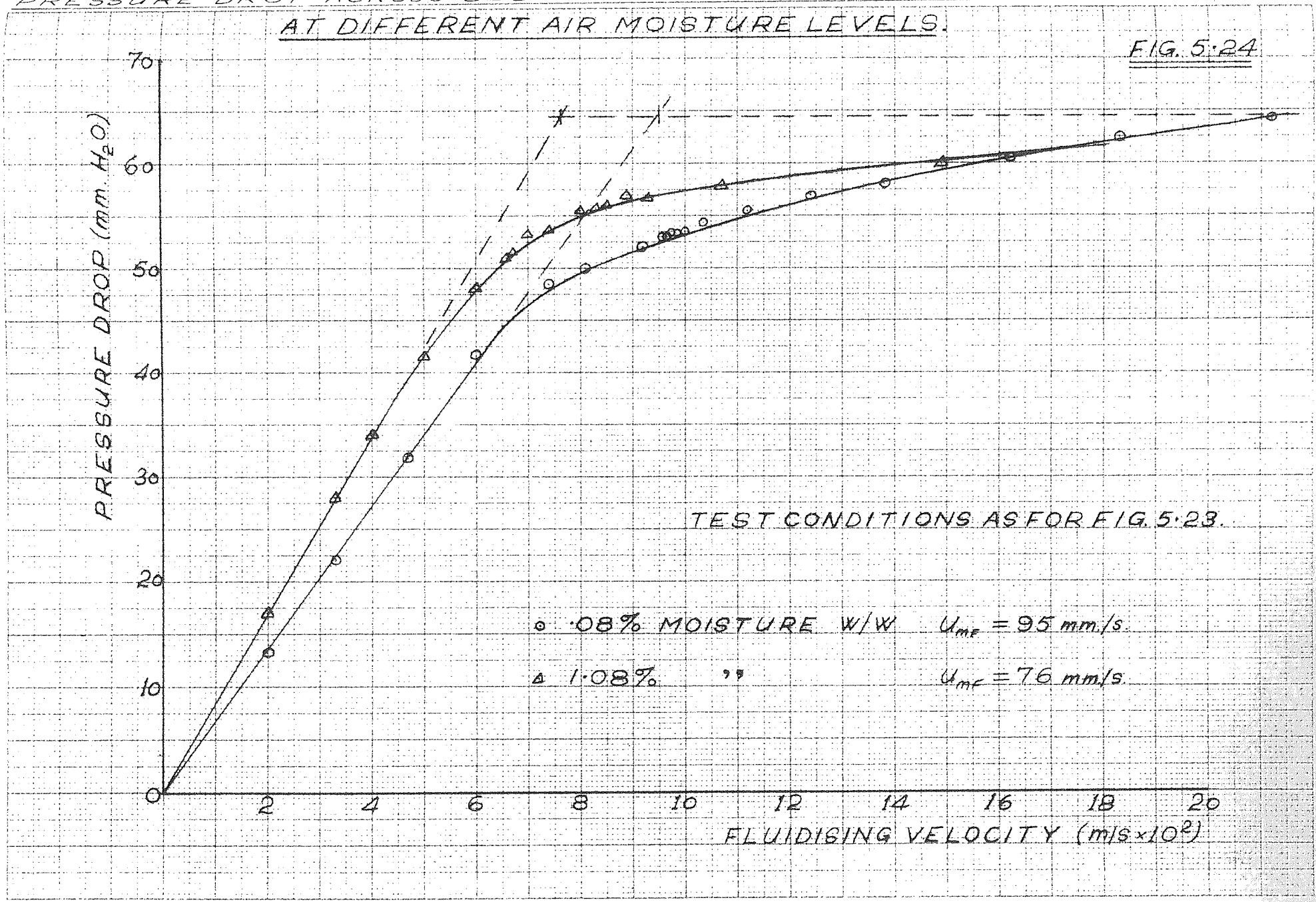

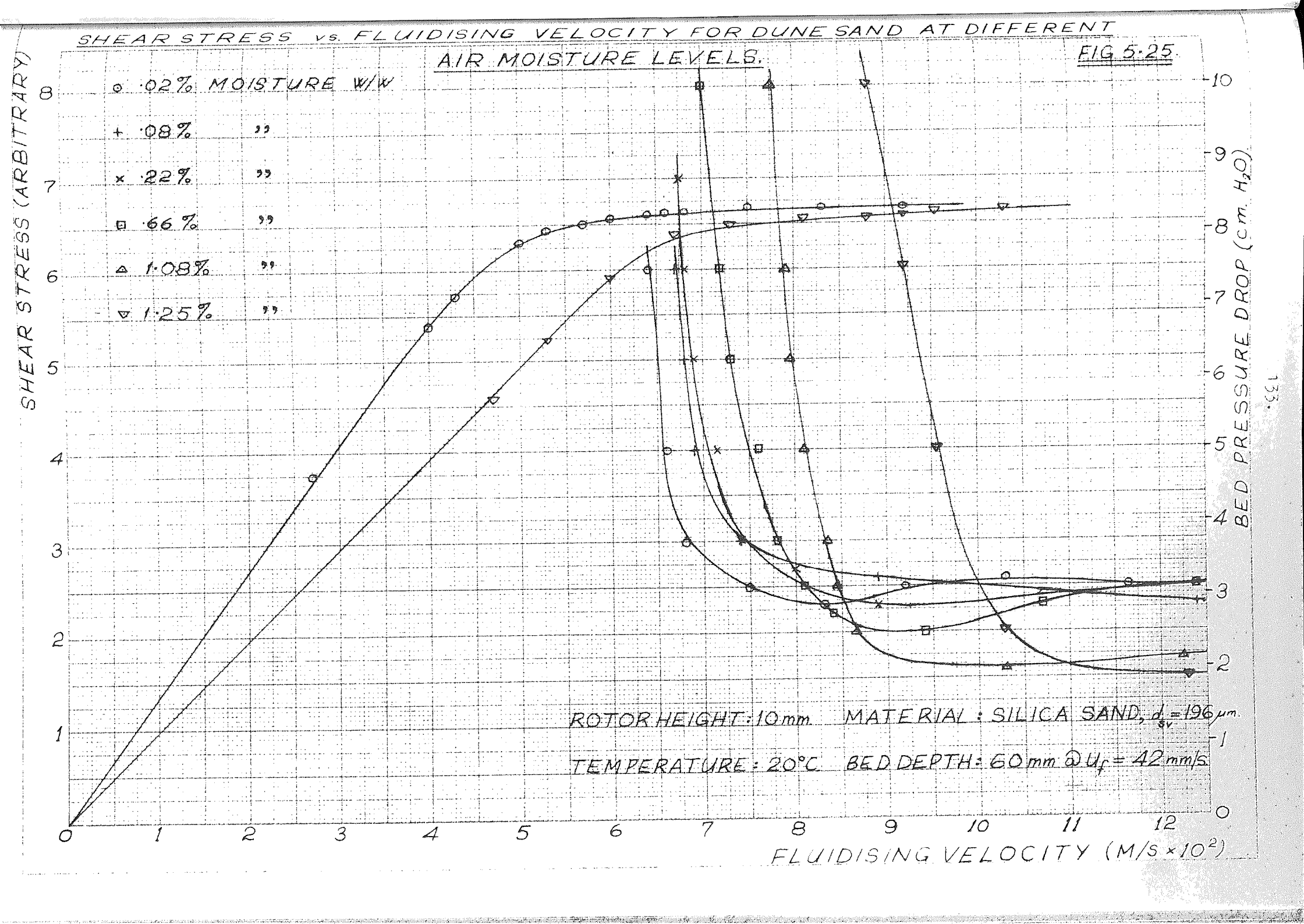
SHEAR STRESS vs. FLUIDISING VELOCITY FOR DUNE SAND AT DIFFERENT AIR MOISTURE LEVELS.
FIG 5·25
○ ·02% MOISTURE W/W
+ ·08% ,,
× ·22% ,,
□ ·66% ,,
△ 1·08% ,,
▽ 1·25% ,,
SHEAR STRESS (ARBITRARY)
BED PRESSURE DROP (c.m. H2O)
FLUIDISING VELOCITY (M/S × 10²)
ROTOR HEIGHT: 10mm MATERIAL : SILICA SAND, dsv = 196 μm.
TEMPERATURE : 20°C BED DEPTH: 60mm @ Uf = 42 mm/s.
0 1 2 3 4 5 6 7 8 9 10 11 12
1 2 3 4 5 6 7 8
0 1 2 3 4 5 6 7 8 9 10

SHEAR STRESS vs FLUIDISING AIR MOISTURE CONTENT FOR 420 - 180 μm SILICA SAND

FIG 5·26

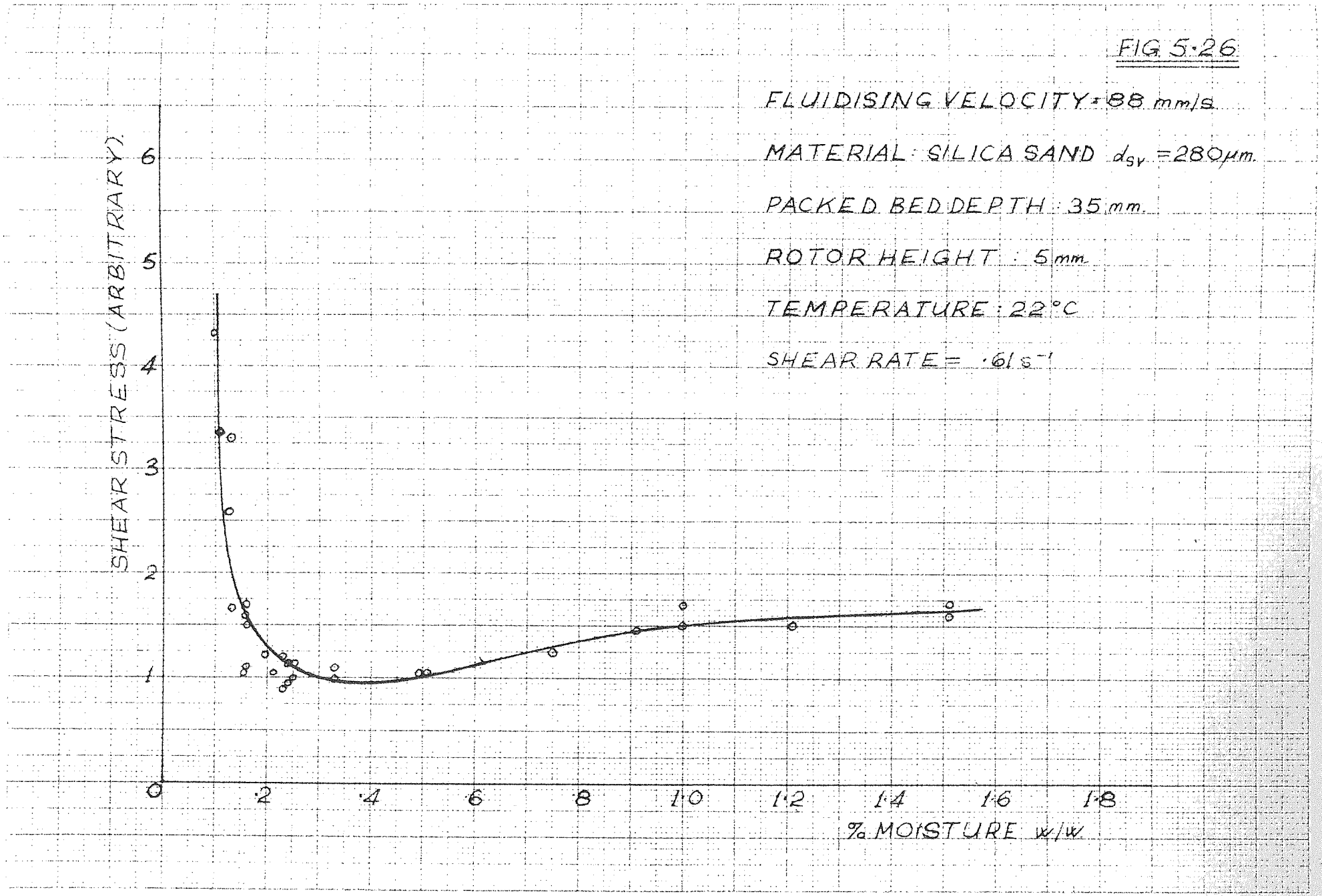

SHEAR STRESS vs. MOISTURE CONTENT OF FLUIDISING AIR FOR 140 μm ZIRCON SAND

FIG 5·27

FLUIDISING VELOCITY = ·09 m/s.

MATERIAL : -180 + 125 μm ZIRCON SAND, d_{SV} = 140 μm.

TEMPERATURE : 25 °C

PACKED BED DEPTH : 35 mm.

ROTOR HEIGHT : 5 mm.

SHEAR RATE : ·53 s^{-1}.

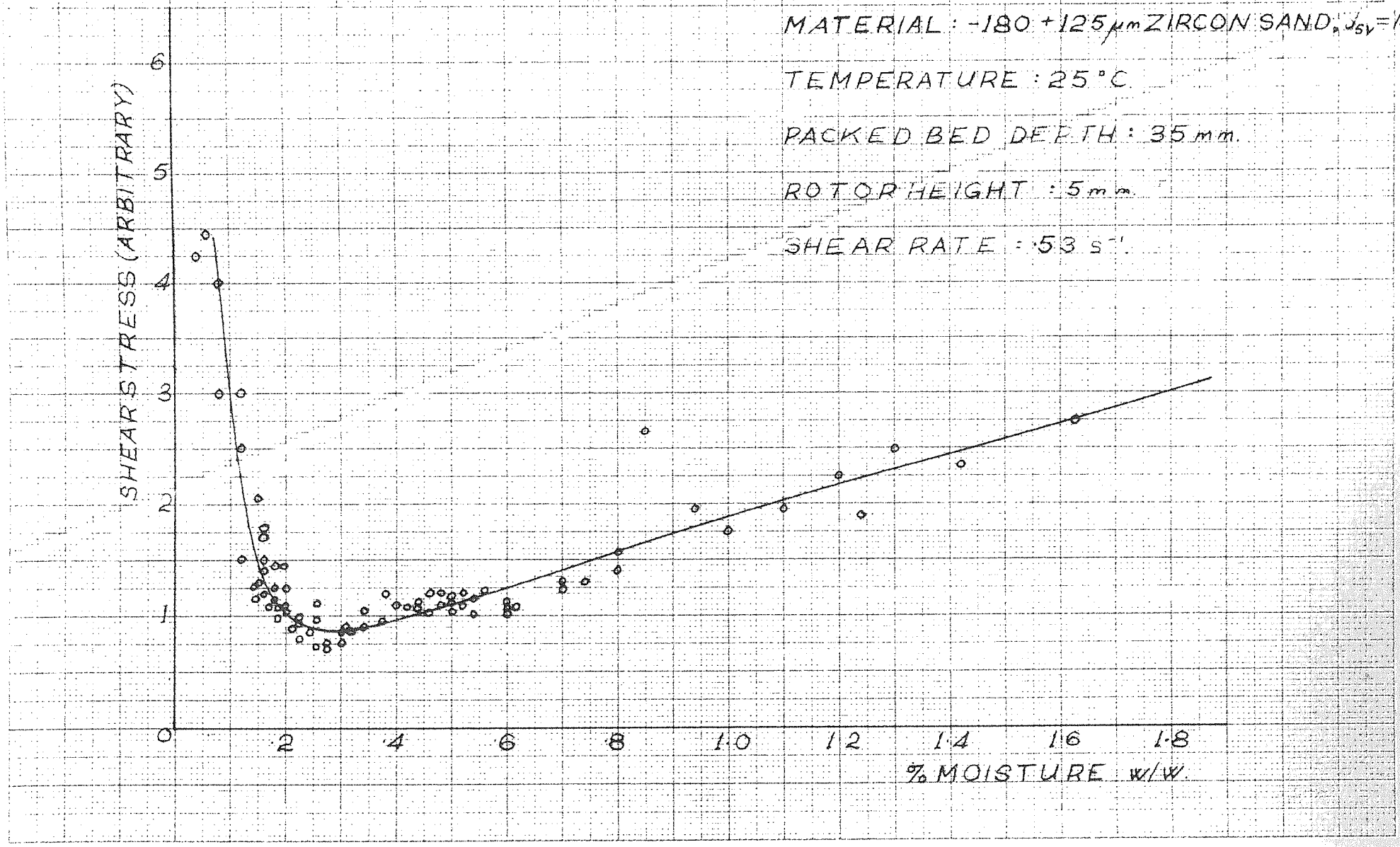

SHEAR STRESS vs FLUIDISING AIR MOISTURE CONTENT FOR 233μm COPPER SHOT.

FIG 5·28.

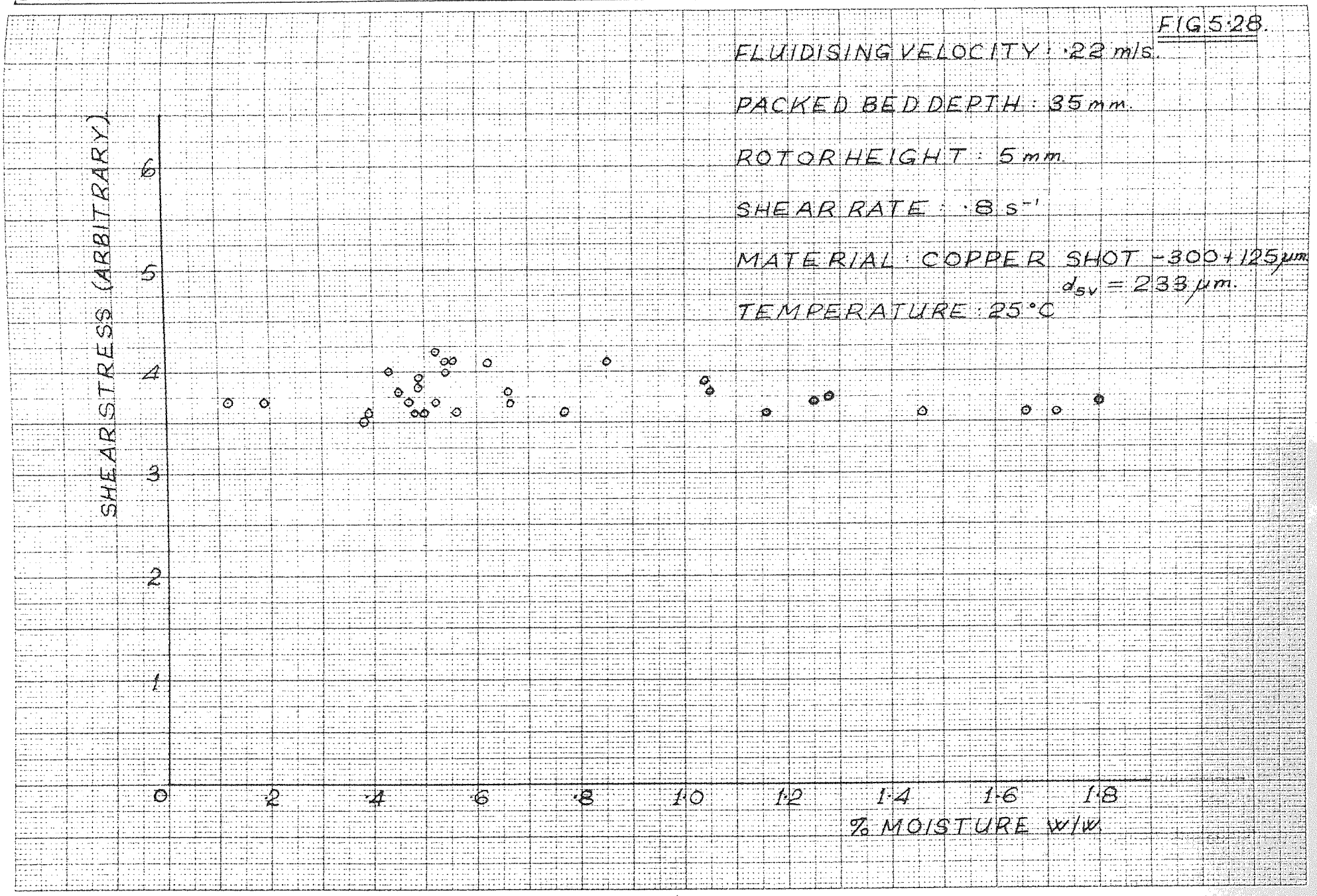

SHEAR STRESS v FLUIDISING AIR MOISTURE CONTENT FOR ZIRCON SAND + 30% Fe_3O_4.

FIG 5.29

FLUIDISING VELOCITY = ·11 m/s.

MATERIAL : -180 + 125 μm ZIRCON SAND
+ 30% w/w Fe_3O_4 $d_{sv} \simeq 150\,\mu m$.

SHEAR RATE : ·53 s^{-1}.

PACKED BED DEPTH : 35 mm.

ROTOR HEIGHT : 5 mm.

TEMPERATURE : 25 °C.

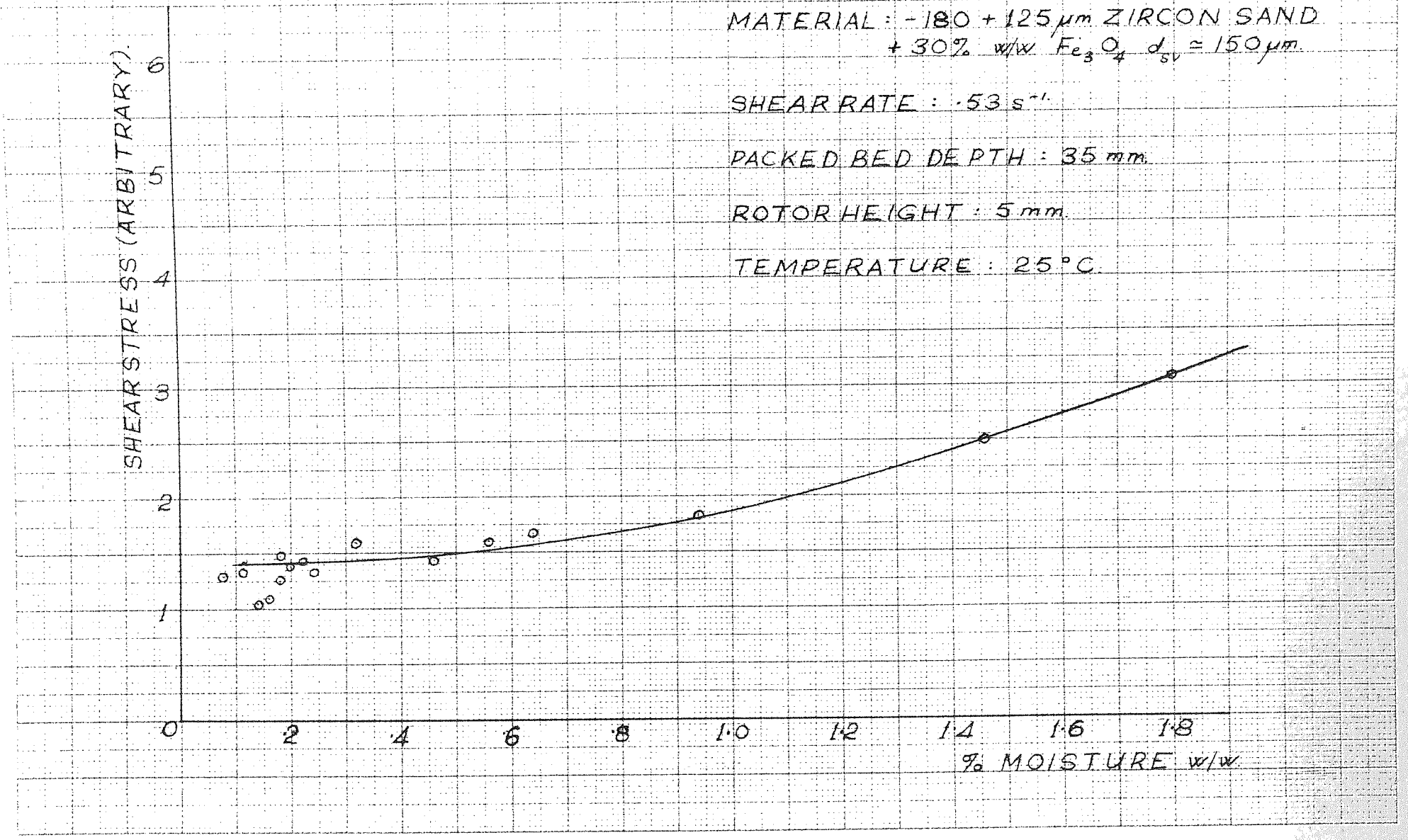

particles in the bed.

The effect of the absorbed water was to make the particles "sticky" so that cohesive forces caused agglomeration and reduced particle mobility. In the case of the sand-like materials tested here the influence upon bed viscosity is less serious than that of electrostatic charges, but will of course persist in hydrophilic materials even if charging is eliminated by increasing their surface conductivity. This is evident from figure 5.29. However, the relative magnitude of moisture and charging effects will depend upon the conductivity and moisture absorbing properties of the particles used. Materials which are hygroscopic rather than hydrophilic are likely to be more adversely affected by fluidising air moisture.

Tests were carried out on steel and copper shot of various sizes and for these materials electrostatic effects were found to be absent. The steel shot behaved unpredictably at high moisture levels, possibly due to incipient surface rusting; but the copper had constant viscosity over the entire relative humidity range at 25°C. This is shown in figure 5.28.

The foregoing tests at constant fluidising velocity clearly show that small variations in fluidising air moisture contents can significantly change the bed viscosity. This would be of considerable importance industrially, for very close control of air humidity would be needed in certain conditions to ensure consistent flow performance. However, it was felt at this stage that it would be instructive to carry out tests over a range of fluidising velocities at a series of constant relative humidity levels.

The results of a test on silica sand are shown in figure 5.23, from which it is clear that the main effect of changes in air moisture is to alter the "flow deterioration velocity". Referring to the pressure drop curves corresponding to the maximum and minimum U_{fd}.

(Figure 5.24), it can be seen that these changes are brought about by changes in minimum fluidising velocity with relative air humidity. The latter has been noted previously by Ciborowski et al[108], and is perhaps not surprising since U_{m_f} will clearly be raised by any tendency to particle agglomeration caused by charging. What is more surprising is that the minimum apparent viscosity is almost constant over the whole range of air humidity. This suggests that once the air velocity is high enough to break up any agglomerates of particles held together by electrostatic forces, the particles do not re-agglomerate and their mobility is little affected by the presence of electrostatic potentials. No quantitative measurements of how electrostatic potential varied with U_f could be made, but according to Ciborowski[108] the potential continues to increase as the fluidising velocity is increased above U_{m_f}. This was confirmed qualitatively here by noting that samples withdrawn from the bed at higher fluidising velocities usually caused the greatest deflection of the gold-leaf electroscope. It is pertinent to note here that changes in the viscosity of air with relative humidity are unlikely to significantly alter U_{m_f}. There is some disagreement in the literature as to the effect of moisture on air viscosity. It is reported[142] that the viscosity of saturated air at 26°C is 1.904×10^{-5} Ns/m^2 compared with 1.863×10^{-5} Ns/m^2 for dry air: conversely DEARNS[143] suggests that the viscosity of dry air at N.T.P is reduced by 0.3% on saturation. There is also some change in specific volume with moisture content but neither should greatly influence the fluidising behaviour of the bed.

The material used for figure 5.23 was a different sample from the same batch as used for Figure 5.26. The bed geometry was slightly different for the two tests but it is of interest that at the same fluidising velocity (.088 m/s) the minimum viscosity occurred in the former case at 1.08% air moisture ($\simeq$ 60% RH) and in the latter at about 0.2 - 0.4% moisture ($\simeq$ 20% RH). Following this, the material of Figure 5.23 was washed in

in water, dried and retested under the same conditions as Figure 5.26: in which circumstances the minimum viscosity was at about 0.5% air moisture. The latter was presumably the result of removal of surface contamination, and although this must have been minute in quantity since no change in weight was detectable before and after washing, it was clearly sufficient to change the surface conductivity and/or hydrophility of the material.

Following the discovery of the influence of air moisture on the flow behaviour of fluidised sands, tests were carried out on material used by BESSANT[141] for fluidised channel flow studies. Shear stress vs. fluidising velocity curves for a range of air moisture levels (Fig 5.25) show that this material is apparently unaffected by electrostatic charging at low air humidity. This was confirmed by visual observation of the bed, since no agglomeration or adhering of particles to the bed wall was evident at low relative humidity. A qualitative test on the dried material with the electroscope showed that its conductivity was much higher than that of the previously tested silica and zircon sands. The high conductivity persisted after washing with water and a number of organic solvents and is presumably not therefore due to surface contamination.

The minimum fluidising and flow deterioration velocities of this 'dune' sand both increased substantially at high air humidity due to moisture absorption causing particle agglomeration. However, once the bed was well fluidised, the minimum apparent viscosity at high humidity was substantially below that under drier conditions despite the increase in minimum fluidisation velocity. This may have been because of some lubrication effect of the surface moisture once the particle agglomeration had been broken up by vigorous bubbling.

In view of the result of the viscometer tests (Fig 5.25) on the 'dune' sand it is surprising that BESSANT[141] reports no substantial effect of humidity changes on his results. However, most of Bessant's work was carried out at around 45-50°C rather than 20-25°C as in this work.

According to Ciborowski et al[108] the minimum fluidising velocity of sand becomes less dependent on air humidity with increasing temperature. This could not be confirmed either by Bessant or the author, since no means of substantially changing the fluidising air temperature was available, but provides a possible explanation of the difference in behaviour.

A point of disparity between the present work and that of Ciborowski[108] concerns the time required for stabilisation of conditions. Ciborowski reported that up to 30 minutes was necessary for the electrostatic potential to reach an equilibrium value under dry conditions. If this was so in the work presented here it was certainly not reflected in the bed flow behaviour. Up to 10 minutes were necessary for the air humidity to stabilise following an adjustment to the supply, but during this time the flow behaviour sensibly followed the changes in air condition and stabilised to its final value virtually as soon as the air condition had reached stability. If the supposition of a dynamic equilibrium between the rate of charge generation and leakage is correct, it would not be expected that long settling times should be necessary unless these represented some unknown change in the surface condition of the material.

It is clear from the foregoing results that the influence of air humidity on fluidised bed flow properties is highly dependent on the surface conditions as well as the material properties of the particles. Spurious changes in behaviour are caused by uncontrollable changes in the degree of surface contamination; a feature which is well known in static electrification work[107]. Clearly it would be desirable to make a more fundamental and searching study of moisture effects on fluidisation. However, it was decided in the present work to rest with the knowledge that results should be repeatable, with the same batch of material, provided that the fluidising air humidity and temperature could be monitored and controlled.

viii. Effect of Viscosity and Temperature of Fluidising Gas

Unlike most liquids, the viscosity of fluidised beds is little altered by small temperature changes. No means was available on the viscometer rig for providing wide variations in fluidising air temperature; but over a range of 15 - 30°C there was no change in bed behaviour, save for a very slight reduction in minimum fluidising velocity. The viscosity of air increases only from 1.72 to 1.91×10^{-3} Ns/m^2 for a temperature rise from 0 to 40°, so that no great change in bed flow behaviour over this temperature range would be expected.

It would clearly be beneficial to the study of high temperature fluidised transport systems to examine the behaviour of hot combusting beds with the viscometer. The latter could be carried out relatively easily with the provision of a heat-shield on the existing rig between the bed and the rotor head, but time has not permitted this to date.

As with temperature effects, the influence of varying the fluidising gas properties has been examined but tentatively to date. A bed of 'Bauxilite' was fluidised with carbon dioxide from a cylinder of the compressed gas and also with dry compressed air. The minimum apparent viscosity was the same with both gases but a 25% higher fluidising velocity was required with carbon dioxide. This is approximately in inverse proportion to the viscosities of the two gases ($CO_2 = 1.46 \times 10^{-3}$ air $= 1.81 \times 10^{-3}$ Ns/m^2 at 20°C), and is as would be expected from the hydrodynamics of the fluidised bed.

ix. Effect of Surface Geometry of Particles and Viscometer Rotor

It would be extremely difficult to assess accurately the effect of particle shape or surface roughness independently of other variables. Even if particles of the same material and size but different shape were available; it is possible that differences in surface contamination

would influence their electrostatic or moisture absorbing properties.

However it is evident from results presented earlier (figures 5.4 - 5.7) that the shear diagrams are of similar form for sharp edged('bauxilite'), cubic (silica sand) and rounded (Zircon) materials. Also, there were no first order differences in the relative magnitude of the viscosities of the different shaped particles. Figures 5.12 to 5.17 show that there is also little difference in the general shape of the viscosity vs. fluidising velocity curves of the different shaped particles.

An attempt was made to assess the effect of particle surface finish by fluidising a silica-sand sample with dry air from a compressed air bottle, and then re-testing the same sample after coating the particles with polytetra fluoro ethylene (PTFE). Dry air was used to eliminate differences in behaviour due to moisture absorption. The electrical conductivity of the raw and coated particles was similar, so that leakage of electrostatic charges would occur at a similar rate in the two conditions, although of course the rate of charge generation may well have been different. The results of these tests for the cases when none, half and all the particles were coated are shown in figure 5.30. Although there is some scatter in the data points it is clear that the coated particles have similar flow properties to the untreated material. There was some doubt as to the efficacy of the coating process, which comprised spraying the particles with an aerosol spray of PTFE dissolved in an organic solvent. However, in view of the extremely low coefficient of friction of PTFE it seems likely that even a partial coating would cause some change in the particle surface condition.

As noted in section 5.(vii), coating the particles with powdered graphite had similarly little effect on the flow behaviour. Here too

VISCOSITY vs FLUIDISING VELOCITY FOR SAND PARTICLES WITH SURFACE COATINGS.

FIG. 5.30

MATERIAL: SILICA SAND, $d_{sv} = 148 \mu m$.

BED DEPTH: 20 mm.

ROTOR HEIGHT: 5 mm.

SHEAR RATE: 4.2 s^{-1}.

o UNTREATED PARTICLES.

× 50% OF PARTICLES PTFE. COATED.

□ 100% OF PARTICLES COATED.

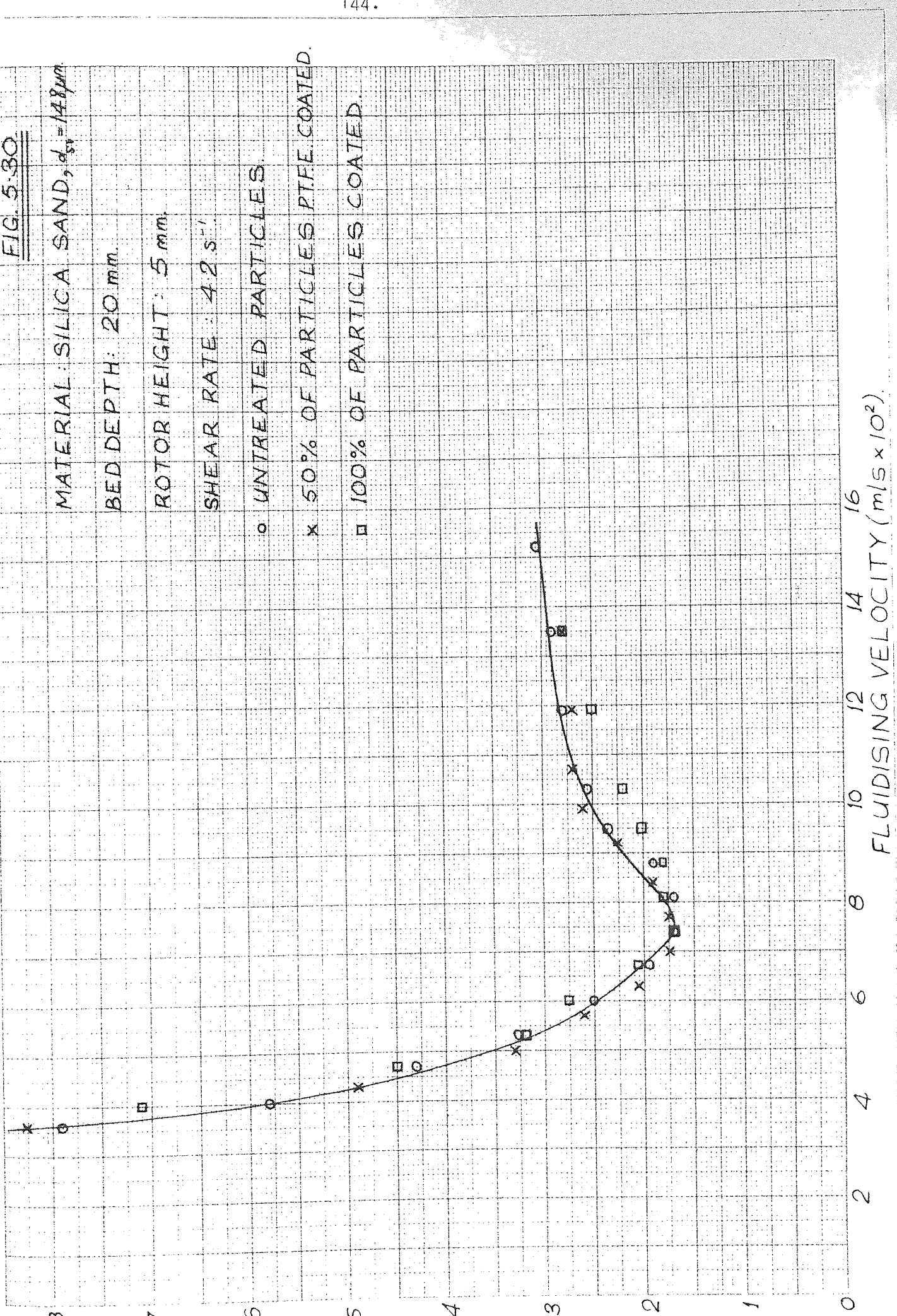

the completeness of coating could not be assessed; although clearly some graphite remained on the particles since the treated material was appreciably darker in colour.

In view of the marked influence of surface water on fluid bed flow properties, it is surprising that the above changes in particle surface condition did not have a similar influence. It is of interest also that BOTTERILL[146] has noted improved heat transfer performance using particles contaminated with minute quantities of oil, which may have been due to improved particle mobility caused thereby. It would perhaps be more useful in assessing particle surface effects to measure also some other surface dependent property such as the angle of repose or internal friction of the unfluidised material. The latter properties have been used to correlate the flow of particulate material through orifices[7,145] but time has not permitted a study of their relationship to fluidised flow behaviour in this work. It is a postulate of the rotational viscometer theory of Kreizer and Maron[132] that no slip occurs between the viscometer surface and the adjacent boundary-layer of fluid. A theoretically rigorous method of assessing slip is available due to MOONEY[147] but cannot be applied to an infinite flow field.

The method adopted here was to use two rotors that were identical other than in external surface finish. In one case the surface was machined smooth; whilst the other was straight knurled to produce a 'washboard' surface, with grooves of similar size to the fluidised particles. Thus if tests with the two rotors produce the same results, either there is no slip, or the slip at both surfaces has an identical finite value. The latter is clearly exceedingly unlikely and it seems reasonable to assume that identical results indicate zero slip.

The results of a typical test using the two rotors is shown in figure 5.31. From this it can be seen that the slip is zero up to a shear rate of about 15 s^{-1}, whereafter the slip velocity tends to a constant value of approximately 5 s^{-1}. It was easy to confirm visually that no slip occurred at low shear rates, since a thin but definite boundary layer of particles moving at the same speed as the rotor could be detected. However the existence of slip at higher rates of shear could not be so confirmed as it was impossible for the eye to follow the rotor movement, even with the aid of a stroboscope.

The onset of slip did not correspond to any particular shear stress or shear rate for a range of materials, nor to a particular Reynolds number as defined by Hetzler and Williams[84] (see section 3.6). However for all the materials tested here, slip commenced at Reynolds numbers well below 2000; that for figure 5.31 being in the region of 5-600. It is of interest that the shear diagram using the 'rough' rotor has no marked change of slope, so that it is reasonable to assume that the slip remains close to zero at higher shear rates. Nevertheless, none of the results presented in this work were taken at shear rates above the onset of slip as determined by the above test.

Figure 5.32 shows the results of a test with the two rotors over a range of fluidising velocities at a shear rate close to the onset of slip at the point of minimum apparent viscosity. From this it is apparent that there is a little slip at low fluidising velocities but this is reduced to zero once the bed becomes more fluid at higher air flowrates.

It is worthy of note that there is little mention of surface slip in the literature on fluid bed viscometry. This is surprising since slip is quite common in non-Newtonian fluids, such as slurries and suspension of solid matter in liquids[75,127]. Several authors have

SHEAR STRESS vs SHEAR RATE FOR 386 μm SAND USING KNURLED & SMOOTH ROTORS

FIG. 5·31

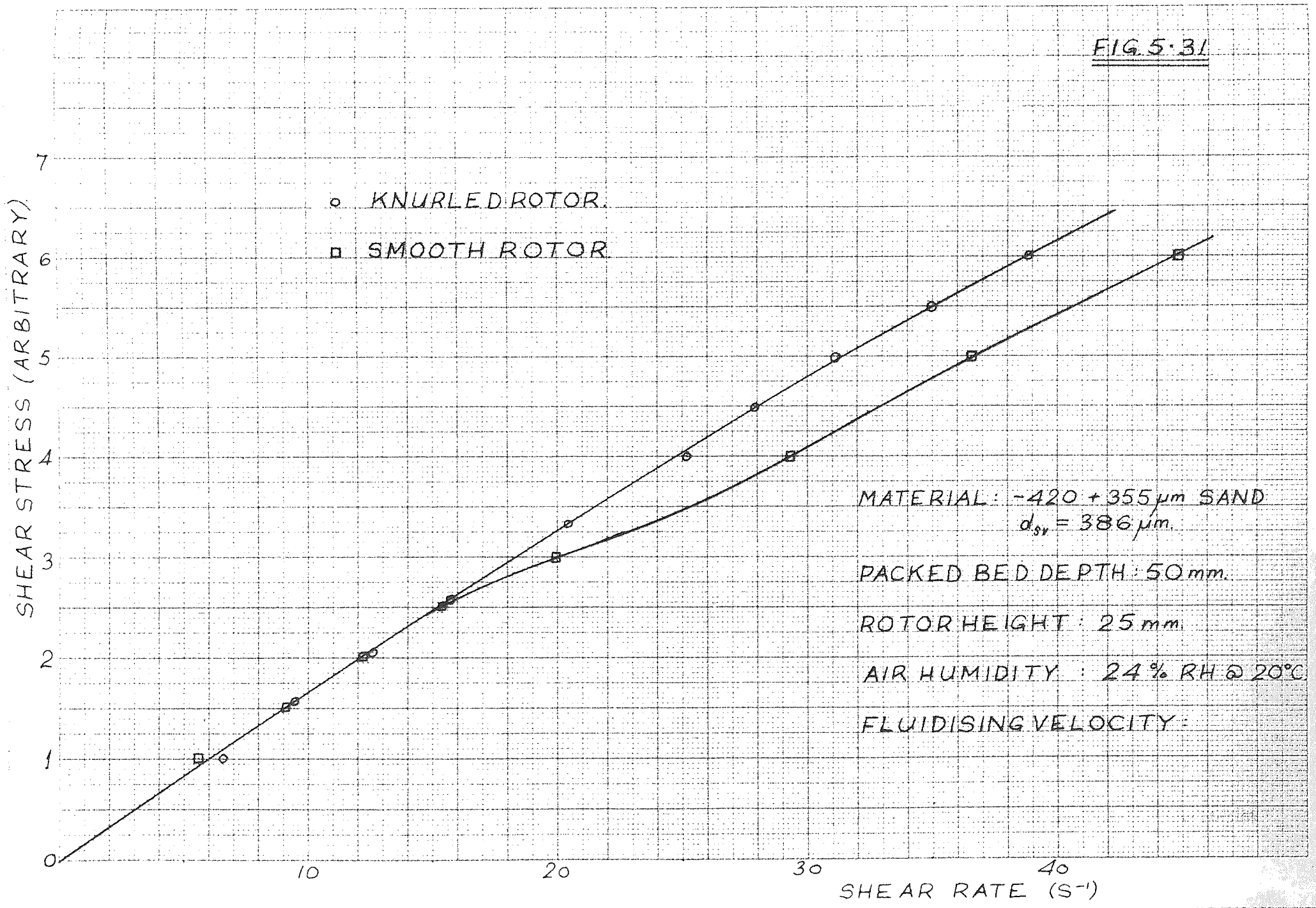

SHEAR STRESS vs FLUIDISING VELOCITY FOR 295 μm SAND USING KNURLED & SMOOTH ROTORS.

FIG. 5·32.

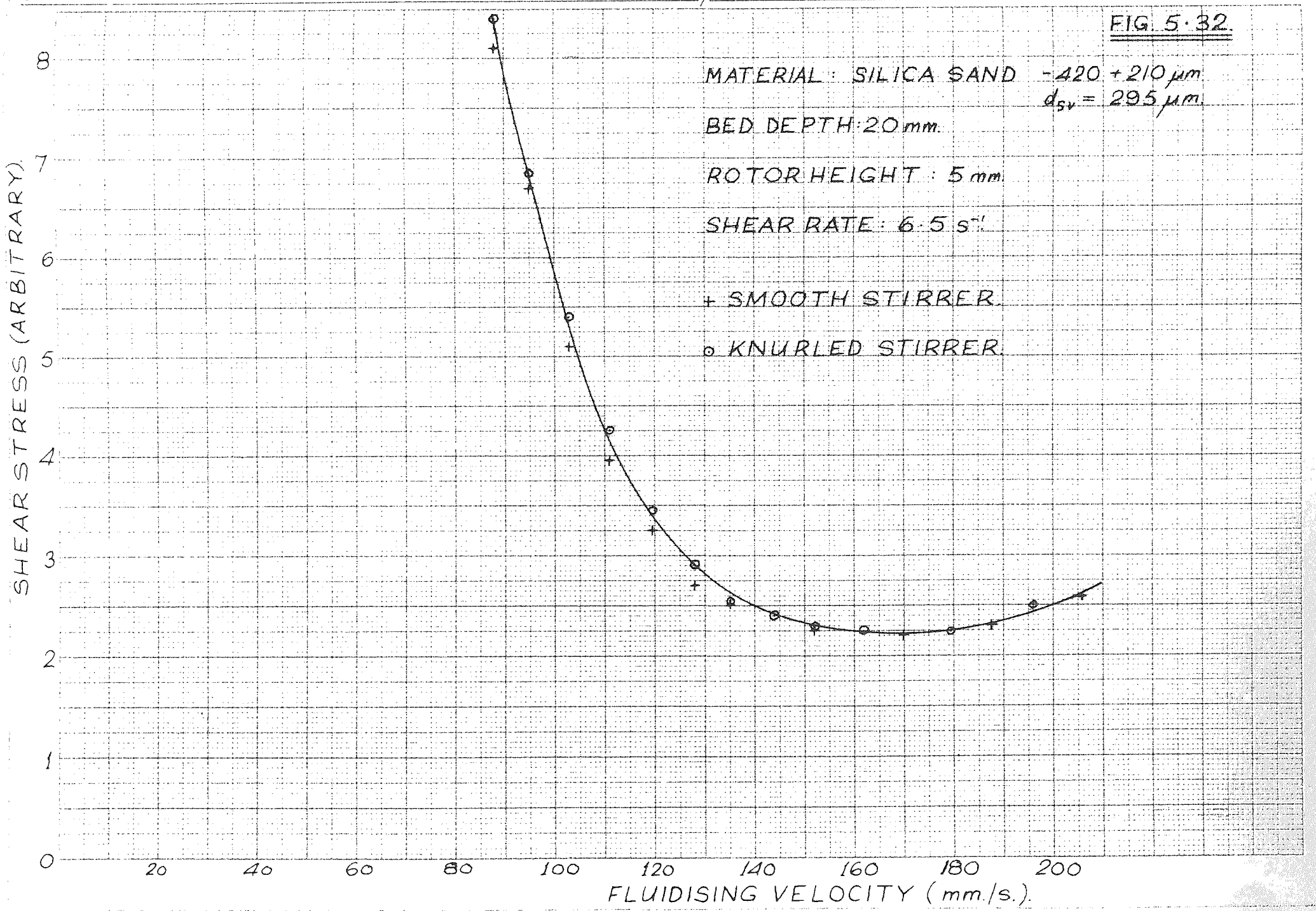

arbitrarily used roughened rotors to eliminate slip in fluid bed viscometry, but only Hetzler and Williams[84] have carried out confirmatory tests in their work with liquid fluidised beds. They used rough and smooth rotors and concluded, as in this work, that the identical results so obtained were indicative of the absence of slip.

It thus appears that, at least at low shear rates, fluidised beds flow without a slip velocity relative to vertical surfaces, and that the flow is not surface dependent. This may not be true in respect of flow over the horizontal distributor however, as inferred by Siemes and Hellmer[97] and Botterill and Bessant[103,105] from channel flow work.

5.3 VISCOMETER TESTS ON MATERIALS FOR USE IN CHANNEL FLOW RIG

i) Effect of Fluidising Air Moisture on Viscosity of Sieved Fractions of Material.

The material used in the channel flow rig was "Buckland 50 FG" silica sand covering a particle size-range from approximately 100-700 μm (for details and size analysis see Table 5.1). This material was chosen because of its cheap and ready availability in large quantities to a consistent specification, and because of its suitability for use in combustion and heat transfer applications. However its flow behaviour was known to be dependent on air moisture content from earlier tests (see section 5.2 (vii)).

It was therefore decided that when the actual batch of material to be used in the channel rig was delivered, it would be instructive to test its flow properties with the viscometer at different air humidity levels. The material was sampled and sieved into fractions in order to see whether the smaller material (due to its greater surface/mass ratio), or the larger (because of the higher electrostatic potentials generated[111]) would be the more susceptible to moisture effects. The raw sample was

sieved into eleven fractions and the six odd ones tested over a range of fluidising air moisture levels between 1.8 and 70% RH at 22°C.

The results are shown in figures 5.33 to 5.38, from which it is clear that changes in air humidity had little effect upon all fractions except the smallest. Even in the latter case (Fig 5.33) the influence was much smaller than for tests on previous batches of the same material (cf figure 5.23).

No reason could be found for the difference in behaviour of the two batches of material; which were to the same specification, but obtained from the supplier at different times. As mentioned previously, washing of the earlier batch made no difference to its behaviour, nor did similar treatment of the second batch. The two batches looked identical, and contact with the supplier revealed that there should have been no difference in their source or preparation. To confirm that the previously noted moisture effects were not due to the wide size of the material used, a raw sample of the second batch was also tested, with negative results (figure 5.39).

Thus although these tests suggested that small material is more likely to be affected by fluidising air humidity changes, the results were not quantitatively conclusive. However the insensitivity of this batch of material to moisture was noted with gratitude, since no provision was initially made in the channel flow rig for control of the humidity of the large quantity of air required for its operation.

Figure 5.40 shows how minimum viscosity, U_{m_f}, U_{fd} and U_{fd}/U_{m_f} varied with particle size for the tests of figures 5.33 - 5.39. It can be seen that the minimum fluidising velocity increases in the manner expected, although the fit of the appropriate correlations due to Kunii[8] and Rowe[11] (shown with pecked lines) is evidently only fair. The value of the ratio of U_{fd}/U_{m_f} lies between 1.15 and 1.4, which is in line with previous results for most materials.

SHEAR STRESS & PRESSURE DROP vs FLUIDISING VELOCITY FOR 'BUCKLAND' SAND d_{sv} = 105μm

FIG.5·33.

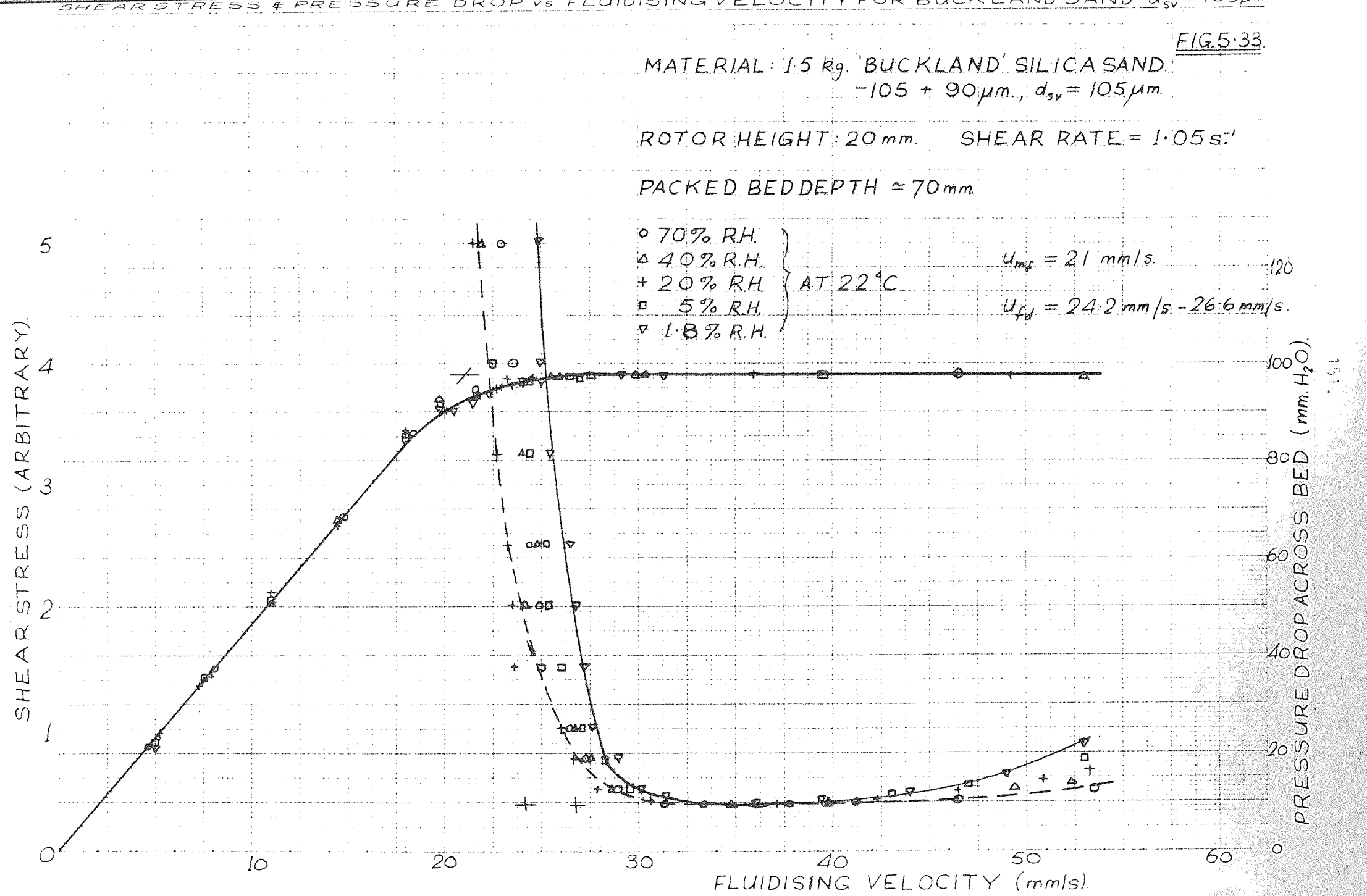

SHEAR STRESS & PRESSURE DROP vs FLUIDISING VELOCITY FOR 150 μm 'BUCKLAND' SAND

FIG. 5.34

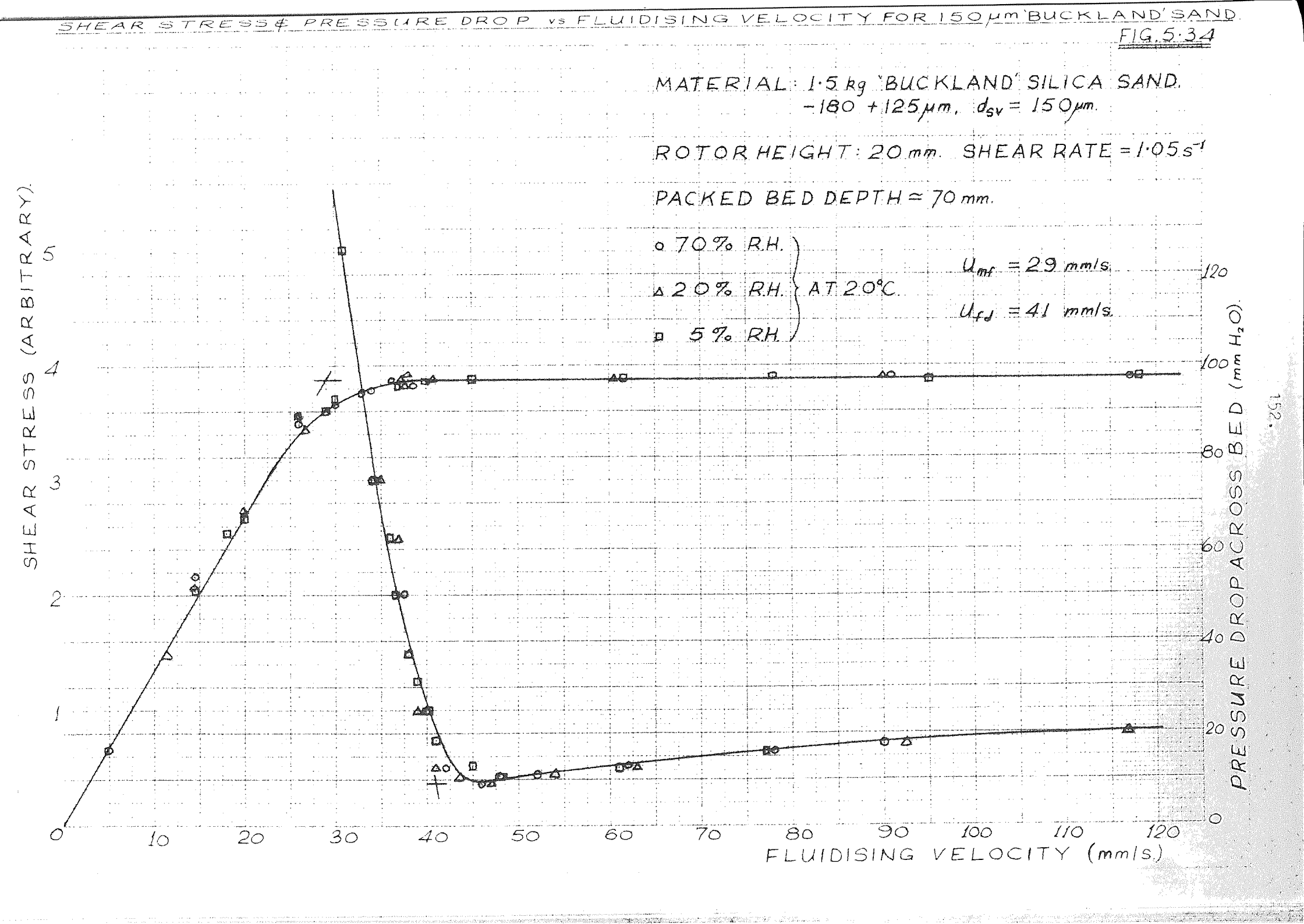

SHEAR STRESS & PRESSURE DROP vs FLUIDISING VELOCITY FOR 230 μm 'BUCKLAND' SAND

FIG 5·35

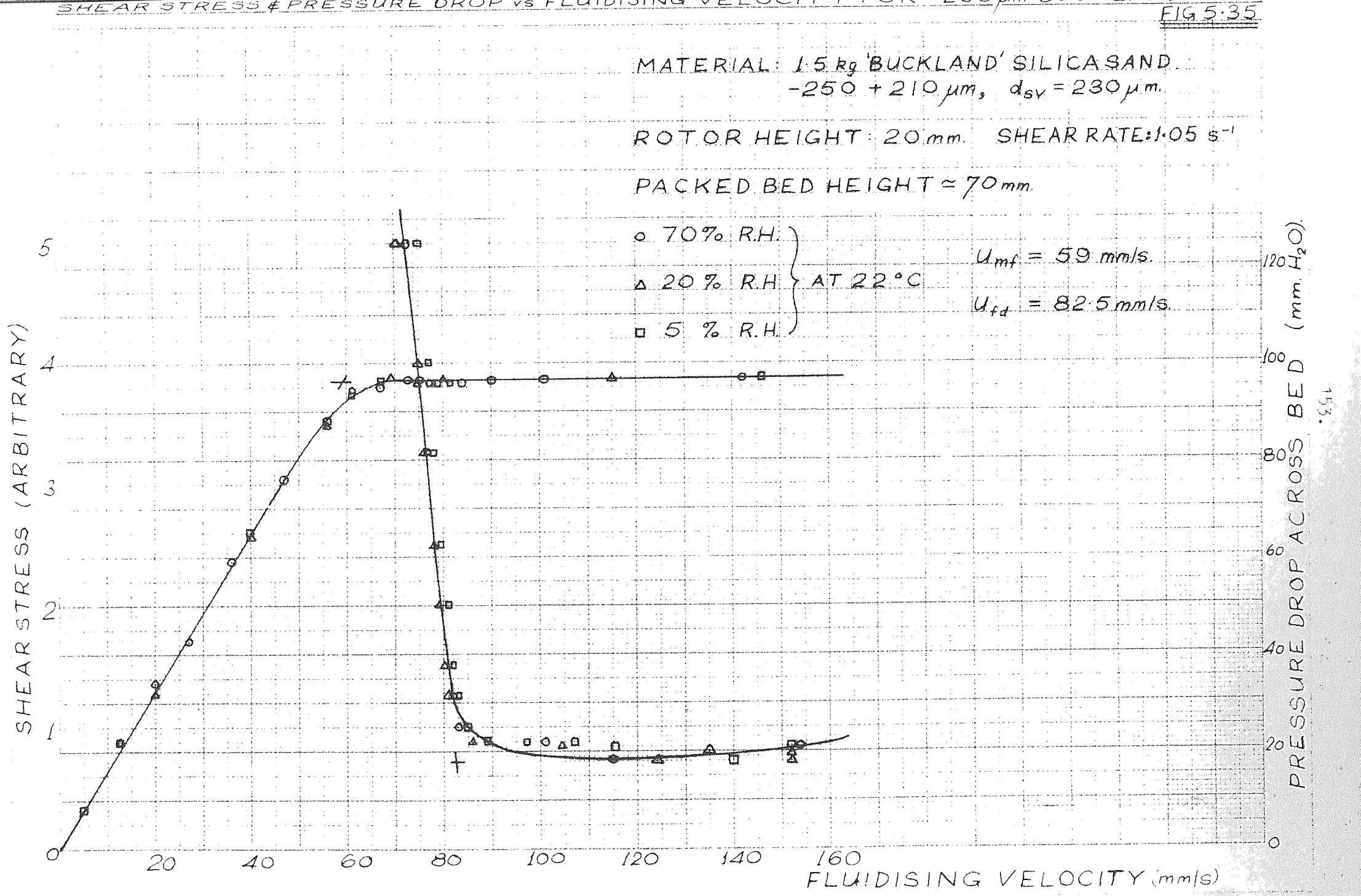

SHEAR STRESS & PRESSURE DROP vs. FLUIDISING VELOCITY FOR 325 μm 'BUCKLAND' SAND

FIG. 5·36.

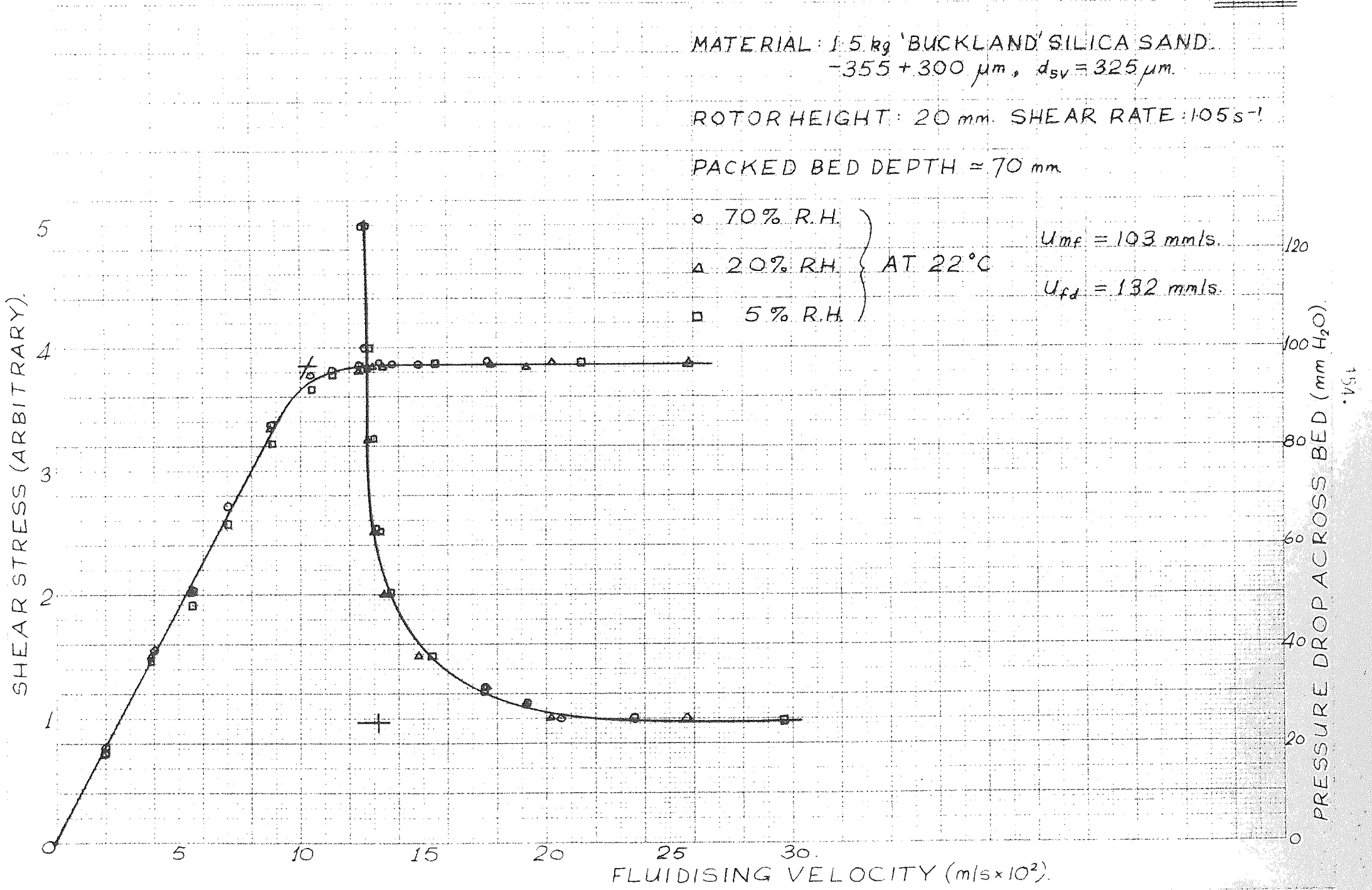

SHEAR STRESS & PRESSURE DROP vs. FLUIDISING VELOCITY FOR 458 μm 'BUCKLAND' SAND.

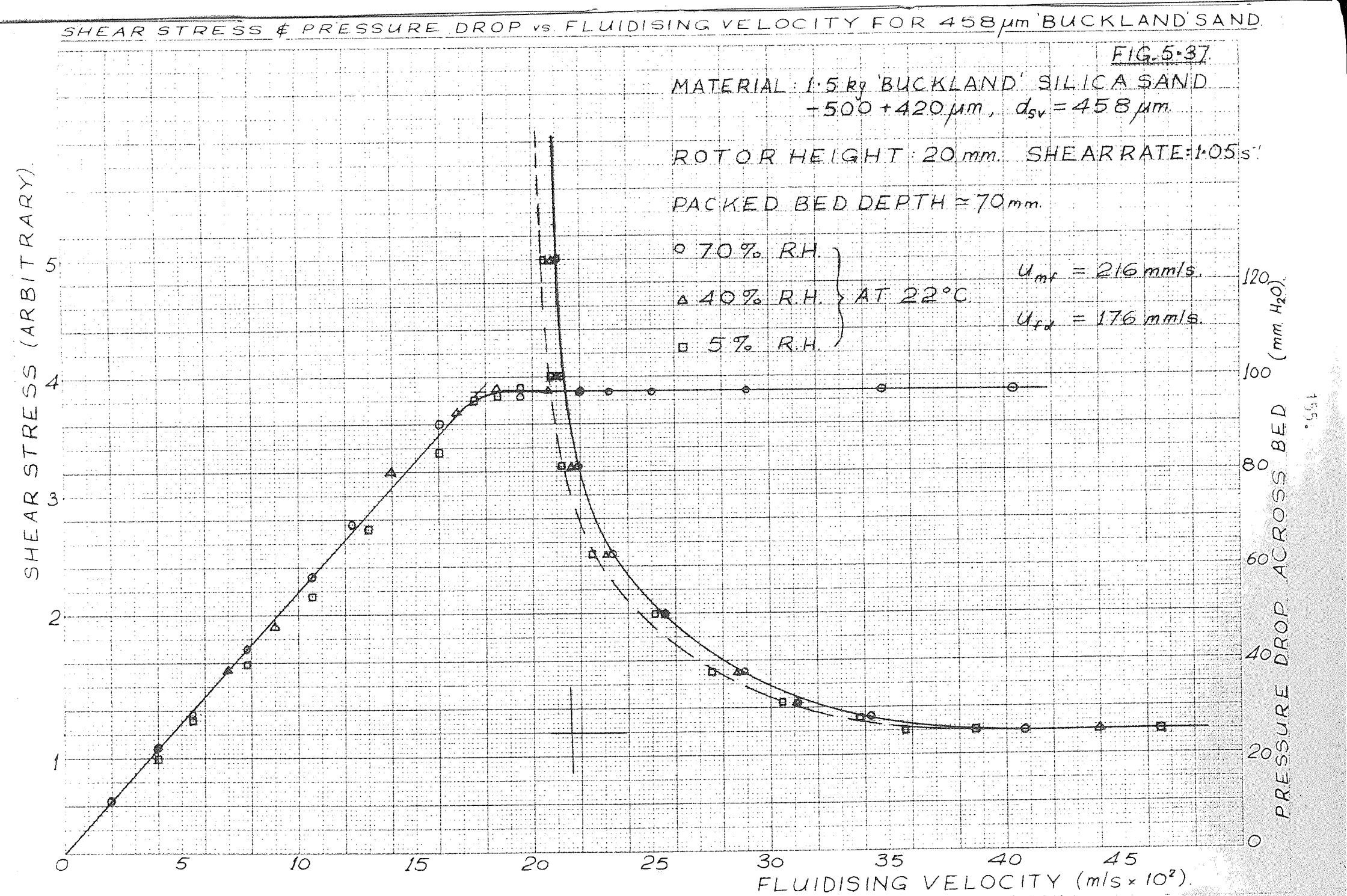

SHEAR STRESS & PRESSURE DROP vs FLUIDISING VELOCITY FOR 655μm 'BUCKLAND' SAND

FIG. 5·38.

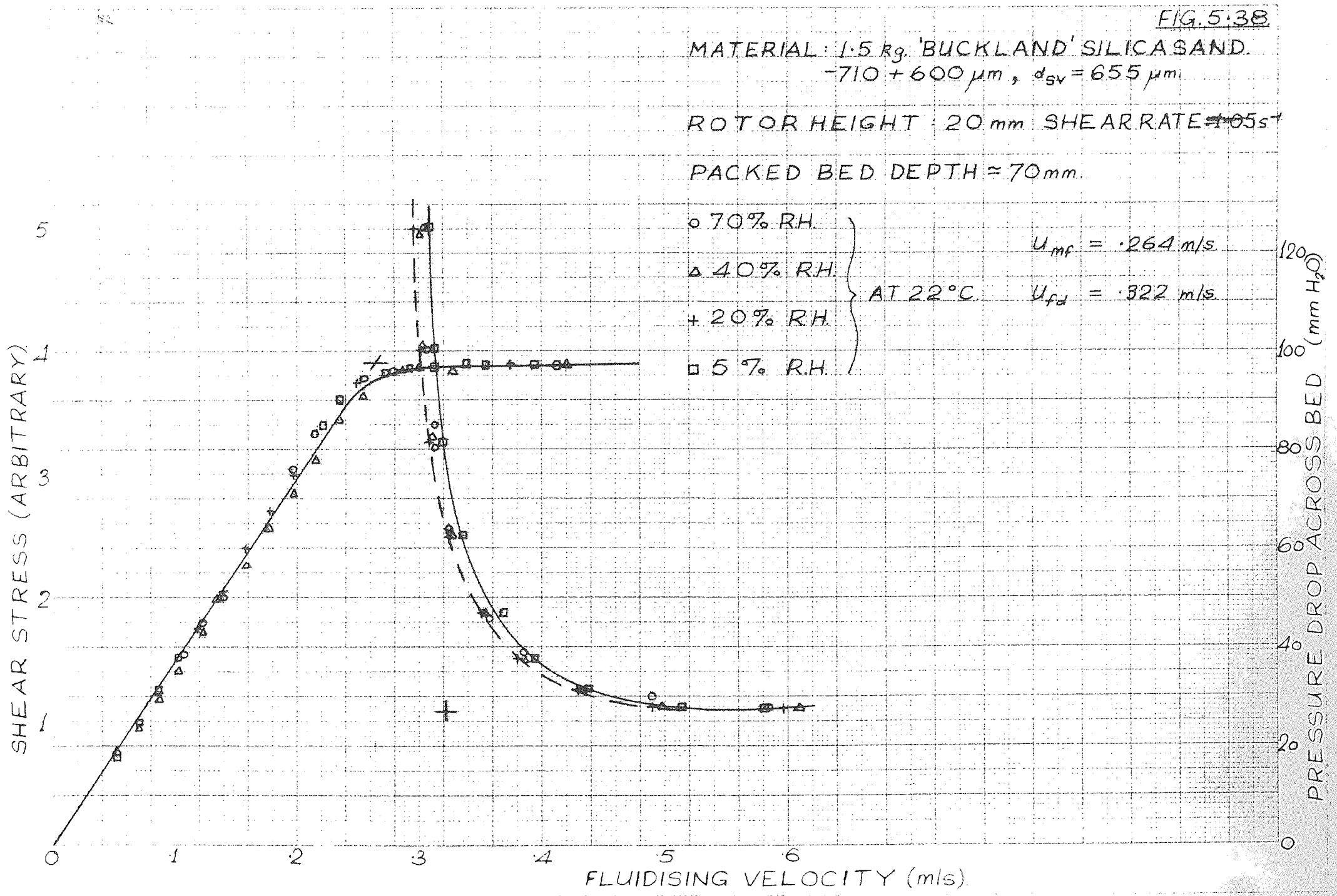

SHEAR STRESS & PRESSURE DROP vs FLUIDISING VELOCITY FOR RAW BUCKLAND 50FG SAND.

FIG 5.39.

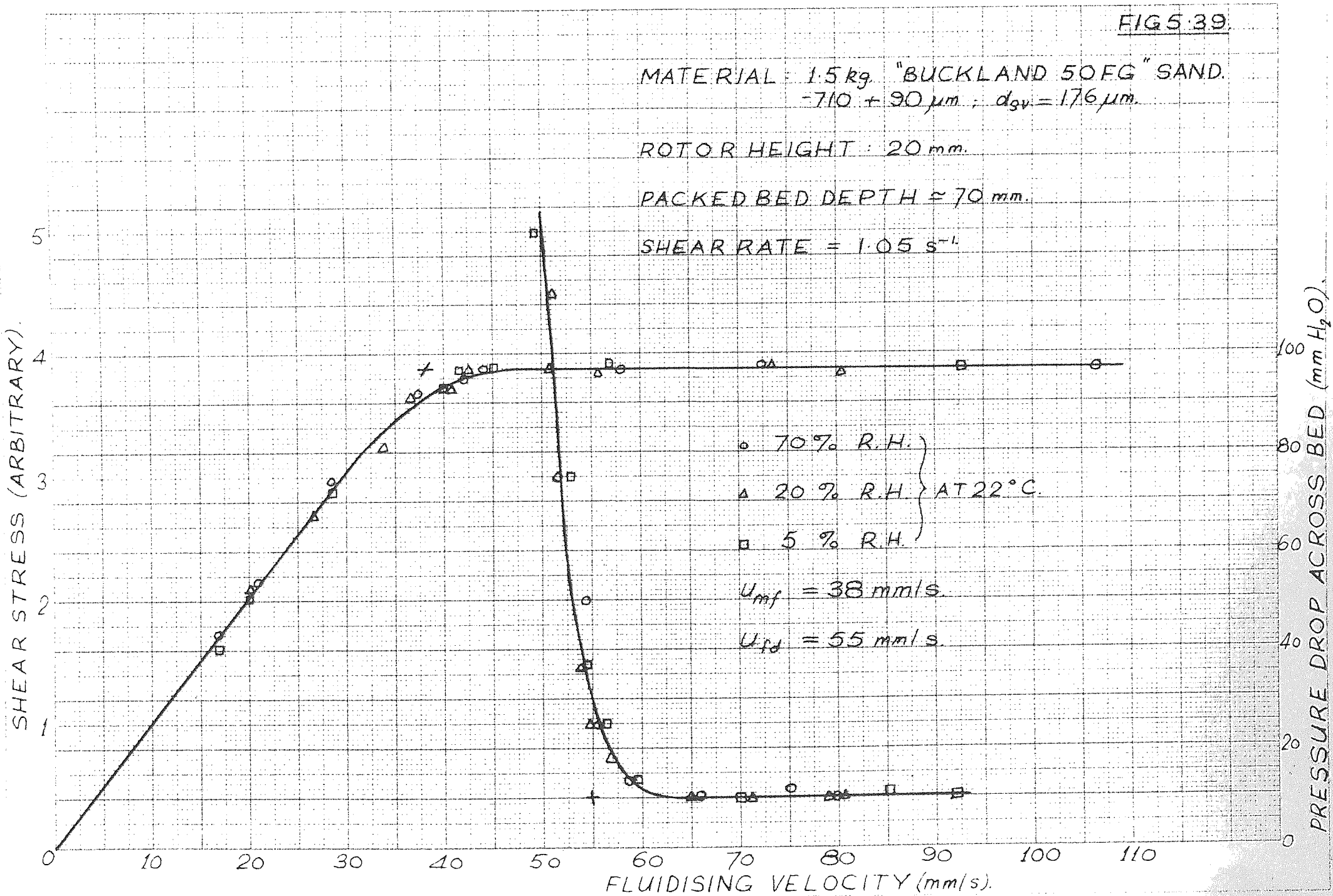

MINIMUM FLUIDISING VELOCITY, FLOW DETERIORATION VELOCITY & MINIMUM APPARENT VISCOSITY vs. SURFACE MEAN PARTICLE DIAMETER FOR 'BUCKLAND' SAND.

FIG. 5·40

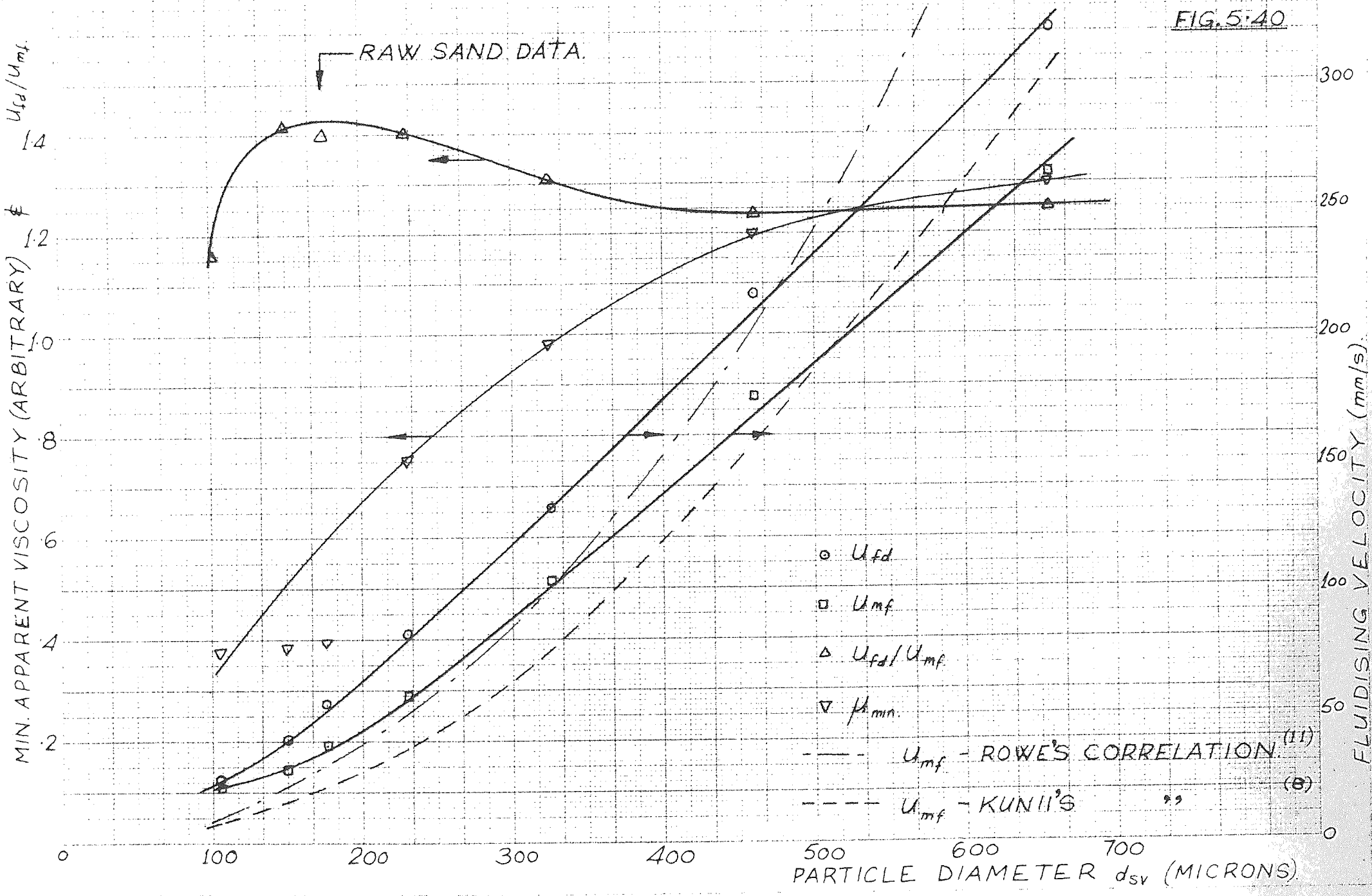

The minimum apparent viscosity increased rather more sharply with particle size than in some previous tests (cf fig 5.12): this may have been due to different bubble growth patterns in the rather deeper bed used for these tests. However, the minimum viscosity of the wide size range unsieved sand is lower than that of the corresponding size narrow cut, which accords with earlier findings.

ii) Absolute Viscosity under Conditions used in Channel Flow Rig

The viscosity of the Buckland 50 FG sand for use in the channel flow rig was measured with the viscometer, using the method of Section 3.5, at two different fluidising velocities at a bed depth of 40 mm. The rotors were positioned approximately midway up the bed in order to measure a mean viscosity, and the same distributor material (Porvair Vyon "F") as in the channel rig was used. The material was sampled by the methods suggested in reference 136 and the size analysis is given in table 5.1. However there are clearly difficulties in sampling from such a large quantity of material (several hundred kilograms) and subsequent samples have given some discrepancies in the proportion of fine and course material, though only minor changes in the surface mean diameter.

TABLE 5.1

Size Range (microns)	Geometric Mean Size (microns)	Weight (gm)
< 105	100	21.9
180 > 105	138	342.2
210 > 180	194	369
250 > 210	229	140
300 > 250	274	94
355 > 300	326	22.4
420 > 355	386	5.4
> 420	450	1.1
		996

SURFACE MEAN DIA, d_{sv} = 177 μm.

The results are shown in figures 5.41 and 5.42, and it is clear that at both fluidising velocities the flow is substantially Newtonian up to the maximum shear rate used of about 6 sec^{-1}. The lower of the two fluidising velocities used corresponds to the minimum apparent viscosity condition (see figure 5.43) and represents approximately 1.9 x U_{m_f}. At the higher fluidising velocity (.135 m/s ≃ 3.5 U_{m_f}) the viscosity has risen to about 2.3 times its minimum value. These results are compared with those from flowing channel experiments in Chapter 4 below.

6. CONCLUSIONS FROM VISCOMETER WORK

The main object of the viscometer studies was to examine qualitatively the trends in the flow behaviour of shallow fluidised beds, and this was achieved with reasonable satisfaction.

SCALE - PAN LOAD vs ROTOR ANGULAR VELOCITY FOR 'BUCKLAND 50FG' SAND.

FIG 5·41

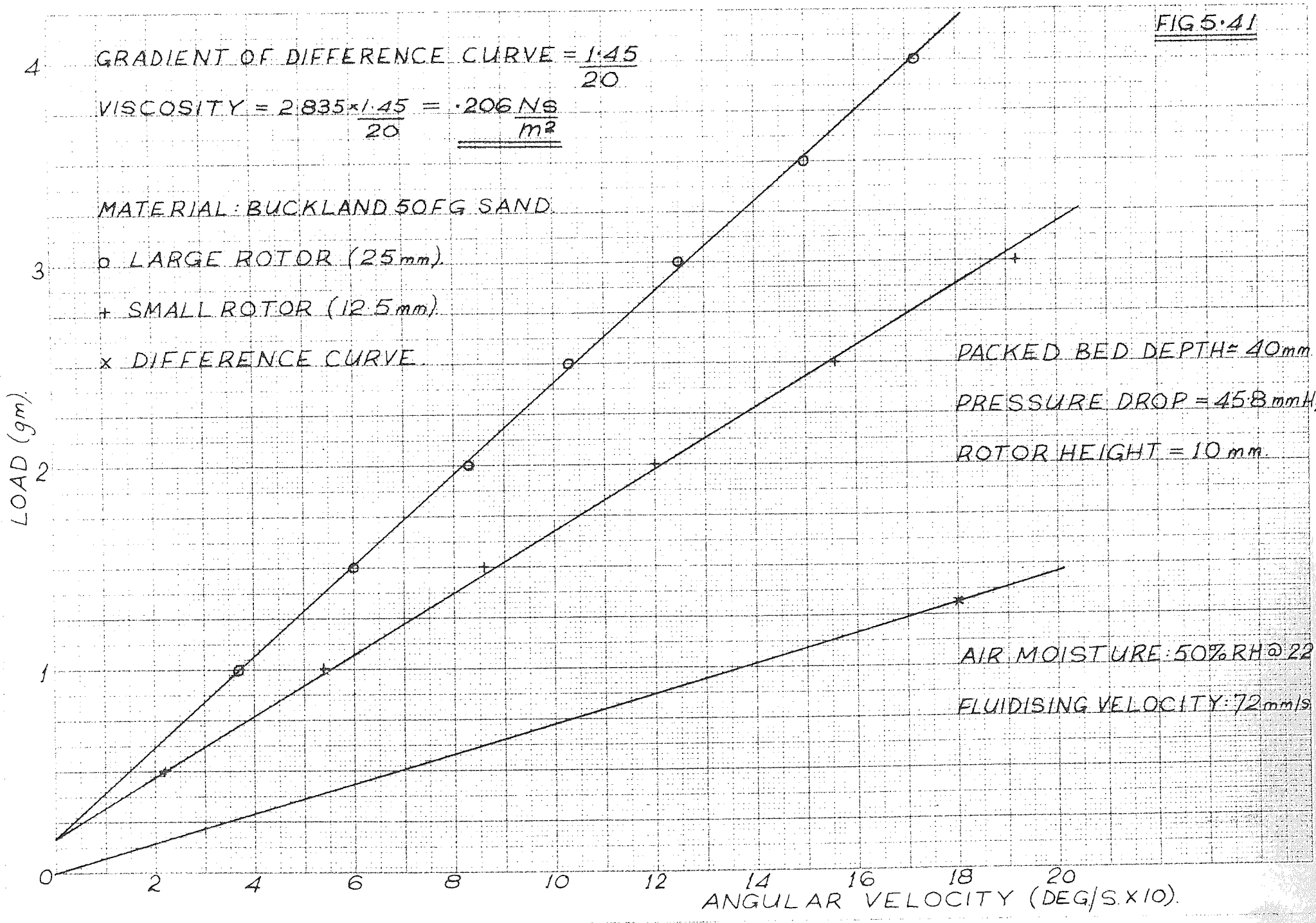

SCALE-PAN LOAD vs ROTOR ANGULAR VELOCITY FOR BUCKLAND 50FG SAND.

FIG 5·42

GRADIENT OF DIFFERENCE CURVE = $\frac{2.39}{14}$

VISCOSITY = $2.835 \times \frac{2.39}{14} = .483 \frac{Ns}{m^2}$

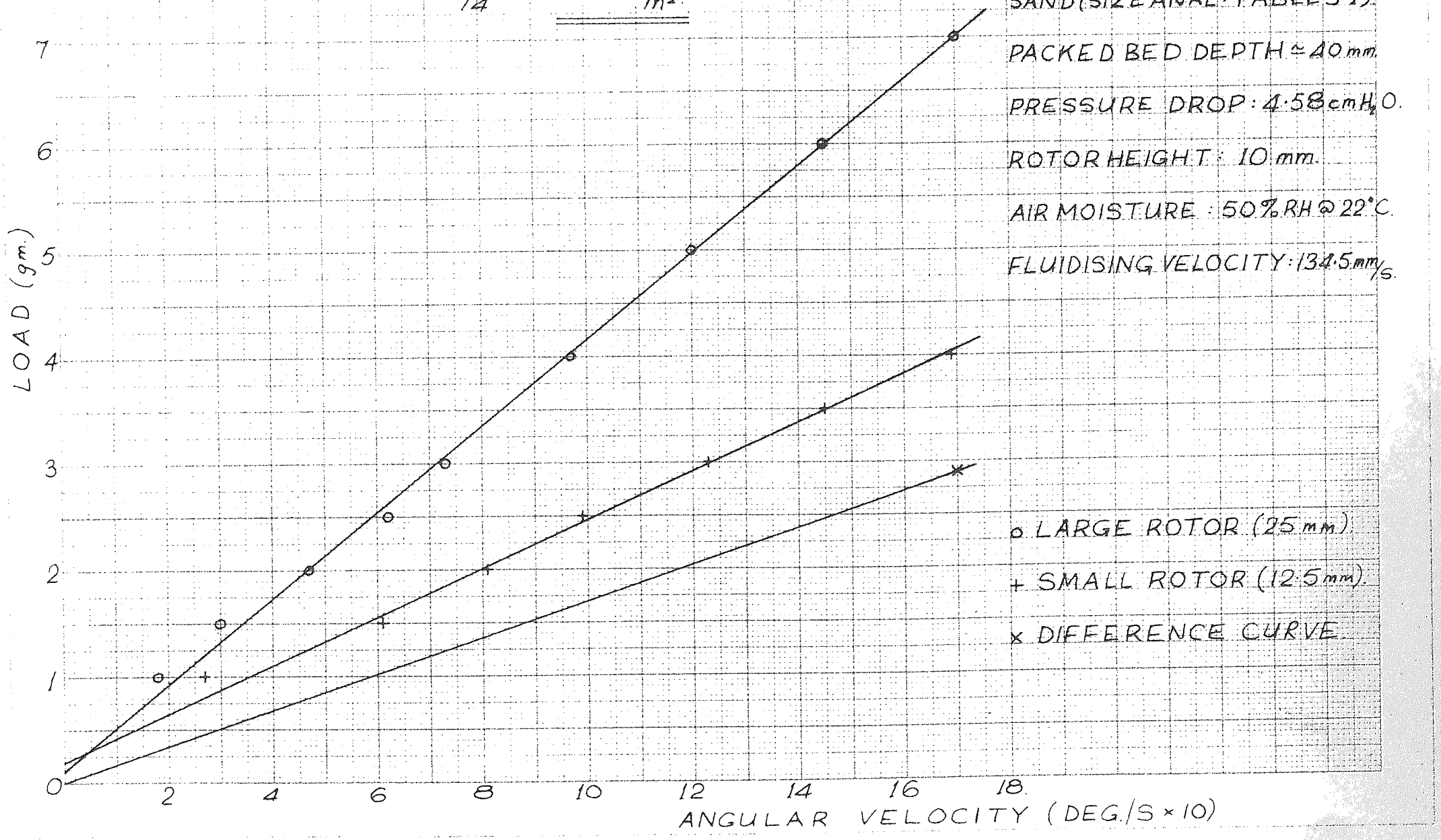

MATERIAL: BUCKLAND 50FG SAND (SIZE ANAL: TABLE 5·1).

PACKED BED DEPTH ≃ 40 mm.

PRESSURE DROP: 4·58 cm H_2O.

ROTOR HEIGHT: 10 mm.

AIR MOISTURE: 50% RH @ 22°C.

FLUIDISING VELOCITY: 134·5 mm/s.

o LARGE ROTOR (25 mm).

\+ SMALL ROTOR (12·5 mm).

× DIFFERENCE CURVE.

APPARENT VISCOSITY vs. FLUIDISING VELOCITY FOR 'BUCKLAND 50FG' SAND.

FIG. 5.43

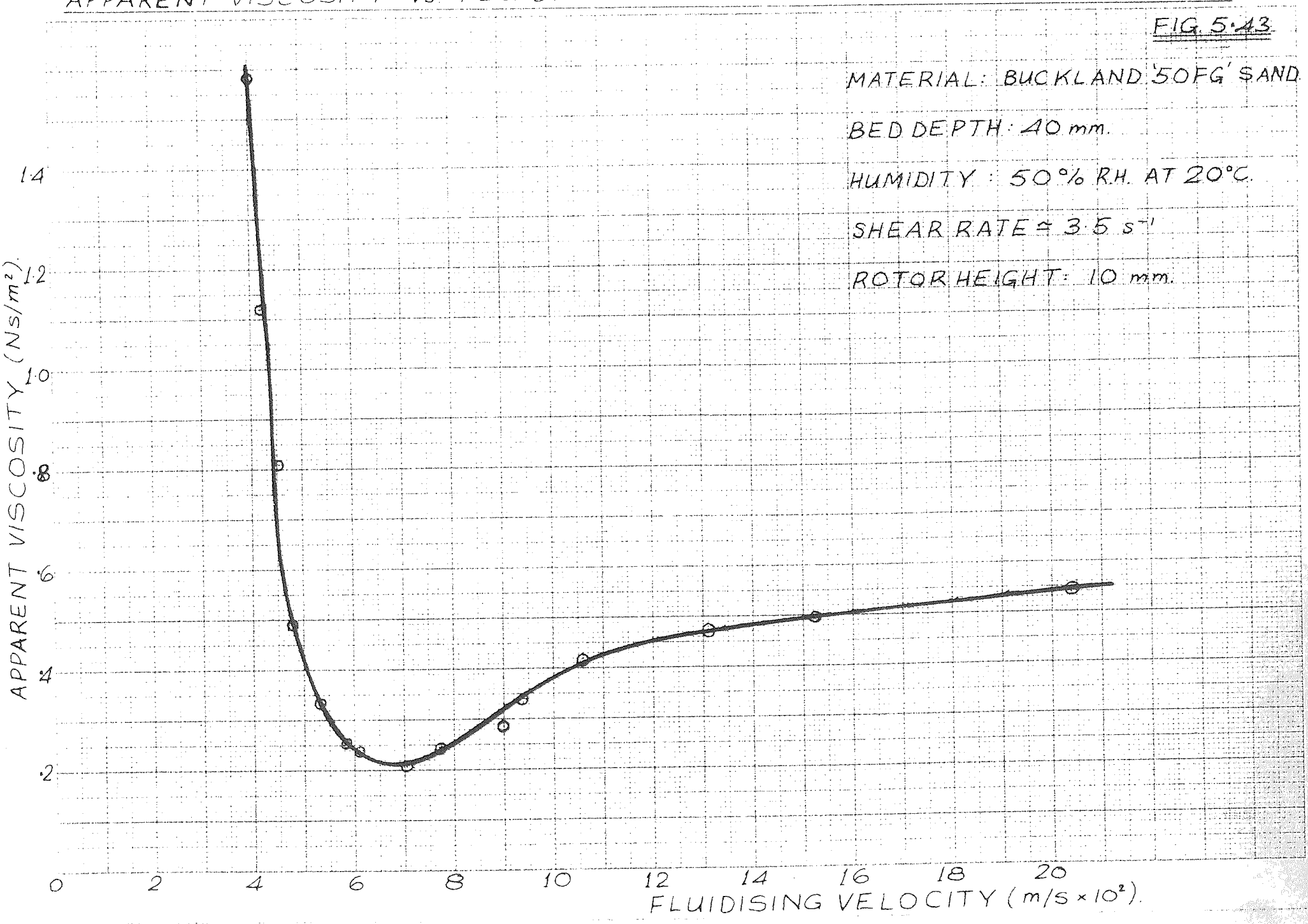

The principal conclusions are as follows:

a. The viscosity of the bed falls to a minimum value at a fluidising velocity of about 1.5 - 2.0 times that for minimum fluidisation. After this, the viscosity may increase or remain constant according to the degree of homogeneity of the bed.

b. At low fluidising velocities the bed behaves as a shear-thinning fluid, due to shear induced improvement in the character of fluidisation local to the shearing surface. The shear diagram cannot normally be represented accurately by a power law expression, and the flow is subject to anomolies due to segregation when using wide size range material.

c. At fluidising velocities above 2 U_{m_f} the flow normally becomes substantially Newtonian for the range of shear rates achievable with the viscometer.

d. Shear at a vertical surface in a fluidised bed takes place without slip up to a certain shear rate; after which slip commences and tends to a constant value, for a particular test, as the shear rate is further increased. The critical shear rate does not appear to have a characteristic value for a given material or fluidising conditions.

e. The viscosity of the bed increases with the density of the fluidised particles; although it is doubtful if the two properties have a unique relationship. The viscosity of two-component mixtures is normally less than that expected by considering the mean density of the components.

f. The viscosity of the bed increases with the mean size of the fluidised particles. The increase is normally more

f (cont)

marked in deeper beds due to the reduced homogeneity therein when fluidising large particles.

g. Wide size range materials have superior flow properties to narrow cuts of the same mean size, in that their minimum apparent viscosity is slightly lower, and the viscosity remains near its minimum value over a greater range of fluidising velocities.

h. Improvements in flow behaviour are possible by blending small dense particles with larger lighter ones. Significant improvements may be possible by mixing components which have closely matched minimum fluidising velocities.

i. The viscosity of a shallow fluidised bed increases with the depth of the bed, due to the disturbing influence of the larger bubbles present in deeper beds.

j. The axial viscosity profile near the distributor of a shallow bed is dependent upon the type of distributor used. Above about 50 mm from the distributor the type of plate has no influence on the behaviour. However, below this depth the viscosity increases with proximity to a pierced plate, but decreases in the case of a porous distributor. This is thought to be due to differences in the initial bubble growth above the distributor.

k. Fluidised particles of low electrical conductivity are subject to a deterioration in flow performance when the fluidising air moisture content is low enough to permit the accumulation of electrostatic charges. The critical relative air humidity depends upon particle properties and also temperature.

ℓ. Absorption of moisture from the fluidising air on to the surface of the fluidised particles may cause agglomeration, and a consequent increase in minimum fluidising velocity. When the bed is well fluidised however, the minimum apparent viscosity may sometimes be reduced at high moisture levels, due possibly to a 'lubrication' effect on the particle surfaces.

m. The presence of minute quantities of surface contaminents may modify the effects of changes in fluidising air humidity.

n. Unlike viscous liquids, the viscosity of fluidised beds is not sensitive to small temperature variations.

o. The influence of particle surface-geometry is difficult to assess independently of other variables but appears not to have any strong influence on fluid bed viscosity.

The foregoing are summarised diagrammatically in figure 6.1, in which the directions of the arrows illustrate the effect of the variables upon a typical viscosity vs. fluidising velocity curve.

It is clear from the above conclusions that the viscosity of a fluidised bed depends upon a much larger number of variables than that of a real fluid. In addition to the physical properties of the fluidised material, it is highly dependent upon environmental factors. Since it is not possible to predict the viscosity of conventional fluids from their other physical properties, it is unlikely that such prediction will be possible for fluidised beds. Because of this, it is vital to try to establish correlations between small-scale viscometer tests and real flow situations, in order to provide more reliable information for their design. It was to this eventual aim that the idea of undertaking both small and large scale experiments in the present work was

SUMMARY OF TRENDS IN FLOW PROPERTIES.

FIGURE 6·1.

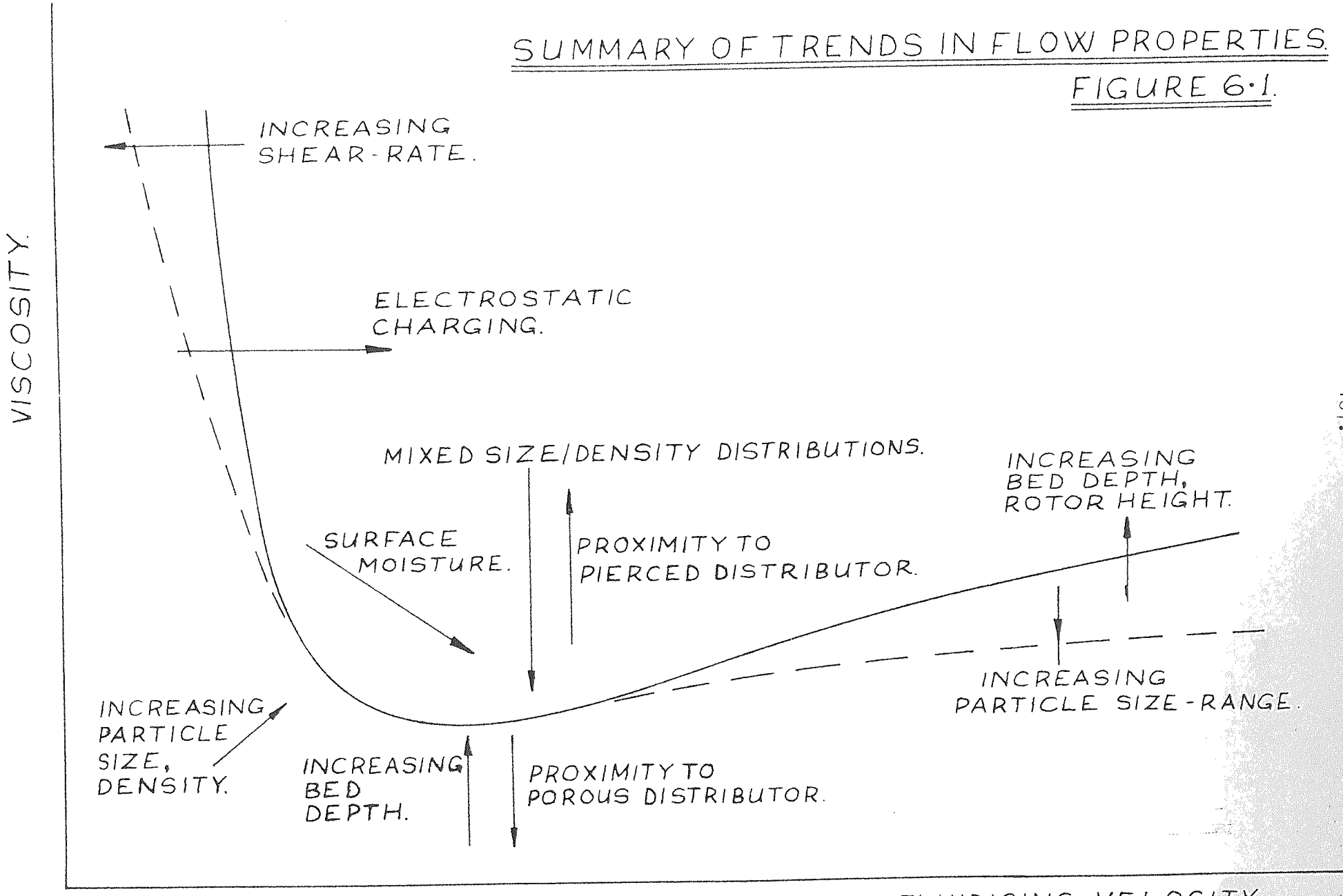

directed.

The viscometer work undertaken represents one of the most wide-ranging investigations of fluid bed flow yet reported, although many authors have made more searching studies over a more restricted field. The influence of some parameters has been examined rather sketchily, but it is considered that the work has formed a useful basis for the design of the channel flow rig described below.

Much further work could be done with the viscometer but this will undoubtedly prove more valuable if carried out in the light of, and in conjuction with, work on channel flow in the large rig. Perhaps the main intrinsic disadvantage of the viscometer is that the maximum usable shear rate is limited by the early onset of slip and other departures from the viscous flows. This means that the high shear-rates achievable in channel flow and of interest industrially, cannot be approached in viscometer studies. This is clearly a limitation in any system likely to be subject to non-Newtonian flows.

The other object of the viscometer work was to devise a method of measuring quantitatively the viscosity of shallow fluidised beds. This has again been achieved satisfactorily with the two rotor method, although the accuracy is clearly limited by the necessity of subtracting two quantities of similar magnitude in order to extract the results from the experimental data. It is likely that, at least in some conditions, the theory of viscometric flows is not rigorously applicable to fluidisation, and comparison with channel flow results must be awaited to see whether viscometer data is useful to engineering accuracy.

7. RECOMMENDATIONS FOR FUTURE WORK

It was noted above that many parts of the work were somewhat limited in depth of study, in order to cover a wide field in a short time; so that almost all aspects would repay further investigation. However, perhaps the most important immediate need is for comparison of small-scale tests and large-scale channel flow experiments. The viscometer is clearly convenient for measuring flow behaviour cheaply and rapidly, but it is as yet uncertain whether the results have any relevance, either qualitative or quantitative to channel flow. Work was commenced to this end in the present study, and is now proceeding.

It would be instructive to carry out measurements of local voidage concurrent with viscometric measurements to test the hypothesis that high viscosity is associated with aggregative fluidisation or lack of homogeneity. It seems likely that much less gas rises in discreet bubbles in very shallow beds, but visual observation of bubbles therein would probably be very difficult.

Of particular importance is the influence of moisture. It would be useful to investigate quantitatively the relationship between electrostatic potential, flow behaviour and inter-particle action. This would probably require extensive electrical measuring equipment and certainly a more specialised knowledge of electrostatics. The influence of surface-absorbed moisture and other contaminants could be examined using photomicrographic techniques.

The limited work done with mixed size and density particles was encouraging in suggesting that the blending of free-flowing mixtures may be possible. Further work in this area in order to provide optimum flow properties consistent with other process requirements would clearly be propitious to industrial acceptance of fluidised flow. The use of mixtures of greater size and density difference than used

to date would be worthy of study.

Lastly, if fluidised flow is to be applied to combustion systems, a study of the effect of high temperatures on the flow properties is essential. Clearly this would present difficulties on a large scale, but the existing viscometer could be easily adapted for measurements in a combusting bed by provision of a heat shield and rotors of suitable material.

CHAPTER 4

CHANNEL FLOW WORK

1. INTRODUCTION

It was decided, after completing a substantial amount of work with the viscometer, to construct an experimental rig with which to study fluidised channel flow.

The object in carrying out channel flow experiments was to investigate the flow behaviour of fluid beds under conditions more similar to those likely to be encountered industrially. The viscometer has been extremely useful in establishing trends of flow behaviour, and is clearly a much more versatile instrument than a large flow rig, because of the smaller quantities of material and fluidising air to be handled. Comparisons of viscometer[102,148] and channel flow data[105, 141,149] have indicated good qualitative agreement in some aspects of the work, but have not generally shown a useful degree of quantitative similarity. In the case of earlier comparisons[102], this was due to inaccurate viscometer calibration; but later results, though in better agreement, still show some disparity. As noted above (Chapter 3, Section ..), the viscometer is limited in its application to low rates of shear; so that even if accurate comparisons with channel flow can be made there, it is possible that these may be of no value at the higher shear rates of interest industrially in channel flow. Very little previous work on fluidised flow has been done at industrially useful shear rates. Thus although much more useful work can be done using viscometry, it is desirable that more is known about its limitations as a technique applied to fluid beds by direct comparison with channel flow.

The design, construction and commissioning of the channel flow rig accounted for a substantial amount of time, so that only a limited period was available on its completion for obtaining results. This initial work with the rig was directed towards obtaining a friction

factor - Reynolds number correlation as an aid to the design of fluidised channels, as well as a preliminary comparison with viscometer data. The former aim was achieved satisfactorily over a limited range of fluidising conditions, though some anomalies were evident in the flow behaviour at low fluidising and solids flow velocities. Further work[150] is now proceeding to assess the generality of the $f - R_e$ correlation, and also toward a more fundamental study of fluidised channel flow.

The large flow rig was designed with a view to studying both horizontal channel flow and flow in vertical conduits, using the same solids return system. However the former mode of flow was considered to be more important initially, so that the specification of the rig was primarily guided by channel flow requirements. Some aspects of the specification and detail design of the rig were necessarily based upon arbitrary decisions, in view of the general lack of knowledge of such systems. Nonetheless the rig has proved to be satisfactory in operation, although clearly some features have come to light as a result of the initial test work which could be improved by minor modification.

The specification for the rig is given below, and a full description of its design and construction is presented in Appendix I.

2. SPECIFICATION FOR CHANNEL FLOW RIG

i) Provision of Continuous Solids Flow

A number of previous workers[97-103,141,151] have used channel flow rigs to study various aspects of fluidisation. Of these, but for Botterill and co-workers none was able to provide for a continuous solids flow over a long period, as material was handled batch-wise. A continuous flow of solids was considered essential for the present work as it was thought (and has since been confirmed) that the establishment of steady flow would take a long while under some conditions. Furthermore, a batch flow system becomes most unwieldy, and therefore least accurate, at conditions of maximum flow; which latter are

clearly of the most importance if the rig is not to be over-designed.

ii) Solids mass flow rate measurement

It was also considered essential to measure the mass flow rate of solids through the channel. From this, knowing the bulk density of the bed and flow cross section, the mean flow velocity may be calculated. The alternative method of measuring mean flow velocity, by a timed float, has been shown to be inaccurate and inconsistent.

iii) Channel Cross Section

It was desired to provide for a maximum bed depth of about 120 mm, similar to that available in the viscometer. There seemed at this stage to be little point in studying deeper beds, even if this was economically possible, as the viscometer work had clearly shown the superiority of shallow bed flow properties.

A further requirement was to be able to measure velocity profiles across the test section. Discussion with Bessant[149], following his work in this area indicated that the minimum viable channel width for this purpose was about 150 mm, owing to measurement difficulties very close to the walls. It was thus decided to specify unit aspect ratio at this dimension for the channel cross section. A larger channel width would be beneficial for some aspects of the work, but this would have meant an unacceptable restriction on flow rates, or necessitated handling an excessively large amount of solids.

A further need was to provide for alterations in the width of the channel without major modification to the rig, in order to investigate the effect of channel geometry on the flow.

iv) Bed Material

Clearly a wide variety of materials could be used in the rig under some conditions, but it was necessary to design around a particular material. The material chosen was 'Buckland' 50 FG sand (for supplier

see Appendix 2, size analysis Chapter 3, Table 5.1), which had been studied previously in the viscometer work. This sand is cheaply and readily available to close specifications and is sufficiently refractory to be used in combustion work. Its only drawback is susceptibility to moisture (see Chapter 3, Section 5.3), but this was not considered serious. A second material, Bauxilite (alumina) was also considered at the design stage. This material is denser than sand, so that it was used as a check on the items of equipment whose performance depends on mass, rather than volume flowrate.

v) Provision for Fully Developed Flow

It was considered essential that the flow in the channel test section should be fully developed, that is such that the fluid free surface is parallel to the channel base. The condition is not a requirement from the fluid dynamics viewpoint, as it is usual[152] to treat accelerating flows in long channels by considering short reaches of channel in which the flow can be assumed uniform. This approach was used by BESSANT[141] because of the design of his apparatus, but it was considered preferable here to ensure uniform bed depth along the test section by using an inclined channel. This is important in order to obviate preferential fluidisation of the downstream end of the channel due to the reduced bed height thereat.

Thus it was necessary to provide a channel of variable inclination, and to furnish means for its accurate measurement. An inclination between zero and 30 degrees was eventually specified: the latter figure is in excess of anticipated requirements but could be easily provided without prejudice to the cost or operation of the rig.

The total channel length was fixed at three metres, the central one metre of which was to comprise the test section. The choice was somewhat arbitrary and governed partly by economic considerations.

One metre was considered the minimum test length for reliable and accurate measurements and the additional upper and lower reaches were provided to eliminate entry and exit effects. A one metre entry length is rather short by conventional hydraulics criteria[152,166] for the highest relevant Reynolds numbers, but previous work[149] had indicated more rapid entry-recovery in fluidised flow.

vi) Fluidising Velocity

It was decided to provide a maximum fluidising velocity of approximately five times that for minimum fluidisation of the design material. Previous work has indicated viscosity minima at between 1.5 and 3 U_{mf} with either deterioration or no further improvement in flow thereafter. Provision of very high fluidising velocities therefore appeared pointless, although larger fans could be provided (if required for denser material for example) at a later date.

vii) Solids Flowrate

One of the main objects of the channel flow work was to study flow at high shear rates. However, the upper limit of flowrate at maximum channel section had to be fixed by considerations of the cost and size of the solids return system. It was decided to base the design maximum flowrate on a solids circulation rate for Bauxilite of 10 kg/s (35 ton/hr) for which the corresponding mean flow velocity is approximately .30 m/s at maximum bed depth. This represents a shear rate of only $12s^{-1}$, but since the same solids mass flow is available at all bed depths, shear rates up to several hundred s^{-1} are possible in shallower beds.

viii) Distributor Material

It was decided to specify a porous fluidising distributor rather than a pierced one, because of the evidence from the viscometer work of an inviscid layer above porous distributors. It is quite possible that such conditions will not obtain in a flowing bed due to the shearing

action of the solids across the plate which is absent in the viscometer. However no previous work is reported on the influence of distributors on fluidised flow in channels. A vital consideration was that of ensuring even fluidisation over the entire distributor area, which is not easy to achieve in such a large bed. However, design criteria were applied which it was hoped would achieve uniform fluidisation with minimum pressure drop.

The material selected was "Vyon" (see Appendix 2) a sintered plastic material which previous experience[153] had shown to be of sufficiently consistent properties to enable even fluidisation of large area beds. The material also met two further important requirements: it is sufficiently flexible to cater for the required variation in channel inclination, and is available in large enough sizes to permit fluidisation of the complete channel without any discontinuities. The latter is particularly vital, as small areas of local absence of fluidising air at distributor joint lines can exert a disproportionately large influence on the flowing bed.

It was also required to be able to change the distributor material with minimum dismantling of the rig.

ix) Vertical Transport

A further requirement at the design stage was provision for the study of vertical fluidised flow, more especially of down-flowing beds; although the latter was not to form part of this work.

A tubular downflowing leg of 140 mm diameter fed and exhausted by the same solids circulation system as the inclined channel was conveniently included in the design, with little increase in cost and none in lack of functionality. However this has not so far been used other than for its secondary function of altering the hold-up of solids when changing the mass flowrate around the rig. The length of the

downflowing leg was specified as two metres, and provision was included for the relocation of its lower receiver to permit the attachment of tubes or ducts to its lower end in order to study their effect on solids efflux.

x) Control and Instrumentation

It was decided to make provision for controlling the solids flowrate at both ends of the fluidised channel. The main control was to be at the channel entry, whilst the downstream control was provided to enable filling the channel without any throughflow. This latter control has also been useful as a means of initiating hydraulic jumps within the channel.

The facility was also included for fitting weirs, sluice gates or other obstructions at entry and exit to the test section of the channel . These were provided in order to study the flow through such devices, rather than as a primary means of flow control.

The following parameters were required to be measured during work with the rig:-

1. Solids flowrate
2. Fluidising velocity
3. Channel inclination
4. Pressure drop across bed
5. Uniformity of flow
6. Depth of Bed
7. Fluidising air humidity

Other more specialised requirements, such as the measurement of velocity profiles, wall drag, and forces on immersed objects were envisaged at the design planning stage. However these were not to be investigated in the initial work with the rig, so that no specific provision was made for their measurement. However, the bed wall of the test section was made

detachable from the remainder, so that it could be replaced by other wall sections containing measuring devices if required.

3). THEORETICAL TREATMENT

i) Choice of a Theoretical Model

Two basic approaches have been used by previous workers to characterise the flow behaviour of fluidised beds. One is to consider the interaction of the fluid and particles on a microscopic scale; and the other is to treat the bed as a continuum and analyse its bulk properties by analogy with liquid flow.

Several authors[18,34,37] using the former approach have considered the rise of an idealised bubble through an inviscid fluid; and BUYEVICH[160] has applied a statistical treatment to the random motion of the dense-phase particles. It is not proposed to discuss these methods in detail, but it is considered that some of the basic assumptions used are questionable; and in any case such treatments are very difficult to apply to a practical flow situation.

The liquid analogy approach, though perhaps little better in providing an accurate description of the internal behaviour of the bed, is at least more readily applicable to real flow fields. From this point alone it is preferable, at least until a fuller understanding of the mechanism of the flowing bed is available. A number of workers using both viscometric[67, 70-72, 74-76] and channel flow[97,98] apparatus have considered the bed to behave as a Newtonian liquid. However there is strong evidence that interparticle contacts occur in the bed, which are likely to be modified by the presence of externally applied shear stresses. Since such structural changes on a molecular scale give rise to non-Newtonian flows in liquids, similar behaviour is likely in fluidised beds. Also, the work with the viscometer has indicated that fluidised beds do not behave in a Newtonian manner. Thus if a liquid analogy is to be applied with any accuracy, a model which takes account of non-Newtonian behaviour must be used.

It is convenient when studying flow in open channels to first consider pipe flow, and use the concept of an equivalent diameter to represent the channel dimensions (see below). Several authors have suggested modification to the normal Newtonian shear stress - shear rate equation ($\tau = \mu \frac{du}{dr}$) to take account of non-Newtonian behaviour. An early attempt by McMILLAN[161] used an empirical expression, and others have fitted power-law or other equations. Many of these have been compared by CRAMER and MARCHELLO[162], from which comparison emerges the fact that the choice of model is of little moment, provided it fits the experimental data.

An extremely useful model is that due to METZNER and REED[130], who use the concept of a generalised Reynolds' Number for non-Newtonian pipe flow. Their approach is based on a power-law model but is not restricted to fluids which follow this law. It has the additional advantage that it is not restricted to laminar flows, and indeed may be used to determine the onset of turbulence. The model may be adapted for use in open channel flow situations, and despite some known shortcomings, it was decided to use it to correlate the initial results obtained from the rig. An outline of the model is presented hereunder.

ii) Flow of a non-Newtonian Fluid in an Open Channel

Considering first the steady flow of a fluid in a circular pipe, it has been shown by RABINOWITSCH[163] and MOONEY[147] that the rate of shear at the wall is related to the pressure drop by the expression:

$$-\left(\frac{du}{dr}\right)_w = 3\left(\frac{8Q}{\pi D^3}\right) + \frac{D\Delta P}{4L} \cdot \frac{d(8Q/\pi D^3)}{d(D\Delta P/4L)} \qquad \ldots(1)$$

This equation requires the following assumptions:-

1. The flow is laminar
2. There is no 'slip' at the wall
3. The fluid does not exhibit rheopexy or thixotropy

Since the mean flow velocity $U = \frac{4Q}{\pi D^2}$, eqn (1) may be rewritten as:

$$\left(-\frac{du}{dr}\right)_w = \frac{3}{4}\left(\frac{8U}{D}\right) + \frac{1}{4}\left(\frac{8U}{D}\right) \cdot \frac{d(8U/D)/(8U/D)}{d(D\Delta P/4L)/(D\Delta P/4L)} \qquad \ldots(2)$$

ie $$\left(-\frac{du}{dr}\right)_w = \frac{3}{4}\left(\frac{8U}{D}\right) + \frac{1}{4}\left(\frac{8U}{D}\right) \cdot \frac{d\,\ell n\,(8U/D)}{d\,\ell n\,(D\Delta P/4L)} \qquad \ldots(3)$$

Now let $$\frac{d\,\ell n\,(8U/D)}{d\,\ell n\,(D\Delta P/4L)} = \frac{1}{n'} \qquad \ldots(4)$$

Then $$-\left(\frac{du}{dr}\right)_w = \frac{3n' + 1}{4n'} \cdot \left(\frac{8U}{D}\right) \qquad \ldots(5)$$

Eqn (4) may be integrated, for constant n', to give

$$\frac{D\Delta P}{4L} = K'\left(\frac{8U}{D}\right)^{n'} \qquad \ldots(6)$$

where K' is also a constant.

It has been found[130] that for most fluids K' and n' are constants over a wide range of the variables $\frac{D\Delta P}{4L}$ and $\frac{8U}{D}$. However the method is not restricted to fluids for which these conditions pertain, in which case equation (6) is that of a tangent to the log plot of the variables at a single point.

By substituting for $\frac{8U}{D}$ in equation (6) from eqn (4), and noting that $D\Delta P/4L$ represents the shear stress at the pipe wall, τ_w, one obtains:

$$\tau_w = K'\left(\frac{4n'}{3n' + 1}\right)^{n'} \cdot \left(-\frac{du}{dr}\right)_w^{n'} \qquad \ldots(7)$$

Thus it is evident that $\frac{8U}{D}$ represents the shear rate at the pipe wall and $K'\left(\frac{\Delta\, n'}{3n' + 1}\right)^{n'} = K$ say, for constant n' represents the plastic viscosity of the fluid as defined by Ostwald's Equation for power-law fluids (see Chapter 3, Section 3.3). Thus n' is an index of non-Newtonian flow, being equal to unity for Newtonian fluids, and less than and greater than unity for shear-thinning and shear-thickening fluids respectively.

The next step is to define a friction factor and Reynolds Number for non-Newtonian flow. Regarding the former, the Fanning and D'Arcy friction factors may be defined in the usual way, as for Newtonian flow:

$$f_{Fanning} = \frac{D\Delta P}{4L} \Big/ \frac{\rho U^2}{2} \qquad \ldots(8)$$

or

$$f_{D'Arcy} = 4 \frac{D\Delta P}{4L} \Big/ \frac{\rho U^2}{2} = 4 \times f_{Fanning} \qquad \ldots(9)$$

To define a generalised Reynolds Number it is necessary to allow for the non-Newtonian flow by including the index n':

$$N_{Re} = \frac{\rho U^{2-n'} D^{n'}}{\gamma} \qquad \ldots(10)$$

Under laminar flow conditions, the usual relationship $f_F = \frac{16}{N_{Re}}$ may be obtained by substituting for $D\Delta P/4L$ in eqn (8) from eqn (6):

$$f_F = \frac{2 K' 8^{n'}}{D^{n'} U^{(2-n')} \rho} \qquad \ldots(11)$$

Thus γ in eqn (10) = $K' 8^{n'-1}$

$$\therefore f_F = \frac{16 \gamma}{\rho U^{(2-n')} D^{n'}} = \frac{16}{N_{Re}} \qquad \ldots(12)$$

$$\text{Similarly } f_D = \frac{64 \gamma}{\rho U^{(2-n')} D^{n'}} = \frac{64}{N_{Re}} \qquad \ldots(13)$$

The above expressions are completely general for laminar flow of any fluid, the parameters K' and n' being obtained from the local slope of the logarithmic plot of $D\Delta P/4L$ vs $8U/D$. With the onset of turbulent flow, eqn (6) becomes invalid, so that the relationship $f_F = 16/N_{Re}$ no longer holds. The method may therefore be used to predict the onset of turbulence.

Modifications for Open Channel Flow

In order to apply the foregoing to flow in open channels, two modifications are required. The first is to replace the pipe diameter by a characteristic channel dimension [164]. This is the hydraulic or equivalent diameter D_ℓ, where:

$$D_\ell = \frac{4 \times \text{flow area}}{\text{wetted perimeter}} = \frac{4b\,h}{b + 2\,h}$$

The other modification is the replacement of the factor 16 or 64 in the relationship between f_F or f_D and N_{Re} by a factor appropriate to

the aspect ratio of the channel. Values of this factor have been tabulated by STRAUB et al[165] for channels of various geometries, and its variation with the aspect ratio of a rectangular channel is plotted in Figure 3.1.

In a sloping channel the pressure head is provided by the component of the weight of the fluid down the channel. The shear stress term is thus given by:

$$\tau_w = \frac{\rho g D_\ell S}{4} \qquad ..(14)$$

where S is the slope of the channel (that is, S = Sin θ, where θ is the angle of inclination).

iii) Validity of the Model when applied to Fluidised Beds

The analysis of Section (ii) is subject only to the three main assumptions stated therein: other than these it is general for any real fluid. The accuracy of the model therefore depends on how closely these assumptions are satisfied, and also the extent to which a fluidised bed behaves as a real fluid.

It is known[101] that shearing a bubbling fluidised bed causes a redistribution of the bubbles and therefore a change in the internal structure; and also that the plastic viscosity of the bed varies throughout its depth (see Chapter 3, Section 5.2 (vi)). However neither of these is necessarily outside the postulation of a generalised non-Newtonian fluid.

Clearly a fluidised bed is not a homogeneous medium since the fluid and solids have disparate motions; in which respect the bed differs from a true fluid. However, in a gas fluidised bed the path taken by the gas is of interest only insofar as it influences the motion of the solids and their interaction with the bed containment. It has been observed by many previous workers that the bulk flow of the bed is analogous to an incompressible fluid, although the local behaviour may

COEFFICIENT 'C' IN $f_D = C/R_e$ VS ASPECT RATIO OF RECTANGULAR CHANNEL.

(AFTER STRAUB ET. AL.[165]).

FIG. 3·1

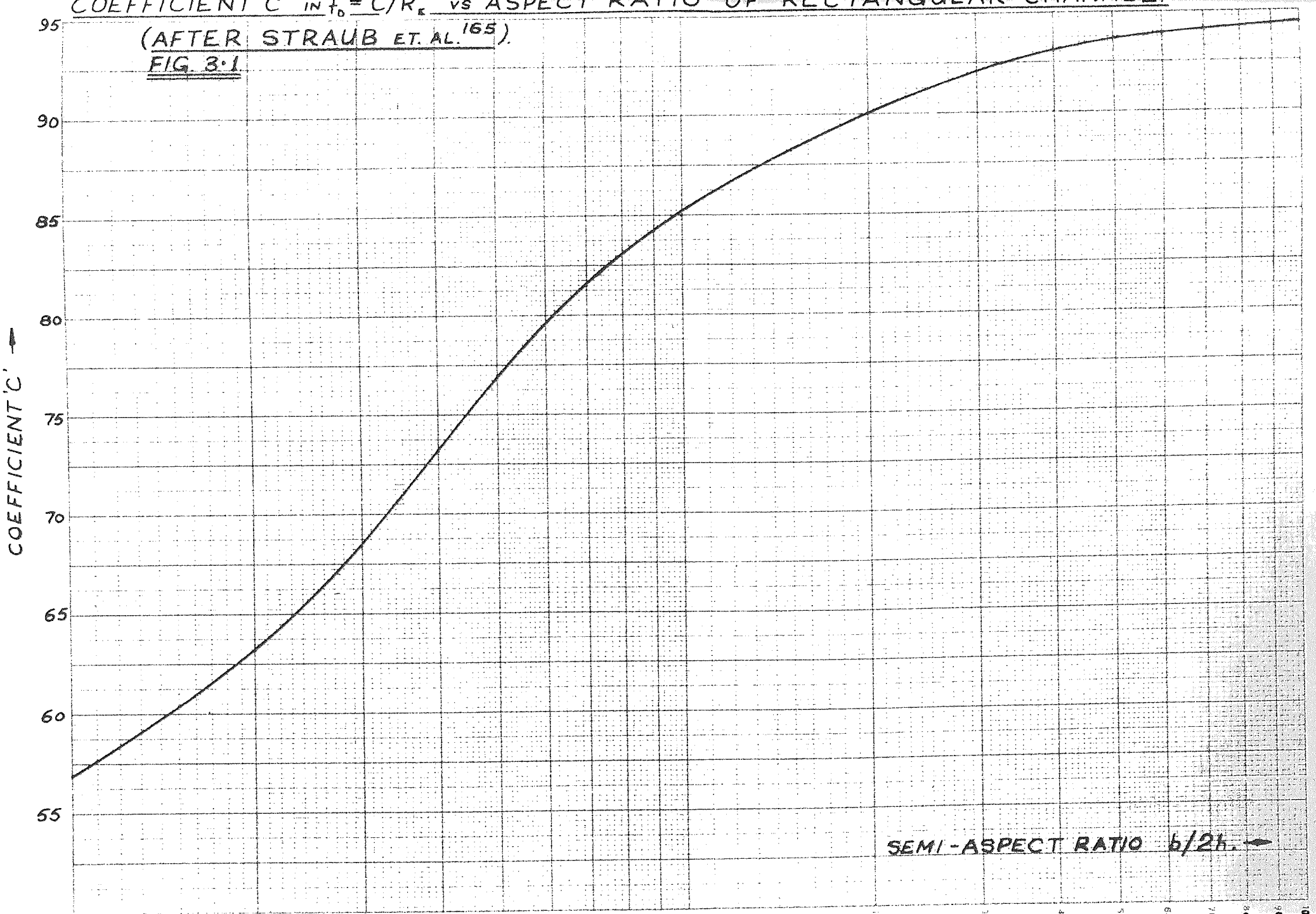

be considerably disturbed by bubbling. This observation has been confirmed in the present work, with the proviso that the whole bed remains fully fluidised.

A condition for the f vs N_{Re} relationship of Section (ii) is that the flow should be laminar. Clearly what is normally understood as laminar flow is inapplicable to any bubbling fluidised bed; as the rising bubbles promote considerable local eddies, and gross disturbance of the free surface of the bed. Also, tests in this work (see below) have shown that stable streamlines rarely exist in fluidised channel flow. Nevertheless, Bessant[141] has measured velocity profiles in a fluidised channel which are appropriate to a non-Newtonian laminar flow field, and , and other work[97, 100-102] requiring the assumption of laminarity has generally been quite successful. Thus it appears that the gross, as opposed to local, behaviour of a flowing bed may be considered laminar to an adequate approximation.

The condition of fully developed uniform flow is considered to be easily satisfied in the fluidised channel. The differential manometer normally indicated uniform bed depth across the section; except on occasion, when particle segregation caused anomolous flow. No results were taken under such conditions.

For capillary flow of a non-Newtonian fluid, the entry length (from a reservoir before the streamlines become substantially straight and parallel) is generally accepted[167] as following the expression:

$$\ell_e = K D N_{Re} \qquad \ldots(15)$$

where K is a constant having a value between 0.02 and 0.06. It was shown by BOGUE[166] that the entry length decreases with reduction in the non-Newtonian index n', and WILKINSON[168] supports this on the grounds that the flatter velocity profile of plastic flowing fluids will be established more quickly than for Newtonian systems. In no case is the

entry length given by equation (15) greater than that available in the channel, and observation of the channel free surface suggested that uniform flow was actually developed much sooner in the fluidised situation. This confirms the findings of Bessant[141].

No instance of true thixotropy or rheopexy has been observed in this work, and nor to the author's knowledge has any been reported by previous workers on fluidised flow. Some time-dependant behaviour was noted in the channel (see Section 5 below), but this took place so slowly that it would be of little moment with regard to the third postulation of the theory of Rabinowitsch-Mooney.

The most questionable of the assumptions of the theory of Section (ii) as applied to fluidised beds is that of no slip at the fluid boundary. Siemes and Hellmer[97] inferred intheir channel work that the resistance of the distributor was less than that of the vertical walls. Also the work of Bessant[105,141] has suggested that slip occurs across the distributor under some conditions; although the results must be viewed with caution because of inaccurate measurement of the solids flow velocity and some limiting theoretical assumptions required to simplify the mathematical treatment. It is considered here that the low distributor resistance could be due in some measure to the inviscid layer present above a porous distributor; although there is no reason to think that slip may not be present also. Conversely, it appears (see below, also Ref. 141) that under some conditions the effective resistance of the distributor is greater than that of the walls, due possibly to partial settlement of some material on the distributor.

In addition to throwing doubt on the assumption of no distributor slip, these features also preclude the rigorous application of the hydraulic diameter concept; in which no distinction is drawn between the contribution of the vertical and horizontal surfaces to the total wetted area.

Notwithstanding these limitations, the simple non-Newtonian liquid analogy appears to correlate the results presented below quite well. The accuracy is certainly sufficient for many design purposes; and it was not considered worthwhile to pursue a more sophisticated analysis at this stage in the absence of more detailed information on behaviour adjacent to the fluidising distributor.

4. EXPERIMENTAL APPROACH

The initial test programme with the channel rig was commenced after carrying out a number of exploratory runs to verify its satisfactory working up to the design maximum flowrate, and to enable the operators to become familiar with its control.

The aim of the tests was firstly to ascertain whether the modified Metzner and Reed theory is adequate to provide a reasonable correlation of flow properties over a range of conditions, and secondly to compare the channel flow results with those from the viscometer.

The bulk of the work was carried out at two bed depths (and therefore channel aspect ratios), and covered a range of fluidising conditions. The bed depths chosen were 27.5 and 40 mm; these being well within the design capacity of the channel, to enable a large range of flow velocities to be easily achieved. The results obtained at the 40 mm bed depth could also be directly compared with viscometer test results at this depth. It is clearly more difficult to control the humidity and temperature of the fluidising air in the channel rig than with the viscometer. However, viscometer tests with the Buckland sand for use in the rig indicated little influence of humidity on the flow behaviour over the usual ambient range. The humidity in the plenum chamber was maintained between 35 and 55% RH for all the tests, which condition was achieved by feeding water droplets to the fan inlet at appropriate intervals. The fluidising air temperature has been shown to have

similarly little influence on flow behaviour. This was kept at or slightly below 25°C by controlling the amount of air bypass in the feedline. The lowest fluidising velocity that could be used over a reasonable range of shear rates was just below 2 U_{m_f}. This limit was fixed by difficulties due to build up of solids in the header tank (see Appendix I). The highest fluidising velocity used was about 5 U_{m_f}. The size analysis of a sample of the Buckland 50 FG sand used for all the tests appears in Table 5.1 of Chapter 3, Section 5.3.

The experimental procedure used is set out in Appendix I, section 4. The only problem encountered was some difficulty in achieving uniform flow at low shear-rates and fluidising velocities, due to particle segregation. This sometimes gave rise to an excessive differential pressure drop over the test section, or an assymetric velocity profile across the width of the channel. These features are elaborated below.

5. RESULTS

Introduction

The results of the channel flow tests are presented in Table 5.1, and are conveniently treated by consideration under three sub-headings. The first discusses the analysis and correlation of the results, and trends observed in the flow behaviour. The second gives a brief comparison of the channel flow and viscometer data obtained under similar conditions; and the third comments upon some visually observed phenomena noted during the test work. It is interesting to note here that steady uniform flow was achieved over the entire range of fluidising velocities (1.9 - 4.7 U_{m_f}) and shear-rates (up to 500s^{-1}) used. Although the author could never foresee circumstances prejudicial to this, Quassim[99] in his channel work reported that steady flow was impossible outside the range of 1.5 - 4.5 U_{m_f}.

i) Correlation and Discussion of Channel Flow Data

The shear diagrams (calculated using the theory of Section 3 (ii)) for the data of Table 5.1 are plotted logarithmically in figures 5.1 to 5.5.

It is immediately clear that only at the highest fluidising velocity (fig 5.5) of about 4.7 U_{m_f} does the flow approximate to that of a power law fluid over the whole range of shear rates. In the other cases the logarithmic plots are of variable slope, indicating that the non-Newtonian index (n') varies with the shear rate. The latter is an extremely unusual occurrence in real fluids[130]; for which n' normally remains nearly constant over the whole range of shear rates. This anomaly is thought to be due to shear induced changes in the structure of the bed, which are more predominant at lower fluidising velocities.

Under the latter conditions, it can be seen from figures 5.1 to 5.3 that, as the shear-rate is increased, there is a region in which the shear stress remains nearly constant or perhaps falls slightly. At shear rates below this transition, it is thought that a segregated layer of large particles accumulates close to the distributor. This layer is only partially fluidised and remains relatively stagnant, thus impeding the flow of the fully fluidised particles above it. As the shear rate is increased (by increasing the channel slope) the segregated layer is gradually swept away, so that the full wetted cross-section of the channel is again available for flow. Visual confirmation of this hypothesis is sometimes possible through the perspex channel walls, when a stagnant layer of large particles near the distributor is apparent. Also, further confirmation has recently been afforded[150] by size analysis of samples taken from the channel at flowrates below transition. These have indicated a higher percentage of large material than is present in the raw sand. The region of transition is also accompanied by a change in observed bubbling pattern at the bed surface: this is discussed more

TABLE 5·1

$\dot{m}$	U	τ	α	f_D	N_{Re}	$Sx10^2$
U_f = 72mm/s. h = 27.5mm.						
0·180	0·037	0·84	3·70	4·025	12·5	0·367
0·240	0·050	1·53	5·00	4·225	18·0	0·667
0·380	0·079	2·33	7·90	2·560	30·5	1·02
0·650	0·135	3·09	13·5	1·160	55·5	1·35
1·22	0·253	4·81	25·3	0·515	114	2·10
1·59	0·329	7·10	32·9	0·449	153	3·10
2·34	0·484	9·39	48·4	0·273	239	4·10
3·11	0·644	8·17	64·4	0·135	474	3·57
4·10	0·849	9·31	84·9	0·089	679	4·07
5·65	1·17	12·1	117	0·060	1028	5·27
U_f = 72mm/s. h = 40mm.						
0·480	0·068	0·81	5·21	1·18	20·6	0·267
0·700	0·099	3·42	7·59	2·37	30·6	1·13
0·970	0·137	3·52	10·5	1·27	43·5	1·17
1·44	0·203	5·74	15·6	0·944	66·3	1·90
1·97	0·278	4·93	21·3	0·433	–	1·63
2·63	0·371	4·53	28·4	0·223	291	1·50
3·88	0·549	6·24	42·0	0·141	457	2·07
3·61	0·510	6·19	39·1	0·158	420	2·05
4·32	0·610	6·54	46·7	0·119	517	2·17
kg/s.	m/s.	N/m^2	s^{-1}	–	–	–

TABLE 5·1 (Continued).

$\dot{m}$	U	τ	α	f_D	N_{Re}	$Sx10^2$
U_f = 81mm/s. h = 27·5mm.						
5·80	1·22	10·65	122	0·050		4·73
5·32	1·12	4·74	112	0·054		4·33
4·17	0·880	8·33	88·0	0·075		3·70
3·00	0·633	7·72	63·3	0·135		3·43
2·40	0·506	6·94	50·6	0·189		3·08
1·44	0·304	7·43	30·4	0·561		3·30
2·64	0·557	7·24	55·7	0·163		3·22
1·73	0·365	8·17	36·5	0·428		3·63
1·35	0·285	7·88	28·5	0·675		3·50
0·92	0·194	8·03	19·4	1·49		3·57
0·75	0·158	7·58	15·8	2·12		3·37
0·75	0·158	5·70	15·8	1·59		2·53
U_f = 81mm/s. h = 40mm.						
0·47	0·067	0·395	5·17	0·600		0·133
0·50	0·072	1·68	5·50	2·25		0·567
0·65	0·093	3·17	7·16	2·50		1·07
1·07	0·154	4·80	11·8	1·40		1·62
1·65	0·237	5·44	18·2	0·669		1·83
2·50	0·359	4·49	27·5	0·294		1·85
3·47	0·499	4·75	38·2	0·132		1·60
4·52	0·649	6·68	49·8	0·109		2·25
5·78	0·831	7·82	63·6	0·078		2·63

UNOBTAINABLE.

TABLE 5·1 (Continued).

Photo. No.	$\dot{m}$	U	τ	α'	f_D	N_{Re}	$Sx10^2$
	U_f = 98·5mm/s h = 27·5mm.						
5·15a	0·085	0·018	0·364	1·75	8·55	15·0	0·167
	0·240	0·052	2·18	5·20	5·79	11·1	1·00
5·15b	0·360	0·079	2·83	7·90	3·27	20·4	1·30
5·15c	0·850	0·175	3·63	17·5	0·855	75·9	1·67
5·15d	1·50	0·328	4·43	32·8	0·296	221	2·03
5·15e	2·15	0·469	5·09	46·9	0·166	383	2·33
	2·95	0·646	6·18	64·6	0·106	675	2·83
	4·17	0·910	7·56	91·0	0·066	968	3·47
5·15f	4·88	1·07	8·65	107	0·055	1143	3·97
	5·93	1·29	11·05	129	0·047	1403	5·07
	U_f = 98·5mm/s. h = 40mm.						
5·16a	0·420	0·061	0·440	4·67	0·825	87·5	0·150
	0·800	0·117	0·920	8·97	0·475	111	0·317
	1·13	0·165	1·95	12·6	0·502	132	0·667
	2·35	0·344	3·80	26·4	0·225	278	1·30
	3·50	0·512	5·06	39·2	0·125	448	1·73
	4·70	0·687	6·81	52·6	0·101	637	2·33
5·16b	5·95	0·870	7·88	66·7	0·073	846	2·70

TABLE 5·1 (Continued).

$\dot{m}$	U	τ	α	f_D	N_{Re}	$Sx10^2$
U_f = 134·5mm/s. h = 27·5mm.						
6·10	1·45	10·85	145	0·041	1664	5·40
4·00	0·948	7·04	94·8	0·061	1024	3·50
2·90	0·687	5·23	68·7	0·086	707	2·60
1·77	0·419	3·78	41·9	0·168	400	1·88
0·950	0·225	2·35	22·5	0·362	195	1·17
0·630	0·149	1·81	14·9	0·637	101	0·90
0·133	0·032	0·235	3·15	1·85	32·8	0·117
U_f = 134·5mm/s. h = 40mm.						
0·860	0·132	0·51	10·1	0·216	–	0·183
1·06	0·163	1·25	12·5	0·347	191	0·450
1·60	0·246	1·95	18·9	0·237	241	0·700
2·21	0·339	3·15	26·0	0·202	322	1·13
2·68	0·412	3·70	31·6	0·161	407	1·33
3·72	0·571	4·91	43·7	0·111	599	1·77
5·10	0·783	6·12	60·0	0·074	873	2·20
6·03	0·926	7·09	71·0	0·061	1066	2·55
U_f = 179·0mm/s. h = 15mm.						
0·180	0·095	1·16	15·4	1·22	83·6	1·13
0·360	0·191	2·62	30·7	0·685	184	2·55
0·650	0·344	3·42	55·5	0·275	360	3·33
0·850	0·455	3·71	73·4	0·171	494	3·62
1·41	0·741	4·18	119	0·072	861	4·07
1·80	0·953	5·10	154	0·053	1145	4·97
2·11	1·12	5·58	180	0·042	1372	5·43
2·60	1·38	7·10	222	0·036	1739	6·91
3·47	1·84	8·97	299	0·025	2415	8·73
4·18	2·21	9·62	357	0·019	2986	9·37
5·23	2·77	12·7	447	0·016	3852	12·33
5·90	3·12	15·7	504	0·0153	4417	15·30
2·30	1·22	5·51	196	0·035	1514	5·37

TABLE 5·1 (Continued)

$\dot{m}$	U	τ	α	f_D	N_{Re}	$Sx10^2$
U_f = 179mm/s. h = 21·5mm.						
0·073	0·025	0·25	2·95	3·61	14·4	0·167
0·117	0·040	0·55	4·77	3·03	25·3	0·367
0·338	0·115	0·999	13·7	0·66	88	0·667
0·495	0·168	1·60	20·1	0·49	139	1·07
0·613	0·208	1·80	24·9	0·36	178	1·20
0·775	0·263	1·95	31·5	0·25	235	1·30
0·923	0·313	2·52	37·5	0·23	289	1·68
1·15	0·392	3·49	46·9	0·20	377	2·33
1·47	0·498	3·55	59·7	0·13	501	2·37
1·15	0·388	3·17	46·5	0·18	373	2·12
1·61	0·546	3·55	65·4	0·104	558	2·37
1·97	0·668	4·04	80·0	0·079	708	2·70
2·40	0·814	4·79	97·5	0·063	894	3·20
1·49	0·505	3·70	60·5	0·127	509	2·47
0·175	0·059	0·33	7·07	0·81	39·9	0·217
2·08	0·705	4·32	84·4	0·074	755	2·88
2·66	0·902	5·67	108	0·061	1009	3·78
3·43	1·16	6·84	139	0·044	1362	4·57
4·79	1·62	10·09	194	0·034	2020	6·73
0·93	0·315	2·85	37·7	0·25	291	1·90
0·52	0·176	1·35	21·1	0·39	147	0·933
2·68	0·908	5·42	109	0·057	1017	3·62
4·85	1·64	9·91	197	0·032	2051	6·62
5·40	1·83	12·23	219	0·032	2328	8·17
6·55	2·22	13·9	266	0·025	2924	9·30
7·28	2·47	11·3	296	0·016	3312	7·53
U_f = 179mm/s. h =35mm.						
0·960	0·179	0·84	15·0	0·204	179	0·350
1·20	0·224	1·35	18·7	0·212	231	0·567
1·84	0·347	2·47	28·7	0·164	379	1·03
2·23	0·416	2·87	34·9	0·130	475	1·20
3·00	0·560	3·71	46·9	0·093	669	1·55
3·63	0·678	4·94	56·7	0·084	836	2·07
4·32	0·807	5·10	67·5	0·061	1023	2·13
5·31	0·992	5·74	83·0	0·046	1300	2·40
6·18	1·15	6·37	96·6	0·037	1549	2·67

TABLE 5·1 (Continued).

U_f = 179mm/s. h = 55mm.						
$\dot{m}$	U	τ	α	f_D	N_{Re}	$Sx10^2$
0·980	0·107	0·81	6·73	0·506	124	0·223
1·76	0·191	1·27	12·01	0·251	212	0·367
2·38	0·259	0·865	16·3	0·093	283	0·250
2·40	0·261	2·77	16·4	0·292	284	0·800
3·50	0·380	2·94	23·9	0·146	403	0·850
4·14	0·450	3·92	28·3	0·139	473	1·13
4·90	0·531	4·59	33·5	0·116	553	1·33
5·65	0·612	5·42	38·6	0·103	631	1·57
6·22	0·680	5·94	42·5	0·093	690	1·72

FIG. 5·1

SHEAR STRESS vs. SHEAR RATE IN FLOWING CHANNEL.

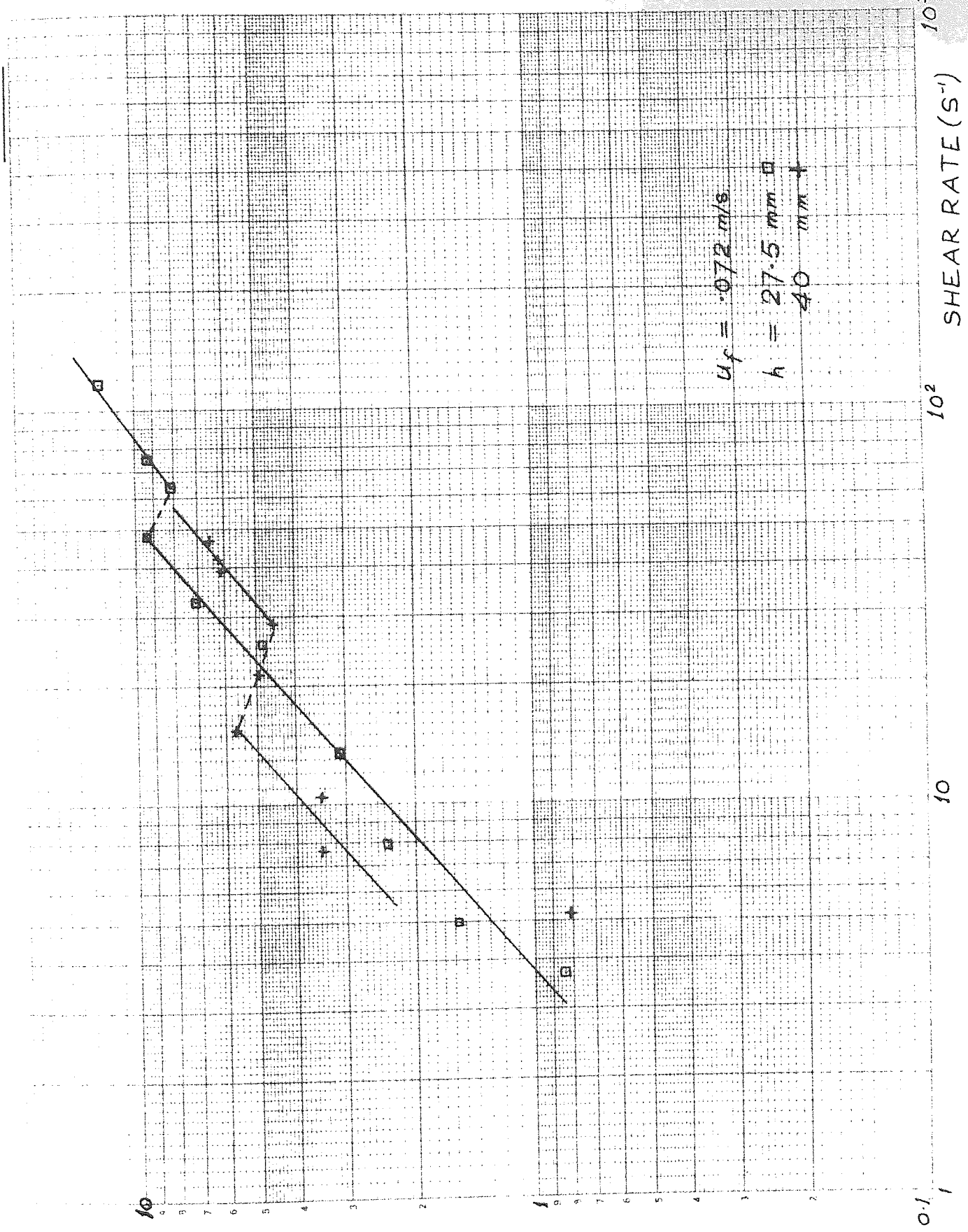

SHEAR STRESS vs SHEAR RATE IN FLOWING CHANNEL.

FIG. 5·2

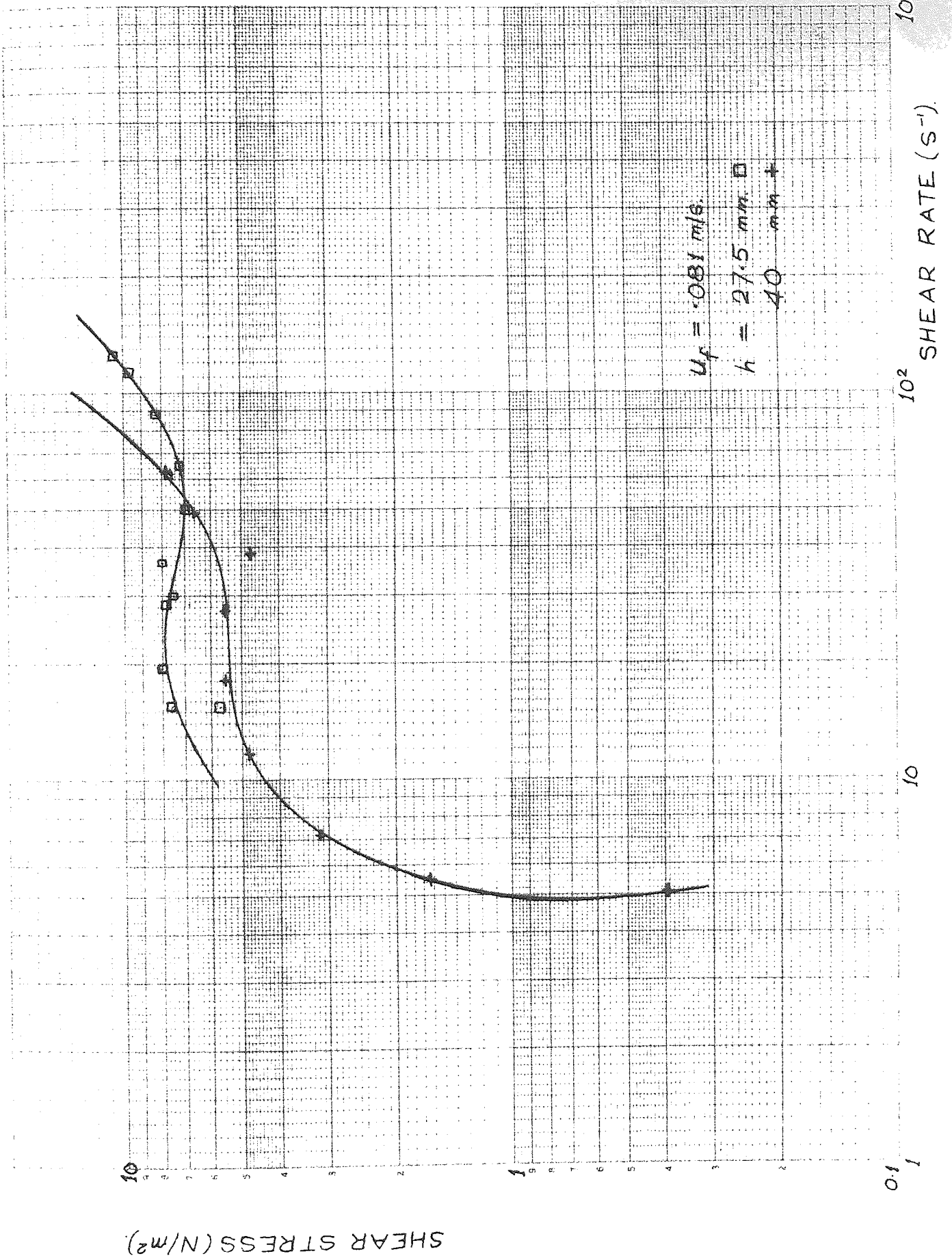

FIG 5·3.

SHEAR STRESS vs SHEAR RATE IN FLOWING CHANNEL.

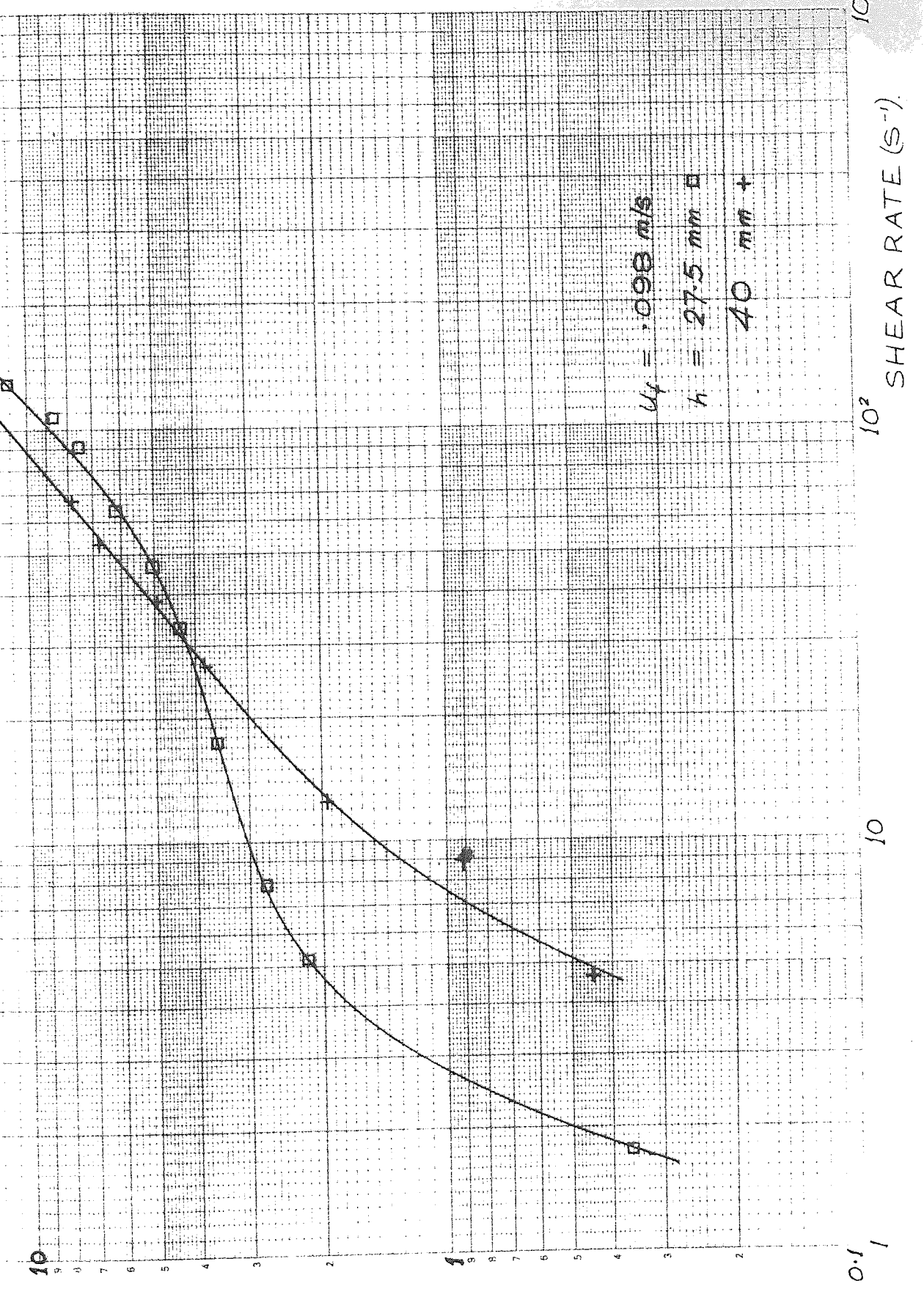

FIG. 5.4

SHEAR STRESS vs SHEAR RATE IN FLOWING CHANNEL

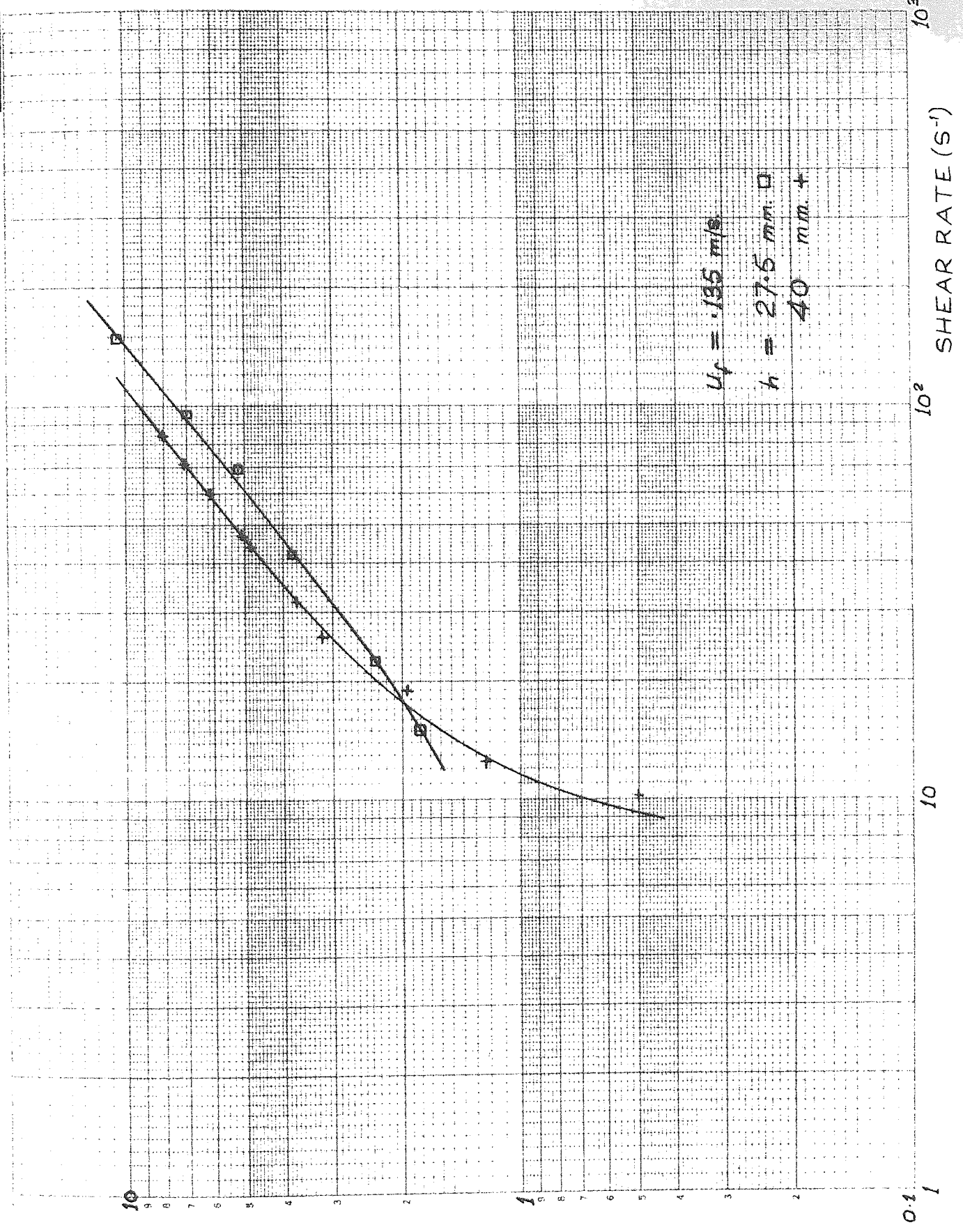

SHEAR STRESS vs. SHEAR RATE IN FLOWING CHANNEL.

FIG. 5.5.

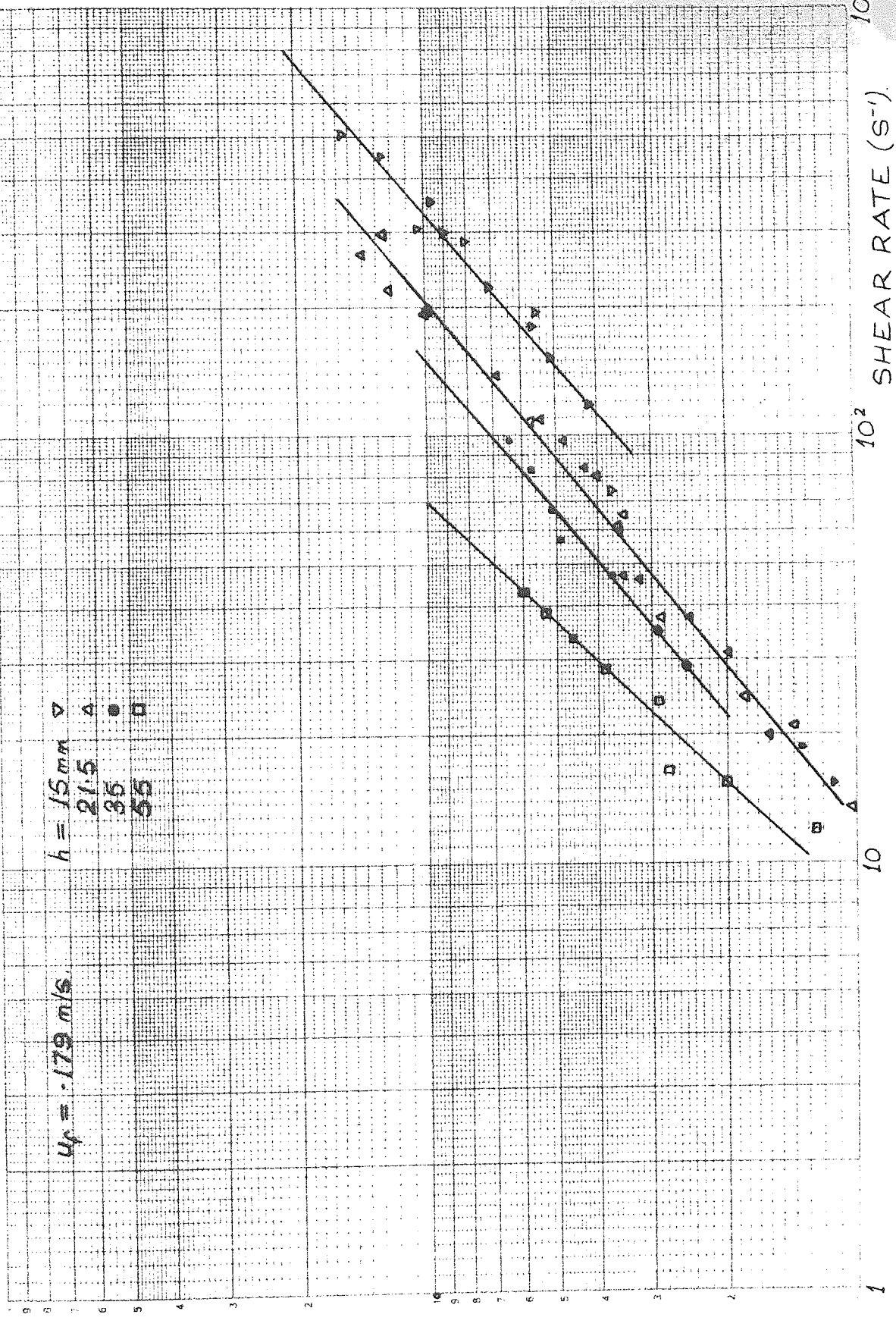

fully in Section 5 (iii) below.

It is at first sight surprising that segregation should occur under these conditions. Even the lowest fluidising velocity used represents 1.9 U_{m_f}, at which condition bubble induced particle circulation would normally be easily sufficient to ensure good mixing. The reason for this behaviour is that as the large mass of material contained in the flow circuit passes through the fluidised channel, the larger size fractions are gradually removed from suspension and settle out on to the distributor. Thus all particles above a certain size from the whole batch of material in circulation become concentrated in the channel, therefore increasing the mean particle size (and hence the minimum fluidising velocity) therein compared with the raw sand. When the fluidising velocity is increased past the transition region the air flow is then sufficient to re-fluidise the segregated layer. Thus eventually the channel mean particle size is reduced to its former value, thereby increasing the relative fluidising velocity.

The magnitude of this effect will clearly increase with the size-range of the material being transported, but is likely to depend also upon whether the flow system is of the circulatory or "once through" variety. In a continuous loop system, such as that of Bessant[141], in which all parts of the circuit are fluidised equally, the effect may be absent. (In fact the shear rates used by Bessant were almost an order of magnitude below those of this work, and would thus be insufficient to exceed the transition region . Nonetheless, he did report evidence of increased drag at the distributor at low relative fluidising velocities, which could be indicative of some segregation). However, in any flow system containing regions of disparate fluidisation (or comprising fluidised and other modes of transport), dumping of coarse material in one region at the expense of another is likely. This may explain the flow asymmetry and other anomalies observed by Bessant[141] when using baffles and guide vanes in his

channel; which latter would clearly upset the uniformity of the flow loop.

In any flow system containing a fluidised leg in which fresh material is to be continuously transported, rather than circulating the same material around a closed circuit, the effects of this segregation phenomenon could be very serious. Unless the fluidising velocity is high enough to prevent segregation starting, then the effect will be cumulative as the larger fractions of the through-flowing material are progressively deposited, until the channel is completely choked.

The shear rate at which transition occurs in a particular circumstance is not very definite. Time has not allowed a thorough investigation of this, but since the establishment of a steady-state flow situation near transition may take tens of minutes, the shear diagram in this region will depend upon the previous shear history of the flow. This cannot be regarded as thixotropy or rheopexy in the conventional sense, since the mean particle size of the bed is changing. This is analogous to a change in the physical properties of a real fluid, rather than merely a shear induced molecular rearrangement. However, the effect is clearly a form of time dependence, and as such may affect the applicability of the theory used; although the influence will be small in view of the slow time rate of change of properties.

As the fluidising velocity is increased, it becomes sufficient to prevent segregation and fully support the larger particles at all shear-rates. Thus the transition region disappears with increasing airflow and the shear diagram becomes closer to that of a power-law fluid. Insufficient data is yet available to propound any general rules for an upper limit of fluidising velocity at which such transition occurs, and this is in any case likely to depend on the size-range of the particles used. However, a transition is still evident in figure 5.3 at a fluidising velocity of $2.6\ U_{m_f}$. It would appear from figures 5.1 to 5.3 that the results of

the segregation are more marked at the shallower of the two bed depths, since transition occurs there at a higher shear rate. Also the shape of the shear curves of figure 5.3 suggests that segregation persists at that fluidising velocity for the shallower bed, but is absent in the deeper one. This may be due to greater vertical particle mobility in the shallow bed, allowing dumping of the coarse particles to occur more readily. It would be of interest in connection with this segregation phenomenon to compare the flow over pierced and porous distributors. The former have been clearly shown to give inferior results in the viscometer. However, in channel flow at low fluidising velocities the high velocity air jets of the pierced plate may assist in keeping the larger particles in suspension, and therefore give superior results.

It is easy to fit equation (6) of Section 3(ii) to the linear portions of the shear diagrams of figures 5.1 to 5.5, and the resulting values of n' and K' are given in Table 5.2. All the values of the non-Newtonian index n' are just below unity; except for one curve on Figure 5.5 in which the data is rather scattered, and may therefore be subject to error in fitting a best straight line. These values are indicative of pseudo-plastic or shear-thinning behaviour; which accords with the results from the viscometer experiments of this work, and with the channel flow rseults of Botterill and Bessant[102, 103, 141]. The shear-thinning character of the flow has been interpreted in both cases as consequent upon an improvement in homogeneity of fluidisation brought about by the shearing action. However, many of the viscometer tests indicated a tendency to Newtonian flow at fluidising velocities above 2 U_{m_f}; a trend which is not in evidence in the channel results. This could be due to the differences in shear across the distributor in the two flow situations.

The values of n' reported by Bessant of 0.4 to 0.8 are rather lower than those obtained here. This is probably because his work was largely concerned with lower fluidising velocities, which, as the viscometer tests

TABLE 5.2

U_f (mm/s)	U_f/U_{mf}	h (mm)	C	n'	K' ($Ns^{n'}/m^2$)	$(\mu)_{\alpha=10^2}$ (Ns/m^2)
7·2	1·89	27·5	67	0·86 0·70	0·33 0·44	0·11
7·2	1·89	40	62·5	0·93 0·84	0·46 0·27	0·13
8·1	2·1	27·5	67	-	-	0·089
8·1	2·1	40	62·5	-	-	0·13
9·85	2·59	27·5	67	0·948	0·105	0·087
9·85	2·59	40	62·5	0·80	0·28	0·11
13·45	3·54	27·5	67	0·85	0·15	0·075
13·45	3·54	40	62·5	0·81	0·22	0·092
17·9	4·71	15	74	0·86	0·069	0·036
17·9	4·71	21·5	71	0·82	0·13	0·055
17·9	4·71	35	64	0·84	0·15	0·070
17·9	4·71	55	59·5	1·07	0·107	0·15

Where two values of n' and K' are quoted, these refer to conditions before and after 'transition' respectively.

No values are quoted for U_f=8·1 due to insufficient data to provide realistic accuracy.

have shown, lead to increasingly non-Newtonian behaviour.

It is also clear that the non-Newtonian index (n') does not alter substantially with depth of the bed. This accords with the viscometer results, for which although no numerical evaluation of non-Newtonian behaviour was made, the flow is seen to have a similar shear-thinning character over a range of bed depths. (eg Figure 5.18, Chapter 3).

It is to be expected that the values of n' in Table 5.2 show some scatter, since its magnitude is sensitive to the slope of the appropriate logarithmic τ vs a plot. These curves were drawn by inspection rather than using a mathematical fitting technique. For accurate work it would be preferable to employ some form of curve-fitting method, but this is not justified here in view of the small number of data points available. The values of the consistency index (k') cannot be directly compared with one another when examining trends in flow behaviour, since the magnitude of k' is not a direct indication of relative fluidity except when comparing data having a common value of n'. For this reason, the apparent viscosity (τ/a) for a shear-rate of $100s^{-1}$ also appears in Table 5.2. The latter shear-rate is well beyond the end of the transition region, and so provides a useful point at which to compare flow properties, although of course the absolute value of the apparent viscosity is unique to the chosen shear-rate.

The apparent viscosity data of Table 5.2 confirms the dependence of flow on bed depth found with the viscometer (Chapter 3, Section 5.2 (vi)). The viscosity at $4.7\ U_{m_f}$ (Fig 5.5) increases from 0.036 Ns/m^2 to 0.15 Ns/m^2 as the depth is increased from 15 to 55 mm. This change is of a similar order to that shown in Chapter 3, Figure 5.17; the slightly greater depth dependence in the channel being due possibly to the much higher shear-rate, or to differences arising from shear across the distributor.

Unlike the viscometer results, which showed a minimum in the apparent viscosity at 1.5 - 2 U_{m_f}, the channel work suggests that the flow behaviour continues to improve with increasing fluidising velocity, over the range investigated (1.9 - 4.7 U_{m_f}). This is rather surprising, as the viscometer also indicated a reduced non-Newtonian index (increasing pseudoplasticity) at lower fluidising velocities; which would suggest improved fluidity under these conditions at the higher shear-rates obtaining in the channel. A possible explanation for this, suggested by Bessant[141] is that the inviscid layer above a porous distributor (inferred from his own findings as well as this work) is swept away at high shear rates, thus increasing the drag at the distributor surface.

The magnitude of the apparent viscosities obtained (.036 - .15 Ns/m^2 at $100s^{-1}$) is rather lower than those reported by Bessant[141] of 0.2 - 2.0 Ns/m^2, and considerably lower than values quoted in some published data[70,77,83]. It is difficult to comment on the latter without fuller details of their test conditions, but Bessant's results were undoubtedly higher because of his much lower shear rates ($\sim 10\ s^{-1}$) and because he studied deeper beds (up to 118 mm). Only the work of Quassim[99] has given lower apparent viscosity values (.002 - .2 Ns/m^2) than those obtained here. As noted in Chapter 2, his results appear to contain a number of anomalies, but could be realistic in view of the shallow bed depths used (< 25 mm).

An attempt is made to correlate the channel flow results, by the use of the generalised Reynolds Number approach of Section 3 (ii) in Figures 5.6 to 5.11. It should be noted that a different value of C (in the equation $f_D = C/N_{Re}$) is appropriate to each channel aspect-ratio: the values of C are obtained from the work of Straub et al[165].

Evidently this method of correlation is quite good in practice, in spite of obvious theoretical limitations due to the disparate shearing action at the vertical and horizontal 'wetted' surfaces. There is naturally some scatter of experimental data (which is masked to some

D'ARCY FRICTION FACTOR vs. GENERALISED REYNOLDS NUMBER. FIG.5·6.

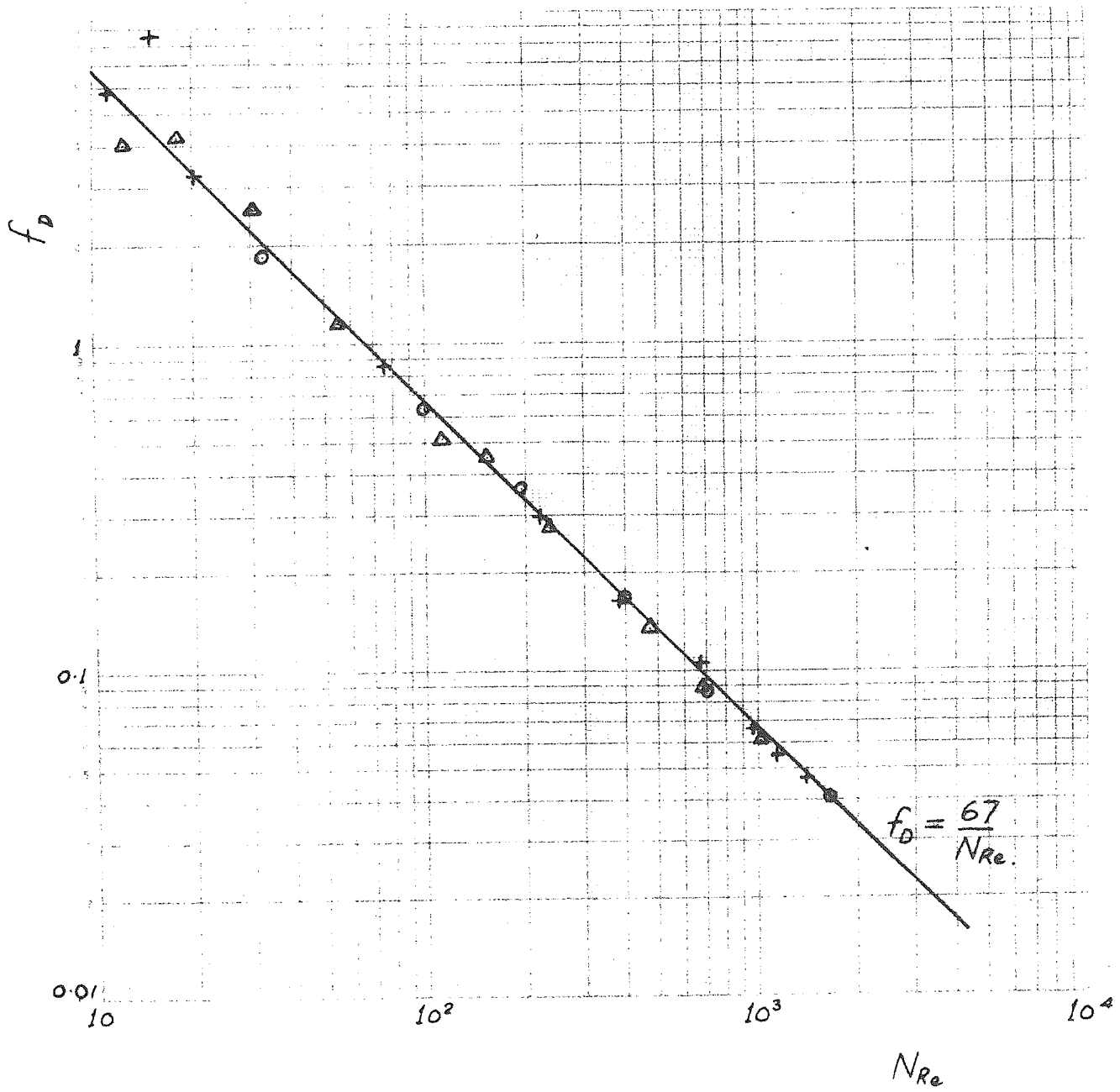

h = 27·5 mm.

u_f : △ ·072 m/s.

\+ ·098 m/s.

o ·135 m/s.

D'ARCY FRICTION FACTOR vs GENERALISED REYNOLDS NUMBER. FIG 5·7.

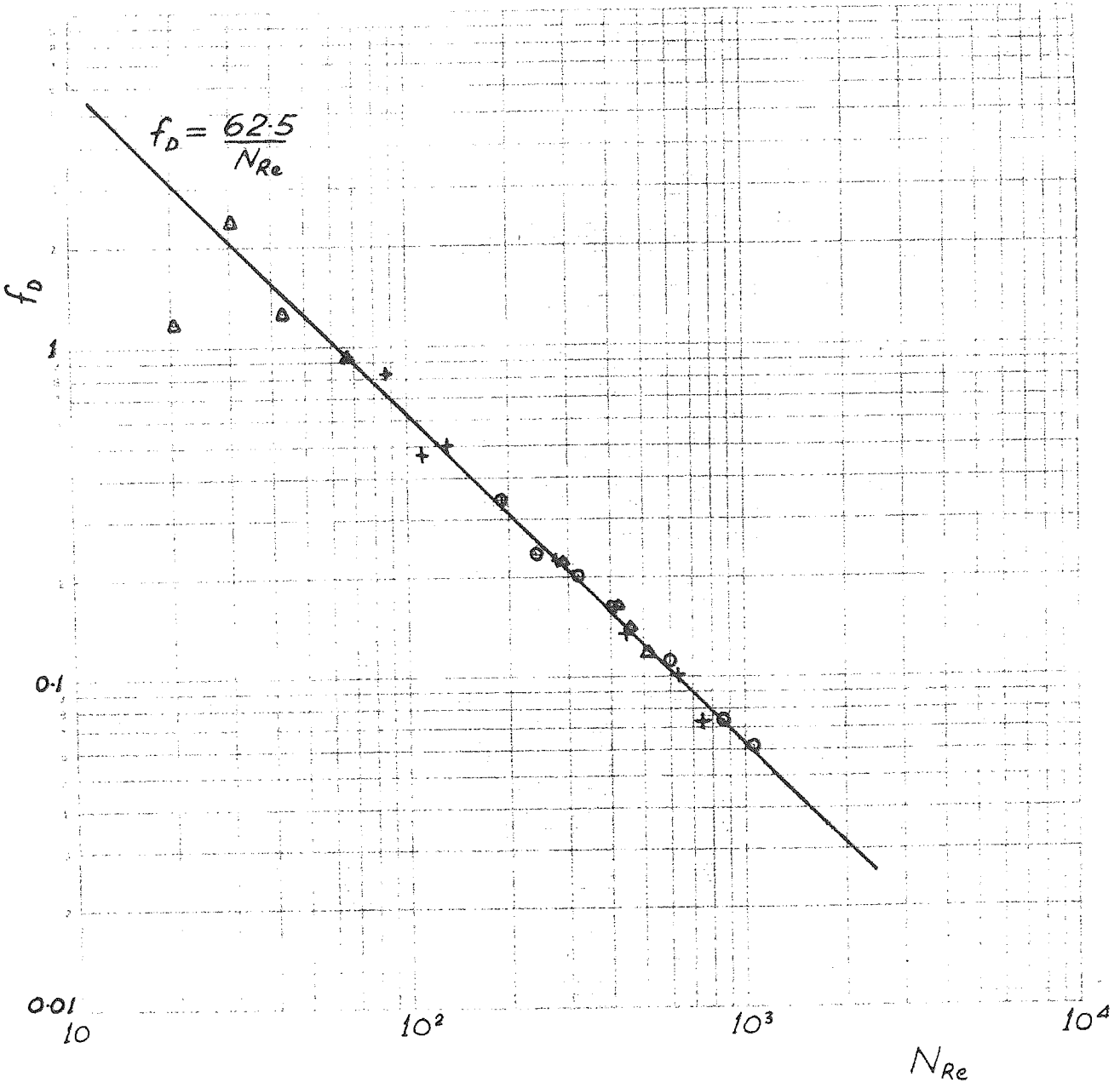

h = 40 mm.

u_f : Δ ·072 m/s.

\+ ·098 m/s.

o ·135 m/s.

D'ARCY FRICTION FACTOR vs. GENERALISED REYNOLDS NUMBER. FIG. 5·8.

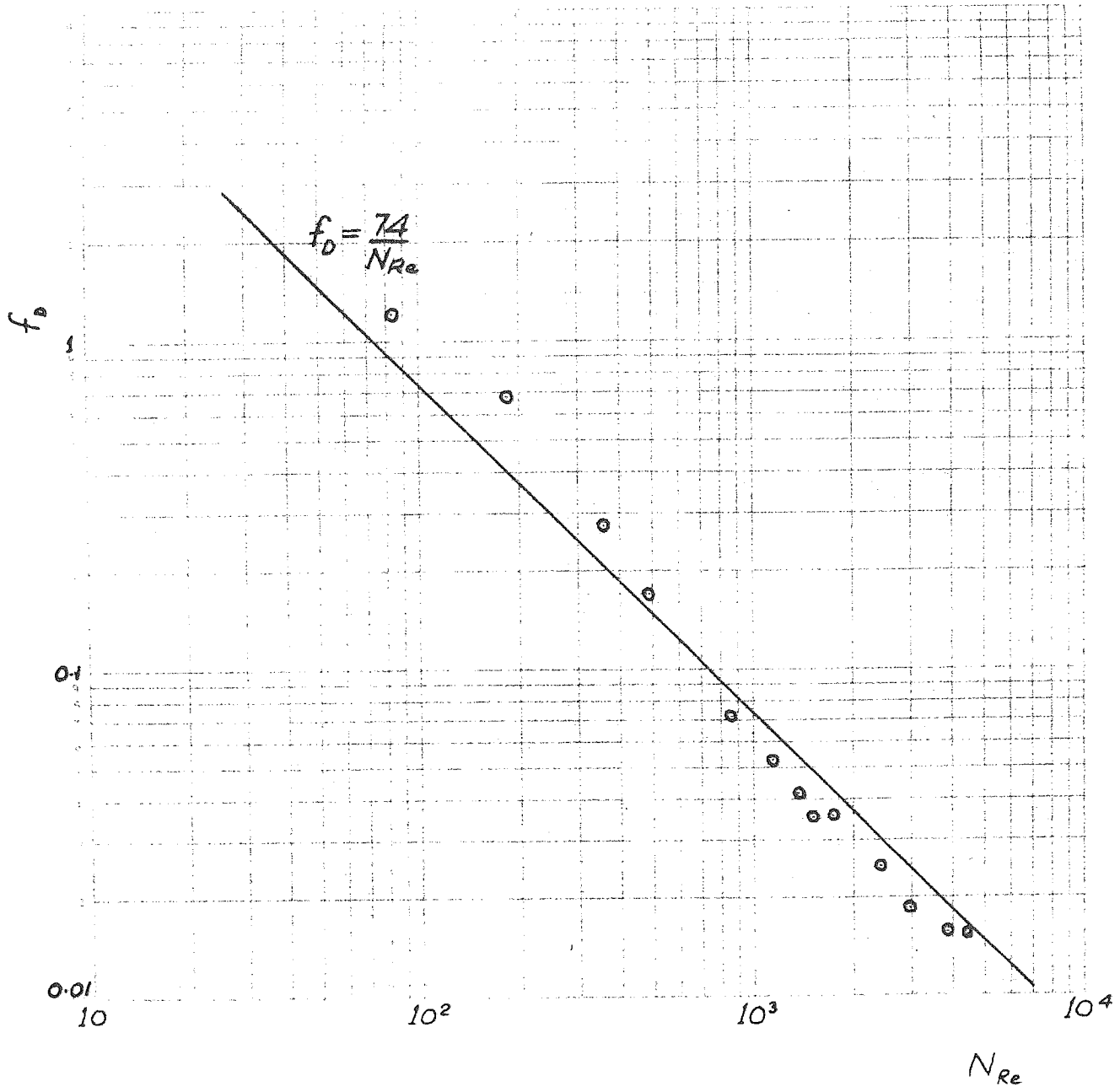

$h = 14·9$ mm.

$u_f = ·179$ m/s.

D'ARCY FRICTION FACTOR vs. GENERALISED REYNOLDS NUMBER. FIG. 5·9.

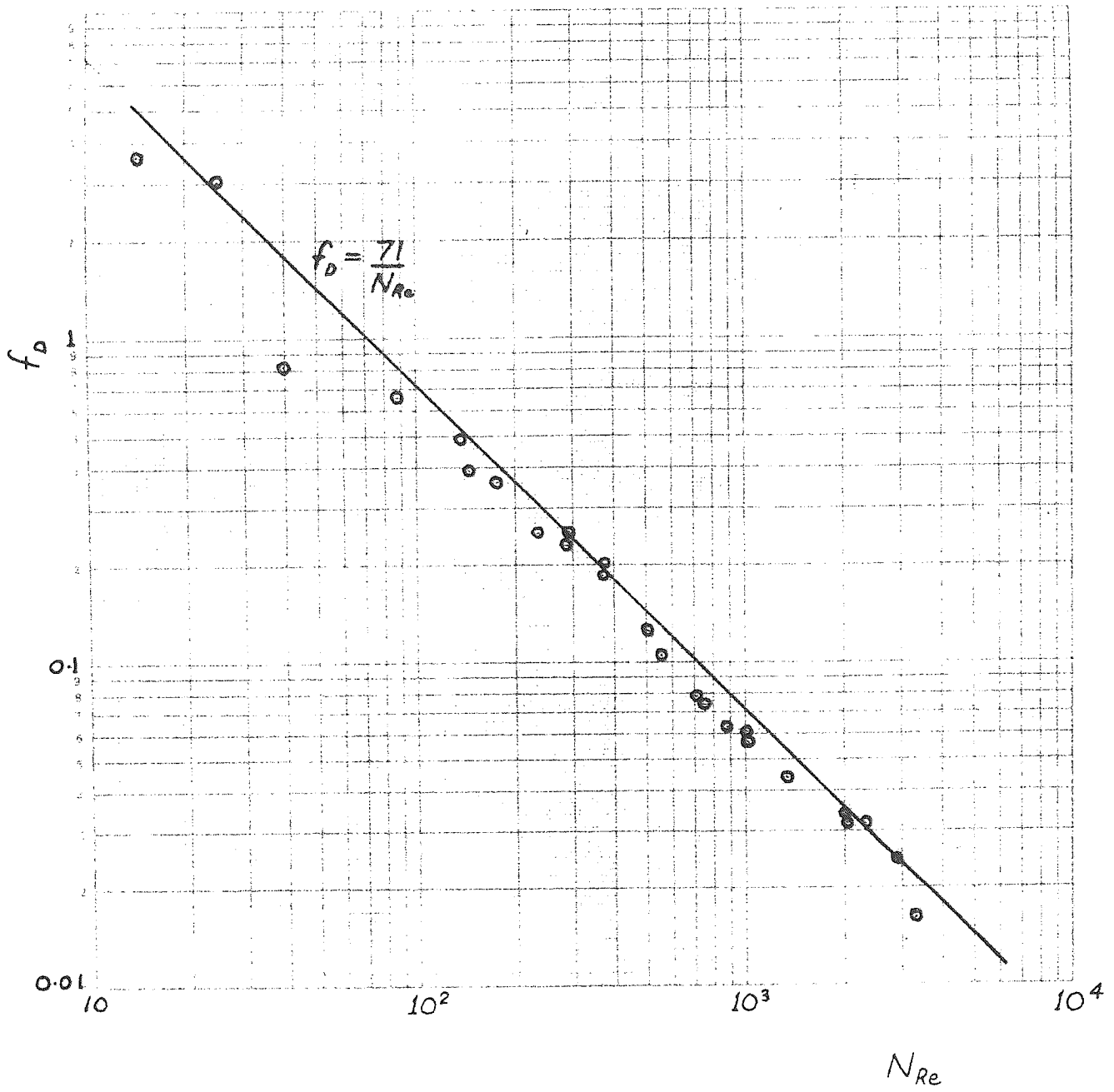

$h = 21·5$ mm.

$u_f = ·179$ m/s.

D'ARCY FRICTION FACTOR vs. GENERALISED REYNOLDS NUMBER

FIG 5·10.

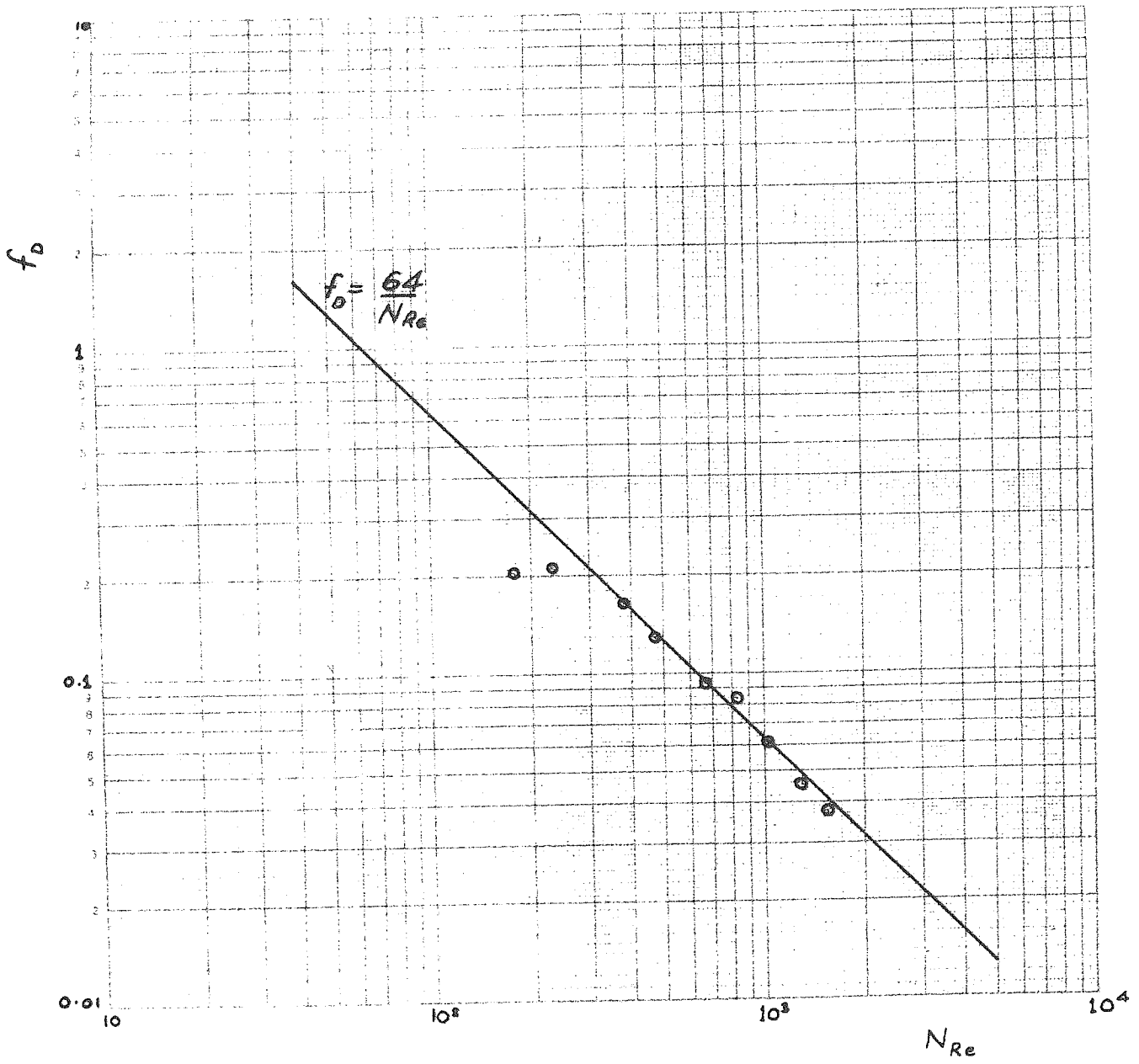

$h = 35$ mm.

$u_f = \cdot 179$ m/s.

D'ARCY FRICTION FACTOR vs GENERALISED REYNOLDS NUMBER. FIG. 5·11.

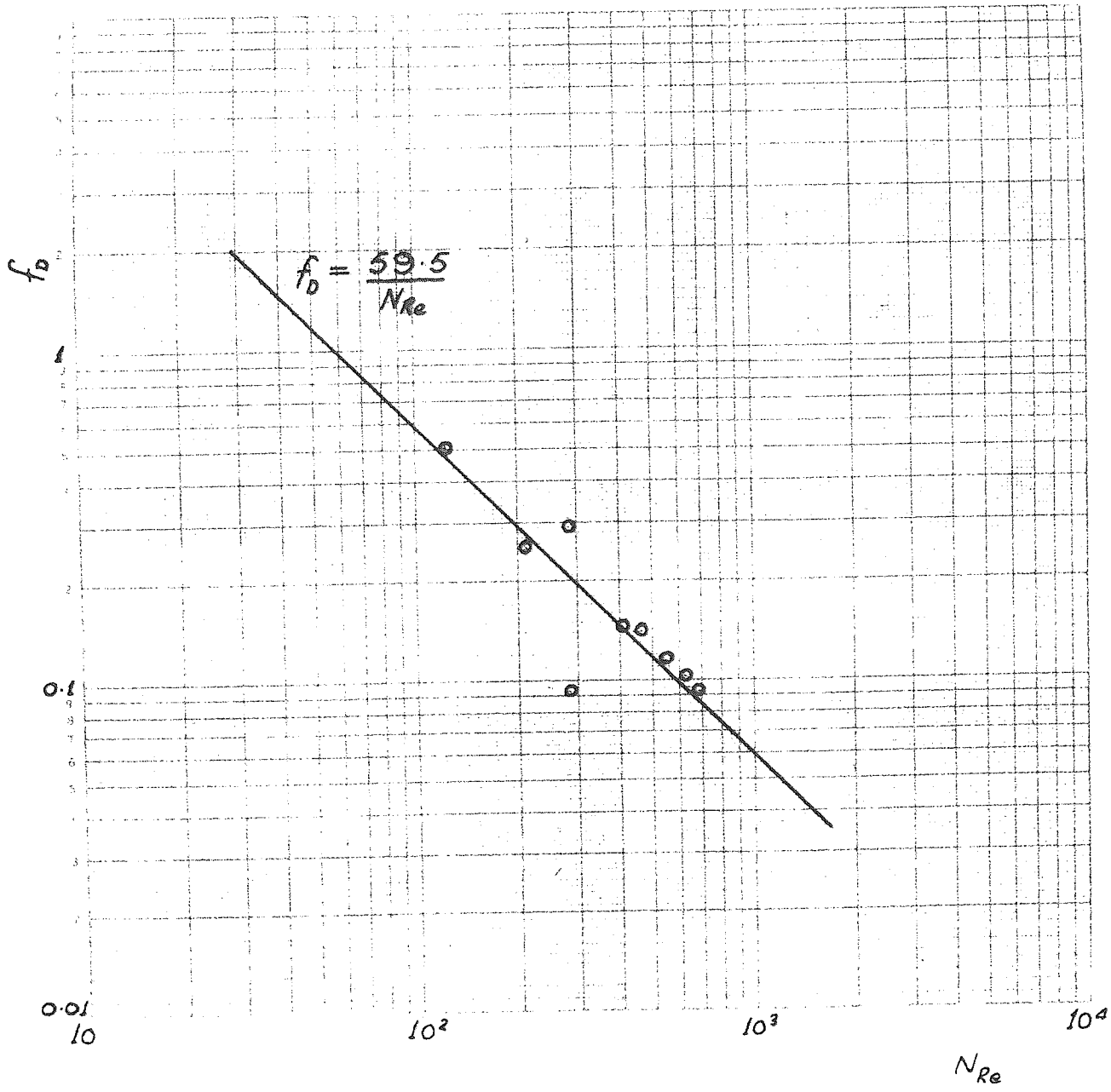

$h = 55·2\,mm.$
$u_f = 0·179\,m/s.$

extent by the logarithmic axes), since the Reynolds numbers are calculated from the flow and consistency indices of figures 5.1 - 5.5. However, most scatter is confined to low Reynolds Numbers and fluidising velocities: and elsewhere the agreement with the theoretical lines is usefully close. The only instance of any consistent departure from the f_D vs C/N_{Re} lines is in Figure 5.8, where the curve is pessimistic at low Reynolds Numbers and optimistic at higher ones. This would be consistent with the presence of an inviscid layer at the plate which is swept away at higher flow velocities, but since the trend is absent from the other curves it could be coincidental.

The data of figures 5.6 to 5.11 may be compared to the single curve $f_D = \frac{64}{N_{Re}}$ appropriate to tube flow by dividing either variable by 64/C. The result is shown in figure 5.12, for which the overall standard deviation is 13.0%. Further recent tests by Pugh[150] under similar conditions, and also using a narrower channel of 100 mm width, have shown that this level of accuracy may be improved upon by taking smaller shear stress increments so that a better shear curve can be plotted, and using a simple curve fitting technique. Also, earlier work by Botterill and van der Kolk[101] at much lower Reynolds Numbers and greater bed depth than employed here gave similarly close agreement to an $f = K/N_{Re}$ curve. It would thus appear that this type of equation describes the fluidised channel flow reasonably accurately over the entire range of Reynolds Numbers corresponding to what in a true fluid would be considered laminar flow. The method therefore constitutes quite a powerful design tool for fluidised transport systems. It is still necessary to assume a value of the non-Newtonian index when attempting to predict flow performance, but the results of this and other work[101,103,141,169] should enable a realistic choice to be made within the range of conditions so far investigated.

D'ARCY FRICTION FACTOR vs. GENERALISED REYNOLDS NUMBER.

FIG. 5·12.

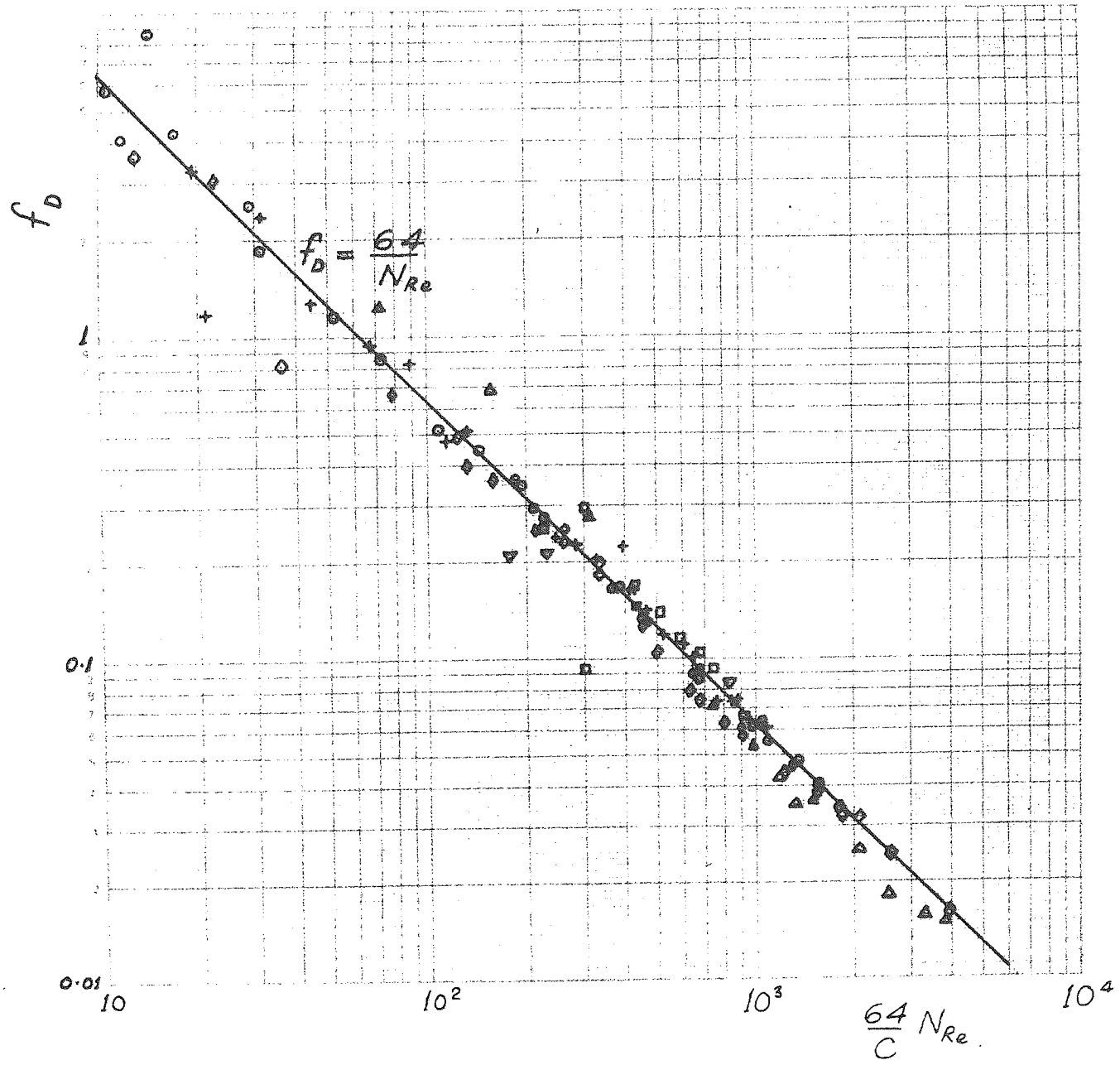

o fig. 5·6
+ " 5·7
△ " 5·8
◇ " 5·9
▽ " 5·10
□ " 5·11

No work has been previously reported on fluidised flow at Reynolds Numbers exceeding 2000, at which point turbulence normally commences in pipe flow of Newtonian fluids. Some data in the latter region is presented here (Figures 5.8 and 5.9), but even at the high mass flow rates available with the new rig it will not be possible to substantially exceed such Reynolds Numbers except with very shallow or narrow channels.

However, unlike natural water conduits, it is the laminar region that will normally be of most interest in fluidised channel flow because much smaller channels are involved and the effective viscosity is higher.

There is no evidence in figures 5.8 and 5.9 to suggest transition to turbulent flow. However, OWEN[170] has pointed out that turbulence in small open water channels does not commence until Reynolds numbers of at least 4000. Also, Metner and Reed[130] found that even for flow in circular pipes, the transition region encompasses a higher range of Reynolds Numbers where shear-thinning fluids are concerned. Thus it is possible that the validity of the normal $f = C/N_{Re}$ equation may extend to Reynolds Numbers as high as 10^4 in fluidised channel flow.

It is perhaps surprising, in view of the likelihood of differences in velocity gradient at the channel walls and distributor, that the foregoing treatment based on a simple hydraulic diameter to represent the channel dimensions is so accurate in practice. No work has been possible here, in the time available, to study the shearing action at the walls and distributor. There is little doubt from viscometer tests, and also from Bessant's work[141] that disparate shear stresses occur at the horizontal and vertical wetted surfaces under some conditions. However, some of Bessant's observations (particularly concerning the effect of channel aspect-ratio and increasing shear-rate) may be open to doubt because of inaccurately measured flow velocities. In Bessant's work the latter were estimated by timing the motion of a float on the channel surface, as no

direct measurement of flowrate was possible. Tests were carried out in this work to compare float measurements with velocities calculated directly from mass flowrate data. Figure 5.13 indicates that the float method is optimistic at low flow velocities and pessimistic at higher ones. Also there is a very wide scatter at low velocities, with which Bessant's work was largely concerned. Some of Bessant's results were handled using a theoretical treatment[106] requiring the assumption of a slip velocity at the distributor which is invarient with bed depth; which assumption does not seem realistic for fluidised flow.

ii) Comparison of Channel Flow and Viscometer Data

Brief references to the parity of the results from the viscometer and channel flow rig were made in the previous section. More direct comparison, at two fluidising velocities and a bed depth of 40 mm is furnished by Figure 5.14, in which the results of Chapter 3, Figures 5.41 and 5.42, and Figures 5.1 and 5.4 of this Chapter are plotted on the same axes.

Since extrapolation of the viscometer results is required for comparison with the channel data, any conclusions drawn must be tentative, but clearly there is considerable divergence in results from the two sources. Whilst the viscometer indicated Newtonian flow as opposed to pseudoplastic in the case of the channel; the former's range of shear-rates is very narrow and the flow may have become pseudo-plastic if higher rates of shear were possible.

The viscosity recorded in the channel at the higher of the two fluidising velocities is much lower than that of the viscometer. At the lower fluidising velocity, in which conditions the channel flow is subject to a transition at about $a = 15\ s^{-1}$, the extrapolated viscometer curve falls between the two sections of the channel flow curve. This pattern is seen as further confirmation of variable drag at the distributor; remembering that the viscometer measures shear at a vertical surface only,

MEAN FLOW VELOCITY IN FLUIDISED CHANNEL vs VELOCITY OF FLOAT ON FREE SURFACE.

FIG 5·13

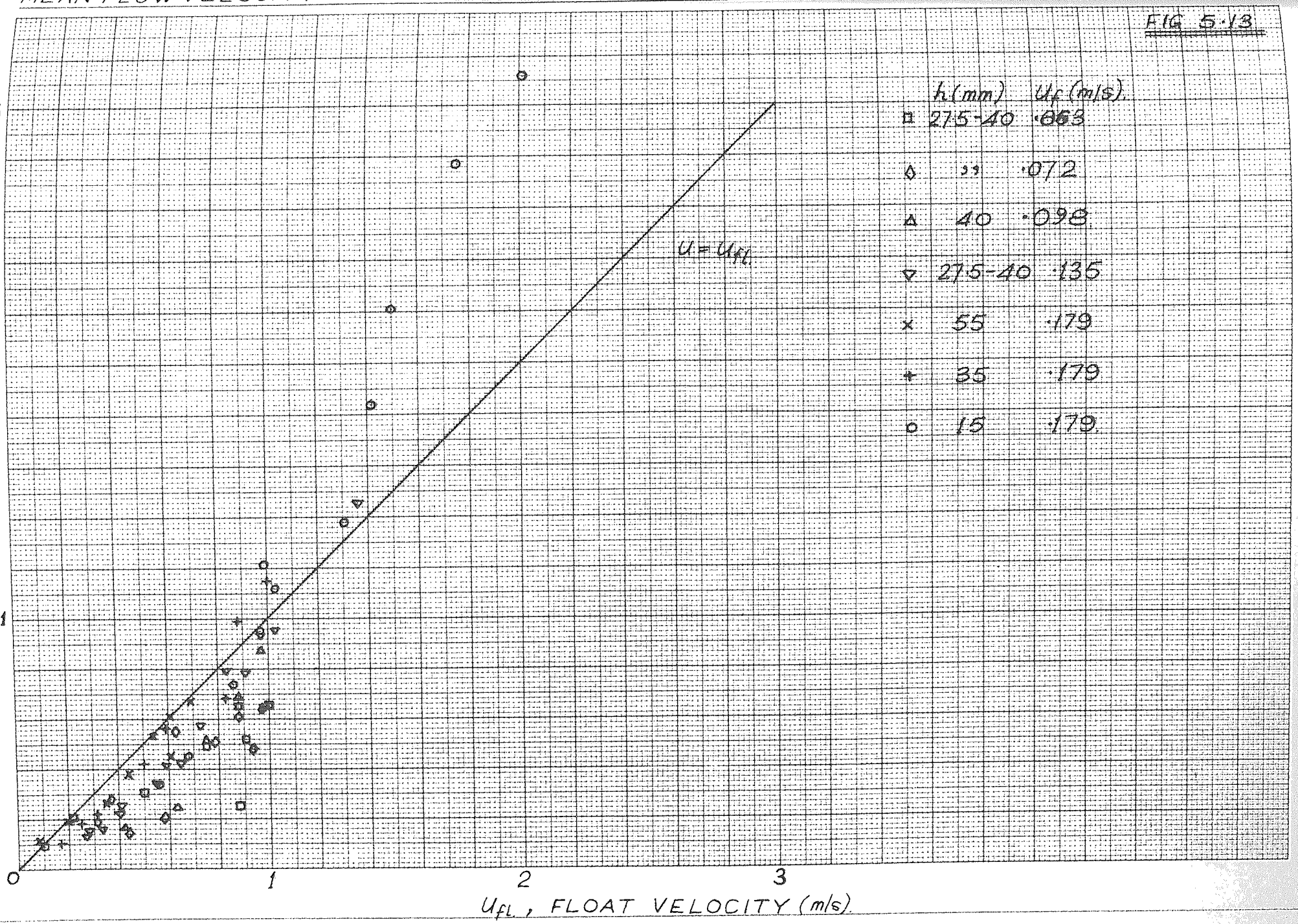

SHEAR DIAGRAMS FOR BUCKLAND 50FG SAND FROM VISCOMETER AND CHANNEL.

FIG. 5·14

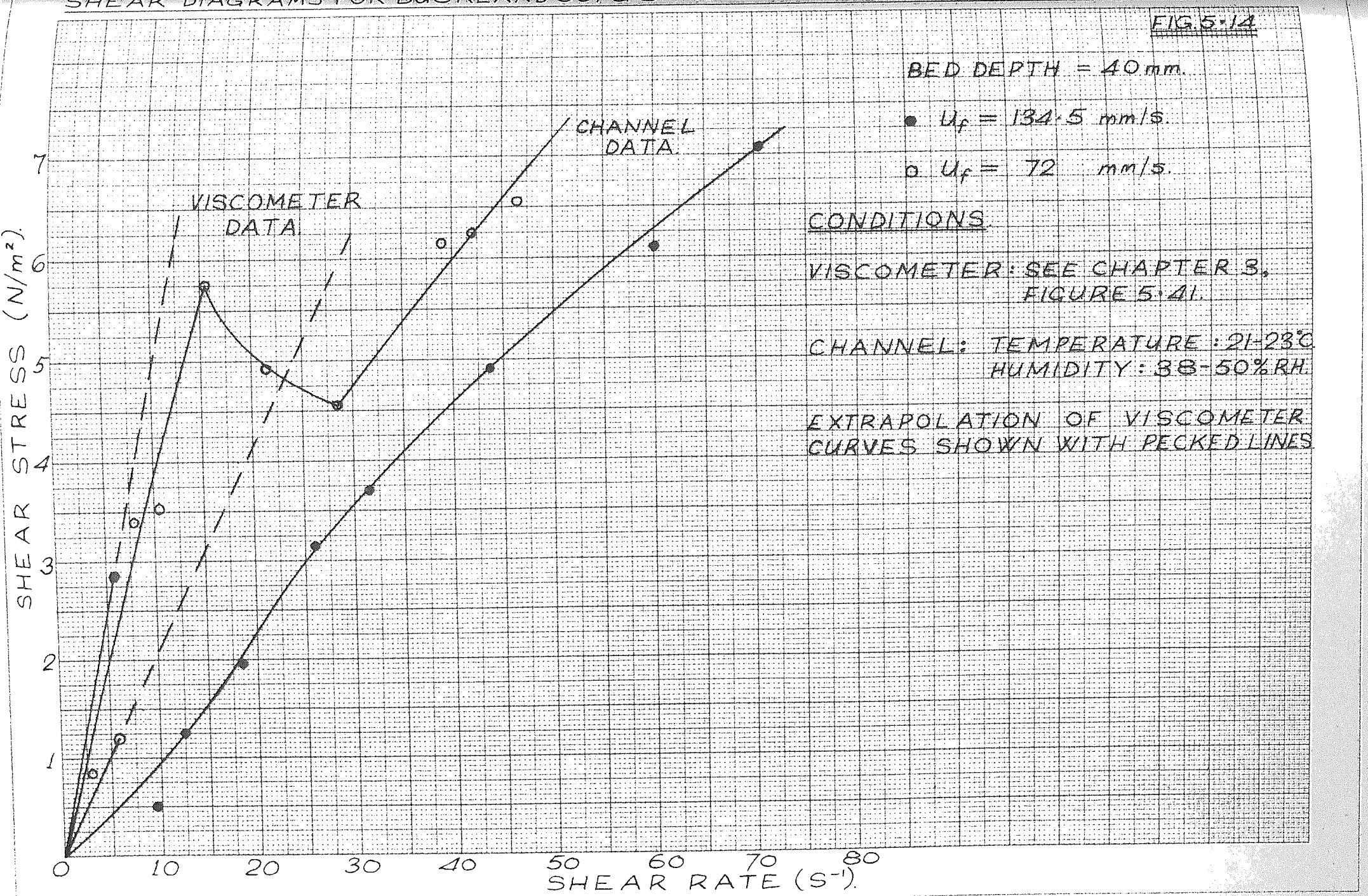

whereas the channel data pertains to an average shear stress over the entire wetted area. Before 'transition' at the lower fluidising velocity, the segregated layer at the distributor causes a high resistance to flow and therefore a high average viscosity. After transition, and at all shear-rates at the higher fluidising velocity, the inviscid layer above the distributor gives a lower average viscosity than measured in the viscometer. The fact that the viscosity under these conditions increases with fluidising velocity in the viscometer but reduces in the channel may be due to the relatively greater effectiveness of the air layer at higher fluidising velocity.

This explanation, based on the results of a single series of tests only, must be regarded as speculative. However it does fit the available facts, and the behaviour is in line with other experimental findings[141].

iii) Visually Observed Phenomena

A number of photographs were taken during trials with the channel rig, some of which are of value in providing confirmation of trends in the tabulated results. Others are usefully included to illustrate observed features of the flow behaviour.

The views of the surface of the bed shown in Figures 5.15 (a-f) are of interest, as they illustrate the change in bubbling pattern over the transition region of Figure 5.3. The test conditions to which the pictures refer are given in Table 5.1. Frames (a) and (b) pertain to shear-rates of 1.75 and 7.9 s^{-1} respectively, both of which are below the start of the transition region. The bubbling pattern here has the even, rhythmic appearance typical of a shallow bed; and a slight reduction in bubbling is evident at the higher of the two shear-rates. This confirms earlier evidence[101,141] of shear induced bubble suppression at moderate shear-rates.

Frames (c), (d) and (e) refer to conditions within the transition region; and here there is a progressive increase in the size of the bubbles. Also, the bubbling becomes more even across the whole channel,

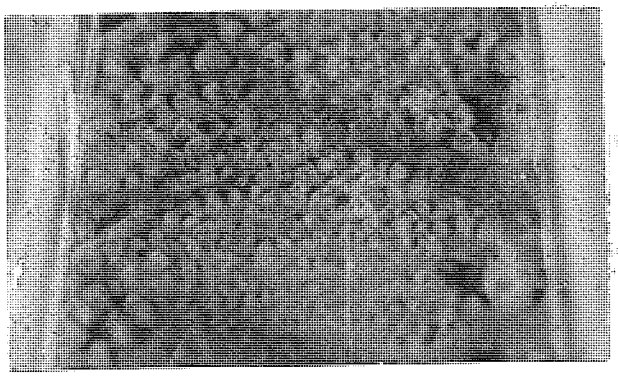

a.

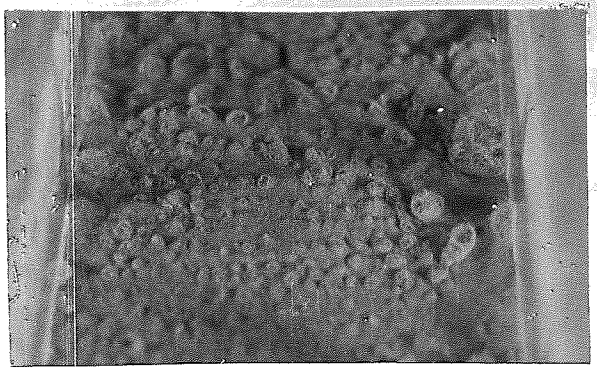

b.

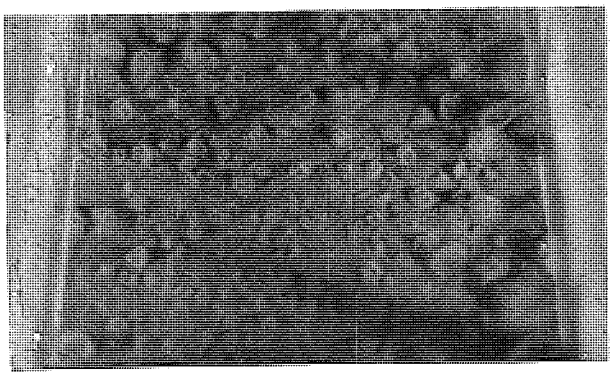

c.

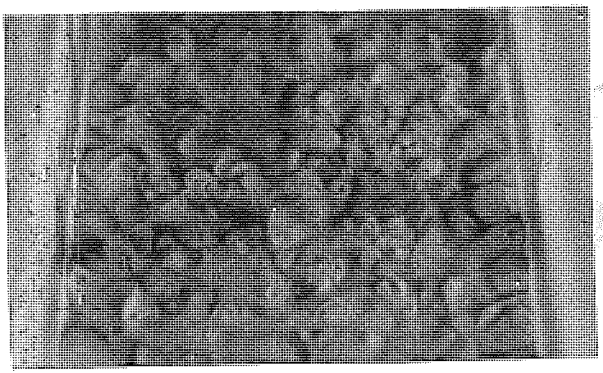

d.

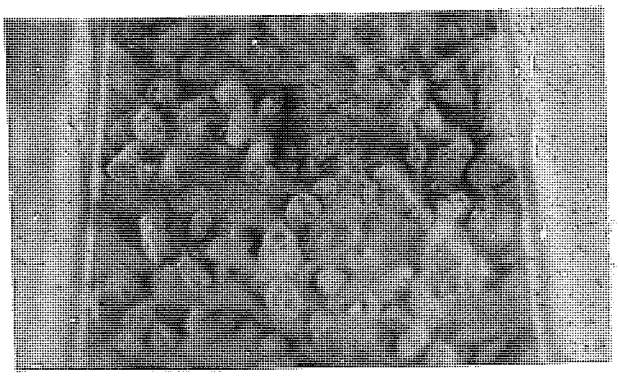

e.

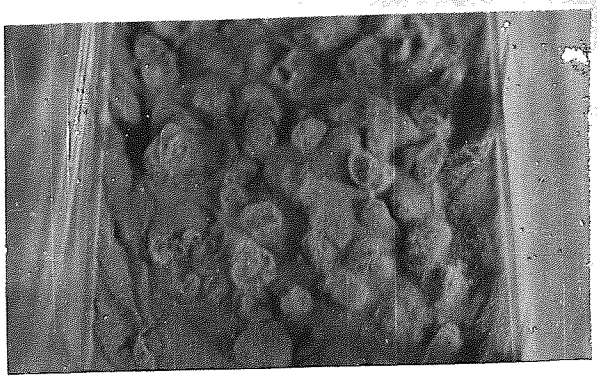

f.

FIG. 5·15 CHANGE IN BUBBLING PATTERN WITH INCREASING SHEAR-RATE.

in contrast to the preferential bubbling at the walls noticeable at lower shear-rates. This increase in bubbling during transition was at first thought to be due to the sweeping away of the segregated layer, which at lower shear rates acts as a secondary distributor, and therefore promotes the even bubbling character of shallower beds. This explanation may be partly correct, but further observations indicate that other factors are also involved.

Frame 5.15(f) illustrates the bubbling at the highest shear rate on Figures 5.3, which is well beyond the transition region. A further increase in bubble size is evident here, and the bubbling is much more vigorous than would be expected in a stationary (ie non-flowing) bed of 27 mm depth at 2.5 U_{m_f}. Referring now to Figure 5.16, which illustrates the bubbling at the same fluidising velocity but at the greater bed depth of 40 mm; a similar trend is evident. However it is clear that the shear diagram for this latter case (Figure 5.3) contains no transition region, so that de-segregation is clearly not entirely responsible for the increase in bubbling.

At high shear rates, the bubbles are rapidly transported horizontally as well as rising vertically. It is thought that this may promote bubble coalescence and also possibly reduce the bubble rise rate: so that at any given air flowrate more bubbles are contained within the bed than would otherwise be so. The latter could, if the dense phase voidage remained constant, entail some increase in bed expansion at high shear rates. However this would not be easy to measure, especially in a shallow bed, as the bed surface becomes extremely diffuse under these conditions.

Mention was made above of preferential bubbling at the walls at moderate flow velocities. This was noticed particularly at low fluidising velocities and is shown in Figure 5.17. It will be seen that the increased bubbling is attendant to a region of high velocity gradient

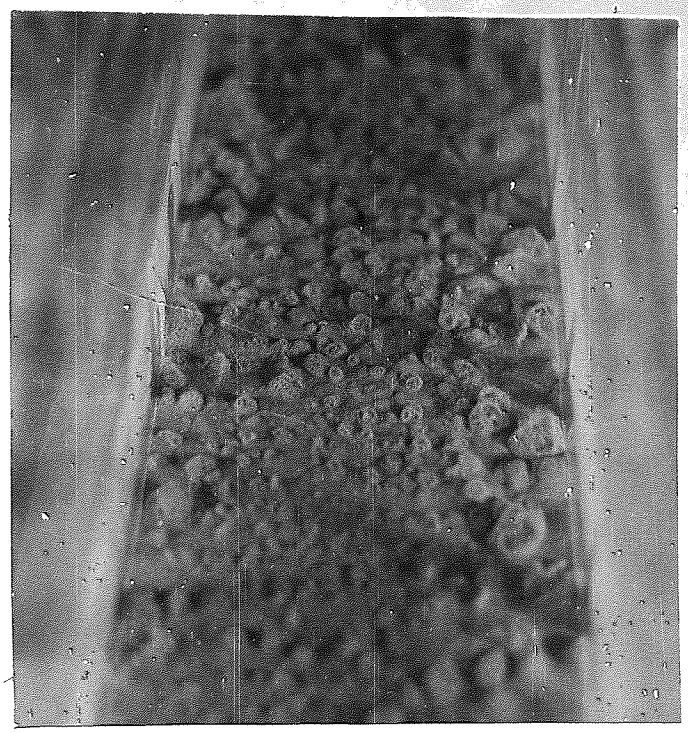

a.

b.

FIGURE 5-16.

FIGURE 5.17

HYDRODYNAMICAL BUBBLING AT CEILING WALL.

U_f = 65 cm/s

h = 27.5 mm

ρ = 3.25 kg/m

S = 0.039

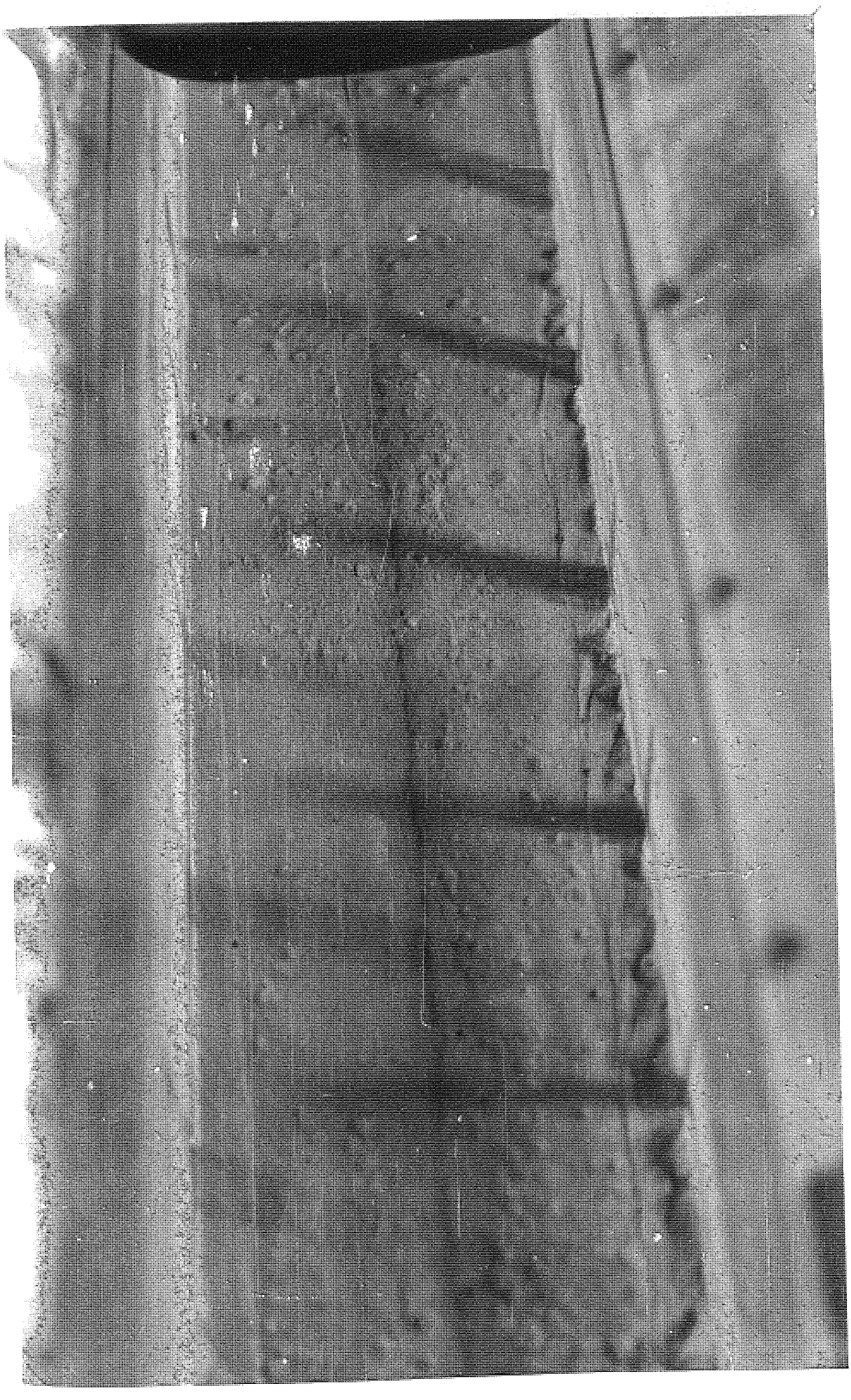

extending about 20 mm from the walls, the central section of the channel (which is virtually innocent of bubbles) moving at an almost uniform surface velocity. Such a region of preferential fluidisation was also noted around the rotor of the viscometer under similar fluidising conditions (see Chapter 3, Section 5.2 (iii)), and is thought to be partly responsible for the shear-thinning character of the flow. Similar conditions obtain at the higher fluidising velocity shown in Figure 5.18, although there the air flow is sufficient to maintain some bubbling in the central region of the channel also.

Clearly the existence of a 'boundary layer' in which the majority of the horizontal velocity gradient is developed is contrary to the concept of laminar flow. Also, the injection of a stream of coloured tracer material indicated that the range of conditions under which streamlines are present in the flow is extremely limited. Under circumstances of anything more than vestigial bubbling, the injected stream was immediately dispersed within the local particle circulations. The coloured dye used does not show up well on black and white photographs, but a central streamline is just visible in Figure 5.17. At the higher fluidising velocity (1.9 U_{m_f}) of Figure 5.18 the streamline has been largely broken up, although a diffused line of dyed material is just visible; but even this completely disappears at higher fluidising velocities (Figure 5.16). It is surprising, in view of this evidence of departure (both local and general) from true laminar flow, that the theory of Section 3 (ii) has proved so readily applicable to the fluidised state.

It will be noted from Figure 5.17 that there is some disparity between the amount of bubbling at the two bed walls. Such asymmetry of air flow often occurred at low fluidising velocities: to such an extent in some cases that the solids flow was completely arrested on one side of the channel, as the bed became locally defluidised. Subsequent examination

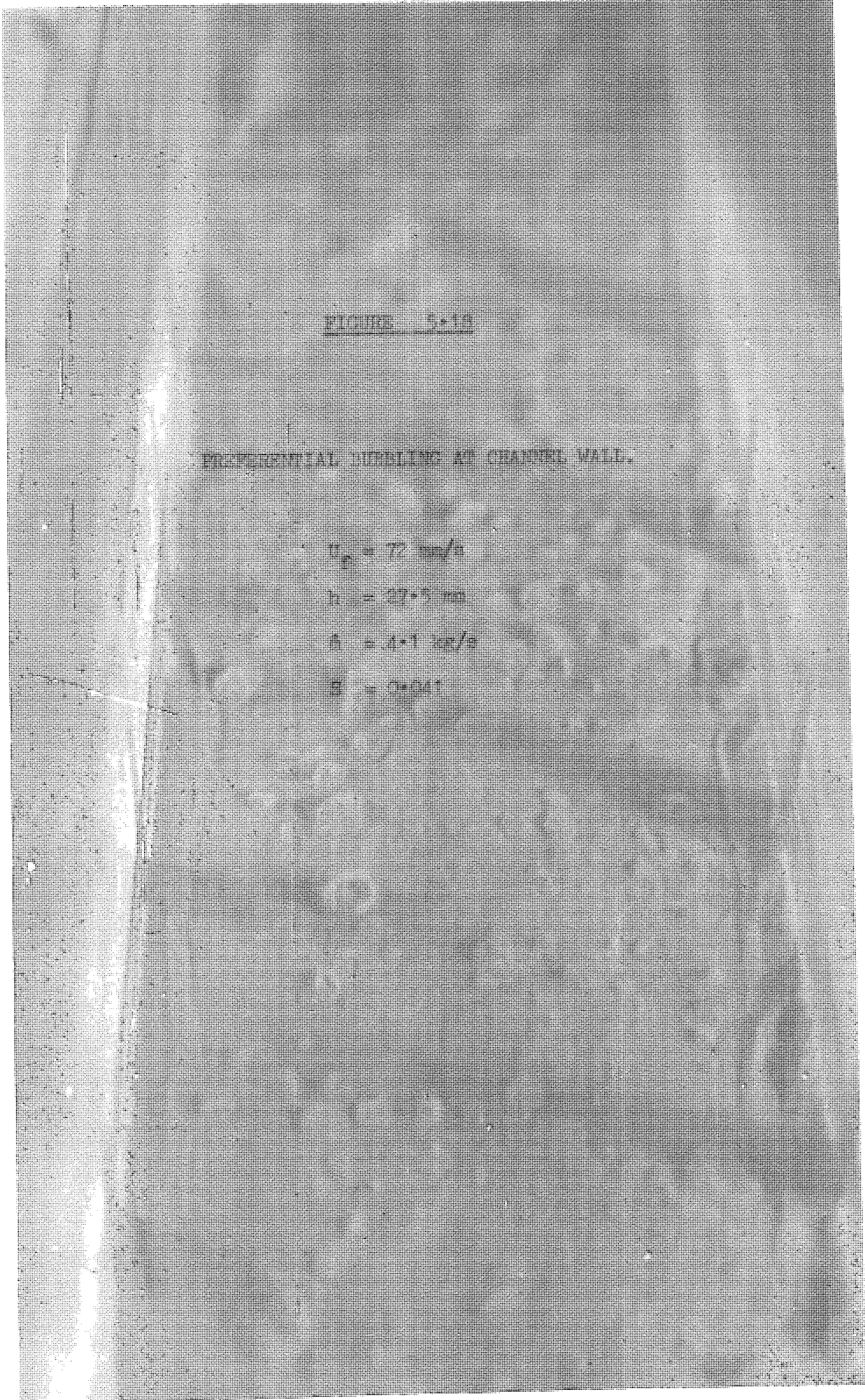

PICTURE 5·13

PREFERENTIAL BUBBLING AT CHANNEL WALL.

U_F = 72 mm/s

$h_{\ }$ = 27·5 mm

$\dot{m}$ = 4·1 kg/s

B = 0·041

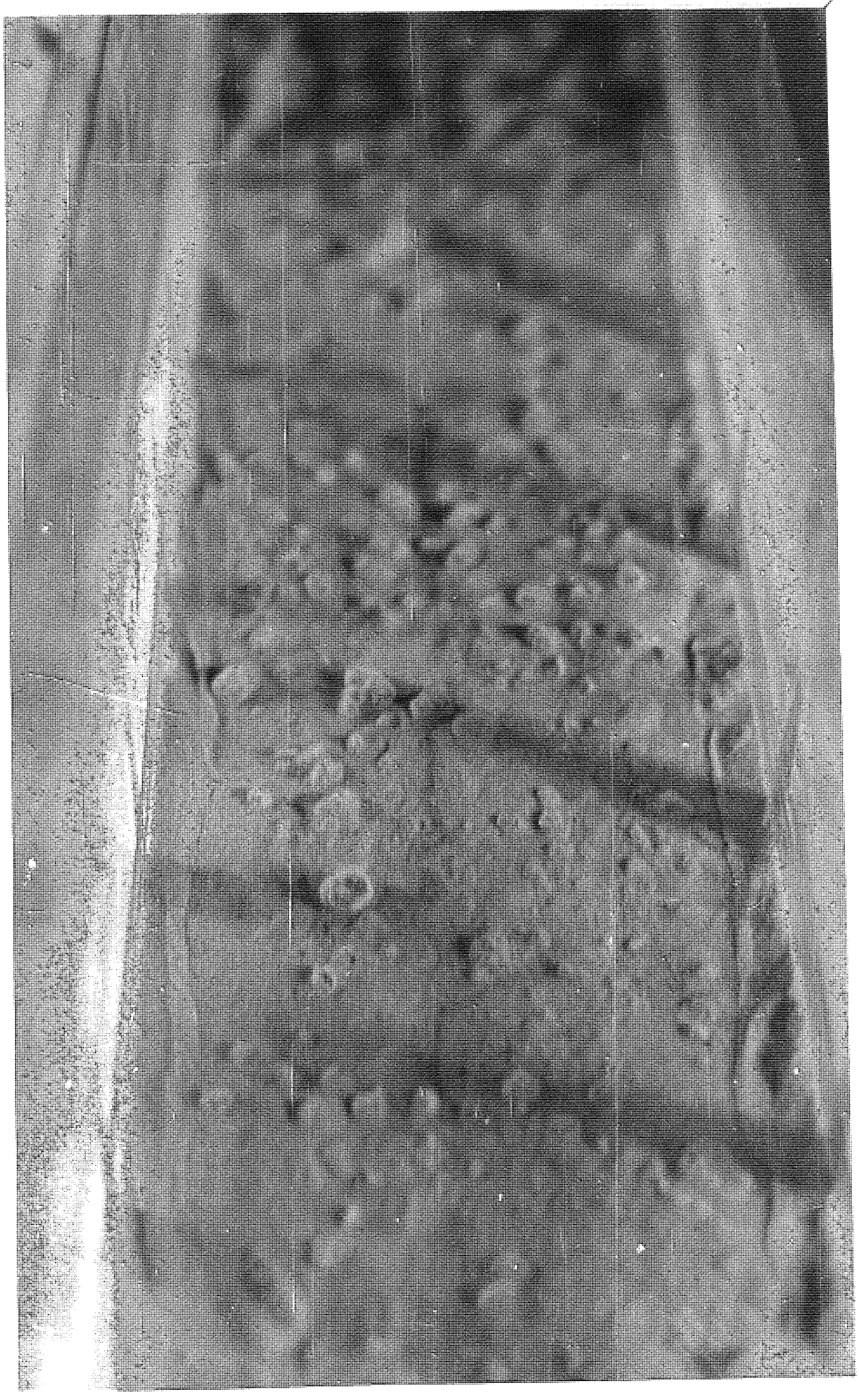

of the bed material revealed that the cause was again segregation of large particles, which process will clearly be cumulative as the air flows preferentially through the other side of the channel. Similar behaviour was noticed by Bessant[141], although at the time this was attributed to other reasons than segregation.

The other main observation of interest in the channel work was the hydraulic jump. An example is shown in Figures 5.19, in which the bed depth is seen to increase abruptly in the direction of flow. Hydraulic jumps are common in water conduits at points of change from a steep to a mild slope[164], but have not to the author's knowledge been previously observed in fluidised channels.

Jumps could be initiated quite readily at fluidising velocities below about 2.5 U_{m_f} by restricting the outlet to the lower receiver. This normally resulted in a series of jumps which travelled up the channel at slow speed and then collapsed, but sometimes stationary jumps were obtained which persisted when the downstream restriction was removed. Hydraulic jumps are not found in liquid flow except near reductions in channel slope or other hydraulic discontinuities, but are possible in fluidised flow in a uniform channel for two reasons. Firstly the bed viscosity increases with depth. Secondly the deeper post-jump section of the channel becomes defluidised relative to the upstream section, as a result of the higher pressure drop across the increased bed depth, which again increases the downstream flow resistance. The extent of the second-named effect will depend upon the pressure-drop across the distributor. With a high pressure-drop plate, less air redistribution will occur, so that presumably the formation of a jump will be less likely.

It is not proposed to discuss the theory of hydraulic jumps here. A condition for the formation of a jump in liquid flow is that the upstream Froude number (U^2/gh) exceeds unity[164]. This condition is satisfied for

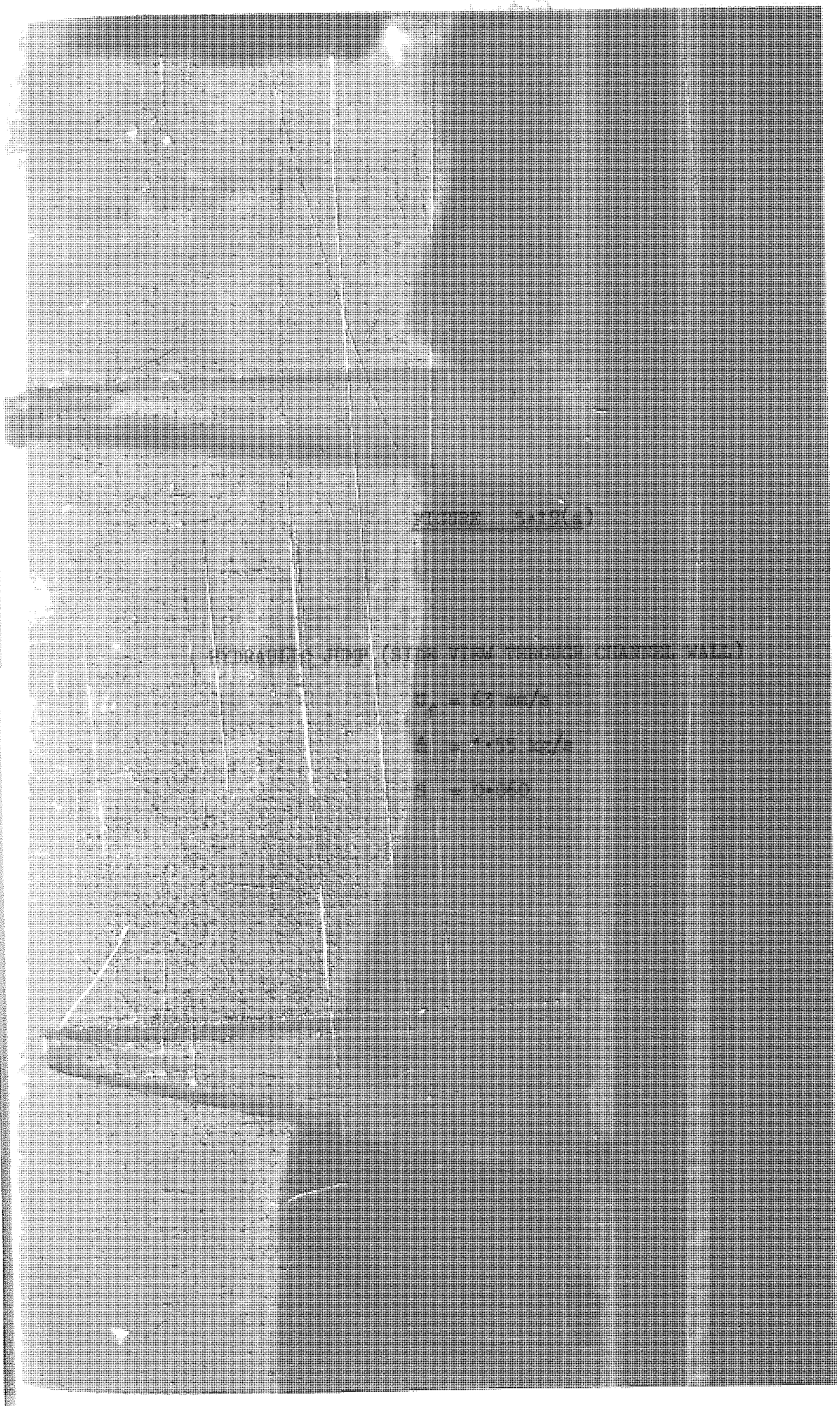

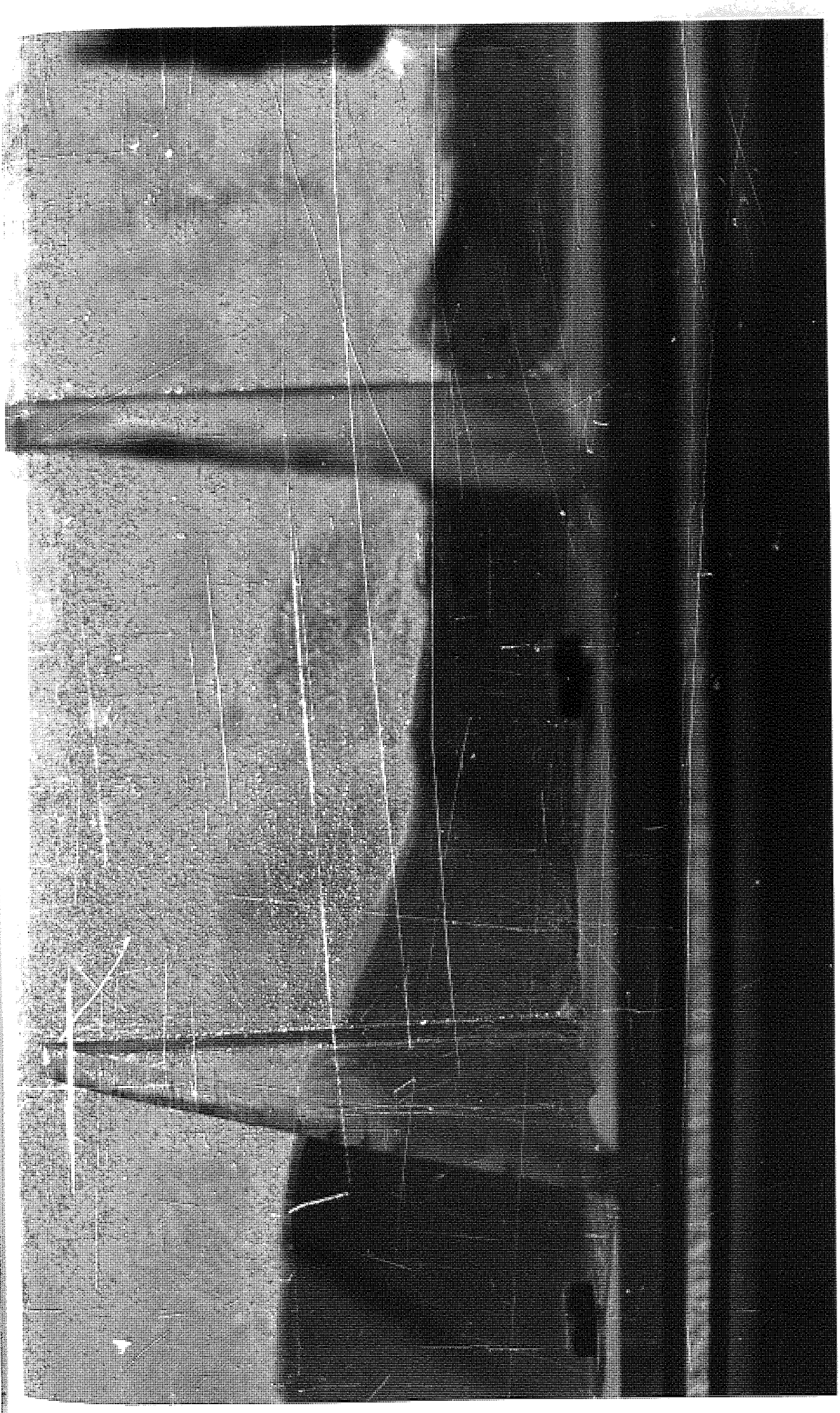

DIRECTION OF FLOW.

DIRECTION OF FLOW.

the case of Figure 5.19. However, further analysis is likely to be complicated in fluidised flow because the jump will be accompanied by a change of density due to the difference in fluidising velocity upstream and downstream.

6. CONCLUSIONS

The main conclusions from the channel flow work are as follows:

a) At fluidising velocities above approximately 2.5 U_{m_f} (for the material tested), the flowing bed normally behaved like a shear-thinning fluid. The shear diagram could not generally be represented by a power-law expression over the whole range of shear-rates.

b) At lower fluidising velocities the flow was adversely affected by segregation of large particles on to the distributor at low shear-rates. This is likely to be aggravated in a through-flowing system by progressive build-up of segregated material. The effect appeared to be more marked in shallow beds.

c) The value of the non-Newtonian flow index varied between 0.8 and unity, but showed no consistent variation with either bed depth or fluidising velocity over the range investigated.

d) The channel results confirmed the deterioration of flowability with increasing bed depth found with the viscometer.

e) The apparent viscosity at a shear-rate of 100 s^{-1} varied between 0.036 and 0.15 Ns/m^2. These values are lower than most of those previously reported, because of the higher shear rates at which they were calculated.

f) The apparent viscosity of the flowing channel continued to decrease with rising fluidising velocity over the range 1.9 to 4.7 U_{m_f} investigated in this work. This is contrary to the viscometer results, which showed a minimum apparent viscosity at 1.5 - 2.0 U_{m_f}

and may be caused by removal, at high shear-rates, of the inviscid layer existing close to the distributor at the latter fluidising velocities.

g) The friction factor/generalised Reynolds Number correlation of Section 3(ii) fits the experimental data with reasonable accuracy over the whole range of Reynolds numbers so far investigated. The standard deviation of all the experimental data points from the appropriate $f_D = C/N_{Re}$ curve is 13%. The level of accuracy could be improved quite easily, and the method is seen as a useful basis for the design of fluidised channels.

h) Although the concepts of laminarity and turbulence cannot be applied rigorously to fluidised flow, no departure from the lamina region of the f_D vs N_{Re} curve was evident up to Reynolds numbers exceeding 4000.

i) The use of a timed float moving with the fluid stream cannot be expected to give a reliable measurement of the flow velocity in the channel.

j) Direct comparison of the viscometer and channel data is difficult because of the wide disparity in shear rates between the two situations. However, it appears that the flow behaviour in the channel is modified by virtue of the variable resistance of the fluidising distributor, compared with the vertical walls.

k) There is little doubt that the flow resistance at the distributor is greater than at the walls in some conditions (eg when segregation is present) and less in others (eg higher fluidising velocities and low shear rates). However, it is not possible to say as yet whether this is due to slip, or to an inviscid region at the distributor in which exists a high velocity gradient.

l) A change of bubbling pattern at the bed surface is evident with increasing shear rate. At moderate shear rates, bubble suppression in the bulk of the bed is evident, due to preferential bubbling at the walls. At higher shear rates, the bubbling becomes more vigorous, due to absence of the segregated layer evident in some conditions at low shear rates, and also possibly to greater hold-up of bubble gas within the bed.

m) Visual observations indicate departure from true laminar flow even at the lowest flow velocities; both locally in terms of absence of streamlines and generally because of lack of developed laminar velocity profiles.

n) Hydraulic jumps or standing waves could be occasioned at fluidising velocities below 2.5 U_{m_f}, by restriction of the downstream flow.

7. RECOMMENDATIONS FOR FUTURE WORK

The work with the flowing channel has indicated above all else the great potential of fluidised transport as a means of conveying large volumes of particulate material with great ease at high velocity. However, it has also shown that there are many problems to be investigated and overcome (segregation for example), and that a much more thorough knowledge of the character of the flow is required before continuous, reliable industrial operation at high throughputs is readily achieved.

A simple correlation has been shown to provide a fairly accurate description of the flow over a reasonable range of conditions, but provides little insight into the true mechanism of fluidised flow. Nonetheless, this treatment would provide a useful design tool in the short term, if its applicability to a wider range of conditions could be confirmed. This would encompass greater bed depths; different distributors, channel widths and fluidising velocities; different types

and size-ranges of materials; and especially, a greater range of Reynolds numbers. All these could be investigated reasonably quickly now that the apparatus is available and proven.

However, the foregoing must be regarded in the long term as an expedient until a fuller knowledge of the true nature of fluidised flow is available, for it is clear from the work done already that it is a more complex process than is capable of representation by a simple liquid analogy. Accurate representation of fluidised flow will not be easy: some aspects of liquid flow in channels remain an empirical art, and fluidised flow, being both non-Newtonian and non-homogeneous is clearly more complicated.

The first priority must be to carry out a thorough investigation of the disparity in behaviour between the distributor and vertical walls. The work of Bessant[141] was helpful here, but was hampered by apparatus which was not designed for the job. Also some of the assumptions of the theory used due to Suzuki et al[106] (which was chosen for its simplicity) are not appropriate to fluidised flow. Any theoretical analysis is made considerably more difficult if the flow has a two dimensional velocity profile. It is probable that by irrigating the channel walls with air, the wall drag would be reduced to the point where treatment of the channel as having infinite width would be reasonable. This would simplify the analysis of the distributor resistance considerably. Further direct measurements, such as velocity profiles and wall-drag forces could be made easily, at higher velocities than hitherto, and provide a valuable complement to other measurements.

It is to be hoped that anomalies between viscometer and channel flow data can be resolved when the behaviour at the channel distributor is understood. The convenience and low solids

requirement of the viscometer make it an invaluable means of studying the behaviour of new materials or fluidising conditions; though until the resulting data can provide a direct indication of channel flow performance its value for quantitative measurements is limited.

All the foregoing applies to flow in a simple, uniform channel. However, if fluidised flow is to be applied to real transport situations, a study of the flow through changes of section, notches, weirs, and entry and exit from reservoirs is equally necessary. Also, for operation at elevated temperature or pressure, a knowledge of the effect of a closed freeboard of limited volume would be useful. It would be interesting to look at the performance of the extended surface heat-exchanges developed at Aston in a rapid-flowing bed.

The second object in building the channel rig - that of studying vertical transport - has not as yet been started. Again this must complement horizontal or inclined channel flow if the fullest industrial usage of fluidised transport is to be realised. Although some work has been done on efflux from orifices, virtually nothing is knwon of this mode of flow.

CHAPTER 5

NOMENCLATURE

NOMENCLATURE.

b	= Breadth(of channel or settling chamber)	mm,m
B_6, B_7	= Constants in saltation velocity equations.	
C	= Constant in f_D vs N_{Re} eqn for channel flow.	
C_d	= Drag coefficient.	
d	= Characteristic dimension in Reynolds Number eqn.	mm,m
d_b	= Bubble diameter.	mm
d_p	= Particle diameter.	mm
d_{sv}	= Surface mean diameter.	mm
d_t	= Tube diameter (pneumatic transport)	mm,m
D	= Pipe diameter.	mm,m
D_e	= Hydraulic diameter.	mm,m
f_D	= D'Arcy friction factor.	
f_F	= Fanning friction factor.	
g	= Acceleration due to gravity.	m/s^2
G	= Air mass velocity in pneumatic transport	kg/m^2s
G_s	= Solids mass velocity in pneumatic transport	kg/m^2s
h	= Height or Depth.	mm,m
K	= Constant in equivalent length eqn.	
K'	= Consistency index in non-Newtonian flow.	$Ns^{n'}/m^2$
l	= Length,of rotor,pipe etc.	mm,m
l_e	= Entry length in channel or pipe flow.	mm,m
L	= Length of channel.	m
$\dot{m}$	= Mass flow rate.	kg/s
n'	= Non Newtonian flow index.	
q,Q	= Volume flowrate.	m^3/s
N_{Re}	= Generalised Reynolds Number.	

R	=	Radius (of rotor)	mm
R_{e_p}	=	Particle Reynolds Number	
S	=	Slope of channel (= Sin α)	
u	=	Velocity	mm/s, m/s
U_b	=	Bubble Velocity	
U_{Ch}	=	Choking Velocity	
U_{cs}	=	Saltation velocity (pn. transport)	
U_f	=	Superficial fluidising velocity	
U_{f_d}	=	Flow deterioration velocity (Chapter 3, Sect 5.2(i))	
U_ℓ	=	Air velocity in pneumatic line	
U_{m_f}	=	Minimum fluidisation velocity	
U_s	=	Solids velocity in pneumatic transport	
U_{s_f}	=	" " in settling chamber	
U_t	=	Terminal velocity (of particle)	
U_w	=	Velocity at a wall	
U	=	Mean flow velocity	
V	=	Volume of bed	m^3
y	=	Direction normal to velocity in a shear field	m
α	=	Shear rate (S^{-1}), Angle of inclination of channel (Deg)	
Δp	=	Head loss, Pressure drop	mm/m H_2O
ϵ	=	Voidage fraction	
γ	=	Constant in eqn 10, Chapter 4, Section 3 (ii)	
Ω	=	Angular velocity of rotor	s^{-1}
ρ_b	=	Bed density, Bulk density	kg/m^3
ρ_f	=	fluid density	
ρ_s	=	Particle true density	
ϕ	=	Sphericity	

ν	=	Kinematic viscosity	m^2/s
τ	=	Shear stress	N/m^2
τ_R	=	" " at rotor surface	
τ_w	=	" " at wall	
τ_y	=	Yield shear stress	
μ	=	Viscosity	kg/ms Ns/m^2
μ_a	=	Apparent Viscosity	
$\mu_{(b)}$	=	Viscosity of bed	
μ_f	=	Fluid viscosity	
μ_g	=	Gas viscosity	
μ_o	=	Viscosity at zero shear rate (limiting)	
μ_∞	=	Viscosity at infinite shear rate	

CHAPTER 6

LIST OF REFERENCES

AND

AUTHOR INDEX

SECTION 6a

REFERENCES

1. RICHARDSON, J F: in DAVIDSON AND HARRISON, "FLUIDIZATION" Acad. Press, 1971.
2. ERGUN S: CHEM ENG PROG. 48, 89, (1952).
3. CARMEN, P C: TRANS I CHEM E 15, 150, (1937).
4. WEN C Y and YU Y H: A I CHEM E JNL, 12, 610, (1966)
5. LEVA M: "FLUIDISATION" McGraw Hill, N.Y, 1959.
6. FRANZ J F: CHEM ENG 69, 161 (1962).
7. ZENZ F A and OTHMER D F: "FLUIDIZATION AND FLUID PARTICLE SYSTEMS" Reinhold, N.Y, 1960.
8. KUNII D and LEVENSPIEL O: "FLUIDISATION ENGINEERING", J Wiley, N.Y, 1968.
9. BROWN G et al: "UNIT OPERATIONS", J Wiley, N.Y, 1950.
10. PINCHBECK P and POPPER F: CHEM ENG SCI, 6, 57, (1956).
11. ROWE P N: TRANS I CHEM E, 39, 175, (1961).
12. MOTAMEDI M and JAMESON G: CHEM ENG SCI., 23, 791, (1968).
13. WILHELM R and KWAUK M : CHEM ENG PROG. 44, 201, (1948).
14. ROMERO J and JOHANSON L: CHEM ENG PROG (Symp Ser) 58, 28, (1962).
15. SIMPSON H and ROGER B: CHEM ENG SCI, 16, 153, (1961).
16. MURRAY J D: J FL MECH 21, 465 (1965).
17. PIGFORD R and BARRON D: IND and ENG CHEM FUND, 4, 81, (1965).
18. JACKSON R: TRANS I CHEM E, 41, 13, (1963)
19. MOLERUS O: PROC INT SYMP ON FLUIDS, EINDHOVEN, 1967.
20. HARRISON D, DAVIDSON J F and de KOCK J: TRANS I CHEM E, 39, 202 (1961).
21. VERLOOP J and HEERTJES P: CHEM ENG SCI. 25, 825, (1970).
22. GELDART D: 4tn INT CHISA CONGRESS, PRAGUE, SEPT 1972.
23. GELDART D: POW TECH, 1, 355, (1967/8).

24. BAUMGARTEN P and PIGFORD R: A I CHEM E JNL, 6, 115 (1960).

25. ROWE P. and STAPLETON W: TRANS I CHEM E, 39, 181, (1961).

26. YASUI G and JOHANSON L: A I CHEM E JNL, 4, 445, (1958).

27. de GROOT H: PROC INT SYMP ON FLUIDN., EINHOVEN 1967.

28. TOOMEY R and JOHNSTONE H F: CHEM ENG PROG, 48, 220, (1952).

29. ROMERO J and JOHANSON L: CHEM ENG PROG (SYMP SER) 58, 28, (1962).

30. ROMERO J and SMITH D: A I CHEM E JNL, 11, 595, (1965).

31. TOOMEY R and JOHNSTONE H F: CHEM ENG PROG (SYMP.SER) 49, 51, (1953).

32. DAVIDSON J F and HARRISON D: CHEM ENG SCI, 21, 231, (1966).

33. ROWE P N in DAVIDSON J F and HARRISON D: "FLUIDIZATION" Acad Press 1971

34. DAVIDSON J F: TRANS I CHEM E 39, 230 (1961)

35. STEWART P: TRANS I CHEM E 46, 60, (1968).

36. JACKSON R: TRANS I CHEM E 41, 13, (1963).

37. MURRAY J: J FL MECH 22, 57, (1965).

38. DAVIES R and TAYLOR G: PROC ROY SOC A200, 375, 1960.

39. KADLEC R, WILLIAMS B, and RUDD D: 54th NAT MTG A I CHEM E.

40. STEWART P: DOCT THES, CAMBRIDGE 1965.

40a) HOVMAND S and DAVIDSON J F in DAVIDSON and HARRISON "FLUIDISATION" Acad. Press, 1971.

41. JOTTRAND R: CHEM ENG SCI 3, 12, (1954).

42. BOLAND D: DOCT THES, BRADFORD 1972.

43. WHITEHEAD A B in DAVIDSON and HARRISON "FLUIDIZATION" Acad Press, 1971.

43A. HIBY J: CHEM ING TECH, 36, 228 (1964).

44. GREGORY S A: PROC INT SYMP FLUIDN, EINDHOVEN 1967, p 751.

45. ZUDERWEG : " " " " " " p 739.

46. MORSE R and BALLOU C: CHEM ENG PROG 47, 199, (1957).

47. GROHSE E: A I CHEM E JNL 1, 358 (1955).

48. HARRISON D and GRACE J in DAVIDSON and HARRISON, "FLUIDIZATION" Acad Press, 1971.

49. BENENATI R F and BROZILOW E: A.I.CHEM.E.J. 8,(3),359,(1962).

50. YAGI S andKUNII D: CHEM.ENG.SCI. 16,364,372,380,(1961).

51. EINSTEIN V & GELPERIN N in DAVIDSON & HARISON, "FLUIDISATION" Acad. Press 1971.

52. MICKLEY H & TRILLING C: IND. & ENG.CHEM. 41,1135,(1949).

53. MICKLEY H & FAIRBANKS D: A.I.CHEM.E.J. 1,374,(1955).

54. MICKLEY H, HAWTHORN R & FAIRBANKS D: CHEM.ENG.PROG.(SYMP.SER) 57,(32),51,(1961).

55. BASKAKOV A in DAVIDSON & HARISON,"FLUIDISATION", Acad.Press, 1971.

56. BOTTERILL J S M,REDISH K,ROSS D & WILLIAMS J: PROC. SYMP. "INTERACTION BETWEEN FLUIDS & PARTICLES", I.CHEM.E.,1962.

57. BOTTERILL J S M & WILLIAMS J: TRANS.I.CHEM.E. 41,217,(1963).

58. BOTTERILL J S M, BRUNDRETT G, CAIN G & ELLIOTT D E: CHEM.ENG. PROG.(SYMP.SER) 62,(62),1,(1966).

59. BOTTERILL J S M, BUTT M, CAIN G & REDISH K: INT.SYMP. ON FLUIDISATION,AMSTERDAM,1967, p442.

60. BOTTERILL J S M & HAMPSHIRE N: CHEM.ENG.SCI. 23,400,(1968).

60A. KUBIE J, UNIV OF ASTON, PRIV. COMN.

61. VREEDENBERG H: CHEM.ENG.SCI. 9,52,(1958).

62. BOTTERILL J S M & van der KOLK M: CHEM.ENG.PROG.(SYMP.SER) 66,(101),61,(1970).

63. PEPRIE J, FREEBY W & BUCKHAM J: CHEM.ENG.PROG. 64, (7), 45, (1968).

64. ATKINSON G, CITY OF B'HAM. POLYTECH., PRIV. COMN.

65. SINGH J & WOOTEN E: UNIV OF ASTON, UNDERGRADUATE PROJECT REPORT, 1972.

66. McGUIGAN S J,"PRELIMINARY REPORT ON THE PERFORMANCE OF AN EXTENDED SURFACE HEAT EXCHANGER IN A FLUIDISED BED",Internal Report, Univ. of Aston, 1970.

67. MATHESON G L, HERBST W A and HOLT P H 2nd., IND and ENG CHEM 41, 1099, (1949).

68. GELDART D: POW TECH 6, 201, (1972).

69. TRAWINSKI H: CHEM ING TECH 4, 201, (1953).

70. KRAMERS H: CHEM ENG SCI 1, (1), 35, (1951).

71. DIEKMAN R and FORSYTHE W L Jnr: IND and ENG CHEM 45, 1174 (1953).

72. PETERS K and SCHMIDT A: "OESTERREICH CHEMIKER ZEITUNG, 54 253, (1953)

73. Van WAZER J, LYONS J, KIM K and COLWELL R: "VISCOSITY AND FLOW MEASUREMENTS", J Wiley N Y, 1963, p 272.

74. FURAKAWA J and OHMAE T: IND and ENG CHEM 50, 821 (1958).

75. SHUSTER W and HAAS C: J CHEM ENG DATA 5, 525 (1960).

76. FA-KEH LIU F and ORR C Jnr: J CHEM ENG DATA 5, 431 (1960).

77. SCHUGERL K in DAVIDSON and HARRISON "FLUIDIZATION" Acad.Press 1971.

78. SCHUGERL K, MERZ M and FETTING F: CHEM ENG SCI. 15, 1, 39 and 75 (1961).

79. EYRING H: J CHEM PHYS. 4, 283, (1936).

80. LEEDEN P and BOUWHUIS G: APP SCI RES A10, 78, (1961).

81. MARTYUSHIN I and KHARAKOZ V: INT CHEM ENG, 7, 255 (1967).

82. PRUDHOE J and WHITMORE R: BRIT CHEM ENG 2, (6), 371 (1964).

83. HAGYARD T and SACERDOTE A: IND and ENG CHEM FUND, 5, 500 (1966).

84. HETZLER R and WILLIAMS M: IND and ENG CHEM FUND, 8, 668 (1969).

85. GRACE J R: CAN JNL CHEM ENG 48, 30, 1970.

86. -

87. JONES D and DAVIDSON J F: RHEOL ACTA 4, 180 (1965).

88. MASSIMILLA L, BETTA V and DELLA ROCCA C: A I CHEM E J 7, 502, (1959).

89. MASSIMILLA L, VOLPICELLI G and ZENZ F: IND and ENG CHEM FUND, 2, 1964, (1960).

90. STOCKHELL I: CHEM ENG PROG (SYMP SER) 58, (38), 106, (1962).

91. YOSHIKI M and FUJIMOTO I in KUNII and LEVENSPIEL: "FLUIDIZATION ENG" J Wiley, N.Y, 1968.

92. TREES J: TRANS I CHEM E 40, 286 (1962).

93. MASSIMILLA L. in DAVIDSON and HARRISON "FLUIDIZATION" Acad.Press 1971.

94. WEN C Y and GALLI A in DAVIDSON and HARRISON "FLUIDIZATION", Acad. Press 1971.

95. WEN C Y and SIMONS H: A I CHEM E J, 5, 263, (1959).

96. ELLIOTT D E and GLIDDON B J: "HYDROTRANSPORT 1", Paper G2, B.H.R.A, 1970.

97. SIEMES W and HELLMER L: CHEM ENG SCI, 17. 555, (1962).

98. NEUŽIL L and TURCAJOVÁ M: COLL CZ CHEM COMN, 34, 3652, 1969.

99. QUASSIM R Y: DOCT THES. LONDON, 1970.

100. BOTTERILL, J S M, CHANDRASEKHAR R, and van der KOLK M: CHEM ENG PROG (SYMP SER) 66, (101), 81; 66, (105), 277, (1970).

101. BOTTERILL J S M and van der KOLK M: A I CHEM E (SYMP SER) 67, 70 (1971).

102. BOTTERILL J S M, van der KOLK M, ELLIOTT D E and McGUIGAN S J: POW TECH 6, 343, 1972 (Also Appendix II).

103. BOTTERILL J SM and BESSANT D J: "POWTECH" CONF. HARROGATE 1973.

104. WHEELER J and WISSLER E: A I CHEM E J, 11, 207, (1965).

105. BOTTERILL J S M and BESSANT D J: INT CONF ON FLUIDN, TOULOUSE, SEPT 1973.

106. SUZUKI A and TANAKA T: IND and ENG CHEM FUND, 10 (1), 84, (1971).

107. HARPER W: "CONTACT and FRICTIONAL ELECTRIFICATION", Clarendon Press, 1967.

108. CIBOROWSKI J and WLODARSKI A: CHEM ENG SCI, 17, 23 (1962).

109. KISEL'NIKOV V, VYALKOV V and FILATOV V: INT CHEM ENG 7, 428 (1967).

110. KATZ H: ARGONNE NAT LAB USA, US ATOM EN COMM. ANL-5725 (1957).

111. GELDART D and BOLAND D: POW TECH, 5, 289, (1971/2).

112. FORREST J: BR JNL APP PHYS, SUPP No 2, 537, (1953).

113. LOEB L: "STATIC ELECTRIFICATION" Springer-Verlag, Berlin, 1958.

114. WINKLER F: D R P 437,970.

115. "DISCUSSION MEETING ON FLUID BED BOILERS" I Mech E, London, 20/1/1971

116. ELLIOTT D E: CHARTERED MECHANICAL ENGR, JULY 1970.

117. ELLIOTT D E: INST OF FUEL TOTAL ENERGY CONF, Paper 23, BRIGHTON, 1971.

118. HARRIS V R, UNIVERSITY OF ASTON: UNDERGRAD PROJECT REPT. 1973.

119. ELLIOTT D E and BROUGHTON J: "COMBUSTION IN SHALLOW FLUIDISED BEDS", TO BE PUBLISHED.

120. ELLIOTT D E: 2nd INT SYMP ON FLUID BED COMBN, HEUSTON WOODS, OHIO 1970, p 0-2-1.

121. MOSS G: DITTO p 11-6-1.

122. VIRR M J and REYNOLDSON R: IND PROC HTG, DEC 1972.

123. PILLAI K K, UNIV OF ASTON: INTERNAL REPORT.

124. TUCKWELL D E, POLYSIUS LTD., PRIV COMN.

125. SQUIRES A M: US Pat 3,268,264 (1966).

126. GLIDDON B J: "SOME NON-NEWTONIAN FLOW PROPERTIES OF P F ASH/WATER SLURRIES," Central Electricity Generating Board Research Report, RD/M/N 283.

127. SKELLAND A H P: "NON-NEWTONIAN FLOW AND HEAT TRANSFER", J Wiley, N.Y 1967.

128. OLDROYD J: RHEOL ACTA 1, 337, (1961) and PROC ROY SOC, A 245, 278, (1958).

129. Von KARMAN T: J AERO SCI, 1 (1), 1, (1936).

130. METZNER A and REED J: A I CHEM E J 1(4), 434, (1955).

131. KREIGER I and MARON S: J APP PHYS 25, 72, (1954).

132. KREIGER I and MARON S: J APP PHYS 23, (1), 147, (1952)

133. KREIGER I and ELROD H: J APP PHYS, 24 (2), 134, (1953).

134. INT CRIT TABLES 5, 23.

135. SEGUR and OBERSTAN: IND and ENG CHEM 43, 2117, (1951).

136. "TEST SIEVING MANUAL", ENDECOTTS (FILTERS) LTD, ACTON, LONDON SW19.

137. ATKINSON G, CITY OF B'HAM POLYTECH: PRIVATE COMN.

138. GELDART D: DOCT THES. BRADFORD 1970.

139. BAERNS M: IND and ENG CHEM FUND. 5, 508, (1966)

140. KUNKEL W B: J APP PHYS 21, 820, (1950).

141. BESSANT D J: DOCT THES., BIRMINGHAM 1973.

142. INT CRIT TABLES 5, 1.

143. STEARNS J: PHYS REV 27, 116, (1926).

144. BROUGHTON J: UNIV OF ASTON, PRIV COMN.

145. RAUSCH J M: DOCT THES., PRINCETON, N.J., 1948.

146. BOTTERILL J S M, UNIV OF BIRMINGHAM, PRIV COMN.

147. MOONEY M, : J RHEOL 2, 210, (1931).

148. McGUIGAN S J and ELLIOTT D E: Paper C2.6,4th Int. CHISA Congress, Prague, Czechoslovakia, Sept 11-15, 1972.

149. BESSANT D J: Priv Comm.

150. PUGH R R, Univ of Aston: Priv. Comm.

151. MUSKETT W J, LEICESTER A R and MASON J S: Paper F1 'Pneumotransport-2', BHRA, Cranfield, Sept 5-7, 1973.

152. DAUGHERTY R L and FRANZANI J B: "Fluid Mechanics with Engineering Applications", McGraw Hill, N Y., 1965.

153. THOMAS J J, Univ. of Aston: Priv Comm.

154. RYDER G H: "Strength of Materials" McMillan and Co.Ltd 1965

155. PORVAIR Ltd., "VYON".

156. ENG. EQUIP. USERS ASSOC: "Pneumatic Handling of Powdered Materials", Constable and Co Ltd. 1963

157. ROSE H E and BARNACLE H E: ENGINEER 203, (5290), 898,939 (1957)

158. STAIMAND C J: TRANS I CHEM E 29, 1951.

159. PERRY J H: "CHEMICAL ENGINEERS HANDBOOK" McGraw-Hill, N Y, 1963.

160. BUYEVICH Y A : J. FL. MECH. 52, 345 (1972).

161. McMILLAN E L: CHEM. ENG. PROG. 44, 531 (1948).

162. CRAMER S D and MARCHELLO J M: A I CHEM E J. 14, 980 (1968).

163. RABINOWITSCH B Z: PHYS CHEM 145A, 1, (1929).

164. VENNARD J K: "ELEMENTARY FLUID MECHANICS" J Wiley, N Y, 1961.

165. STRAUB L G, SILBERMAN E and NELSON H C: TR.A.S.Civ.E. 685, 123, (1958).

166. BOGUE D C: IND and ENG CHEM. 51, (7), 874, (1959).

167. KNUDSEN J G and KATZ D L: "FLUID DYNAMICS & HEAT TRANSFER" McGraw-Hill, N.Y. 1958.

168. WILKINSON W L: "NON-NEWTONIAN FLUIDS", Pergamon, London (1960).

169. PUGH R R, UNIV. of ASTON: DOCT. THESIS (IN PREPARATION).

170. OWEN W M: TRANS A.S.CIV.E. 119, 1157 (1954).

SECTION 6b.

AUTHOR INDEX (ALPHABETICAL)

Name	Reference No
Gregory S	44
Grohse E	47
de Groot H	27
Haas C	75
Hagyard T	83
Hampshire N	60
Harper W	107
Harris V	118
Harrison D	20,32,33,48
Hawthorn R	54
Heertjes P	21
Hellmer L	97
Herbst W	67
Hetzler R	84
Hiby J	43a
Holt P	67
Hovmand S	40a
Inst Mech Eng	115
Int Crit Tables	134,142
Jackson R	18
Jameson G	12
Johanson H	28,31
Jones D	87
Jottrand R	41
Kadlec R	39
von Karman T	129
Katz D	167
Katz H	110

Name	Reference No
Reed J	130
Reynoldson R	122
Richardson J	1
Roger B	15
Rowe P	11,25,33
Romero J	14,30
Rose H	157
Ross D	56
Rudd D	39
Ryder G	154
Sacerdote A	83
Schmidt A	72
Schügerl K	77,78
Segur	135
Shuster W	75
Siemes W	97
Silberman E	165
Simons H	95
Simpson H	15
Singh J	65
Skelland A	127
Smith D	30
Squires A	125
Stairmand C	158
Stapleton W	25
Stearns J	143
Stewart P	35,40
Stockell I	90

Name	Reference No
Wooten E	65
Yagi S	50
Yoshiri M	91
Yasui G	26
Yoshiri M	91
Yu Y	5
Zenz F	7
Zuderweg	45

APPENDICES

APPENDIX I

DESIGN, CONSTRUCTION AND OPERATION OF CHANNEL FLOW RIG

(The design and construction of the fluidised channel flow rig was carried out with the collaboration of R R Pugh, B Sc, M Sc).

1. INTRODUCTION

The design of the channel flow rig was commenced when the viscometer work had reached a stage at which it was considered that some comparison and confirmation of the results obtained with channel flow data would be valuable before proceeding further. Concurrently with this, the need was expressed by one of the author's colleagues, Mr R Pugh, for an apparatus with which to study fluidised downflow in vertical conduits. Since both these requirements could be met with largely common hardware, the design of the rig was undertaken as a collaborative effort; although the vertical transport work has not yet been commenced in view of increased interest in channel flow studies.

The design of the rig took approximately twelve months to complete, and the construction four months. The rig operated successfully on initial start-up and has been run efficiently up to and slightly above the design maximum flowrate, although some difficulty is encountered in achieving the latter at low fluidising velocities. This, though, could be easily rectified by some simple development work in the light of the initial test running.

2. EVOLUTION AND LAYOUT OF THE DESIGN

It would be facile to report that the rig was designed to the specification laid out in Chapter 4. In practice several aspects of the specification could not be fixed until some calculation and drawing-board work had been done to establish the extent of the constraints of finance, and space in which to build the rig.

It was decided at an early stage to separate the functions of flow measurement and solids return. A continuous fluidised flowing system such as that used by Bessant[141] has two major disadvantages: firstly the head of fluid upstream must be provided by increased bed depth, and secondly, there is no direct method of measuring solids flow-rate. It was thus decided to use a straight inclined channel fed by a header tank which would receive solids from a separate return system, and exhaust into a receiver which would then deliver the material back into the return system for recirculation. This layout enables the head of fluid across the test section to be changed by altering the inclination of the channel, and the solids flow-rate to be measured by direct weighing at a convenient point in the return system. It is however undoubtedly greater in capital cost, physical size, and amount of solids required in circulation for a given flow-rate.

Much deliberation was given to deciding on the type of solids return system to employ, from which emerged the choice between a specially designed pneumatic conveying system and a mechanical system utilising proprietory main components. These two systems were considered sufficiently comparable to warrant a complete design scheming and costing exercise before making a final choice.

A particular requirement of the specification was for continuous monitoring of the solids flow-rate around the rig, for which a weigh-belt feeder was required. This was the most expensive single capital

item required for the rig and its cost and capacity determined to some degree the maximum solids flow-rate that could be employed. It was decided to place the weigh-feeder to discharge directly into the header tank for the channel and to supply it from a small hold-up hopper fitted with a flow control valve. With the feeder so positioned, any lack of uniformity in the operation of the solids return system would not upset the constant rate of delivery of solids to the channel. At this stage two provisional schemes were drafted as a basis for comparing the proposed solids return systems, using similar layouts for the channel and feeding arrangements. These are shown diagrammatically in Figures 2.1 and 2.2. It became apparent from these provisional schemes that the overall height of the rig was greater than anticipated, so that it could not be housed in the originally proposed location without considerable revision of the design and consequent reduction in versatility. However, by good fortune, an alternative location was found in which much of the solids return system could be located below floor level. This had the additional advantage of obviating the need for a raised walkway to gain working access to the channel.

The design study of the two solids return systems indicated that the mechanical system would be preferable. Having taken this decision, a more detailed design scheme of a layout using the latter system was prepared, including the arrangement of the supporting structural steelwork and other scantlings of the rig. This scheme formed the basis for the detail design of the components of the rig, and also for some further design calculations which could not be made until that stage. A number of additional schemes were later drafted to lay-in details of alternative return system components from different manufacturers. However these were completed after some major items had been designed and put out for manufacture in order to minimise the design lead time. Fortunately all the structural steelwork could be assembled locally so

FIGURE 2-1. SCHEMATIC ARRANGEMENT OF RIG USING PNEUMATIC RETURN SYSTEM

ARROWS ⟶ INDICATE SOLIDS FLOW PATH.

'C' = SOLIDS CONTROL POINTS.

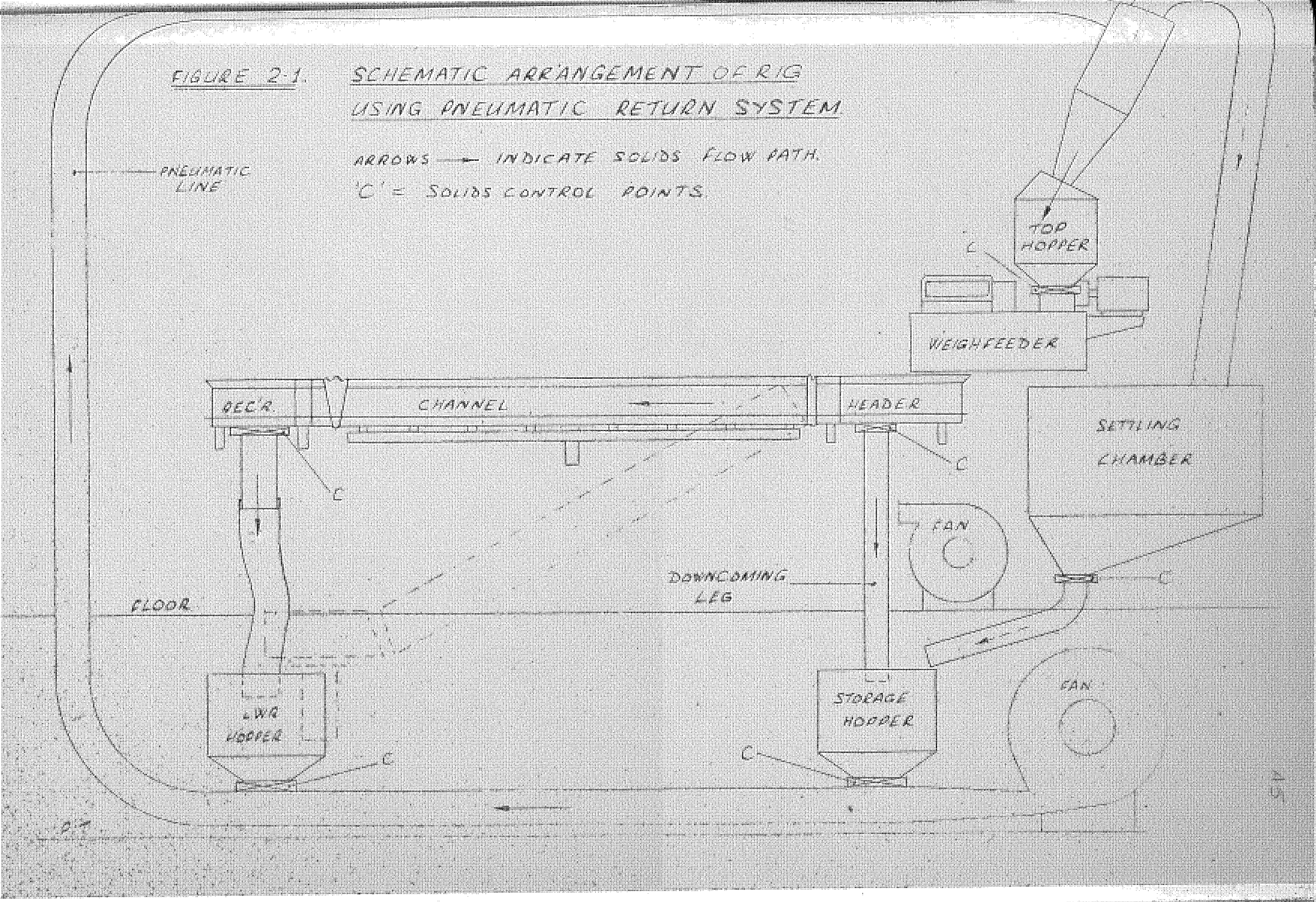

FIGURE 2-2 SCHEMATIC ARRANGEMENT OF RIG USING MECHANICAL RETURN SYSTEM

ARROWS ——→ INDICATE SOLIDS FLOW PATH.
'C' = SOLIDS CONTROL POINTS.

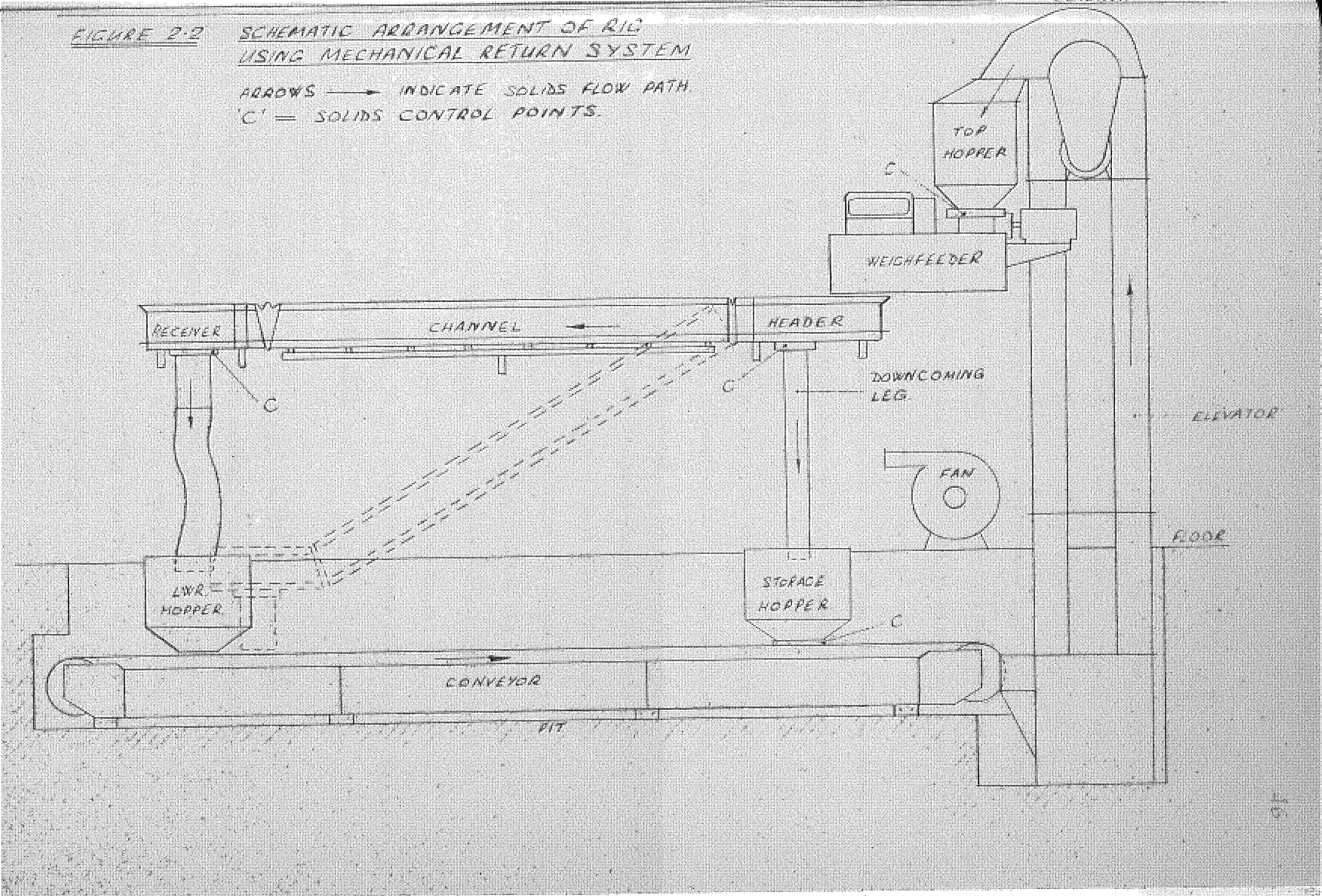

that it was unnecessary to finalise its design details until a late stage.

The finally chosen flow circuit is comprised as follows, referring again to Figure 2.2: The solids delivered by the weigh feeder are collected and fluidised in the header tank and flow into the channel. The fluidised solids flow down the inclined channel under their own head and are collected in the receiver. The outflow from the receiver passes through a control valve and via a collection hopper on to the horizontal belt conveyor. The latter delivers the solids to the boot of the vertical bucket elevator, from the top of which the flow is taken through a small hopper and discharged on to the weigh-belt feeder once more.

It was considered prudent to limit the hold-up of solids in the actual circulation loop to the minimum required for steady flow, in order to simplify control and remedial action if the flow became out of hand. The small hopper discharging into the weigh-feeder is for this purpose, and is fitted with a control valve to regulate the solid flow.

The main storage hopper is located below the downcoming leg, via which the channel is drained when shutting-down the rig or reducing the amount of solids in circulation. This hopper feeds directly on to the horizontal conveyor in order to charge the flow circuit with material. Photographs of the completed rig are shown in Figures 4.1 - 4.5 below.

3. DETAILS OF MAJOR COMPONENTS

i. Introduction

The foregoing section gave an outline of the layout and salient features of the rig. This section deals with the selection and design of the main functional and structural components. These will be treated in discrete sections, and some design calculations are appended where these are considered sufficiently important. Most of the design and all the construction was carried out using Imperial units, so that

relevant figures are mainly quoted in these units for convenience.

ii. Fluidised Channel

The main fluidised channel is three metres long by 150 mm wide, and is fluidised without interruption over its entire length. The fluidising air is supplied via a plenum chamber of the same width as the channel and 50 mm deep, which is fed from a manifold underneath the channel. The manifold is connected to the plenum chamber by eight short pipes, so proportioned that the air velocity therein is three times that in the manifold to promote even distribution. A baffle is placed above each plenum inlet pipe to prevent the issuing jet of air impinging directly on the distributor. A cross section of the channel assembly is shown in Figure 3.1. The plenum chamber walls and top flanges are of 2" x 3/16" mild steel angle, to which is welded a base of 10 SWG (.128 in) steel sheet. The manifold (of 3 in square x 10 SWG steel hollow section) is welded to the plenum chamber base via the eight 1" BSP connecting pipes, to form a beam of high flexural rigidity in the vertical plane. The central deflection of the fully loaded channel was estimated by the method of Macauley[154] to be less than 1 mm, the equivalent maximum bending stress being only 1700 $\frac{lbf}{in^2}$ (11.73 MN/m^2).

The channel walls are of 1/4 inch thick Perspex, flanged at the base for attachment to the plenum chamber, with triangular braces between the wall and flange for extra rigidity. The walls are 0.2 m high, to allow a 50 mm free board above the design maximum bed depth of 0.15 m; and are furnished with .1 m high splash guards at 45° to minimise the egress of solids from vigorously bubbling beds. The walls are made in three 1 m long sections for ease of manufacture, and to allow the central test section wall to be replaced by other features as required. The wall sections are butted together at their joints and assembled with steel fish-plates attached by countersunk screws, so as to cause no interruption to the flow. Steel spacing pieces are fitted between the walls at the

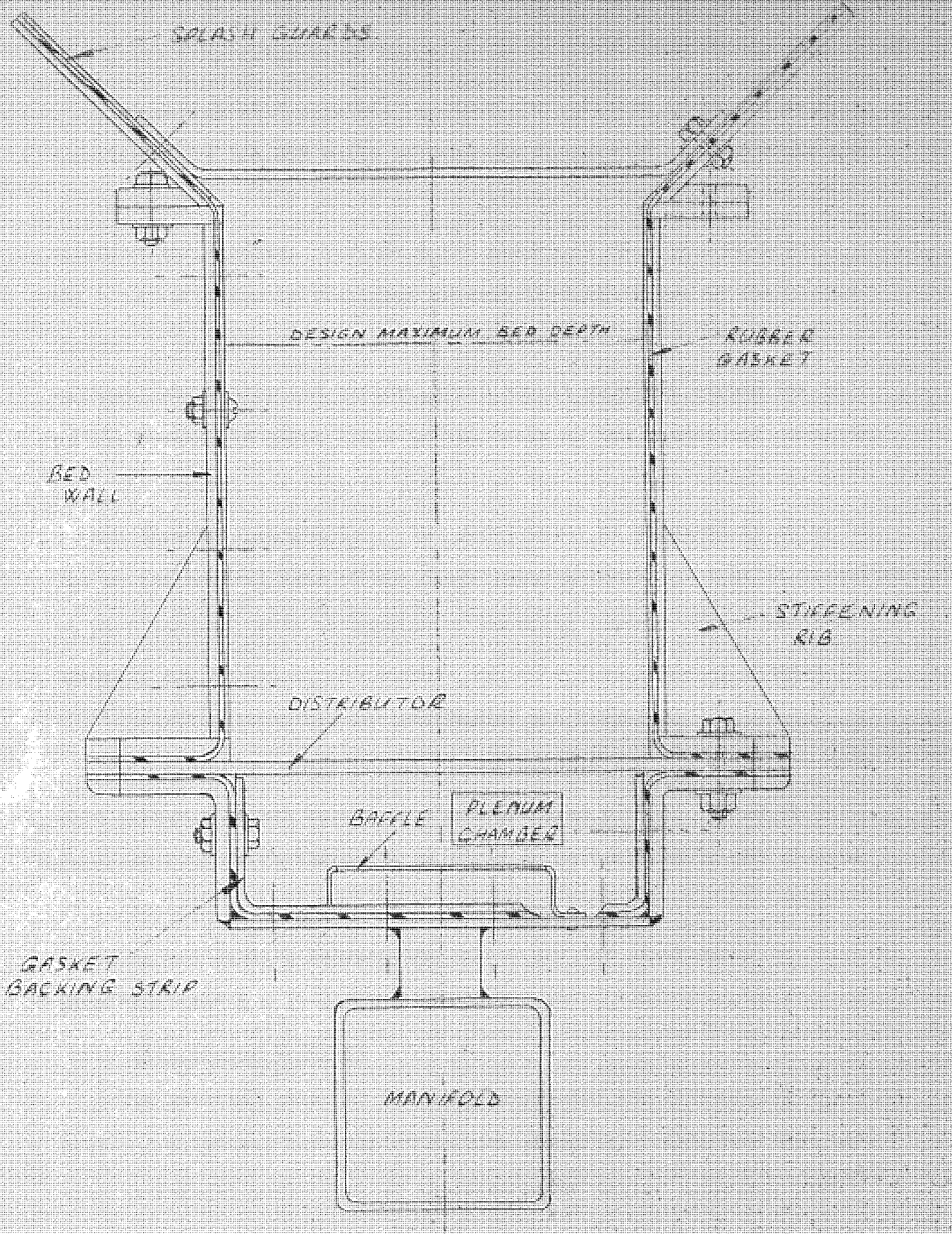

FIGURE 3.1 CROSS-SECTION OF FLUIDISED CHANNEL

(SCALE - HALF SIZE)

ends and joints to maintain parallelism.

The distributor material is sandwiched between rubber gaskets and clamped by 1/4 BSF bolts between the flanges of the bed walls and plenum chamber. All joints in the gaskets are of labyrinth form to minimise air leakage; and the lower gasket is of foamed neoprene, which is sufficiently resilient to seal irregularities in the plenum chamber flange resulting from welding distortion. The distributor is without joints over its entire length and is extended beyond the ends of the channel to joint lines in the necks of the header and receiver.

The channel assembly is pivoted at the upper and lower ends on $\frac{1}{2}$ inch diameter pin-joints. The pivot point is adjusted by shims to lie on the neutral axis of the distributor material so that it is subject to pure bending, with no tensile or buckling loads. The attachment brackets are bolted to the channel and mate with suitable pummels on the supporting structure for the header and receiver.

The flexible joints in the plenum chamber and bed walls are made with rubber sheeting backed by steel clamping plates: these being recessed flush with the walls to offer no restriction to the channel cross section. Labyrinths are again used at joints in the rubber sheeting and sealing between the rubber and the distributor is effected with "Loctite" I S 12 contact adhesive.

iii. Distributor Material

The material selected for the distributor was Porvair 'Vyon', a sintered polythene material of uniform porosity. This had been used with satisfaction for some of the viscometer tests, and other work[153] had shown it to be suitable for providing even fluidisation of large beds. The only serious drawback is the low elastic modulus of the material which gives rise to hogging of the distributor under high pressure-drop conditions if it is used unsupported over larger areas.

It is suggested by some authorities[1] that the distributor pressure drop should be equal to or greater than that across the bed, for even fluidisation. The design maximum bed pressure drop for a 150 mm deep bed of Buckland sand is approximately 180 mm water, which is rather less than that across Vyon filter grade material of 4.75 mm thickness at the design maximum fluidising velocity of 0.2 m/s[155]. Samples were obtained of this material, but these were judged to be of insufficient flexibility to permit good sealing at the channel pivot locations. The next thinner grade of material (3.2 mm thick) has a pressure-drop of only 100 mm water at .2 m/s, but is much more flexible. In view of generally satisfactory experience with low pressure drop distributors in shallow bed work at Aston, it was decided to use the latter material in the channel rig. This also meant that it was possible to use an existing fan for supplying the fluidising air, whereas the higher pressure-drop material would have necessitated ordering a larger fan to deliver the required air flow.

iv. Fluidised Header and Receiver Tanks

The header and receiver tanks for the fluidised channel follow similar construction to the latter, except that the walls are of steel instead of perspex. The header is mounted in a fixed position to receive the solid flow from the weigh-feeder and deliver it to either the channel or the vertical transport leg as required. The receiver is attached to the lower end of the channel and moves with it as the channel inclination is adjusted; but is maintained horizontal by a parallelogram linkage pivoting from the main supporting structure.

Both header and receiver have lead-in passages to the channel of length 0.2 m, their walls being equipped with slots for the location of weirs or sluice gates as required. The joints between the distributor material for the channel and tanks are also located in these lead-in sections. The solids flow into the header is controlled upstream of

the weigh feeder, and the efflux is diverted from the channel or vertical leg as required by a control valve and sluice plate respectively. The solids outflow from the receiver occurs centrally through its base, via a short pipe and control valve to the return conveyor.

The header tank is .61 x .46 m in plan, whilst the receiver is .46 m square. These dimensions were decided on as the minimum consistent with solids efflux around the complete periphery of the outlet orifices, and also, in the case of the header, the minimum for accepting the solids feed direct from the weigh feeder outlet.

The fluidising air plenum chamber for the two tanks is common with that for the channel, though both are fed by their own air ducts so that they could be fluidised separately if necessary by subdividing the plenum chamber. Both air supplies are via manifolds feeding a number of separate, baffled, intakes in a similar manner to the channel.

vi. Solids Return System

The original conception of the rig design called for a pneumatic transport line to return the flowing solids to the supply point after leaving the channel. The basic layout is shown in Figure 2.1. It comprises a pipeline carrying high velocity air to entrain and transport the solids from the delivery points at the end of the test sections, and a recovery system to return the material to the supply hopper. The recovery system consists of a cyclone separator followed by a large settling chamber to retain a further proportion of the material escaping from the cyclone.

This system was chosen originally as the cheapest likely means of providing solids return, the main alternative being a mechanical handling system. A fluidised system was also considered, but rejected on the grounds of unpredictability of behaviour and lack of available design information. A design study for the pneumatic system was completed

(and is summarised at the end of this section) in order to prepare a cost estimation. However the design study revealed a number of disadvantages in using such a system. Perhaps the principal one is again the uncertainty of achieving the design performance in the absence of pilot scale testing. Although the design of such systems is fairly well established, the available design methods involve making a number of arbitrary assumptions on important parameters, and using correlations of rather limited accuracy. Also, the author had no practical experience of the design of pneumatic handling systems.

Pneumatic transport systems also have some more general disadvantages from the viewpoint of this work[8,156]. When transporting wide size-range material they are likely to handle the small fractions preferentially, and so alter the effective mean particle size of the material in the fluidised section. Also, if designed for high solids loading, the performance with materials denser or larger than the design material will be below par. Particle attrition, abrasion of the carrying lines and electrostatic charging are also likely. Further, unless a filter is used on the carrying line exhaust, considerable loss of fine material and detritus to the atmosphere will occur: clearly this is undesirable from functional as well as environmental considerations. A control difficulty also exists with a pneumatic return system, in that it is necessary to maintain sufficient head of solids in the feed hopper to overcome the carrying line air pressure. This would necessitate keeping a constant manual watch on the hopper level and adjusting the line feed valve at intervals as necessary. The latter could be obviated by providing a positive displacement rotary feed valve at each line inlet, but these are expensive and would certainly render a pneumatic system economically unattractive.

For these reasons it was decided that a mechanical return system would be preferable, unless the pneumatic system showed a very clear cost advantage.

Several mechanical systems were investigated, each comprising two main functional components: a horizontal conveyor and a vertical elevator. Both were specified to handle the maximum solids flow rate of 35 ton/hr (equivalent to 705 ft^3/hr).

The elevator was required to lift the solids through a vertical distance of some 5m. The choice of equipment was restricted to the type comprising a series of buckets mounted on a belt or chain running on wheels in the head and boot. Quotations and technical details were obtained from a number of suppliers, and the equipment was subsequently ordered on Simon-Barron Ltd., Gloucester.

Their equipment was chosen mainly because it had provision for feed and delivery on the same side of the machine, which considerably simplified the design of the rest of the rig. It was also lower in overall height than most of the others, although it was still necessary to sink a small pit in the floor of the laboratory to accommodate the boot. The accessability for maintenance, adjustments and emptying the boot of solids is also good because of the largely bolted-up modular construction. The price was slightly cheaper than most of the competitors, and only one fifth of the most expensive quotation.

The equipment comprises a 10 inch wide rubberised fabric belt, with 8 inch wide 10 SWG pressed steel buckets at 10 inch pitch, running over 18 diameter pulleys. The belt is driven at 240 ft/min via a chain to the top pulley from a 3 HP geared induction motor mounted between the vertical legs. The belt is tensioned and centralised by draw-bolts on the bottom pulley, and the complete unit is self-supporting.

For the horizontal conveyor, both screw and belt conveyors were considered. However, as the former were somewhat more expensive and are also prone to blocking and abrasive wear by the solids, a belt conveyor was deemed preferable. The unit eventually selected (manufactured by Numec Ltd. Chesterfield) utilises a belt with flexible corrugated rubber side-walls. This means that a greater solids loading for a given belt width is possible than with conventional concave or flat belting.

This equipment is again of modular construction and comprises a 16 inch wide rubber belt running on 12 inch diameter drums at 15 ft centres. The belt is driven at 80 ft min by a 1 HP motor contained within the delivery-end drum. The idle feed-end drum is of crowned spiral self-cleaning design and is mounted on draw-bolts for belt tensioning. The cost of the unit was competitive with conventional flat belt conveyors of similar capacity, but it is of interest that a fluidised conveyor with self-contained fan would probably cost little more than half as much, if manufactured using similar production methods. It would also be considerably more compact.

The costing comparison between this mechanical system, with its attendant hoppers and steel work, and a simple pneumatic system without rotary feed valves indicated that the mechanical system was about 15% more expensive. However this extra cost was considered tolerable in view of the guaranteed performance of the mechanical system, and also the likely protracted manufacturing time for the pneumatic system, most items of which would have to be produced as 'one-offs'.

The design calculations for the pneumatic system are given below. The figures presented are those for Bauxilite, which is the critical material for the pneumatic line because of its higher density. Repeat calculations (not shown here) for Buckland sand confirmed the suitability

of the system for the lighter material.

Air Requirement

Fluidised Channel Cross Section = 0.15 m square

$\therefore$ Area of flow = $.0225\ m^2$

Design maximum flow rate = $0.3\ \frac{m}{s}$

Fluidised density of bed (maximum, determined empirically in small bed) = $1.5 \times 10^3\ \frac{kg}{m^3}$

$\therefore$ mass flow rate of solids = $1.5 \times 10^3 \times .3 \times .0225 = 10.12\ \frac{kg}{s}$

Assume a maximum solids loading of $\frac{15\ kg\ solids}{kg\ air}$ (156)

$\therefore$ Air requirement = $\frac{10}{15}\ kg\ \frac{air}{s} \simeq .556\ \frac{m^3}{s}$

For satisfactory operation the air velocity in the line (U_l) must be above the saltation velocity (U_{cs}) for horizontal pipes, and the choking velocity (U_{ch}) for vertical upflow.(7) For wide size-range material $U_{ch} \leqslant \frac{U_{cs}}{3}$(7), so that U_{cs} is the critical velocity in systems containing both modes.

Calculation of Saltation Velocity, U_{cs}

Using procedure due to Zenz and Othmer[7,8]

$$\frac{d_p}{B_7} = d_p \Big/ \left[\frac{3\,\mu_g^2}{4_g\,\rho_g\,(\rho_s - \rho_g)}\right]^{1/3}$$

ρ_s for bauxilite = $3.8 \times 10^3\ \frac{kg}{m^3}$, $\mu_g = 1.8 \times 10^{-5}\ \frac{Ns}{m^2}$

$\therefore$ $B_7 = 1.796 \times 10^{-5}$ m

Assume particle size range $90\ \mu m < d_p < 170\ \mu m$

$$\left(\frac{d_p}{B_7}\right)_{min} = 5.0\ , \quad \left(\frac{d_p}{B_7}\right)_{max} = 9.5$$

$\therefore$ From Ref 8, $\frac{U_{cs}}{B_6} = 3.3$

$$B_6 = \left[\frac{4g\mu\ (\rho_s - \rho_g)}{3\rho_g^2}\right]^{1/3} = 87 \text{ cgs}$$

$\therefore U_{cs} = 3.3 \times 87 = 2.87 \frac{m}{s}$

This is for a 63.5 mm pipe.

Using an initial assumption [8,156] of 30 ft/s ($9.15 \frac{m}{s}$) for U_t :

Necessary pipe cross section = $\frac{.556 \text{ m}^3.\text{s}}{9.15 \text{ m.s}} = .0608 \text{ m}^2$

$\therefore$ Pipe diameter = $\sqrt{\frac{4 \times .0608}{\pi}} = .278 \text{ m}$

[Or, using square pipes $\doteq$ .25 m square sides.]

Now correcting U_{cs} for .28 dia pipe

$$U_{cs} = U_{cs_{63.5}} \times \left(\frac{d_t}{.0635}\right)^{0.4} = 2.87 \times \left(\frac{.278}{.0635}\right)^{0.4}$$

$$= 5.18 \frac{m}{s}$$

$\therefore$ Chosen velocity of $9.15 \frac{m}{s}$ is almost twice the saltation velocity. This should provide a reasonable safety margin without incurring excessive pressure drop.

Calculations of Pressure Drop in Pneumatic Line

Vertical Section: Length = 4 m , dia = .28 m

Horizontal Sections: Total Length 6.25 m, dia .28 m

Mean $d_p = 120\ \mu_m$, $\rho_s = 3.8 \times 10^3 \frac{kg}{m^3}$

From Ref. 9, Terminal Velocity of a particle in a pipe, $U_t = \left[\frac{4g\ d_p\ (\rho_s - \rho_g)}{3\ \rho_g\ C_d}\right]^{\frac{1}{2}}$

$$C_d\ Re_p^{\ 2} = C_d \left[\frac{d_p\ \rho_g\ U_t}{u_g}\right]^2 = \frac{4g\ d_p^{\ 3}\ \rho_g\ (\rho_s - \rho_g)}{3\ \mu_g^{\ 2}}$$

$$= 300$$

Sphericity of Particles: Particles are of angular shape - assume tetrahedral for calculation purposes.

For a regular tetrahedron of unit side:

$$\text{Volume} = \frac{1}{3} \times \frac{\sqrt{3}}{4} \times \sqrt{\frac{2}{3}} = \frac{\sqrt{2}}{12}$$

Surface area $= \sqrt{3}$

Radius of sphere of volume $\frac{\sqrt{2}}{12} = 0.304$

$\therefore$ Surface area $= 4\pi \times (.304)^2 = 1.16$

$\therefore$ Sphericity of particles $= \frac{1.16}{\sqrt{3}} = \underline{\underline{0.67}}$

From Refs 8,9 for $Cd\ Re_p^2 = 300$, $\phi_s = .67$

$$Re_p = 4 = \frac{d_p \rho_g U_t}{\mu_g}$$

$\therefore$ Terminal velocity $= \underline{\underline{.52 \frac{m}{s}}}$

a) Horizontal Sections, length = 6.25 m (total) (8)

Total Pressure drop $\Delta P = \Delta P_f + U_s (\rho_g U_l) \frac{G_s}{G}$

(1st term = frictional pressure drop, 2nd term = kinetic energy term - due to acceleration of solids from rest at entry point).

$U_s = U_l - U_t = 9.15 - .52 = 8.63 \frac{m}{s}$

$\therefore$ K.E term $= 8.63 \times 1.18 \times 9.15 \times 15 = \underline{\underline{1.398 \frac{kN}{m^2}}}$

Friction Term:

From ROSE AND BARNACLE[157]

$$\Delta P_f = \Delta P_{f_s} + \Delta P_{f_g}$$

Where ΔP_{f_g} = Friction due to air alone $= \frac{2 f_g \rho_g U_l^2 \ell}{d_t}$ (Fannings Eqn)

$$Re_t = \frac{\rho_g U_l d_t}{\mu_g} = \frac{1.18 \times 10^{-3} \times 915 \times 28}{1.846 \times 10^{-4}} = 1.64 \times 10^5$$

$\therefore$ From Ref 157 $f_g = .0008 + .0552 \left(\frac{\rho_g U_t d_t}{\mu_g} \right)^{-.237}$ for $10^5 < R_e < 10^8$

$\therefore$ $f_g = .0008 + .0552 (1.64 \times 10^5)^{-.237} = \underline{4.00 \times 10^{-3}}$

$\therefore$ from Fanning's Eqn., $\Delta P_{fg} = \dfrac{2 \times 4 \times 10^{-3} \times 1.18 \times (9.15)^2 \times 6.25}{.28}$

$= .018 \ \frac{kN}{m^2}$

ΔP_{f_s} = Friction due to solids:

$\Delta P_{f_s} = \frac{\pi}{8} \cdot \frac{f_p}{f_g} \cdot \left(\frac{\rho_s}{\rho_g}\right)^{\frac{1}{2}} \cdot \frac{G_s}{G} \cdot \Delta P_{f_g}$

where f_p is here assumed[157] to be 0.65×10^{-4}

$\therefore \ \Delta P_{f_s} = \frac{\pi}{8} \times \frac{.65 \times 10^{-4}}{4 \times 10^{-3}} \times \left(\frac{3.3 \times 10^3}{1.18}\right)^{\frac{1}{2}} \times 15 \times .018 = .091 \ \frac{kN}{m^2}$

$\therefore$ Total $\Delta P_f = \underline{.109 \ \frac{kN}{m^2}}$

b) Vertical Section, length 4 m

Static head $= \bar{\rho} \, g \, (h_2 - h_1)$, $\bar{\rho} = \rho_s (1-\epsilon) + \rho_g \epsilon = \frac{G_s}{u_s} + \frac{G}{u_l}$

$= 19.9 \times 9.81 \times 4 = \underline{.781 \ \frac{kN}{m^2}}$

$\Delta P_f = .109 \times \frac{4}{6.25} = \underline{.069 \ \frac{kN}{m^2}}$

c) Bends: $2\frac{1}{2}$ bends, $\frac{\text{radius}}{d_t} = 4.$

Pressure drop due to single bend, $\Delta P_b = 2 f_b \bar{\rho} u_l^2$ (156)

where $f_b = .188$ for $\frac{r}{d_t} = 4.$

$\bar{\rho} = \rho_s (1-\epsilon) + \rho_g \epsilon = \frac{G_s}{U_s} + \frac{G}{U_l} = \rho_g \epsilon \left\{ \frac{G_s}{G} \frac{u_l}{U_s} + 1 \right\}$

Assuming $\epsilon \rightarrow 1$ - reasonable for lean phase transport

$\bar{\rho} = 1.18 \left(\frac{15 \times 9.15}{8.63} + 1 \right) = 19.9 \ \frac{kg}{m^3}$

$\therefore$ Total $\Delta P_b = 2.5 \times 2 \times .188 \times 19.9 \times (9.15)^2$

$= \underline{1.57 \ \frac{kN}{m^2}}$

$\therefore$ Total Pressure Drop (Excluding Cyclone) = a + b + c

$= 1.398 + .109 + .781 + .069 + 1.57$

$= 3.93 \ \frac{kN}{m^2} \equiv .400 \text{ m } H_2O$

Design of Cyclone - Taken from STAIRMAND[158]

Using high throughput type:

Gas flowrate = $1500\ D^2\ \frac{m^3}{hr}$ (D in ft)

$\therefore$ Outside diameter D = $\sqrt{\frac{.556 \times 3600}{1500}}$ = 1.15 ft

Inlet Area = $0.75 \times .375\ D^2 = \frac{9\ D^2}{32}$ = .323 ft^2

$\therefore$ Velocity at inlet = $\frac{.556\ m^3}{.323\ ft^2\ s}$ = 60.8 $\frac{ft}{sec}$

Hence[158] pressure drop across cyclone $\simeq$ 4 in H_2O

= .102 m H_2O

$\therefore$ Total Pressure drop in pneumatic circuit including cyclone

= .502 in H_2O at .556 $\frac{m^3}{s}$ air flowrate

(Pressure drop in settling chamber is neglected as small).

Design of Settling Chamber - from PERRY[159]

Efficiency of Chamber $\eta = \frac{U_t\ \ell_s}{h_s\ U_{s_f}} = \frac{U_t\ b_s\ \ell_s}{q}$

Assume an initial value of 1.50 $\frac{m}{s}$ for U_{s_f}

Then cross sectional area of chamber = $\frac{.556}{1.50}$ = .371 m^2

Assume $h_s = 2\ b_s$ $\therefore$ b_s = .43 m

Working on unit efficiency $\frac{q}{U_t} = \ell_s\ b_s$

U_t = .52 $\frac{m}{s}$ $\therefore$ ℓ_s = 2.13 m

and make b_s = .50 m

$\therefore$ Make actual dimensions 2m x 1m x .5m to use standard size sheet steel.

Smallest particle capable of separation, $d_{P_{min}}$:

Assuming unit efficiency, $d_{P_{min}} = \sqrt{\frac{18\ \mu_g\ q}{b_s\ \ell_s(\rho_s - \rho_g)}}$

$= \sqrt{\frac{1.846 \times 18 \times .556 \times 10^{-5}}{.50 \times 2.0 \times 3.8 \times 10^3 \times 9.81}}$ = 7×10^{-5} m = 70 μ m

This should be satisfactory for 'Bauxilite' and Buckland sand, and most other likely materials.

vi) Support and Adjustment Mechanism for Fluidised Channel

The fluidised channel is pivoted at its upper end on the main supporting structure of the rig, and from its lower end is pivoted the fluidised receiver. Provision is made for variation of the channel inclination from -1 to 30^{o} in the direction of flow. The variable inclination is provided by mounting the lower end of the channel on a linkage mechanism supported by a telescopic hydraulic ram.

Hydraulic actuation was chosen because of the ease of making accurate fine adjustments compared with a mechanical system. The ram is pressurised by a double acting hand pump connected via a flexible high-pressure hose. The ram and pump were supplied to specification by Bowes Engineering Ltd., Nottingham. The ram is connected to the channel through a linkage mechanism which was necessary because the closed length of a direct acting ram of the required stroke was too great to be accommodated beneath the channel. The linkage is of 3 inch square x 10 SWG steel hollow-section pivoting on 1 inch diameter mild steel pins. It was designed on considerations of rigidity rather than strength, the maximum nominal stress being only 1.5 tonf/in^{2}. The compressive load on the ram in the worst loading condition is approximately 900 lbf with the channel fully loaded.

The lower end of the channel is mechanically clamped laterally to two 3/8 inch thick mild steel plates mounted on a tubular steel super-structure surrounding the lower receiver. It is also supported vertically on the steel plates, via adjustable eccentric mounting discs bolted in suitably drilled holes. This rather elaborate support system was provided to obviate any vibration or movement of the lower end of the channel and also to relieve the hydraulic ram of continued load once adjustment of the channel inclination is completed.

vii) Fluidising Air Supply

The fluidising air requirement was for a maximum fluidising velocity of 5 U_{m_f} with the design material ($\simeq$ 0.2 m/s) at a pressure sufficient to fluidise the maximum design bed depth ($\simeq$ 0.3 m H_2O). Quotations were obtained for a suitable centrifugal fan, the most competitive being returned by Midland Fan Co Ltd, Birmingham. However for the initial work an existing Alldays - Peacock fan was used, although this cannot quite achieve maximum air flow at full bed depth. The fan inlet is fitted with a butterfly valve to reduce start-up load.

The air flow is metered by a bank of four pre-calibrated type 65 Rotameters, each fitted with its own downstream gate type control valve. Rotameters were preferred to orifice flow meters because of their greater sensitivity at low flow rates, and because such large orifice meters could not be calibrated locally. The inlet manifold to the rotameters is fitted with a quick action by-pass valve exhausting to atmosphere: this was included as a safety device by which the air supply can be interrupted in an emergency.

viii) Solids Flowrate Measurement

A number of indirect methods of solids mass flow measurement were considered, including sampling and feeding through calibrated orifices or flow control devices. However, since the solids flowrate is one of the most important experimental parameters to be measured, it was considered preferable that this should be done by an accurate, direct method in spite of the higher cost.

Two manufacturers were found who could offer weighfeeders of a suitable size for the work: W. and T. Avery Ltd., and Messrs Wallace and Tiernan Ltd. Quotations were obtained from both suppliers, the cheapest being returned by the latter. Their equipment also offered a number of advantages, being more accurate at part load and having an output signal suitable for continuous recording if required.

The equipment eventually ordered was the "Wallace and Tiernan Superweigh 18 inch Pneumatic Gravimetric Meter". This comprises a rubberised flat belt driven by a 1/3 HP synchronous reluctance motor through a worm gear reducer, on to which the material is fed from the top hold-up hopper. The centre section of the top run of the belt passes over a counter-balanced weighing platform which is supported on a pneumatically operated weighing mechanism. The signal from the latter is a pneumatic pressure between 3 and 15 lbf/in^2, which is proportional to the mass flowrate of solids across the belt. The claimed accuracy of the feeder is $\pm$ 1% over a 10:1 range, and low flowrates may be additionally catered for by adjustment of the pneumatic balancing mechanism, or reducing the belt speed using alternative change gears in the reduction gear box. The pneumatic balancing mechanism is actuated by an air supply of 0.1 ft^3/min at 20 lbf/in^2, which is provided in this case by a small reciprocating compressor/reservoir unit.

The complete feeder is mounted on rubber and fed via a flexible rubber inlet duct to eliminate any transmitted vibration. It discharges directly into the header tank for the fluidised channel.

ix) Hoppers

Three hoppers are included in the flow circuit. These are of rectangular cross section constructed in 16 SWG welded mild steel with a base slope of 40°, this being about 5° greater than the angle of repose of the solids to allow for complete emptying.

The top hopper has a capacity of ten times the maximum solids flowrate per second, and its function is merely to maintain sufficient solids hold-up to provide a uniform discharge to the fluidised channel.

The two lower hoppers are 20 inches square by 15 inches deep and serve both to provide the main solids storage for the rig and to guide the material on to the horizontal conveyor. They are employed alternately for these purposes, according to which mode of fluidised flow is being

studied. The hopper below the vertical flow leg is movable laterally to enable different exit pipes to be fitted to the leg as required.

x) Supporting Structure

The supporting framework for the rig was assembled from rectangular hollow-section E.R.W. mild steel tubing. The main members are of 3 inch square x 10 SWG material with some cross members and auxiliary structures of 2 inch x 10 SWG and 1 inch x 12 SWG; all fabrication being by electric arc welding. The complete structure was designed from considerations of rigidity, to ensure minimum transmission of vibrations to the fluidised channel and weigh-feeder. The stresses are thus very low, and are anyway mostly direct compression, so that no stress analysis of the framework was needed.

The main frame (supporting the elevator, top hopper, weighfeeder, and header tank) comprises six columns mounted on cross-members with steel feet attached. Each cross-member is bolted to the floor with eight 3/8 inch Rawlbolts. These main members are cross braced at suitable points to ensure lateral stiffness. The electrical supply to the rig and the main control panel are mounted on the side of the main frame, and the fan and air compressor are mounted on rails on the lower cross-members.

The air rotameters and manifolding are fixed to a floor mounted subframe, which is again cross-braced to the main structure. The curved steady-plates for the lower end of the fluidised channel are attached to a triangular framework bolted to the floor around the lower receiver.

The structure was designed on an intuitive basis, with the thought of adding further bracing or triangulation if required during construction, but this was in fact unnecessary since adequate rigidity was achieved with the main members alone. The only difficulty experienced during erection was some distortion of the main columns due to cooling contraction after welding. The latter is inevitable with any welded structure and did not cause any serious problem.

xi) Controls

The main operating controls for the rig are grouped together around the top end of the fluidised channel. All the electrical switches and starters are mounted on a facia attached to the main framework, together with a 240 volt distributor board for plugging-in auxiliary equipment. The fluidising air rotameters and control valves, the air by-pass valve and the fan inlet damper are positioned beside the electrical controls. A general view of the layout of these items in given in figure 4.4 below.

The flow of solids around the rig is regulated by a number of "Mucon" valves (Manufacturers: Mucon Engineering Company Ltd). These valves provide a variable circular orifice through which the material flows, this being in the form of a nylon membrane working in the manner of the iris of a camera. They have proved eminently suitable for the work, although the action is not without some backlash. The orifice size (and thus the flowrate) through the valve does not vary linearly with the control lever position; but this is of little detriment once the operator becomes familiar with the settings.

The flowrate of solids is controlled during normal operation by an eight inch Mucon valve below the top hopper, to which operating access is gained by a ladder adjacent to the rotameter panel. Notches were cut in the periphery of the valve in order to provide a series of fine adjustments between the fully open and closed positions.It would have been convenient to provide a remote control for this valve at floor level, but this was omitted for reasons of cost.

A further eight inch Mucon valve is centrally located in the lower receiver in order to provide a restricted outlet to the fluidised channel if required. The flow from the fluidised header-tank into the vertical leg is regulated by a six inch Mucon valve. This is kept closed during operation of the sloping channel, but is used to exhaust the system into

the main storage hopper when required. A four inch Mucon valve is fitted to the base of the storage hopper. This discharges directly on to the belt conveyor, and is used to fill the flow-circuit with solids at the start of a test and to increase the amount of material in circulation as required. This latter valve could also be remote controlled with benefit, even though it is used relatively infrequently.

The inclination of the fluidised channel is controlled by means of the hand pump and bleed valve for the hydraulic ram, as mentioned above.

xii) Instrumentation

The three important basic parameters to be measured during work with the inclined channel are solids flow rate, bed depth and channel inclination.

The weighfeeder for measuring solids mass flow has already been described in Section 3 (viii) above. The pneumatic output signal from the feeder is registered on a simple 'U' tube mercury manometer. This is both sensitive and accurate over the required range of pressures. The calibration graph for the feeder, using the manufacturers calibration data, is given in figure 3.2. This calibration was checked at a number of flow-rates near the mid-range of the instrument by timed weighing, although the accuracy of the latter method is undoubtedly less than the manufacturers claimed accuracy of $\pm$ 1%.

The inclination of the fluidised channel is measured by a device similar to a builders water-level. This is shown diagrammatically in Figure 3.3. It comprises two sight-glasses connected by a flexible tube filled with water. One sight glass is positioned adjacent to the fixed header tank for the fluidised channel and the other is attached to the lower receiver. A graduated scale with its zero at the fluidising air distributor is fixed alongside the upper sight-glass, and the lower one has a single datum mark at the distributor. The connecting tube incorporates a variable displacement chamber (made from a large hypodermic

FIG. 3·2.

CALIBRATION CURVE FOR WALLACE & TIERNAN WEIGFEEDER.

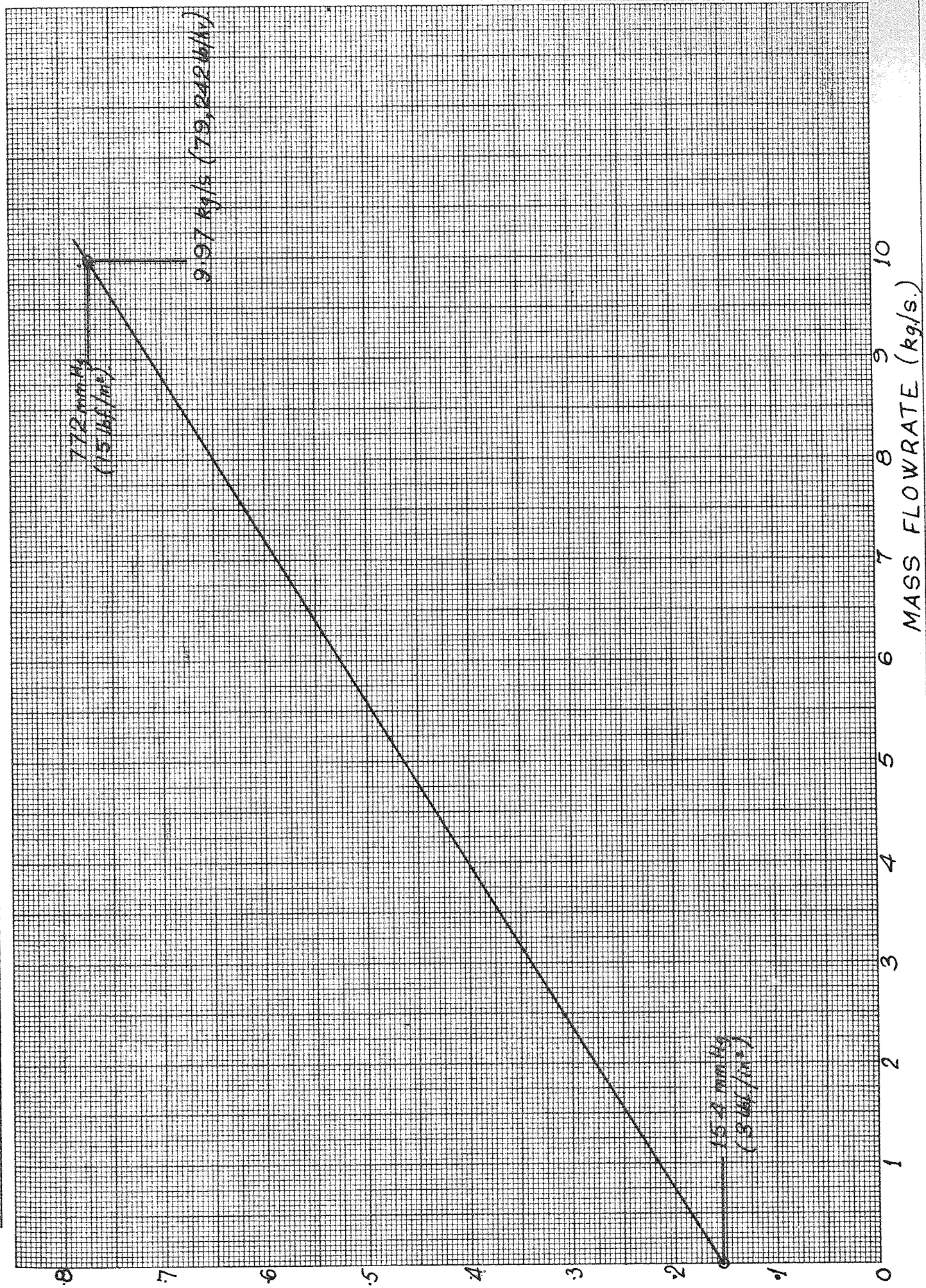

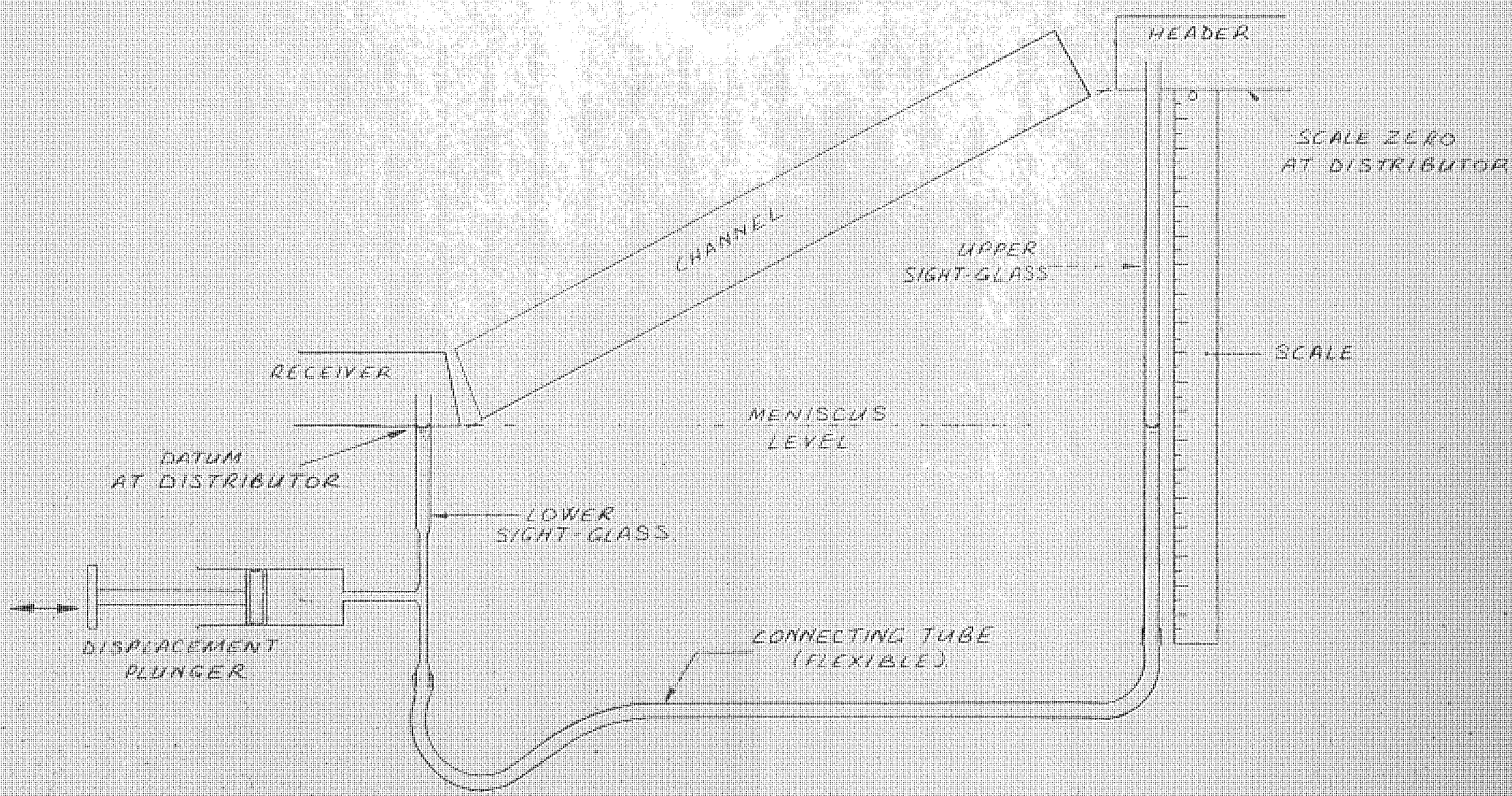

FIG 3.3 DIAGRAM OF WATER LEVEL (NOT TO SCALE)

syringe), by which means the water meniscus in the tube is aligned with the datum mark at the lower sight-glass. The position of the water meniscus in the upper sight-glass with respect to the zero on the graduated scale then gives the depression of the lower end of the channel with respect to the upper. By this method the channel slope is measured to an accuracy better than $\pm$ 1 mm in 3 m.

The position of the free surface of the bed is difficult to discern in the rapidly flowing channel, so that the bed depth cannot easily be measured directly. This parameter is therefore estimated by measuring the pressure drop across the flowing bed, and, and comparing this with an empirical correlation (Figure 3.4) of pressure drop and bed depth obtained from separate tests on a small, non-flowing bed.

In order to calculate the flow velocity along the channel from the above parameters, it is necessary to know the density of the bed under the conditions of the test. This was again found from an empirical correlation obtained from small bed tests, figure 3.5. An inherent assumption in the use of both figures 3.4 and 3.5 is that the density of the bed is the same in the small bed as in the channel. This was known to be approximately true, but it was thought that changes in bed density may occur at high shear rates, due to bubble rearrangement. However, recent work with a traversing pressure probe[150] has confirmed that the mean bed density, under given fluidising conditions, is little altered at high rates of shear.

The pressure drop across the bed is measured in the flowing channel by pressure probes of the type used in the viscometer,(see Chapter 3, fig 2.5) sited at entry and exit to the test section. The upstream pressure is indicated on an Airflow Developments inclined manometer, and the differential pressure between the two probes is indicated on a similar instrument. The latter shows whether or not the flow across the test

FIG. 3·4.

PRESSURE DROP vs. BED DEPTH CORRELATION, FROM SMALL-BED TESTS.

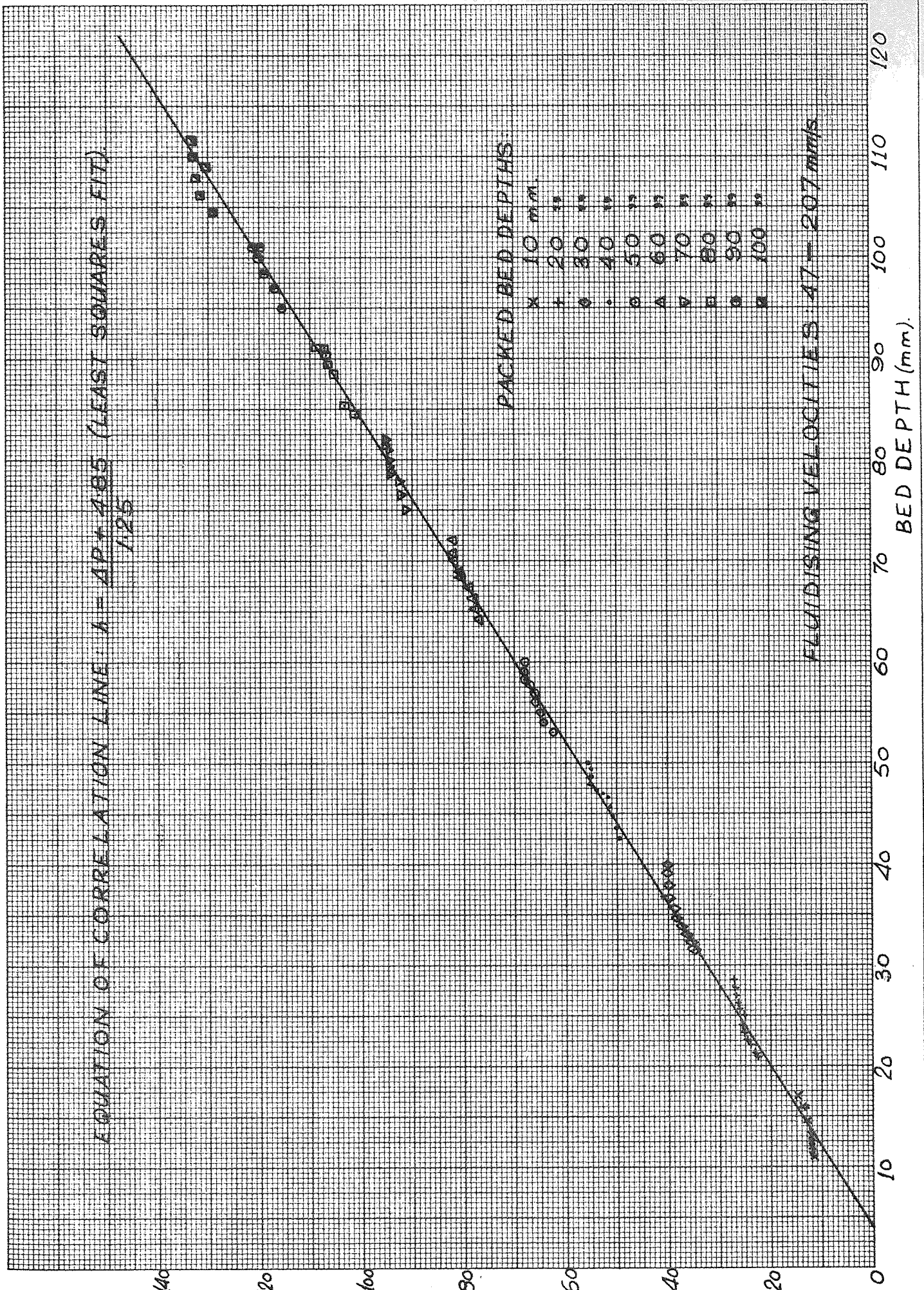

PRESSURE-DROP vs. BED DENSITY FOR BUCKLAND 50FG SAND (SMALL BED TEST RESULTS).

FIG 3.5

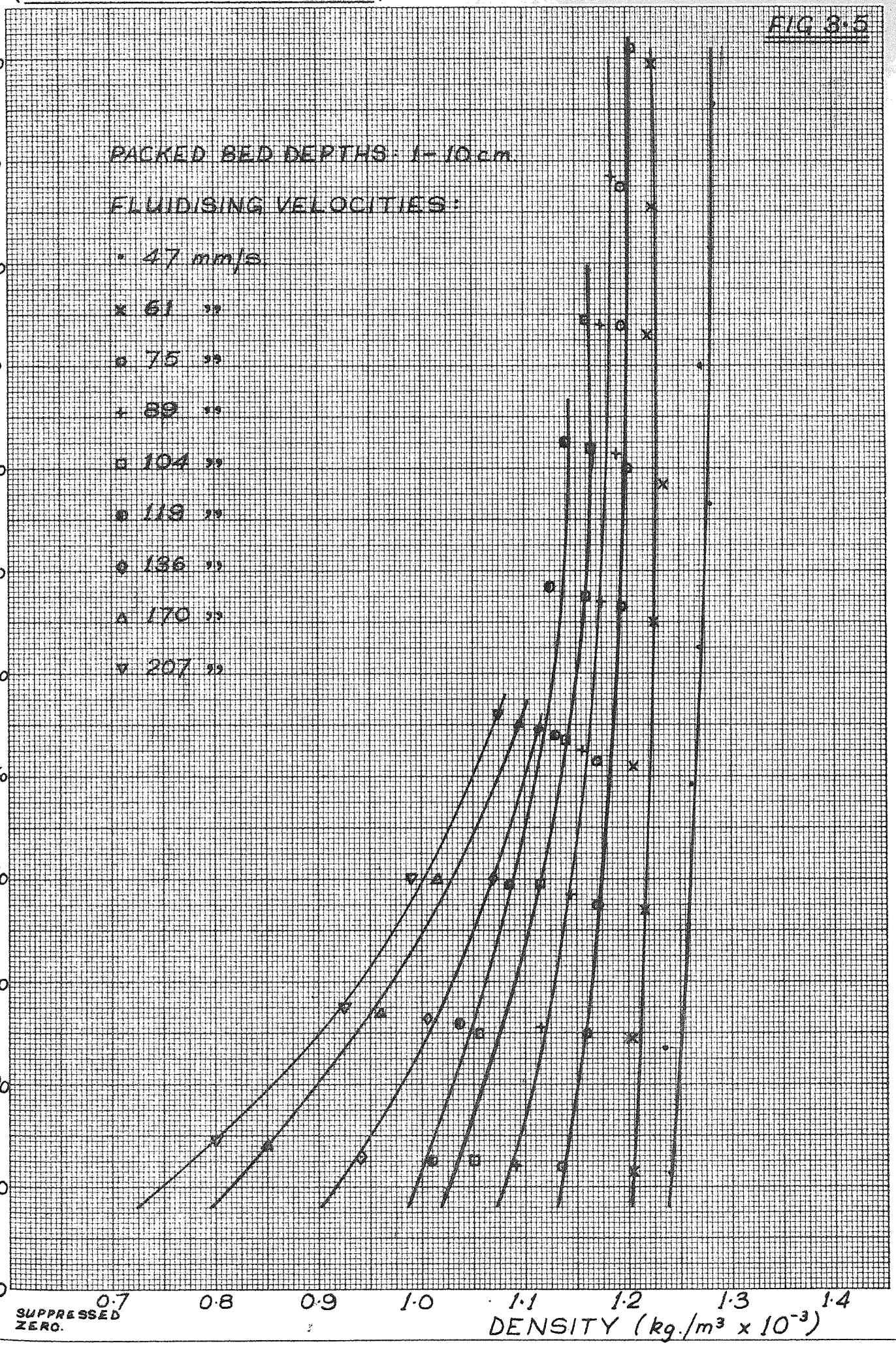

section is uniform. All the manometers are mounted on a free-standing instrument panel, connected to the rig by flexible tubing, which can be moved to the most convenient operating point as necessary.

The flowrate of the fluidising air is measured on a bank of rotameters as noted above. The moisture content of the air is recorded with the Shaw Moisture Meter as used for the viscometer work. The sensing element for the meter is mounted in the plenum-chamber of the test section.

The storage hoppers and the receiver at the lower end of the fluidised channel are fitted with devices which give warning if the level of solids therein approaches the point of overflowing. The devices give an audible warning of impending overflow at any of the three stations, together with a visual display on the control panel of which station is at fault. This precaution was taken because at the design stage there could be no conception of how difficult the rig would be to control during operation. The warning system comprises photo-electric sensors positioned at the critical solids levels, which energise a suitable relay circuit and thus actuate the output signals. Auxiliary lamps are provided for the photo-cells in the hoppers because the ambient illumination is inadequate. The circuit diagram for the warning devices is shown in figure 3.6.

The only warning which has tripped to date is that in the top hopper. This hopper sometimes becomes over-filled when the mass flowrate is reduced if the solids hold-up in the flow circuit is not also appropriately reduced.

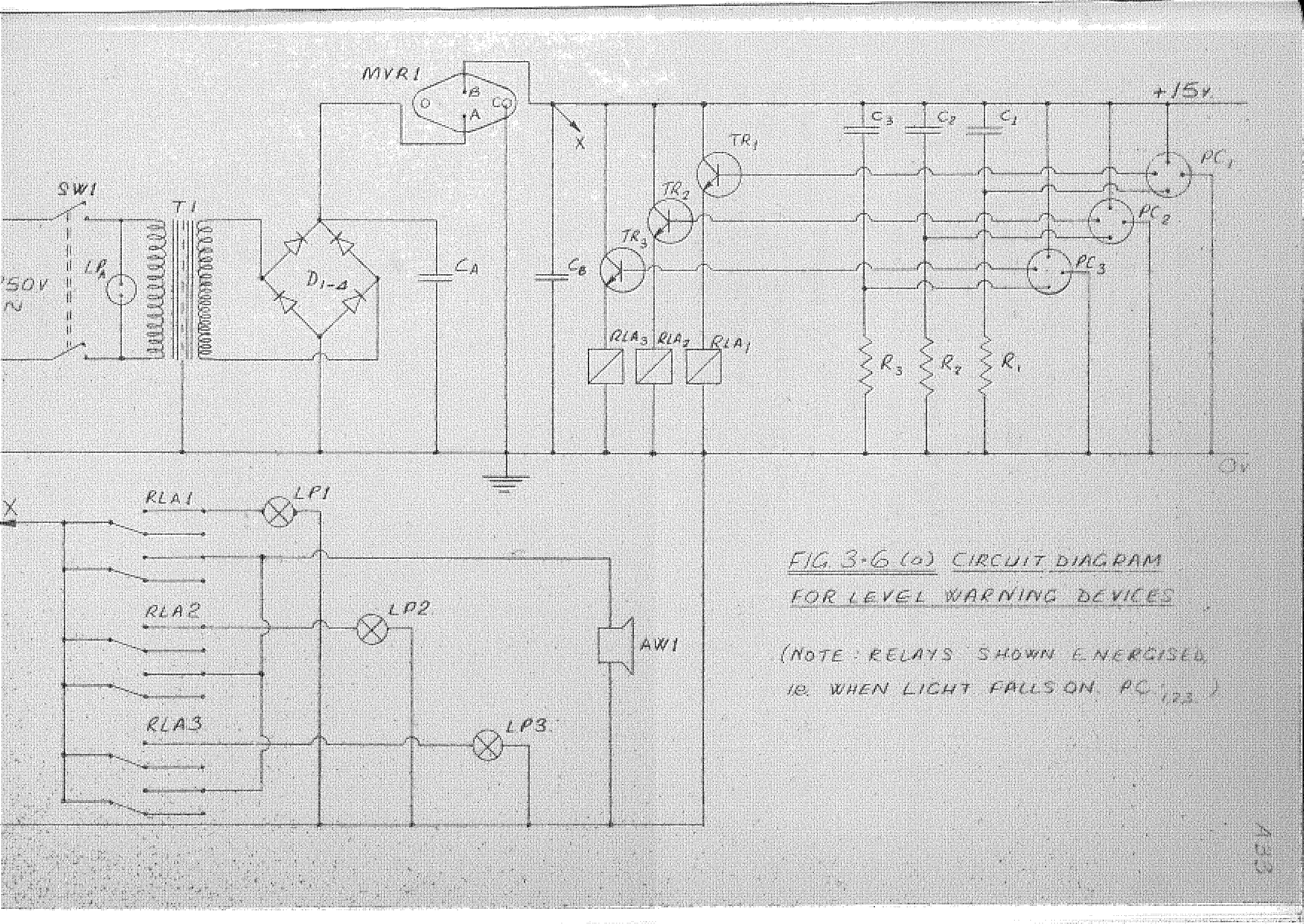

FIG. 3-6 (a) CIRCUIT DIAGRAM FOR LEVEL WARNING DEVICES

(NOTE: RELAYS SHOWN ENERGISED IE. WHEN LIGHT FALLS ON PC 1,2,3)

Figure 3.6 (b) Key to Circuit Diagram for Level Warning Device

A.W.1	:	Audible Warning Device, R.S.
$C_{A,B}$	:	680 µfd, 25v.
$C_{1,2,3}$	:	100 pf Polystyrene 2.5%
D_{1-4}	:	4x IN 4001 or R.S RME 70
LP_A	:	Neon Sub. Min. Indicator
$LP_{1,2,3}$	:	Sub. Min. Indicators, 12v (R.S.)
MVR_1	:	MVR-15v Voltage Regulator, 15v (R.S.)
$PC_{1,2,3}$	:	1 PL PS12 Photocell
$R_{1,2,3}$	:	1 Megohm 0.5 W R.S.
$RLA_{1,2,3}$	:	R.S Low profile relay, 12v.
SW_1	:	D.P.D.T Sub.Min.
T_1	:	R.S 634, 17.5v.
$TR_{1,2,3}$	:	R.S 2N 3053.

4. START-UP, OPERATION AND SHUTDOWN OF THE RIG

The completed rig is illustrated in Figures 4.1 to 4.6. The procedures that were found most convenient for operating the rig are set out below; the numbers in parentheses refer to Figures 4.1 - 4.6.

i) Start-Up Procedure

The following sequence of operations was used when starting the rig:

a) Switch on main 415 v 3 phase supply (1).

b) Switch on compressor (2) and await cut-out when working pressure is reached.

c) Switch on Shaw Moisture Meter and allow to warm-up (2 minutes). Verify check-reading against appropriate element calibration graph, and adjust if necessary.

d) Check weighfeeder air line pressure, and adjust to 20 lbf/in^2 if necessary (3).

e) Verify that Mucon Valve (4) on top hopper (5) is closed.

f) Switch on weighfeeder (6,7) and verify that manometer reading (8) corresponds to zero mass flowrate.

g) Energise photo-cells (9) and lamps (10) of level warning devices.

h) Switch on elevator (13) and conveyor (14) and verify correct operation.

i) Check that main air supply by-pass valve (15) is closed.

j) Close fan inlet butterfly (16), open two rotameter valves (21) about half way and start fan (17). When up to speed, open inlet butterfly.

k) Open Mucon Valve in lower receiver (18) and check that channel has a slight downward inclination. (If not, see adjustment procedure under "Operation").

ℓ) Verify that Mucon valve (19) in channel header-tank (20) is shut.

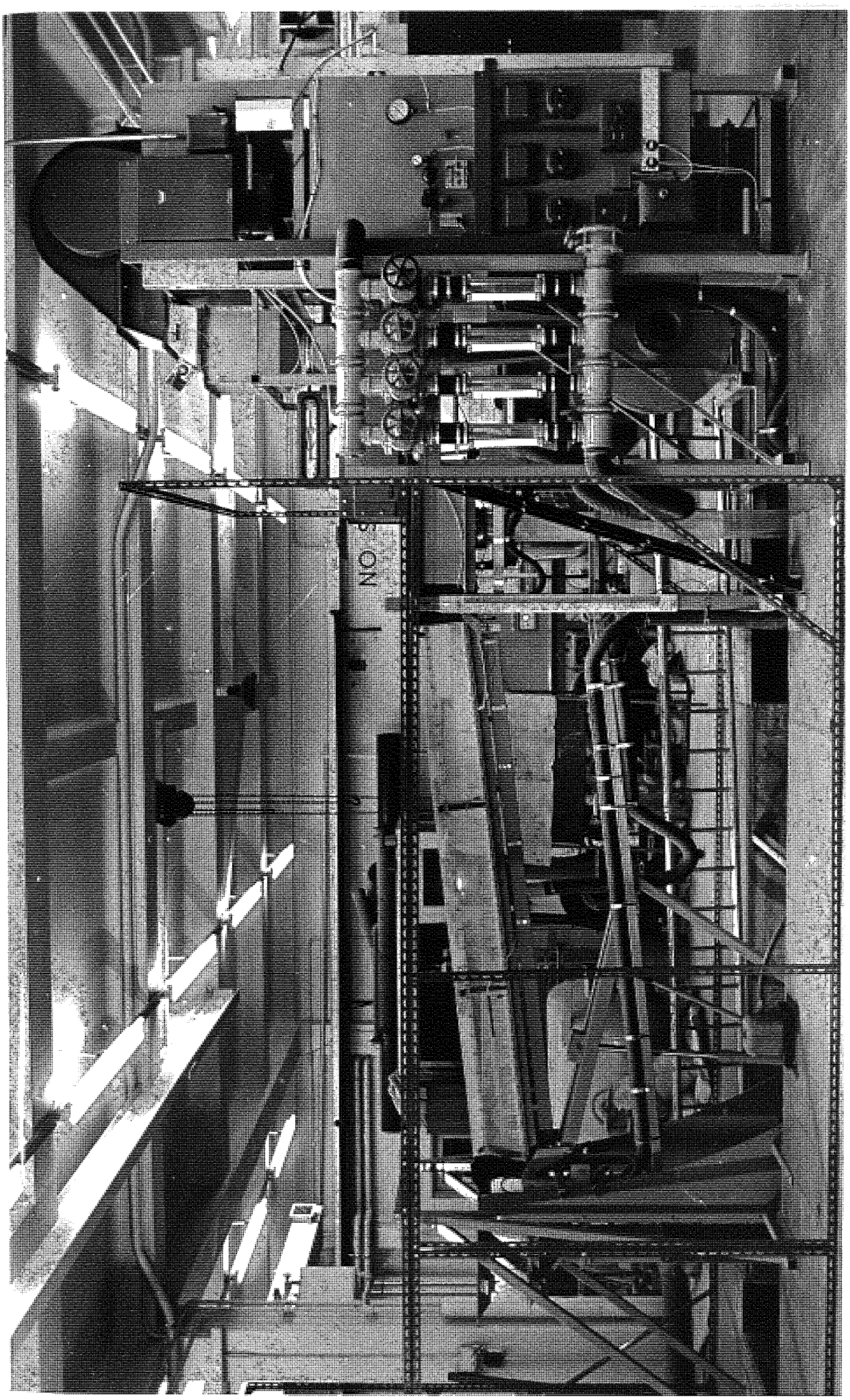

FIG. 4·1 CHANNEL FLOW RIG ~ OVERALL VIEW.

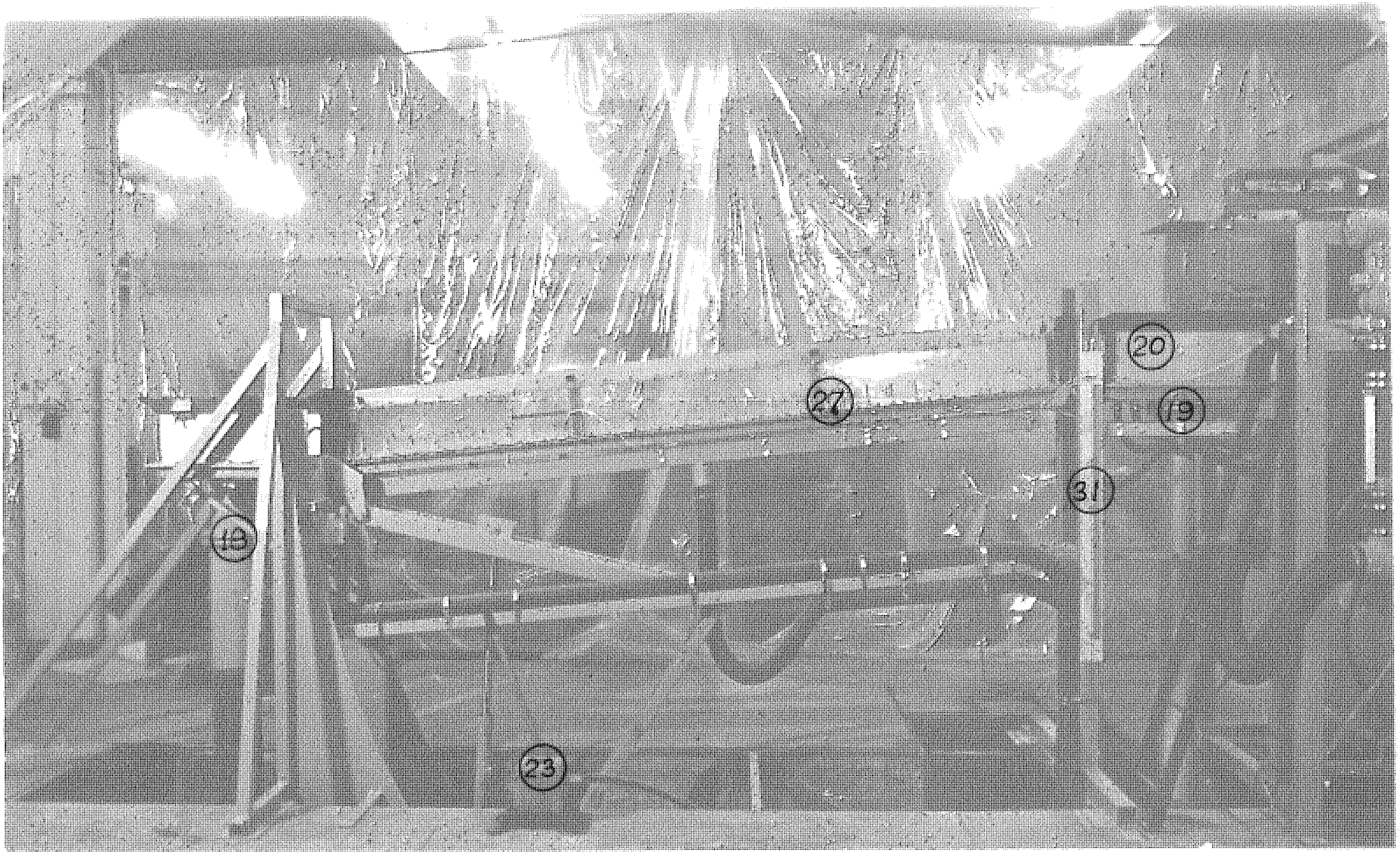

FIG. 4·2 FLUIDISED CHANNEL.

FIG. 4·2 FLUIDISED CHANNEL.

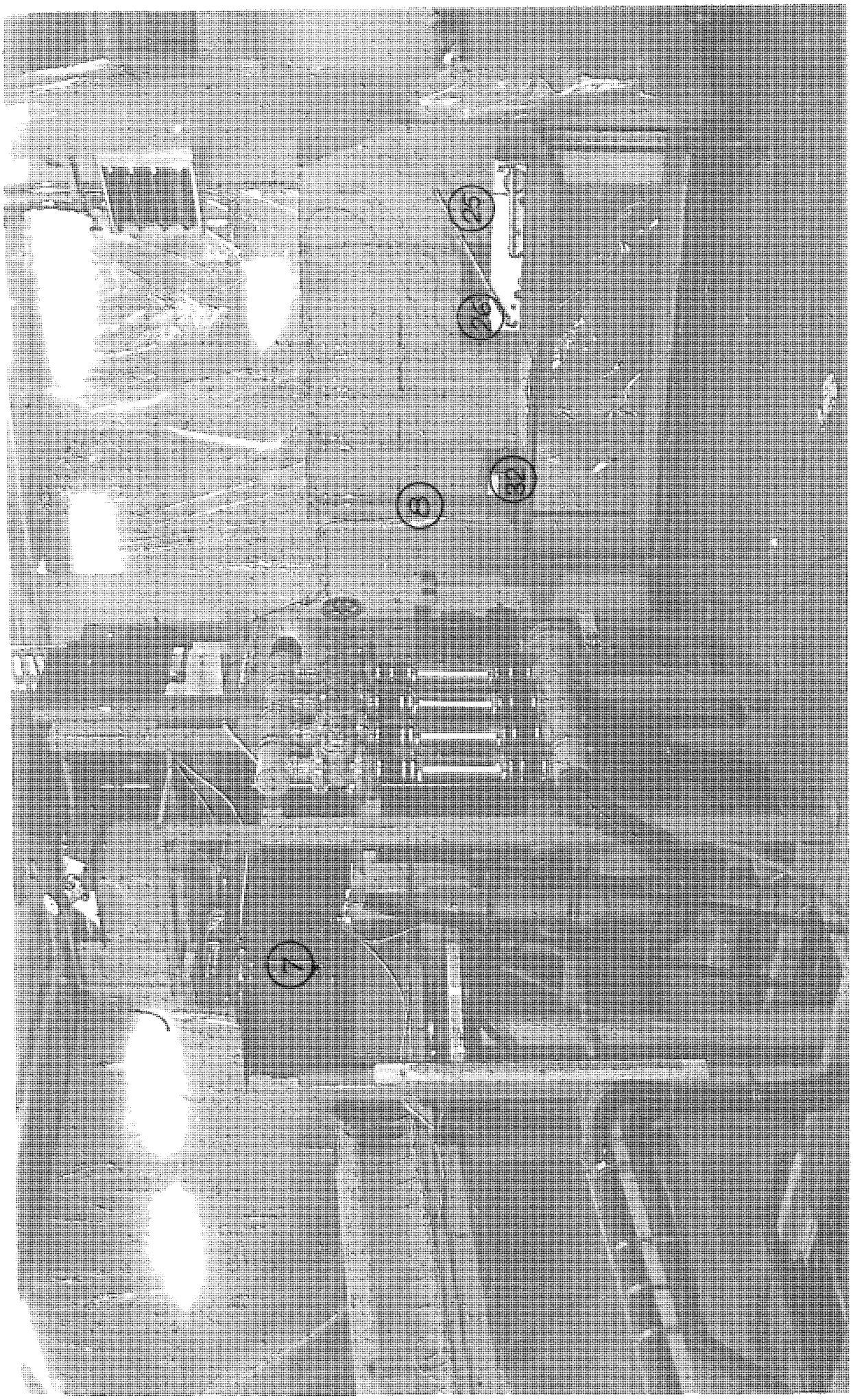

FIG. 4.3 HEADWORK AND WEIGHFEEDER.

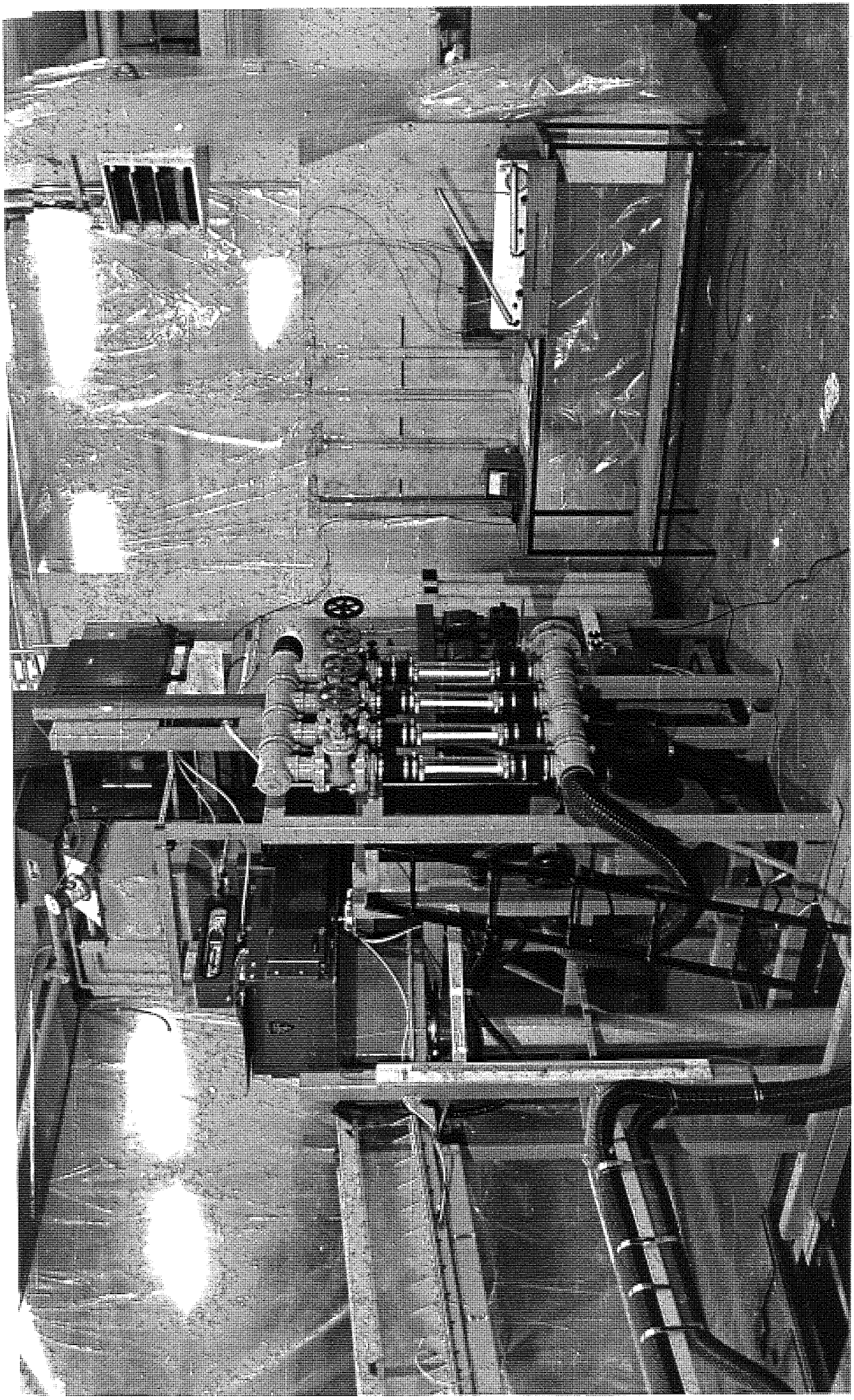

FIG. 4.3 HEADWORK AND WEIGHFEEDER.

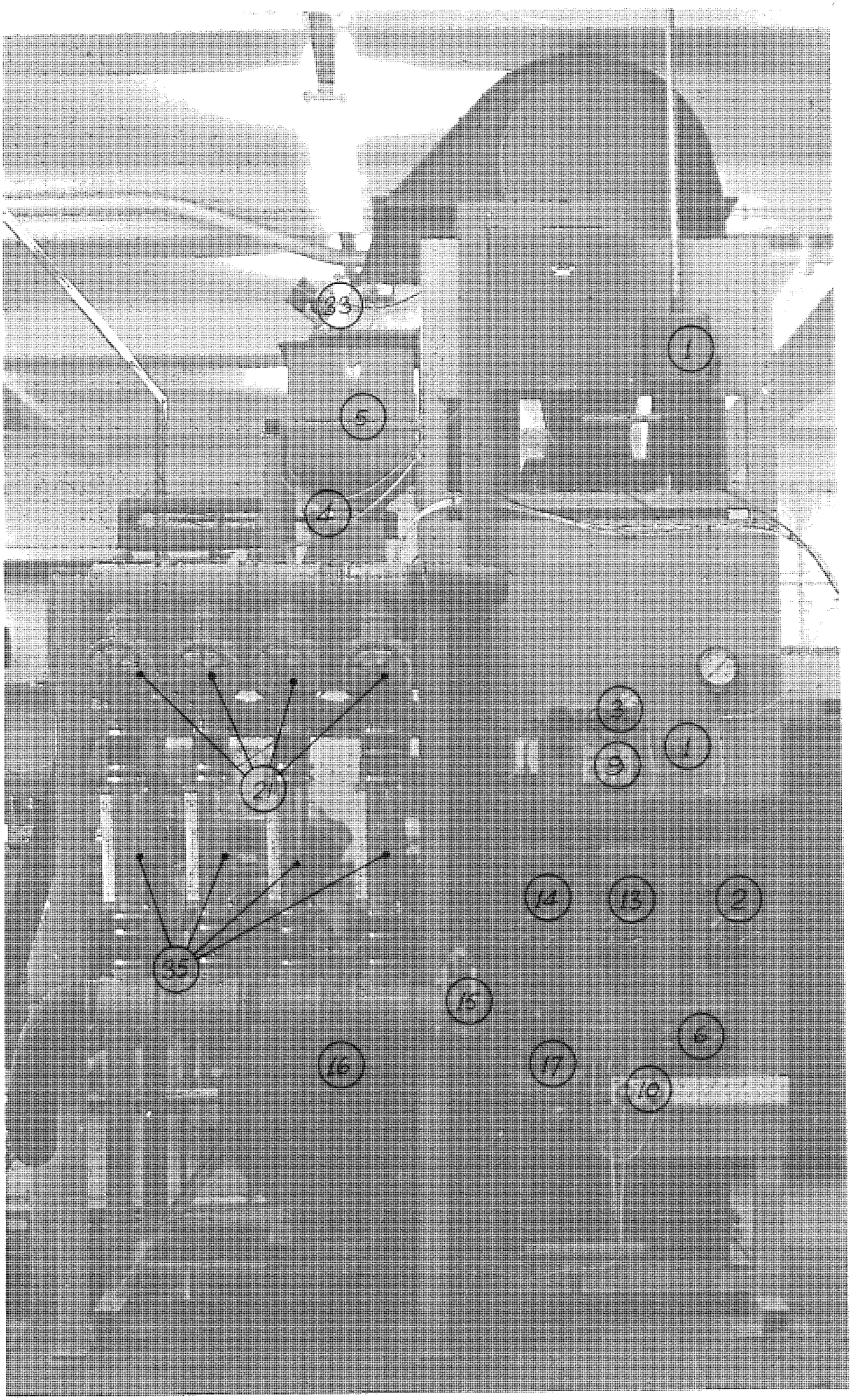

FIG. 4·4 CONTROL PANNEL AND ROTAMETERS.

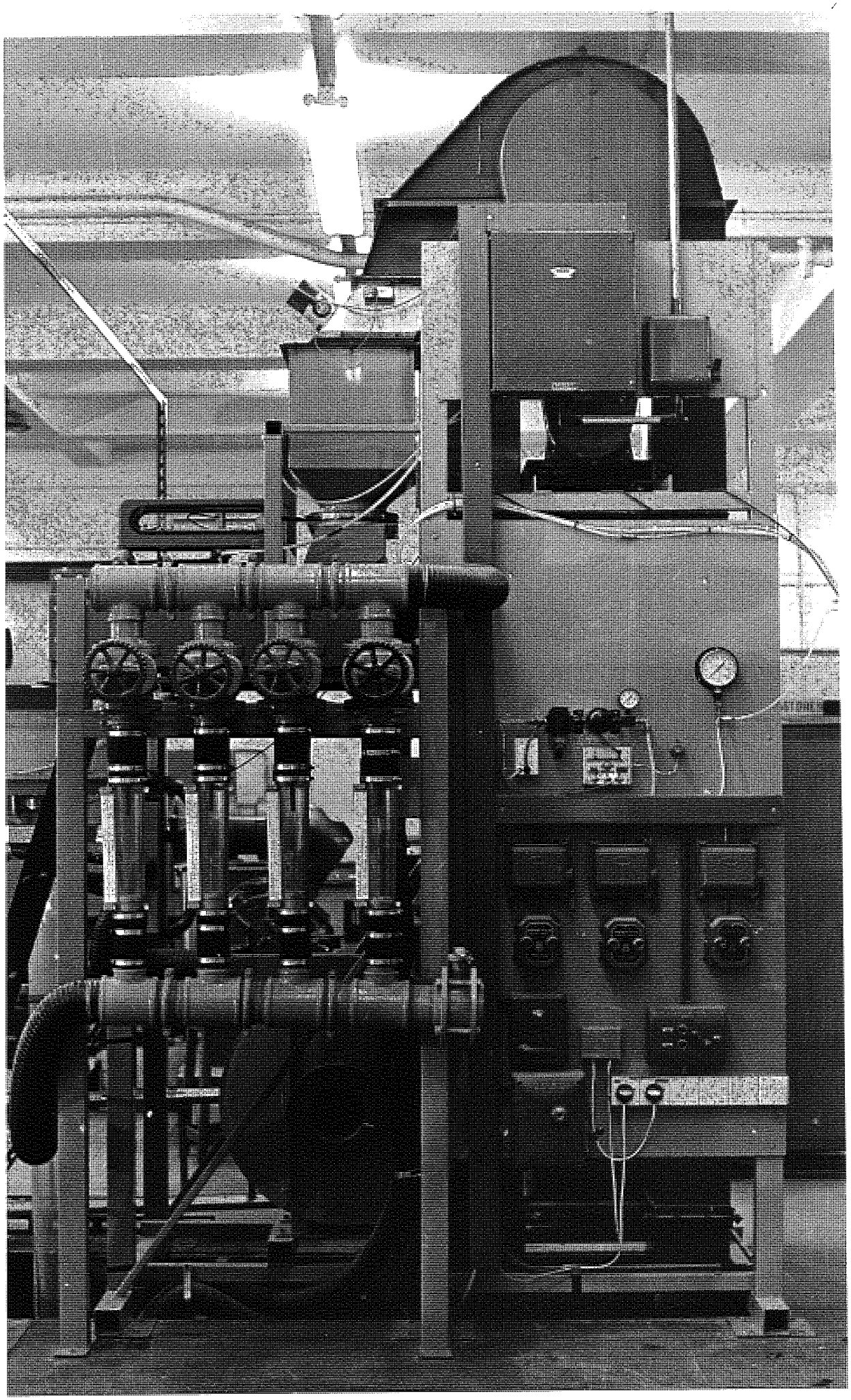

FIG. 4·4 CONTROL PANNEL AND ROTAMETERS.

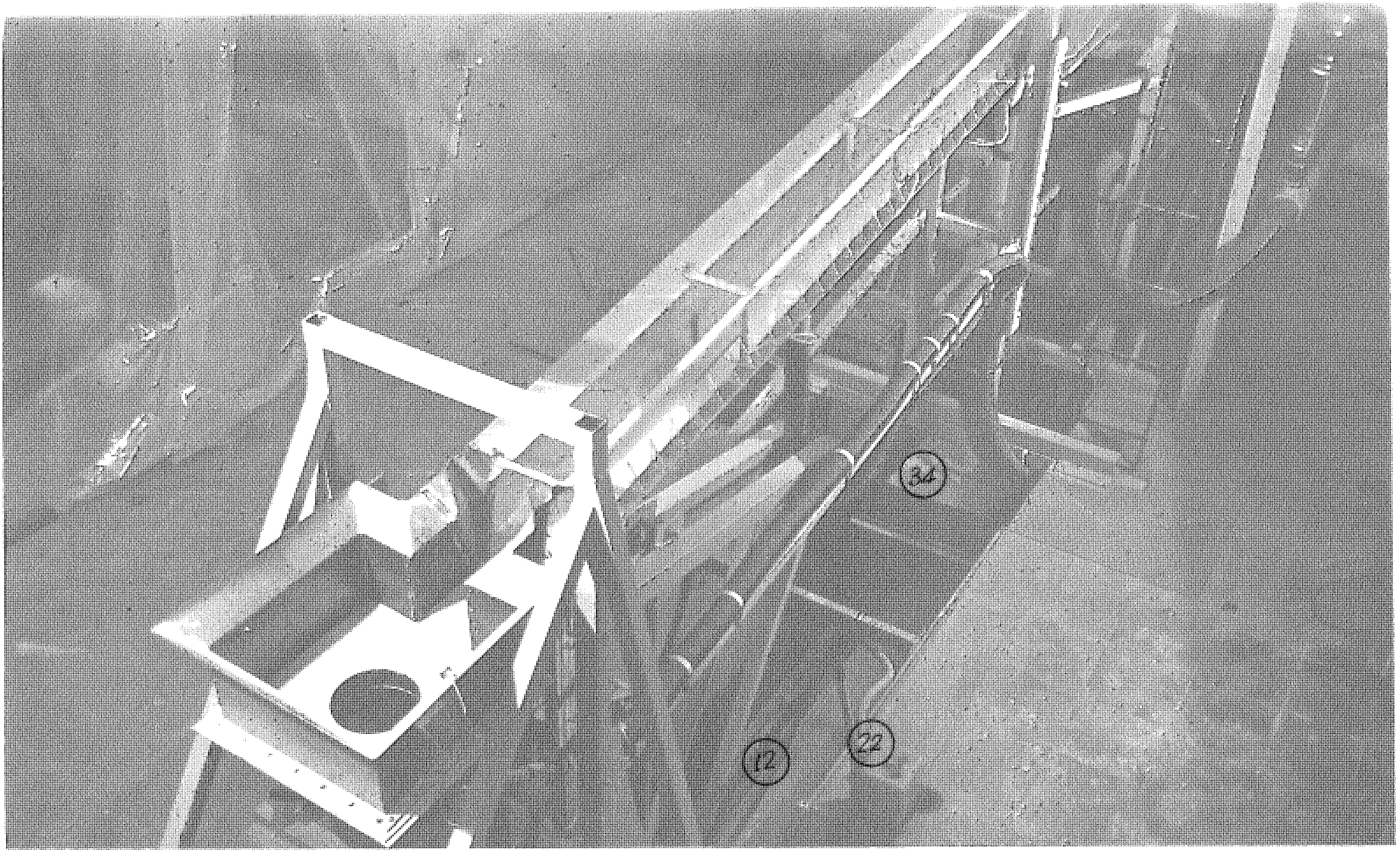

FIG. 4·5 FLUIDISED CHANNEL AND LOWER RECEIVER.

FIG. 4.5 FLUIDISED CHANNEL AND LOWER RECEIVER.

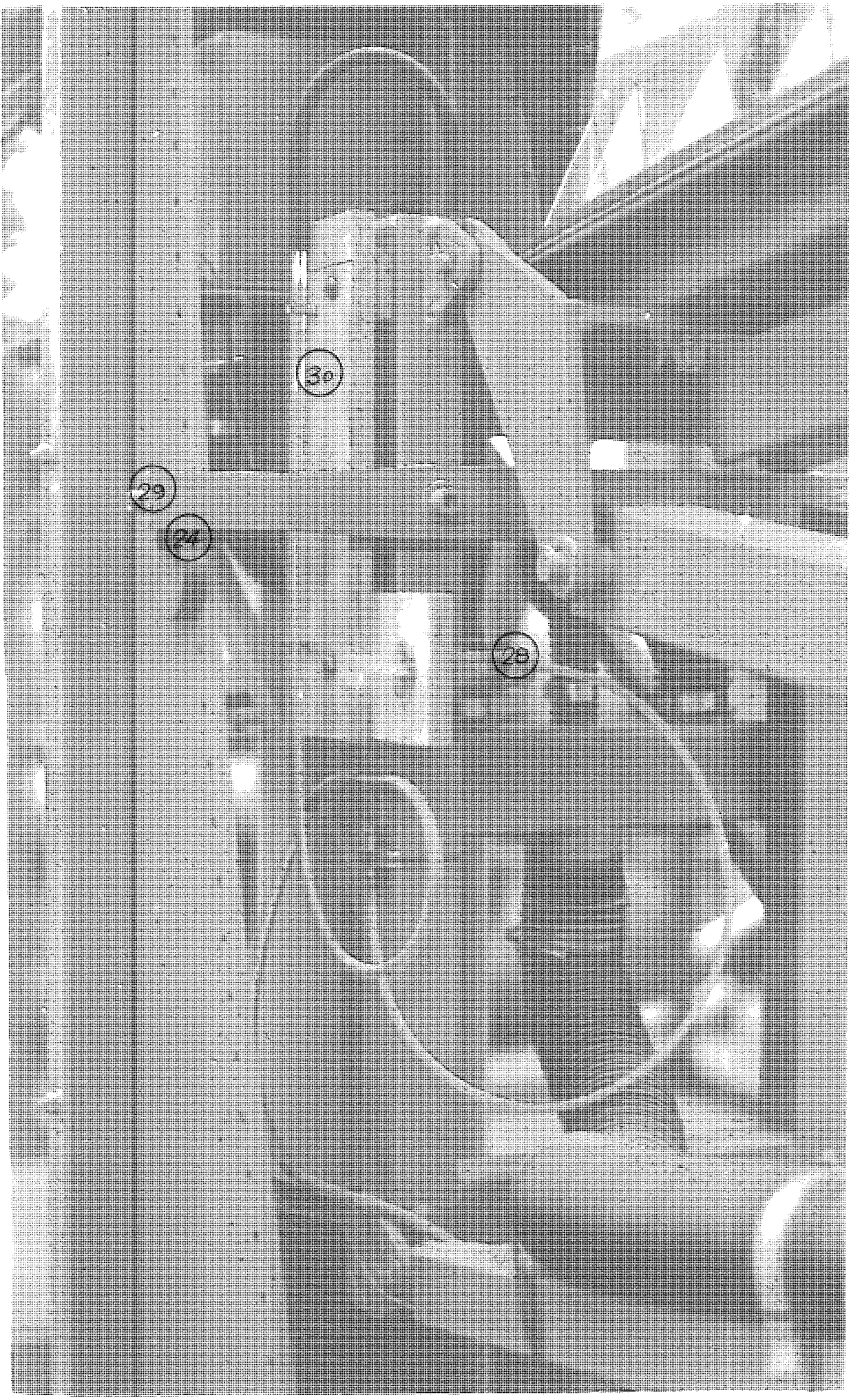

FIG. 4·6. WATER LEVEL AND LOWER CHANNEL SUPPORT.

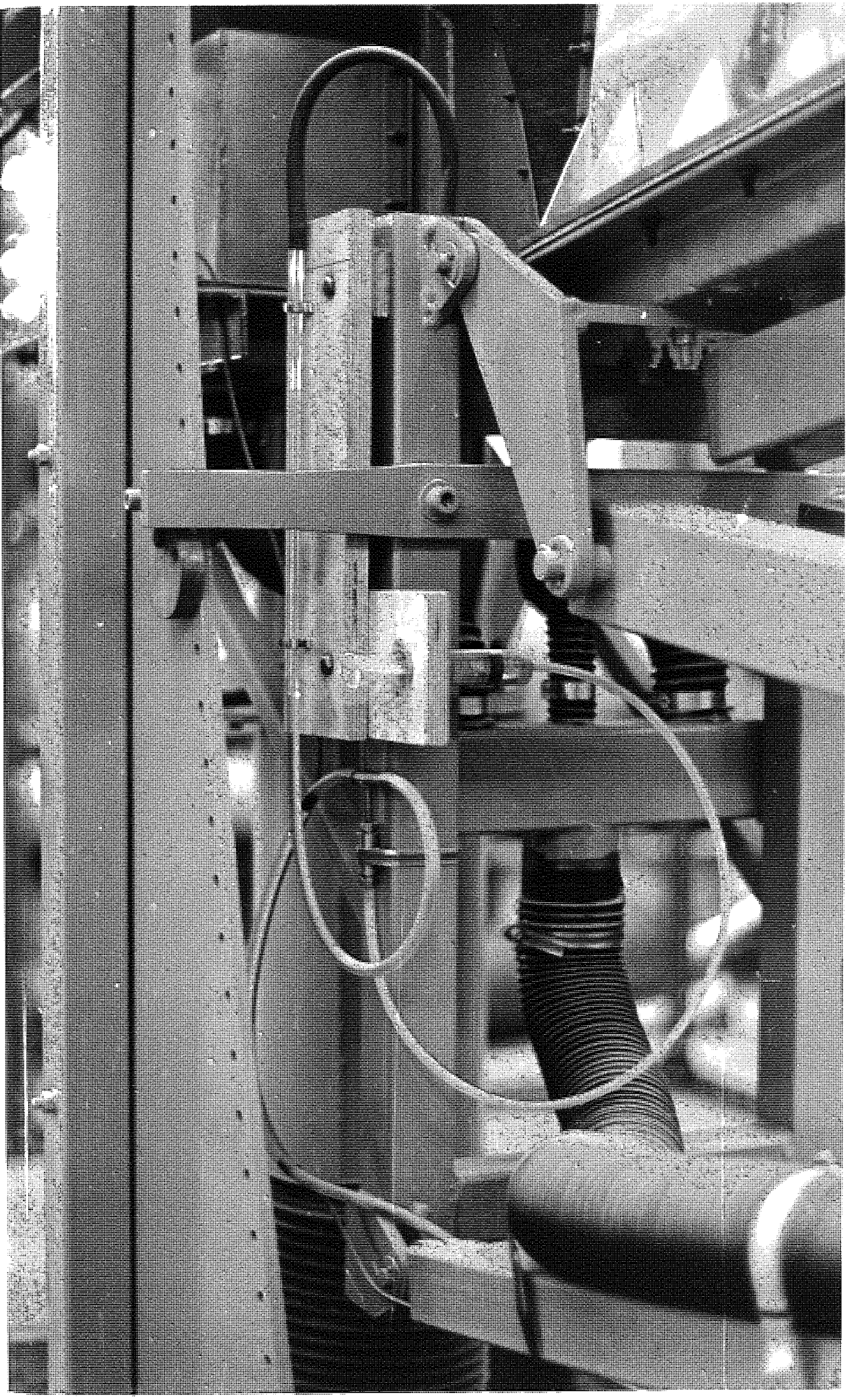

FIG. 4·6. WATER LEVEL AND LOWER CHANNEL SUPPORT.

KEY TO FIGURES 4.1 - 4.6

1. Master Switch, 415v 3ph.supply.
2. Compressor switch and starter .
3. Weighfeeder air-line pressure gauge and regulator .
4. Mucon valve for top hopper .
5. Top hopper .
6. Weighfeeder switch and starter .
7. Weighfeeder .
8. Mercury manometer: weighfeeder output signal .
9. Photocell switches and visual display .
10. Photocell lamp switches .
11. Level sensor audible warning .
12. Horizontal conveyor belt .
13. Elevator switch and starter .
14. Conveyor switch and starter .
15. Main air by-pass butterfly .
16. Fan inlet butterfly .
17. Fan switch and starter (star-delta) .
18. Mucon valve for lower receiver .
19. Mucon valve for header tank .
20. Header tank .
21. Rotameter control valves .
22. Relief valve for hydraulic ram .
23. Pump for hydraulic ram .
24. Eccentric discs, lower channel support .
25.) Inclined manometers (Upstream tapping .
26.) (Differential .
27. Upstream pressure tapping point.
28. Water level adjustment plunger .
29. Clamping screws, lower receiver .

30. Water level lower sight-glass .

31. Water level upper sight-glass .

32. Shaw Moisture Meter .

33. Top hopper lamp .

34. Storage hopper .

35. Rotameters (3 off 65K, 1 off 65A) .

m) Adjust rotameter control valves (21) to give a fluidising velocity of about 2 U_{m_f} for the material under test.

n) Open Mucon valve (4) on top hopper to give the desired minimum mass flowrate for the ensuing test.

o) Level and adjust zero reading on inclined manometers (25,26)

The rig is now ready for use.

ii) Operation

The following sequence of operations was used during testing:

a) Adjust fluidising velocity to desired value with rotameter control valves (21).

b) Shut ram pump pressure relief valve (22) and raise channel slightly with one or two strokes of pump (23).

c) Remove eccentric discs (24) supporting lower end of channel, and adjust channel inclination until manometer (25) from upstream pressure tapping (27) indicates desired bed pressure drop. (Note that the water-level plunger (28) must be adjusted to prevent the level overflowing before lowering the channel).

d) If test is to be of long duration fit and tighten accentric discs (24) and tighten channel clamping screws (29).

e) When conditions have stabilised, check top hopper for sufficient solids level to ensure steady discharge (via peep-hole in lamp (33)). Increase solids hold-up if necessary by releasing additional material from storage hopper (34).

f) Verify that differential manometer (26) is reading substantially zero (indicating uniform flow).

g) Adjust water-level plunger (28) until meniscus in lower sight-glass (30) is aligned with datum mark .

h) Note readings of:

Mass flowrate (manometer 8)

Upstream bed pressure drop (manometer 25)

Differential pressure, upstream/downstream (manometer 26)

Channel inclination (Upper sight-glass 31)

Fludising Velocity (Rotameters 35)

Fluidising air humidity (Meter 32)

Bed temperature (hand-held thermometer)

Also verify that weighfeeder air line pressure remains at 20 lbf/in^2.

i) Increase solids mass flowrate by suitable increments and repeat a-h until desired maximum mass flowrate is achieved.

j) Decrease solids mass flowrate and repeat previous procedure down to the minimum flowrate. Note that it will be necessary to reduce the solids hold-up in the flow circuit during this period by draining solids back into the storage hopper via valve 19, in order to prevent overflow of the top hopper. However, sufficient head of solids to ensure uniform discharge must always be maintained therein.

iii) Shut-down Procedure

The following sequence of operations was used when shutting-down:

a) Close Mucon valve (4) on top hopper and wait for flow circuit to empty (note that if flow circuit still contains sufficient solids to cause overflow of top hopper, some material must first be drained to the storage hopper via valve 19).

b) Check that weighfeeder manometer pressure (8) corresponds to zero mass flow.

c) Close Mucon valve in lower receiver (18).

d) Switch off fan (17).

e) Switch off conveyor (14) and elevator (13).

f) Switch off weigh feeder (6), level warning device (9), lamps (10) and moisture meter (32).

g) Switch off compressor (2) and open blow-down valve on air reservoir.

h) Fit and tighten eccentric discs (24) to support lower end of channel, and release hydraulic pressure in ram (22).

i) Switch off electrical master switch (1).

j) Recheck Mucon valves 4 and 34 for leakage.

Footnote The sensitivity and accuracy of the weigh feeder at low mass flow rates may be increased by reducing the belt speed. Two reductions from the design speed of 72 ft/min are possible with the existing change-gears: see instruction manual for details.

5. SUGGESTED MODIFICATIONS TO RIG IN THE LIGHT OF OPERATING EXPERIENCE

The flow rig has in general performed satisfactorily, and has presented no particular difficulty in operation. It was run successfully on initial start-up, and has been used to its full capacity in terms of volume flowrate on a number of occasions. Clearly though, any piece of equipment designed from such scant previous experience will benefit from some development in the light of experience gained during initial operation.

The only feature of the rig which could be regarded as a serious shortcoming does not affect its functionality but is detrimental to the well-being of the operators and others working near it. This is the dispersal of fines in the spent fluidising air. The problem is only serious when working at high fluidising velocities with fresh samples of material: once the fines have been expelled there is little ensuing trouble until further new material is added.

Protection for the operators can be afforded when necessary with suitable masks, but it would be desirable to build a dustproof enclosure around the rig to shield the rest of the laboratory. Temporary screens were erected to this end using polythene sheeting,

but a permanent enclosure, possibly with an extractor fan would be preferable. This is now in hand.

A problem associated with the latter one is the induction of fines and other atmospheric dust by the fluidising air fan, causing blinding of the porous distributor material. As well as increasing the distributor pressure drop, this could also change the fluidisation pattern by closing the smaller distributor pores and thereby giving less uniform distribution. This problem could be easily solved by fitting a filter to the fan inlet, although this would cause some flow restriction and necessitate a larger fan to maintain the full air delivery.

The only difficulty experienced in the fluidised channel has been build-up of solids in the header tank at high flowrates and low fluidising velocities. This problem arises from the use of a common air supply to the header, channel and receiver. As solids enter the header, the bed depth therein increases and causes the fluidising air to flow preferentially through the channel and receiver, where the pressure drop is slightly lower. The process tends to be cumulative at low fluidising velocities, so that eventually the solids in the header become defluidised and cease to flow freely.

It would be easy to obviate this trouble completely by separating the header plenum chamber from that of the rest of the channel, and providing an independently controlled air supply. By this means the fluidising velocity in the header could be maintained despite local increases in bed depth.

It has been quite easy, because the fluidised solids flow so freely, to exceed the designed maximum flowrate of the rig even at quite moderate bed depths. The weighfeeder and conveyor seem able to cope with some overload, but on a number of occasions the elevator has stalled due to choking of the boot with solids. The elevator manufacturer has

indicated that an increase in belt speed of about 25% is possible, but at the expense of reduced life. This is of little moment since the usage of the rig is very light compared with industrial operation. The modification involves changing the chain drive sprockets, which could be easily accomplished, and would be most useful.

An increase in solids storage capacity would be helpful, and could be provided by enlarging one of the existing bottom hoppers; or preferably by fitting a third hopper. This could be placed adjacent to one of the existing ones, to discharge on to the belt conveyor. The existing solids storage is not really adequate when working with deeper beds at high flow-rates and means that the solids have to be loaded and discharged manually.

In general the rig has proved to be very easy to operate and control, and has allayed fears expressed in some quarters regarding instability of flow. However, greater convenience of operation would be possible by providing remote controls for the Mucon valves on the top and bottom hoppers. These are available from the valve manufacturer, but were omitted at the design stage for cost reasons.

The top solids hopper must run part-full in order to provide a steady discharge, and a positive means of detecting low solids level therein would be of advantage. (At present the latter is indicated only by the sporadic discharge on to the weigh feeder belt). Such detection could be provided by a photo-indicator device similar to the overload warning, or more simply by a sight glass in the wall of the hopper.

Apart from the elutriation of fines mentioned above, some loss of solids occurs as the material falls down the receiver exit pipe and cascades on to the belt conveyor via the lower hopper. This could be minimised by fitting side curtains to the hopper exit to prevent the material 'splashing' up as it hits the belt. This would entail some restriction to the hopper outlet area and it would be prudent to fit an additional level warning device in the hopper to detect excess

solids build-up.

The foregoing are the only apparent difficulties with the rig following the quite considerable amount of work now undertaken. Most of the suggested modifications could be implemented without substantial expenditure or effort.

APPENDIX II

LIST OF MANUFACTURERS

A list of suppliers of equipment used for the experimental work, and their products, is given alphabetically below:

Airflow Developments Ltd, (Manometers)
29, Union Street, Oldham, Lancs.

Alldays and Onions Ltd, (Centrifugal fans)
Sydenham Road, Birmingham 11.

Keith Blackman Ltd, (Centrifugal Fans)
76, Sherlock Street, Birmingham 5.

Bowes Engineering Ltd, (Hydraulics Ram)
29, Porchester Road, Nottingham 3.

British Vacuum Cleaner Co. Ltd, (Blowers)
Leatherhead, Surrey.

Brookfield Engineering Laboratories Inc., (Viscometer)
Stoughton, Mass. USA.

Buckland Sand and Silica Co Ltd., (Sand)
Reigate Heath, Reigate, Surrey.

Crane Packing Ltd., (P.T.F.E.)
Slough, Bucks.

Dick Bearings Ltd., (Ball and Roller Bearings)
48, Upper Gough Street, Birmingham 1.

Douglas-Kane Group Ltd., ('Loctite' Products)
Swallowfields, Welwyn Garden City, Herts.

Associated Lead Manufacturers Ltd., (Zirconia)
Crescent House, Newcastle-upon-Tyne.

A.M.Lock and Co.Ltd., (Hygrometer)
Oldham, Lancs.

Midland Industrial Plastics Ltd., (Plastic conduit)
Mill Street, Birmingham 6.

Midland Tank and Ironplate Ltd., Heneage Street, Birmingham 7.	(Welded Fabircations)
Mucon Engineering Co.Ltd., Winchester Road, Basingstoke, Hants.	('Mucon' Valves)
Numec Ltd., New Whittington, Chesterfield, Derbys.	(Belt Conveyor)
Porvair Ltd., Estuary Road, King's Lynn, Norfolk.	('Vyon' porous plastic)
Rotameter Manufacturing Co.Ltd., (GEC - Elliott Process Instruments Ltd.) Croydon, Surrey.	(Rotameters)
Rubber and Plastic Industries Ltd., 27,Alcester Street, Birmingham 12.	(Rubber and Neoprene sheeting)
Sankeys Ltd., 92,Albert Street, Birmingham 5.	(Pipe Fittings)
Shaw Moisture Meters, Rawson Road, Westgate, Bradford.	(Humidity Meter)
Shell Marketing Ltd., Station Road, Rowley Regis, Staffs.	(Lubricants)
Simon-Barron Ltd., Bristol Road, Gloucester.	(Elevator)
British Steel Corporation. (Rylands-Whitecross and Co.Ltd.) Albion Road, West Bromwich.	(Steel tube and plate)
Venner Electronics Ltd., New Malden, Surrey.	(Digital Counter)

APPENDIX III.

PUBLICATIONS.

APPENDIX III

Some of the work included in this theses has been presented in the literature, and a full reference to each publication is given below.

i) J S M BOTTERILL, M VAN DER KOLK, D E ELLIOTT and S J McGUIGAN[102] :
"The Flow of Fluidised Solids". Paper presented to the 'POWTECH' Internal Conference on Powder Technology, Harrogate, May 1971. Published in Powder Technology, Vol 6, P343, (1972).

ii) S J McGUIGAN and D E ELLIOTT[148] : "The 'Viscosity' of Shallow Fluidised Beds". Paper presented to the 4th International 'CHISA' Congress of Chemical Engineering, Chemical Equipment Design and Automation, Prague, Czechoslovakia, September 11-15, 1972.